



저작자표시-비영리-변경금지 2.0 대한민국

이용자는 아래의 조건을 따르는 경우에 한하여 자유롭게

- 이 저작물을 복제, 배포, 전송, 전시, 공연 및 방송할 수 있습니다.

다음과 같은 조건을 따라야 합니다:



저작자표시. 귀하는 원저작자를 표시하여야 합니다.



비영리. 귀하는 이 저작물을 영리 목적으로 이용할 수 없습니다.



변경금지. 귀하는 이 저작물을 개작, 변형 또는 가공할 수 없습니다.

- 귀하는, 이 저작물의 재이용이나 배포의 경우, 이 저작물에 적용된 이용허락조건을 명확하게 나타내어야 합니다.
- 저작권자로부터 별도의 허가를 받으면 이러한 조건들은 적용되지 않습니다.

저작권법에 따른 이용자의 권리는 위의 내용에 의하여 영향을 받지 않습니다.

이것은 [이용허락규약\(Legal Code\)](#)을 이해하기 쉽게 요약한 것입니다.

[Disclaimer](#)

공학석사 학위논문

Nonlinear Analysis and Design of Tensile Membrane Structures

막구조의 비선형 해석과 설계기술에
관한 연구

2015 년 2 월

서울대학교 대학원

건축학과

Marta Gil Pérez

Nonlinear Analysis and Design of Tensile Membrane Structures

지도 교수 강 현 구

이 논문을 공학석사 학위논문으로 제출함

2015 년 2 월

서울대학교 대학원
건축학과

Marta Gil Pérez

마르타의 공학석사 학위논문을 인준함

2015 년 2 월

위 원 장 _____ (인)

부위원장 _____ (인)

위 원 _____ (인)

Abstract

Nonlinear Analysis and Design of Tensile Membrane Structures

Marta Gil Pérez

Department of Architecture & Architectural Engineering

The Graduate School

Seoul National University

Advisor: Professor Thomas Kang

Membrane structures are one of spatial structures that allow for long span and light weight roofs. In many cases, the membrane roofs are supported with trusses or mats and prestressed together with cables to obtain a resistant shape for a given loading condition. For the design of membrane structures, nonlinear analysis is required.

Besides, modeling of each membrane element and form-finding of the shape are of great importance in the design process. First, an equilibrium-finding analysis is conducted for the purpose of obtaining the optimal shape of the membrane structure, during which the initial stresses of the

membrane and cables must be balanced. Next, the stress-deformation analysis is performed for the required loading condition. This analysis allows understanding the behavior of the structure and confirms that the design of the membrane satisfies the required safety factor for the construction.

In this research, a broad definition and explanation about spatial structures and in particular membranes are given. Then, the detailed procedure for the design and analysis of those is introduced with a complete explanation of the modeling and conditions to be considered. For a better understanding, two case studies are introduced and described where each step for the modeling, design and analysis is illustrated.

At the last part of this thesis, a parametric study on barrel vault shaped membranes is described. In this part, firstly regular membrane panels supported between arches are analyzed, leading to the development of a safe design aid for this type of membranes. Secondly, by adding one grade of irregularity, curved and inclined membrane barrel vault shaped panels are also studied, resulting on a similar safe design combination graph for each of this kind of panels. Finally, by the use of these design charts, simple design examples are illustrated to show the application of this study.

Keywords: Membrane, Cable, Tensile Structures, Spatial Structures, Nonlinear Analysis and Design, Form-Finding, Stress-Deformation.

Student Number: 2013-22464

Table of Contents

Abstract.....	i
Acknowledgements.....	iii
Table of Contents	v
Figures.....	xiii
Tables	xxiii
Notations	xxv
Cable element stiffness equation notations	xxv
Membrane element stiffness equation notations	xxix
Barrel vault shaped membranes notations	xxxvi
Chapter 1. Introduction.....	1
Chapter 2. Review of Spatial and Tensile Structures.....	7
2.1. Spatial structure classification	7
2.1.1. Classification by structural system.....	7
2.1.1.1. Form-active structural systems	9
2.1.1.2. Vector-active structural systems.....	10
2.1.1.3. Surface-active structural systems	11
2.1.2. Spatial structures synthesized classification.....	12

2.1.2.1. Hybrid structures	14
2.2. Environmentally compatible aspects of spatial structures.....	17
2.3. Historical development of tensile structures.....	20
2.3.1. Frei Otto and the natural forms	22
2.3.1.1. The four-point tent	24
2.3.1.2. The Peak tent.....	25
2.3.1.3. The arched tent.....	26
2.3.1.4. The hump tent	27
2.3.1.5. Hybrids and variations	28
2.3.1.6. Olympic Stadium, Munich, Germany	28
2.3.2. Horst Berger	29
2.3.2.1. Inefficient solutions.....	30
2.3.2.2. Point-supported structures.....	31
2.3.2.3. A-frame supported structures	32
2.3.2.4. Arch-supported structures	33
2.3.3. Recent constructions	34
Chapter 3. Design Considerations for Tensile Structures	37
3.1. Tensile structures characteristics and properties	37
3.1.1. Tensile basic forms characteristics.....	39
3.1.1.1. Types of curvature.....	40
3.1.1.2. Types of anticlastic shapes	41
3.1.2. Fabric material properties.....	43

3.2. Design procedure of tensile structures	46
3.2.1. Form-finding analysis	50
3.2.1.1. Dynamic relaxation	53
3.2.1.2. Force density method	54
3.2.1.3. Nonlinear finite element method	55
3.2.2. Stress-deformation analysis	56
3.2.3. Patterning and construction	58
3.3. Loading conditions and safety approach	59
3.3.1. Loads and load combinations	61
3.3.1.1. Prestress	61
3.3.1.2. Self-weight	64
3.3.1.3. Wind	64
3.3.1.4. Snow	65
3.3.1.5. Temperature	66
3.3.1.6. Seismic	67
3.3.2. Safety factors	67
Chapter 4. Purpose of Research	71
Chapter 5. Development of Geometrically Nonlinear Finite Element Equations	73
5.1. Cable element equations	74
5.1.1. Coordinate system and displacement function	74
5.1.2. Displacement-strain relationship	75

5.1.3. Stress-strain relationship	76
5.1.4. Equation of equilibrium using the principle of virtual work.....	77
5.1.5. Coordinate transformation.....	79
5.1.6. Stiffness equation	81
5.1.7. Wrinkling of cable element	82
5.2. Membrane element equations	83
5.2.1. Shape function.....	83
5.2.2. Displacement-strain relationship.....	87
5.2.3. Stress-strain relationship	89
5.2.4. Equation of equilibrium using the principle of virtual work.....	90
5.2.5. Coordinate transformation and global stiffness equation.....	92
 Chapter 6. Nonlinear Analysis and Modeling of Tensile	
Structures.....	97
 6.1. Nonlinear Analysis of Spatial Structures program (NASS)...	98
6.1.1. General chart	99
6.1.2. Element charts	103
6.1.3. Nonlinear analysis chart.....	110
6.1.4. Input and output data.....	115
6.1.5. Application examples.....	121
 6.2. Modeling of membrane and cable elements.....	123
6.2.1. Fabric weave orientation	123
6.2.2. Nodes and elements.....	124

6.2.3. Material properties	125
6.2.4. Initial stresses	126
6.2.5. Loading conditions	127
Chapter 7. Case Studies.....	129
7.1. Seoul Southwestern Baseball Stadium dome.....	129
7.1.1. Membrane model	133
7.1.1.1. Models and panels for analysis	133
7.1.1.2. Material properties	135
7.1.1.3. Initial stress conditions.....	135
7.1.2. Form finding analysis.....	136
7.1.2.1. Initial stress balance	137
7.1.2.2. Perfect shape	139
7.1.3. Stress deformation analysis.....	140
7.1.3.1. Design loading cases	141
7.1.3.2. Displacement results of the deformed shape.....	141
7.1.3.3. Stress, deformed shape and safety factor	143
7.1.4. Conclusion.....	147
7.2. Jeju World Cup Stadium dome	148
7.2.1. Membrane model	151
7.2.1.1. Models and panels for the analysis	151
7.2.1.2. Material properties	153
7.2.1.3. Initial stress conditions.....	153

7.2.2. Analysis results	153
7.2.2.1. Design loading cases	154
7.2.2.2. Results of the deformed shape and displacements	155
7.2.2.3. Stress, deformed shape and safety factor	158
7.2.3. Conclusion.....	161

Chapter 8. Parametric Study and Design of Barrel Vault

Shaped Membranes..... 163

8.1. Assumptions for the models 163

8.1.1. Material properties, loading conditions and initial stress	164
8.1.2. Maximum stress and safety factors	165
8.1.3. Barrel vault shaped membrane parameters for the study	166
8.1.3.1. Regular barrel vault shaped membranes	166
8.1.3.2. One grade of irregularity for barrel vault shaped membranes..	168
8.1.4. Design and analysis procedure	169
8.1.4.1. Modeling of the panels for the analysis	170

8.2. Regular barrel vault shaped membranes..... 171

8.2.1. Arch curvature.....	171
8.2.1.1. Form-finding analysis for various arch curvatures	173
8.2.1.2. Stress-deformation analysis for various arch curvatures.....	176
8.2.2. Width.....	179
8.2.2.1. Form-finding analysis for various widths	179
8.2.2.2. Stress-deformation analysis for various widths	181

8.2.3. Arch scale.....	187
8.2.3.1. Form-finding and stress-deformation analysis for various arch scales	188
8.2.4. Parametric study for regular barrel vault shaped membranes	189
8.3. Curved barrel vault shaped membranes.....	191
8.3.1. Initial model design and analysis for curved panels.....	192
8.3.1.1. Comparison of a regular panel with 6 m width and a curved panel with the same width in the central section	195
8.3.1.2. New parameters defining curved panels	197
8.3.2. Analysis of curved panels with same width in the center and different opening angle	199
8.3.3. Analysis of curved panels with same arch curvature and different width in the center.	203
8.3.4. Parametric study for curved barrel vault shaped membranes.....	206
8.4. Inclined barrel vault shaped membranes	213
8.4.1. Parameters defining the inclined barrel vault shaped membranes .	214
8.4.2. Analysis of inclined panels with same arch curvature and different inclination angle for two different widths	219
8.4.3. Analysis of inclined panels with same inclination angle and same width but different arch curvatures	227
8.4.4. Parametric study for inclined barrel vault shaped membranes.....	230
8.5. Design application examples	237
8.5.1. Regular barrel vault shaped membranes	237

8.5.1.1. Example 1: Regular panels for street market with low buildings	238
8.5.1.2. Example 2: Regular panels for street market with higher buildings.....	240
8.5.2. Curved barrel vault shaped membranes	242
8.5.2.1. Example 3: Regular and curved panels for irregular street market	243
8.5.2.2. Example 4: Regular and curved panels for a green walking path	244
8.5.3. Inclined barrel vault shaped membranes	245
8.5.3.1. Example 5: Regular and inclined panels for domed roofs	245
Chapter 9. Conclusion	249
References	257
Appendices	263

Figures

Figure 2.1-1 Spatial structures classification (reinterpretation) (Engel 1981)	8
Figure 2.1-2 Spatial structures synthesized classification	12
Figure 2.1-3 Types of spatial structures	13
Figure 2.1-4 Quasi-static folding simulation (ESI France) (Haug et al. 2012)	16
Figure 2.2-1 Eden project (Knebel et al. 2002) (left) and Great glasshouse of national botanic garden of Wales (Ali-Nezhad & Eskandari 2012) (right)	18
Figure 2.2-2 Park dome (Sakai et al. 1999) (left) and Millennium dome (Hills et al. 2002) (right)	19
Figure 2.3-1 J. S. Dorton Arena Pavilion in Raleigh, North California (left) and the Yale University hockey rink, New Haven, Connecticut (right) (Fang 2009)	20
Figure 2.3-2 Frei Otto soap film experiments (Otto & Rasch 1996)	23
Figure 2.3-3 For-point tent, woven diagonally to the base area (left), woven parallel with the edges of the base area (center) and Music Pavilion at the 1955 Federal Exhibition in Kassel (right) (Otto & Rasch 1996)	24
Figure 2.3-4 Form finding study, high and low points with cable loops (left), Swiss Regional expo 1964 in Lausanne (center and right)	

(Otto & Rasch 1996).....	25
Figure 2.3-5 Arched tent and the entrance of the Federal Garden Exhibition (Otto & Rasch 1996).....	26
Figure 2.3-6 Hump tent (left) and canopy of the Interbau café in Berlin (right) (Otto & Rasch 1996).....	27
Figure 2.3-7 Studies for membranes and cable nets (left) and matrix of nets dependent on the four different shapes (Otto & Rasch 1996).....	28
Figure 2.3-8 Olympic Stadium, Munich, Germany (Fang 2009)	29
Figure 2.3-9 Canada Place (left) and Jeddah Haj Terminal (right) (Berger 1999).....	31
Figure 2.3-10 Jeppesen Terminal, Denver International Airport (Berger 1999).....	31
Figure 2.3-11 Cynthia Woods Mitchell Center (http://www.eventfinda.com/).....	32
Figure 2.3-12 McClain indoor practice facility (https://www.flickr.com).....	33
Figure 2.3-13 Millennium Dome (left) and London 2012 Olympic Stadium (right) (Bridgens & Birchall 2012).....	34
Figure 2.3-14 Foshan Century Lily Stadium (left) and Shenzhen Bao'an Stadium (right) (Lan 2012).....	35
Figure 3.1-1 Skysong at ASU campus, USA (FTL design engineering studio) (http://sgustokdesign.com).....	38
Figure 3.1-2 Example of anticlastic shape (left) and synclastic shape (right)	40
Figure 3.1-3 Three fundamental tensile forms by manipulation of boundary conditions (Bridgens & Birchall 2012).....	41

Figure 3.1-4 Architectural fabric cross-sections showing highly crimped, woven yarn bundles encased in PTFE or PVC coating (Bridgens & Birchall 2012).	44
Figure 3.1-5 Base components of technical woven fabric (Ambroziak & Kłosowski 2014)	44
Figure 3.2-1 Design procedure of tensile structures (organized by Marta Gil Pérez)	47
Figure 5.1-1 Local coordinates system and displacements of a cable element.	74
Figure 5.2-1: Local coordinates system and displacements of a membrane element.	83
Figure 6.1-1 Synthesized general chart of NASS program	101
Figure 6.1-2 Extended general chart of NASS program (organized by Marta Gil Pérez)	102
Figure 6.1-3 Cable element stiffness matrix chart (organized by Marta Gil Pérez)	104
Figure 6.1-4 Membrane element stiffness matrix chart (organized by Marta Gil Pérez)	105
Figure 6.1-5 Nonlinear analysis chart (organized by Marta Gil Pérez)	112
Figure 6.1-6 Membrane application examples of the program NASS	122
Figure 6.2-1 Typical wave (warp and fill) directions for the three basic tensile structure shapes.	123
Figure 6.2-2 Example of membrane elements connectivity order	125
Figure 6.2-3 Example of the equivalent nodal loads for the snow loading	127
Figure 6.2-4 Example of the equivalent nodal loads for the uplift wind	

loading.....	127
Figure 7.1-1: 3D view and elevation of the stadium (Kim et al. 2010).	130
Figure 7.1-2 Structural system of the dome.....	131
Figure 7.1-3 Interior and exterior of the Seoul Southwestern Baseball Stadium construction	132
Figure 7.1-4: Models A and B of the membrane structure and panels chosen for the analysis.....	133
Figure 7.1-5 Definition of the warp and fill directions and connectivity of the triangular elements.....	134
Figure 7.1-6 Prestressing of the cable for Model B.....	136
Figure 7.1-7 Initial shapes of panels 2 and 8 (Models A and B).....	137
Figure 7.1-8 Balance of initial stress in cable and membrane for panels 2 and 8 and Models A and B.....	138
Figure 7.1-9 Comparison of transverse displacements at the central section from the shape finding analysis.....	140
Figure 7.1-10 Displacements of panel 2 and panel 8 at the central longitudinal section.....	142
Figure 7.1-11 Final deformed shape under downward loading	146
Figure 7.1-12 Final deformed shape under uplift loading	147
Figure 7.2-1 Original dome of Jeju Stadium (up) (http://ojakgyoo.com.ne.kr), new dome of the Stadium (down)....	148
Figure 7.2-2 Plan view (left) and section (right) of the structure of the dome (Brzozowski et al. 2005).....	149
Figure 7.2-3 Original model of one strip of Jeju dome (left), new model of the same strip (right).....	150
Figure 7.2-4 Representative panels chosen for the analysis	151

Figure 7.2-5 Initial models of the panels chosen for the analysis.....	152
Figure 7.2-6 Uplift wind loading condition.....	154
Figure 7.2-7 Comparison of displacement of panels 1, 2 and 3 of the surface in the z direction.....	156
Figure 7.2-8 Displacements of panels 1, 2 and 3 at the nodes of the central longitudinal section.....	157
Figure 7.2-9 Deformed shapes of the 3 panels under uplift wind loading condition.....	160
Figure 8.1-1 Barrel vault shaped membrane structures.....	164
Figure 8.1-2 Regular barrel vault shaped membrane's parameters.....	167
Figure 8.1-3 One grade of irregularity barrel vault shaped membrane parameters.....	168
Figure 8.1-4 Node and element numbers for the base model.....	170
Figure 8.2-1 Angle subtended by the arch.....	171
Figure 8.2-2 Arch curvature initial models.....	172
Figure 8.2-3 Arch curvature initial shape and final shape after form- finding analysis.....	173
Figure 8.2-4 Maximum stresses in warp and fill directions for the different arch curvature models.....	177
Figure 8.2-5 Stress distribution in the warp direction under upwards loading condition.....	178
Figure 8.2-6 Width parameter models.....	179
Figure 8.2-7 Final shapes of width models for different arch curvatures.....	180
Figure 8.2-8 Initial stress distribution after form-finding analysis in the elements of the longitudinal section for 74 degree arch curvature and variable width models.....	181

Figure 8.2-9 Maximum stress of width models for the different arch curvature	183
Figure 8.2-10 Behavior with respect to width models under downwards loading	184
Figure 8.2-11 Behavior with respect to width models under upwards loading.....	185
Figure 8.2-12 Stress distribution in the fill direction under upwards loading condition for 6 meter width models	186
Figure 8.2-13 Scale parameter models.....	187
Figure 8.2-14 Maximum stress of scale models for 38 degree curvature and 6 m width	188
Figure 8.2-15 Regular barrel vault shaped membrane limitations.....	190
Figure 8.3-1 Parameters to define the curved barrel vault shaped membrane panels	191
Figure 8.3-2 Parameter nomenclature for curved panels.....	191
Figure 8.3-3 Initial shape in plan and final shape of curved panels with 38° of curvature, 12 m span (C), 3 m of initial width (W_I) and different opening angles (β).	193
Figure 8.3-4 Maximum stress in the warp and fill directions for the different opening angles (β) in panels with 38° of curvature and 3 m of initial width (W_I)	194
Figure 8.3-5 Regular panel with 6 m width and 38° curvature and curved panel with the same curvature and 6 m width in the central section of the panel	195
Figure 8.3-6 Comparison of stress distribution, maximum stress and deformed shape under downwards and upwards loadings	

between a regular panel of 6 m width and a curved panel with the same width in the central section	196
Figure 8.3-7 New parameters defining curved panels	197
Figure 8.3-8 Initial shape in plan and final shape of curved panels with 56° curvature, 12 m span (C), 6 m width in the center (M), and different opening angles (β) and initial widths (W_1).....	199
Figure 8.3-9 Maximum stress in the warp and fill directions for the different opening angles (β) in panels with 56° curvature and 6 m width in the center (M).....	200
Figure 8.3-10 Stress distribution in the fill direction, maximum stress and deformed shape of curved panels with 56° curvature, 12 m span (C), 6 m width in the center (M), and different opening angles (β) and initial widths (W_1).	201
Figure 8.3-11 Limitations for curved barrel vault shaped membranes considering the arch curvature and the width in the center of the panel (M).....	202
Figure 8.3-12 Comparison of regular and curved panels with the same curvature of 38°, span of 12 m (C), and width in the center M of 3 m, 6 m and 9 m.	204
Figure 8.3-13 Maximum stress in the fill direction under downwards loading for models with the same curvature of 38° and different width in the center (M) when increasing the opening angle (β)	205
Figure 8.3-14 Increase of maximum stress slope for models with different arch curvatures when increasing the opening angle (β)..	205
Figure 8.3-15 Explanation of how to obtain the maximum opening angle for the selected model	206

Figure 8.3-16 Slope values m for the increase of maximum stress in models with different arch curvature when increasing the opening angle	208
Figure 8.3-17 Maximum stress under downwards loading in the fill direction with the increase of the curvature of the arch for different widths in regular panels (n).....	208
Figure 8.3-18 Maximum width in the center M for different opening angles β when increasing the arch curvature	210
Figure 8.3-19 Combination of the M and β limitations found under downwards loading and upwards loading.....	211
Figure 8.3-20 Final design chart for arch curvature, width in the center M , and opening angle β of curved barrel vault shaped membrane panels.	212
Figure 8.4-1 Parameters to define the asymmetry about the longitudinal axis models	213
Figure 8.4-2 Parameters defining the scale of the second arch with consideration of the inclination between the arches	214
Figure 8.4-3 Representation of the H_I function and its solution.....	217
Figure 8.4-4 Different inclination angles α for 3 and 6 m width W inclined panels	219
Figure 8.4-5 Plan of the models with 50° curvature and 3 m width for the various inclination angles α and corresponding scale of the second arch S	220
Figure 8.4-6 Plan of the models with 50° curvature and 6 m width for the various inclination angles α and corresponding scale of the second arch S	221

Figure 8.4-7 Final shape for 50° curvature models with 3 and 6 m width for the various inclination angles α	222
Figure 8.4-8 Maximum stresses in the warp and fill directions for the different inclinations angles between arches with 3 and 6 m width	223
Figure 8.4-9 Stress distribution in the warp direction and deformed shape under downwards and upwards loadings for inclined panels with 6 m width and 50° curvature and various inclinations between arches (α).....	225
Figure 8.4-10 Stress distribution in the fill direction and deformed shape under downwards and upwards loadings for inclined panels with 6 m width and 50° curvature and various inclinations between arches (α).....	226
Figure 8.4-11 Final shape for models with different arch curvatures θ , with the same width of 3 m and the same inclination angle of 30°	227
Figure 8.4-12 Comparison of maximum stress in the fill direction under upwards loading between models with different arch curvatures, but with the same width and inclination angles	228
Figure 8.4-13 Central transverse section of the models with different arch curvatures θ , but with same width and inclination angle.....	229
Figure 8.4-14 Increase of maximum stress slope for models with different widths for the increasing of inclination angle between arches	230
Figure 8.4-15 Explanation of how to obtain the maximum inclination between arches for the selected model.....	231

Figure 8.4-16 Slope m values for the increase of maximum stress in models with different widths when increasing the inclination angle between arches	232
Figure 8.4-17 Maximum stress under upwards loading in the fill direction with the increase of the curvature of the arch for different widths	233
Figure 8.4-18 Maximum inclination between arches α for various combination of arch curvatures and panel widths.....	235
Figure 8.4-19 Maximum inclination between arches α for various combinations of arch curvatures and panel widths excluding combinations where wrinkle appears.....	236
Figure 8.5-1 Membrane roof of Hatikva Market in Tel Aviv, Israel	237
Figure 8.5-2 Regular panels used for the design example 1	238
Figure 8.5-3 Example 1: 3D view.....	239
Figure 8.5-4 Example 1: interior view	239
Figure 8.5-5 Regular panels used for the design example 2	240
Figure 8.5-6 Example 2: 3D view.....	241
Figure 8.5-7 Example 2: interior view	241
Figure 8.5-8 Regular and curved panels used for examples 3 and 4	242
Figure 8.5-9 Example 3: 3D view.....	243
Figure 8.5-10 Example 3: interior view	244
Figure 8.5-11 Example 4: 3D view	244
Figure 8.5-12 Assumptions for the example 5	245
Figure 8.5-13 Panels chosen for the design example 5.....	246
Figure 8.5-14 Example 5: 3D view of the dome.....	247

Tables

Table 2.2-1 Three categories of eco-friendly spatial structures	17
Table 6.1-1 Zoom into the cable element stiffness matrix chart (organized by Marta Gil Pérez).....	106
Table 6.1-2 Zoom into the membrane element stiffness matrix chart (organized by Marta Gil Pérez).....	107
Table 6.1-3 Zoom into the nonlinear analysis chart (organized by Marta Gil Pérez).....	113
Table 6.1-4 Control data for the input data file.....	116
Table 6.1-5 Macro data for the input data file	118
Table 7.1-1 Membrane properties for the dome.....	135
Table 7.1-2 Valley cable properties for the dome	135
Table 7.1-3 Load combinations for the analysis	141
Table 7.1-4 Deformed shape, stress distribution in warp and fill directions, maximum stress and safety factor (γ) of panel 8.....	144
Table 7.1-5 Deformed shape, stress distribution in warp and fill directions, maximum stress and safety factor (γ) of panel 2.....	145
Table 7.2-1 Membrane properties for the dome.....	153
Table 7.2-2 Valley cable properties for the dome	153
Table 7.2-3 Stress distribution and maximum values of each panel in the warp and fill directions	159
Table 7.2-4 Factor of safety for wind up loading for the two types of	

fabric, Sheerfill-II and Sheerfill-I	159
Table 8.1-1 Membrane properties for the models	165
Table 8.1-2 Load combinations for the analysis	165
Table 8.1-3 Membrane properties for the models	166
Table 8.2-1 Initial stress distribution after form-finding analysis.....	174
Table 8.3-1 Maximum width in the center M for different combinations of opening angles β and arch curvature.....	209
Table 8.4-1 Maximum inclination between arches for different combination of arch curvatures and width.....	234

Notations

Cable element stiffness equation notations

Roman lower and upper case letters

x	Coordinate of any point of the element in the local axis x
X_i	Coordinate of the i node in the global axis X
Y_i	Coordinate of the i node in the global axis Y
Z_i	Coordinate of the i node in the global axis Z
x_i	Coordinate of the i node in the local axis x
X_j	Coordinate of the j node in the global axis X
Y_j	Coordinate of the j node in the global axis Y
Z_j	Coordinate of the j node in the global axis Z
x_j	Coordinate of the j node in the local axis x
A	Cross sectional area
b_1	Derivative of the shape function of node i over axis x
b_2	Derivative of the shape function of node j over axis x
D_{xi}	Displacement of node i in the global x direction
D_{yi}	Displacement of node i in the global y direction
D_{zi}	Displacement of node i in the global z direction
u_i	Displacement of node i in the local x direction
v_i	Displacement of node i in the local y direction
w_i	Displacement of node i in the local z direction
D_{xj}	Displacement of node j in the global x direction

D_{yj}	Displacement of node j in the global y direction
D_{zj}	Displacement of node j in the global z direction
u_j	Displacement of node j in the local x direction
v_j	Displacement of node j in the local y direction
w_j	Displacement of node j in the local z direction
F_{xi}	Force scalar of node i in the global x direction
F_{yi}	Force scalar of node i in the global y direction
F_{zi}	Force scalar of node i in the global z direction
f_{xi}	Force scalar of node i in the local x direction
f_{yi}	Force scalar of node i in the local y direction
f_{zi}	Force scalar of node i in the local z direction
F_{xj}	Force scalar of node j in the global x direction
F_{yj}	Force scalar of node j in the global y direction
F_{zj}	Force scalar of node j in the global z direction
f_{xj}	Force scalar of node j in the local x direction
f_{yj}	Force scalar of node j in the local y direction
f_{zj}	Force scalar of node j in the local z direction
$u(x)$	Generic displacement function in the global X direction
$v(x)$	Generic displacement function in the global Y direction
$w(x)$	Generic displacement function in the global Z direction
l	Length in the X global direction
m	Length in the Y global direction
n	Length in the Z global direction
L	Length of the element
R_{xi}	Residual force scalar of node i in the global x direction
R_{yi}	Residual force scalar of node i in the global y direction

R_{zi}	Residual force scalar of node i in the global z direction
R_{xj}	Residual force scalar of node j in the global x direction
R_{yj}	Residual force scalar of node j in the global y direction
R_{zj}	Residual force scalar of node j in the global z direction
N_i	Shape function of node i
N_j	Shape function of node j
V	Volume

Greek upper and lower case letters

∂	Differential symbol
Δ	Length of the element calculated with the global coordinates of the nodes
$\sigma_{x'}$	Modified stress due to wrinkling
E'	Modified Young's modulus due to wrinkling
ξ	Relationship between Cartesian coordinates and normalized system for the shape function the elements
ε_x	Strain in the local x direction
σ_x	Stress in the local x direction
$\sigma_x^{(0)}$	Stress in the local x direction (initial condition)
∂U	Virtual external work
∂W	Virtual strain energy
E	Young's modulus for the cable material

Roman underlined lower and upper case letters (vectors and matrices)

\underline{K}_E	Elastic stiffness matrix in the global axis
\underline{k}_E	Elastic stiffness matrix in the local axis
\underline{K}_G	Geometric stiffness matrix in the global axis
\underline{k}_G	Geometric stiffness matrix in the local axis
\underline{D}	Global displacement vector of the element
\underline{D}_i	Global displacement vector of the node i
\underline{D}_j	Global displacement vector of the node j
\underline{F}	Global force vector of the element
\underline{F}_i	Global force vector of the node i
\underline{F}_j	Global force vector of the node j
\underline{R}	Global residual force vector of the element
\underline{R}_i	Global residual force vector of the node i
\underline{R}_j	Global residual force vector of the node j
\underline{d}	Local displacement vector of the element
\underline{d}_i	Local displacement vector of the node i
\underline{d}_j	Local displacement vector of the node j
$\underline{f}^{(0)}$	Local force vector (initial condition) of the element
\underline{f}	Local force vector of the element
\underline{f}_i	Local force vector of the node i
\underline{f}_j	Local force vector of the node j
\underline{r}	Local residual force vector of the element
\underline{A}_1	Strain-displacement matrix
\underline{B}	Strain-displacement matrix for large displacement terms
\underline{T}	Transformation matrix
\underline{T}_0	Transformation matrix diagonal terms

Membrane element stiffness equation notations

Roman lower and upper case letters

A_m	Area of the membrane triangular element
e_x, e_y, e_z	Components of the unit vector of the global coordinate system
X_i	Coordinate of node i in the global X direction
Y_i	Coordinate of node i in the global Y direction
Z_i	Coordinate of node i in the global Z direction
X_j	Coordinate of node j in the global X direction
Y_j	Coordinate of node j in the global Y direction
Z_j	Coordinate of node j in the global Z direction
x_j	Coordinate of node j in the local x direction
X_k	Coordinate of node k in the global X direction
Y_k	Coordinate of node k in the global Y direction
Z_k	Coordinate of node k in the global Z direction
x_k	Coordinate of node k in the local x direction
y_k	Coordinate of node k in the local y direction
$u(x, y)$	Displacement function in the x direction
$v(x, y)$	Displacement function in the y direction
$w(x, y)$	Displacement function in the z direction
D_{xi}	Displacement of node i in the global X direction
D_{yi}	Displacement of node i in the global Y direction
D_{zi}	Displacement of node i in the global Z direction
d_{xi}	Displacement of node i in the local x direction
d_{yi}	Displacement of node i in the local y direction
d_{zi}	Displacement of node i in the local z direction

D_{xj}	Displacement of node j in the global X direction
D_{yj}	Displacement of node j in the global Y direction
D_{zj}	Displacement of node j in the global Z direction
d_{xj}	Displacement of node j in the local x direction
d_{yj}	Displacement of node j in the local y direction
d_{zj}	Displacement of node j in the local z direction
D_{xk}	Displacement of node k in the global X direction
D_{yk}	Displacement of node k in the global Y direction
D_{zk}	Displacement of node k in the global Z direction
d_{xk}	Displacement of node k in the local x direction
d_{yk}	Displacement of node k in the local y direction
d_{zk}	Displacement of node k in the local z direction
F_{xi}	Force scalar of node i in the global X direction
F_{yi}	Force scalar of node i in the global Y direction
F_{zi}	Force scalar of node i in the global Z direction
f_{xi}	Force scalar of node i in the local x direction
f_{yi}	Force scalar of node i in the local y direction
f_{zi}	Force scalar of node i in the local z direction
F_{xj}	Force scalar of node j in the global X direction
F_{yj}	Force scalar of node j in the global Y direction
F_{zj}	Force scalar of node j in the global Z direction
f_{xj}	Force scalar of node j in the local x direction
f_{yj}	Force scalar of node j in the local y direction
f_{zj}	Force scalar of node j in the local z direction
F_{xk}	Force scalar of node k in the global X direction
F_{yk}	Force scalar of node k in the global Y direction

F_{zk}	Force scalar of node k in the global Z direction
f_{xk}	Force scalar of node k in the local x direction
f_{yk}	Force scalar of node k in the local y direction
f_{zk}	Force scalar of node k in the local z direction
X, Y, Z	Global coordinate system
h_m	Height of the membrane triangular element
x, y, z	Local coordinate system
i	Node located in the local coordinate system origin (0, 0, 0)
k	Node located in the plane x-y of the local coordinate system (0, x_k , y_k)
j	Node located in the x axis of the local coordinate system (x_j , 0, 0)
R_{xi}	Residual force scalar of node i in the global X direction
R_{yi}	Residual force scalar of node i in the global Y direction
R_{zi}	Residual force scalar of node i in the global Z direction
R_{xj}	Residual force scalar of node j in the global X direction
R_{yj}	Residual force scalar of node j in the global Y direction
R_{zj}	Residual force scalar of node j in the global Z direction
R_{xk}	Residual force scalar of node k in the global X direction
R_{yk}	Residual force scalar of node k in the global Y direction
R_{zk}	Residual force scalar of node k in the global Z direction
u_x, u_y, u_z	Second row terms of the transformation matrix of one direction or node
N_1, N_2, N_3	Shape function vector terms
a_1	Terms of the geometry matrix inverse, first row
b_1, b_2	Terms of the geometry matrix inverse, second row
c_1, c_2, c_3	Terms of the geometry matrix inverse, third row

v_x, v_y, v_z	Third row terms of the transformation matrix of one direction or node
V	Volume of the membrane triangular element

Greek upper and lower case letters

$\alpha_1, \alpha_2, \alpha_3$	Coefficients for the displacement function $u(x, y)$ in the x direction
$\beta_1, \beta_2, \beta_3$	Coefficients for the displacement function $v(x, y)$ in the y direction
$\gamma_1, \gamma_2, \gamma_3$	Coefficients for the displacement function $w(x, y)$ in the z direction
∂	Differential symbol
$\lambda_x, \lambda_y, \lambda_z$	First row terms of the transformation matrix of one direction or node
$\tau_{xy}^{(0)}$	Initial stress in the local x-y plane
$\sigma_x^{(0)}$	Initial stress in the local x direction
$\sigma_y^{(0)}$	Initial stress in the local y direction
ν	Poisson's ratio of the membrane
γ_{xy}	Strain in the local x-y plane
ϵ_x	Strain in the local x direction
ϵ_y	Strain in the local y direction
τ_{xy}	Stress in the local x-y plane
σ_x	Stress in the local x direction
σ_y	Stress in the local y direction
E_m	Young's modulus of the membrane

Roman and Greek underlined lower and upper case letters (vectors and matrices)

$\underline{\alpha}$	Coefficient vector for the displacement function $u(x, y)$ in the x direction
$\underline{\beta}$	Coefficient vector for the displacement function $v(x, y)$ in the y direction
$\underline{\gamma}$	Coefficient vector for the displacement function $w(x, y)$ in the z direction
\underline{X}_i	Coordinate vector of the i node in the global system
\underline{X}_j	Coordinate vector of the j node in the global system
\underline{X}_k	Coordinate vector of the k node in the global system
\underline{D}	Displacement vector of the element in the global coordinate system
\underline{d}	Displacement vector of the element in the local coordinate system
\underline{d}_x	Displacement vector of the element in the local x direction
\underline{d}_y	Displacement vector of the element in the local y direction
\underline{d}_z	Displacement vector of the element in the local z direction
\underline{D}_i	Displacement vector of the node i in the global coordinate system
\underline{d}_i	Displacement vector of the node i in the local coordinate system
\underline{D}_j	Displacement vector of the node j in the global coordinate system
\underline{d}_j	Displacement vector of the node j in the local coordinate system
\underline{D}_k	Displacement vector of the node k in the global coordinate system

	system
\underline{d}_k	Displacement vector of the node k in the local coordinate system
\underline{E}	Elastic matrix for the stress-strain relationship
\underline{K}_E	Elastic stiffness matrix in the global axis
\underline{k}_E	Elastic stiffness matrix in the local axis
\underline{F}	Force vector of the element in the global coordinate system
\underline{f}	Force vector of the element in the local coordinate system
\underline{f}_x	Force vector of the element in the local x direction
\underline{f}_y	Force vector of the element in the local y direction
\underline{f}_z	Force vector of the element in the local z direction
\underline{F}_i	Force vector of the node i in the global coordinate system
\underline{F}_j	Force vector of the node j in the global coordinate system
\underline{F}_k	Force vector of the node k in the global coordinate system
\underline{K}_G	Geometric stiffness matrix in the global axis
\underline{k}_G	Geometric stiffness matrix in the local axis
$\underline{\Phi}$	Geometry matrix of the element
$\underline{f}^{(0)}$	Initial force vector of the element in the local coordinate system
$\underline{\sigma}^{(0)}$	Initial stress vector of the element
\underline{R}	Residual force vector of the element in the global coordinate system
\underline{r}	Residual force vector of the element in the local coordinate system
\underline{R}_i	Residual force vector of the node i in the global coordinate system

\underline{R}_j	Residual force vector of the node j in the global coordinate system
\underline{R}_k	Residual force vector of the node k in the global coordinate system
\underline{N}	Shape function vector of the element
$\underline{B}, \underline{C}$	Strain-displacement matrices corresponding with the large displacement
$\underline{A}_1, \underline{A}_2, \underline{A}_3$	Strain-displacement matrices rows corresponding with the small deflection
\underline{A}	Strain-displacement matrix corresponding with the small deflection
$\underline{\varepsilon}$	Strain vector of the element
$\underline{\sigma}$	Stress vector of the element
\underline{T}	Transformation matrix
\underline{T}_n	Transformation matrix of one direction or node (diagonal components of the total transformation matrix)
\underline{i}	Unit vector in the local x direction defined with global coordinates
\underline{j}	Unit vector in the local y direction defined with global coordinates
\underline{k}	Unit vector in the local z direction defined with global coordinates
\underline{e}	Unit vector of the global coordinate system
\underline{a}	Vector defining \vec{i}_j in the global coordinate system
\underline{b}	Vector defining \vec{i}_k in the global coordinate system

Barrel vault shaped membranes notations

Roman and Greek lower and upper case letters

s	Arch length
r	Radio of curvature of the arch
C	Span of the panel
C_1	Span of the smallest arch in inclined panels
C_2	Span of the largest arch in inclined panels
W	Width of the panel
W_1	Width of the shortest side in curved panels
W_2	Span of the longest side in curved panels
H	Height of the arch in the center
H_1	Height of the smallest arch in the center in inclined panels
H_2	Height of the largest arch in the center in inclined panels
h	Height difference between the two arches in inclined panels
M	Width in the middle of the panel in curved panels
α	Inclination angle between arches in inclined panels
β	Opening angle in curved panels
θ	Arch curvature
S	Scale of the largest arch in inclined panels when the smallest arch scale is considered equal to one

Chapter 1. Introduction

In a mathematical definition, space is a set of elements or points satisfying specified geometric postulates, but also it is the infinite extension of the three-dimensional region in which all matter exists. From this terminology, it is considered that a spatial structure is the one that can cover a long-span space with a light weight structure.

The shape of structures such as thin concrete shells, grid-shells with steel structure or cable structures including membranes varies from regular geometries, with intrinsic symmetries, as revolution surfaces, to free structures, covering a wide range of possibilities. The mechanical behavior, as well as other physical performances, related to acoustics, energy, light control, weight, etc. are all strictly depending on the shape of the structure, both at the global level and at the local level. For this reason, the structural design takes a greater importance rather than the architectural design, and very specific and technical knowledge is needed in order to perform a good optimization of the structure. It has to be considered that a finite number of parameters must be defined to represent the global shape, paying attention to the fact that when a few parameters are used, only a small subset of solutions is considered, while with many parameters, the process becomes time consuming.

Spatial structure refers to innovative long-span structural systems, primarily roofs and enclosures to house human activities. More specifically, they include many types of structures, such as: space frames or grids; cable-and-strut and tensegrity; air-supported or air-inflated structure; self-erecting and deployable structure; cable net; tension membrane; geodesic domes; folded plates; and thin shells. Tall buildings and long-span bridges are excluded because both of them are addressed separately (Bradshaw et al. 2002).

Therefore, a lightweight structure is defined by the optimal use of material to carry external loads or prestress. Material is used optimally within a structural member if the member is subjected to tensile forces rather than bending. The objective of an optimization procedure to determine layout and shape of a lightweight structure is, therefore, to minimize bending or to minimize the strain energy rather than structural weight (Bletzinger & Ramm 2001).

In particular, membrane structures are one of spatial structures that allow for long span and light weight roofs. In many cases, the membrane roofs are supported by trusses, arches or masts and prestressed together with cables to obtain a resistant shape for a given loading condition. Membrane fabrics are lightweight ($0.7\text{--}1.3 \text{ kg/m}^2$), waterproof and have negligible bending and compression stiffness. By ensuring that the fabric membrane remains in tension at all times, these materials can act as both structure and cladding, efficiently covering large areas, most notably for airports, pavilions or sports stadium.

The shape of the membrane dome is related to its ability to resist all applied loads in tension. To resist both uplift and downward forces the surface of the membrane must be double-curved (with anticlastic curvature) and prestressed. Boundary conditions determine the fabric shape and stress distribution; ideally a uniform prestress is applied to the fabric. Consequently, to achieve a uniform prestress the fabric must take the form of a minimal surface. This means that the surface joins the boundary points with the smallest possible membrane area and has uniform in-plane tensile stresses (Bridgens & Birchall 2012).

Optimization and search algorithms in combination with various analysis procedures have been used to generate spatial structures that are especially capable of responding, for example, to structural, constructional or acoustical demands. These methods serve virtually the same purpose, to gather specific information in a large space of possibilities.

In the case of simulation software, the input they need is too elaborate for the concept stages. That means that in projects with high technical requirements, for economic and time constraints, the designer is forced to consider very few alternatives to shorten the early design phase and to try and make the best out of it in later stages (the traditional optimization process). In the case of optimization algorithms the problem with them lies in the manner in which they have been traditionally used, the way they are formulated, and the focus given to them.

Traditionally, optimization algorithms are left for the final stages, when the technical issues of the project are usually taken into account. However, in the final stages of design, many decisions in many different fields have already been made, and changes in the project can easily conflict with previous decisions. Then, the search space of this optimization algorithm is very small and that limits the possibility of innovation. For all of that, the creation of tools and design criteria that can introduce optimal solutions to diverse and perhaps contrasting technical issues in the early design phase, without hindering creativity, should be proposed (Mendez Echenagucia & Sassone 2012).

This thesis covers the numerical analysis and design of tensile membrane and cable structures. For that, broad definition and explanation about spatial structures and in particular membranes and cables are given. Then, the detailed procedure for the design and analysis of those is introduced. Finally, two case studies and a parametric study on barrel vault shaped membranes are described. In this way, the chapters are distributed as follows:

Chapter 2 covers the Review of Spatial and Tensile Structures. It begins with the spatial structure definition and classification from different points of view. After that, some examples of environmental compatible aspects of spatial structures are given. And then, it focuses more on tensile structures and introduce the historical development of those, going through the research and work of Frei Otto and Horst Berger and finishing with some case studies and current constructions.

Chapter 3 is about the Design Considerations for Tensile Structures. In this chapter a more detailed explanation about the characteristics and properties of tensile structures, including the basic forms, types of curvature and fabric material properties. Afterwards, the design procedure is described and the analysis steps are also shown; form finding analysis, stress deformation analysis and patterning and construction. And finally, more information is given about loading conditions and safety approach for tensile structures.

Chapter 4 explains the purpose of research of this thesis.

Chapter 5 covers the Development of Geometrically Nonlinear Finite Element Equations. The nonlinear equations to find the stiffness matrix for both cable and membrane elements are presented.

In Chapter 6 the Nonlinear Analysis and Modeling of Tensile Structures is described. This includes the non-commercialized software used for this research including charts, required input data and obtained output data, and some application examples. Then, the modeling of membrane and cable elements is shown with detailed specifications.

Chapter 7 develops two case studies. The first one is about the membrane dome of the Seoul Southwestern Baseball Stadium and the second one about Jeju World Cup Stadium dome. In both of them, all steps for the modeling and analysis are described, and results for displacements, stress and safety factors are shown. Conclusions for this case studies are also given.

In Chapter 8, a parametric study of barrel vault shaped membranes is described. It begins with the assumptions for the study that are based on the case studies described in the previous chapter. Then, the parameters related to the regular barrel vault shaped membranes are analyzed in detail. After that, one grade of irregularity is also introduced to have more variety of design possibilities. And finally, some design examples are shown as possible applications of this study.

Finalizing, Chapter 9 discusses the conclusion of this research.

Chapter 2. Review of Spatial and Tensile Structures

2.1. Spatial structure classification

As explained in the previous chapter, the common characteristic of spatial structures is that they are light-weight and can cover long-span areas. Most examples are found in stadiums, music pavilions, exhibition halls, airports, and so on.

There are many ways to classify spatial structures. In this chapter, two classifications are explained. In the first one, spatial structures are classified depending on the structural system they use. With this initial classification it is easier to know the full structural systems thought of spatial structures and the way they work. In the second classification, an additional synthesized approach is introduced to clarify the ideas.

2.1.1. Classification by structural system

From the classification shown in Fig. 2.1-1, it is possible to distinguish three main kinds of spatial structures relying on the various structural systems they use. In the case of form-active structural systems,

structures like cable, tent or membrane, and arch structures have a single stress condition composed by compressive or tensile forces; the forces act principally through the fabric form.

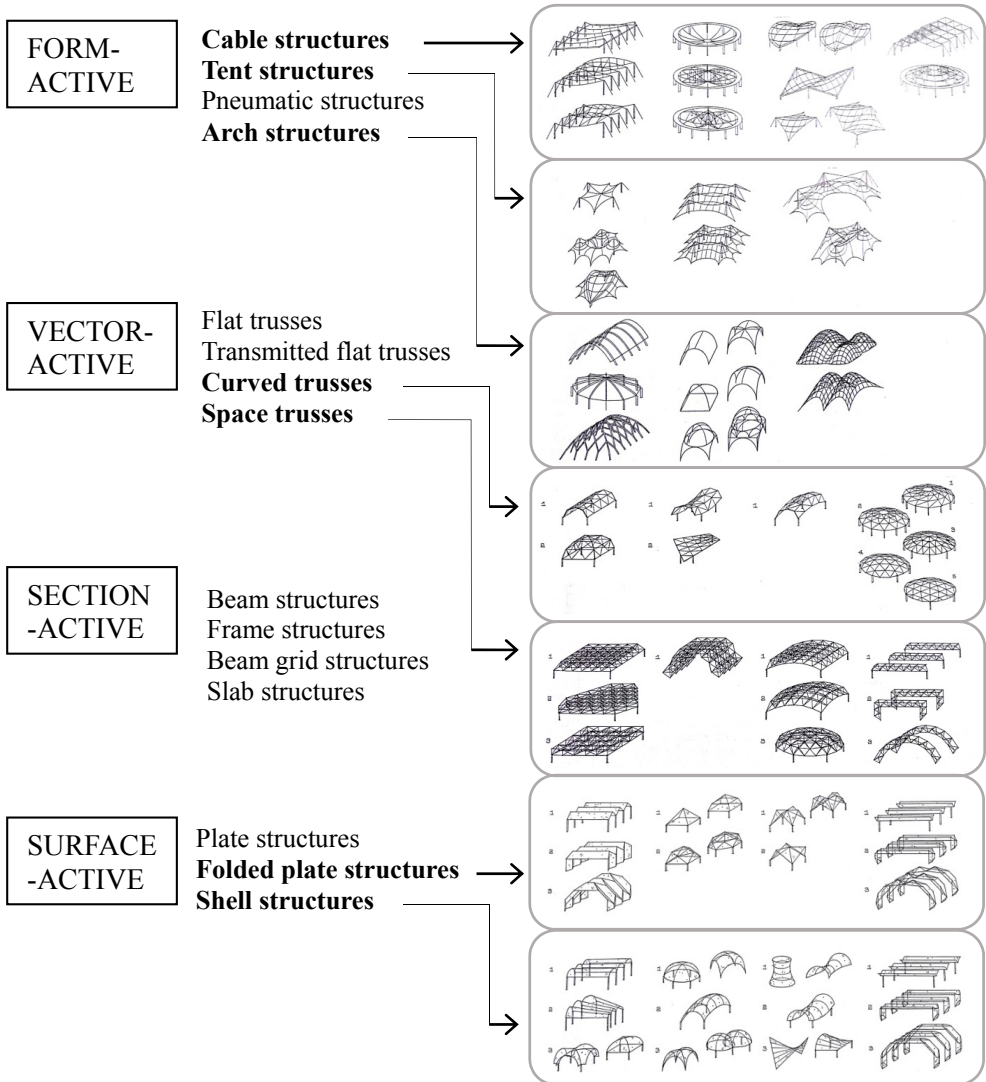


Figure 2.1-1 Spatial structures classification (reinterpretation) (Engel 1981)

The vector-active structural systems induce structures like curved or space trusses where both compressive and tensile forces act through the composition of the members. Finally, on the surface-active structure systems the forces act through the extension and form of the surface, like it happens in folded plate or shell structures (Engel 1981).

2.1.1.1. Form-active structural systems

Form-active structural systems are flexible and non-rigid structural systems secured by fixed ends, in which the redirection of forces is accomplished through explicit form design and characteristic form stabilization.

Distinction of the form-active structural systems is that they redirect external forces by simple normal stresses: the arch by compression, the suspension cable by tension. Form-active structural systems develop at their ends horizontal stresses. The reception of these stresses constitutes a major problem in designing form-active structural systems. The 'natural' stress line of the form-active compression system is the funicular pressure line, or in the form-active tension system the funicular tension line.

Any change of loading or support conditions changes the form of the funicular curve and causes a new structural form. In the case of the load cable, it assumes by itself a new tension line under new loads, but the arch must compensate the changed pressure line with stiffness. Since the suspension cable under different loading changes its form, it is always the funicular curve for the existing load. On the other hand the

arch, since it cannot change its form, can be funicular only for one certain loading condition. Because of their dependence on loading conditions, these structures are strictly governed by the discipline of the 'natural' flow of forces and hence cannot become subject to arbitrary free form design.

The form-active structural systems are the suitable mechanisms for achieving long spans and forming large spaces. Since form-active structural systems disperse loads in the direction of resultant forces they are in effect and essence linear girders. This is true also for cable nets, membranes or lattice domes in which the loads, though being dispersed in more than one axis, are still transferred in a linear way because of lack of shear mechanism.

Form-active qualities can be brought to bear on all other structural systems. Especially in surface-active structural systems they are an essential constituent for the functioning of the bearing mechanism (Engel 1981).

2.1.1.2. Vector-active structural systems

For the vector-active structural system, compressive and tensile members in triangular assemblage form a stable composition complete in itself, that, if suitably supported, receives asymmetrical and changing loads and transfers them to the ends. Those compressive and tensile members, arranged in a certain pattern and put together in a system with hinged joints, form mechanisms that can redirect forces and can transmit loads over long distances without intermediate supports.

Distinction of vector-active structure systems is the triangulated assemblage of straight-line members.

Redirection of forces can be also accomplished both in curved planes or three-dimensional directions. By arranging the members in single or doubly curved planes the advantage of form-active redirection of forces is integrated and thus a cohesive load-carrying and stress resisting mechanism is set up: curved truss system.

The mechanism of vector-active redirection of forces can be applied also to other structural systems, especially if these, because of dead weight increase, have reached the limits of feasibility. Thus arches, frames, or shells can also be designed as trussed systems (Engel 1981).

2.1.1.3. Surface-active structural systems

In the case of surface-active structural system, surfaces, finite and fixed in their form, are instrument and criterion in space definition. If given certain qualities, they can perform load-bearing functions: structural surfaces. Without additional help they can rise clear above space while carrying loads. Structural continuity of the elements in two axes, along with surface resistance against compressive, tensile, and shear stresses, are the first pre-requisites and first distinctions of surface-active structures.

While in horizontal structural surfaces the bearing capacity under gravitational load decreases with increasing surface (slab mechanism), in vertical structural surfaces the bearing capacity increases together

with the surface expansion (plate mechanism). Through inclining the surface toward the direction of the acting force by means of folding or curving, it is possible to reconcile the opposites of horizontal efficiency in the coverage of space and vertical efficiency in the resistance against gravitational forces (Engel 1981).

2.1.2. Spatial structures synthesized classification

After describing the different structural systems that spatial structures can present, it is possible to synthesize the classification into a simpler one. Therefore, in the classification represented in Fig. 2.1-2, spatial structures can be divided between continuous and discrete systems and hard and soft structures.

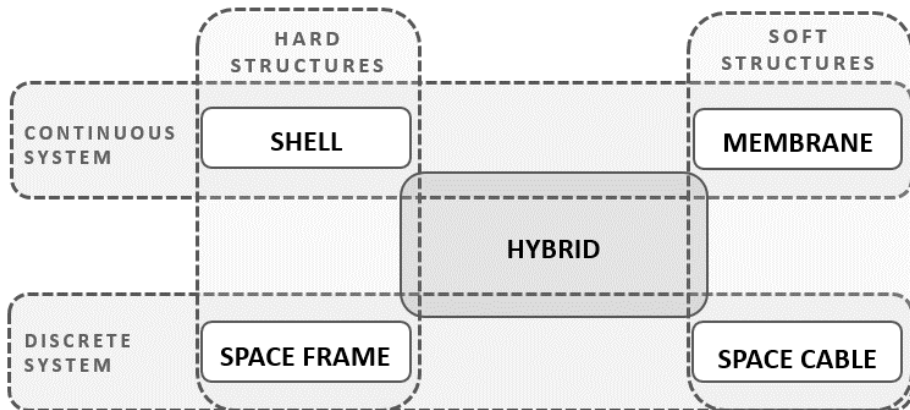


Figure 2.1-2 Spatial structures synthesized classification

By doing this, and also following the examples shown in Fig. 2.1-3, shells are hard structures with a continuous system, normally made of concrete. Space frame are also hard structures but with a discrete system, normally steel trusses. Besides, in a similar way, there are soft structures, membranes with a continuous system and space cables with a discrete system. Besides, the combination of any of them will be considered a hybrid structure.

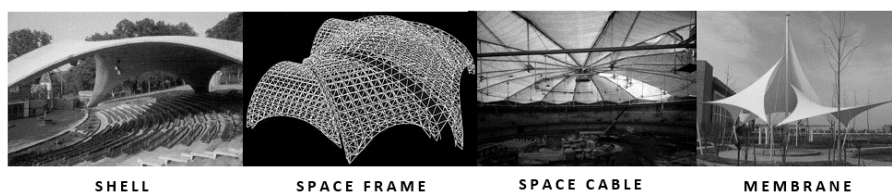


Figure 2.1-3 Types of spatial structures

Following the previous classification of structural systems, these spatial structures can be also categorized into three groups based on the method by which they resist the loads: compression structures (shells); tension structures (tension fabric, air-supported, air-inflated, tensegrity, and cable-net structures); and tension/compression reticulated structures (space grids or frames and geodesic domes) (Bradshaw et al. 2002).

Tension or tensile structures are the target of this study so a further explanation in the definition, history, materials and design will be described in the following sections.

2.1.2.1. Hybrid structures

As explained before, in many cases, spatial structures do not follow just one specific structural system but they can be composed of combinations of them, and they are called hybrid structures.

The variety of possible structures created by the combination of structural system is very wide and it is still a field under development. Some examples of those structures could be the following ones.

There is at least a dozen of air-supported membrane structures used for gymnasium, tennis court or warehouses. The building is usually in barrel shape with semi-spheres at two ends. The transverse span is in the range of 30 to 70 m with a large height. By adjusting the shape of the membrane, pressing of the stiffening cables and increasing the inner air pressure, the membrane structure can resist the effect of rain, snow and wind effectively (Lan 2012).

Another field of wide application of cables is hybrid structures named “Structure with Tensioning Chord” or “String Structures”. The upper chord is usually formed by arch-shaped lattice truss with single-plane or triangular section. By pre-tensioning the lower chord cables, the lattice truss with intermediate struts act integrally with lower cables and then resist much more loads.

For structures with tensioning chord, the upper chord may also be arranged in two ways. The construction is complicated by the curved configuration of the roof and different types of connecting nodes. In

addition to the assembly of a large number of members of the lattice grids, it is also necessary to pretension the chord cables.

For buildings with circular or elliptical plan, if a lattice shell is served as the upper chord, then “Lattice Shell with Tensioning Chord” or “Suspend-Dome” is obtained.

A “Single-layer Kiewit” type lattice shell is used as the upper chord combined with three courses of ring cables. Compared with ordinary lattice shell, the stability of the structure will increase to a large extent. The forces in the members will be about only 1/3 of the original shell and display more even distribution. The horizontal thrusts at the support are also decreased.

A surface net is defined as a hybrid system that combining the behavior and characteristics of a surface component assembly with those of a pre-stressed cable net. Based on the established knowledge in cable nets, surface nets take the discourse one step forward by integrating surface components. Considering that the form of nets relates to the forces acting upon them it is evident that the design of such systems cannot be disconnected from the structural strategy adopted (Symeonidou 2012).

Another type of hybrid structures are the called deployable structures. One example of them are the “umbrellas”. The closing (opening) function of the umbrellas mainly serves to protect pedestrians from direct sunlight during the day, with the umbrellas fully open (deployed), and to radiate heat stored during the day up to the night sky, when the umbrellas are fully closed (stowed) overnight.

The umbrella closing/opening mechanisms are realized by hinged arm segments (folding/unfolding) and/or by telescope arm segments (retraction/extension) as shown in Fig. 2.1-4.

The closing (opening) processes of large umbrella structures are influenced by the initial shape of the suspended membrane, by the nature and sequence of the kinematical umbrella folding/unfolding and



Figure 2.1-4 Quasi-static folding simulation (ESI France) (Haug et al. 2012)

retraction/extension mechanisms; by the self-weight of the membrane; by suspension and guidance elements to control the folds; by collision-contact events of the membrane material itself and with the surrounding structural components; by the folding-retraction (unfolding-extension) speed; and, in the final stage of stowing (un-stowing), by the flexural stiffness of the severely folded and compressed membrane and its reinforcing belts and cables (Haug et al. 2012).

2.2. Environmentally compatible aspects of spatial structures

When spatial structures are used as multiuse facilities covering huge spaces such as dome stadiums or concert halls, they can shelter many people at the same time and might use lots of energy temporarily. For this reason, it is encouraged to implement aspects of environmental compatibility for better energy efficiency. The following chart (Table 2.2-1) shows 3 overall categories and the different strategies or methods for developing a more eco-friendly spatial structure.

Table 2.2-1 Three categories of eco-friendly spatial structures

Energy saving	Indoor comfort	Material saving / recycling
Insulation (use of ETFE) Renewable energy (solar & geothermal power) Heat exchanger Free cooling (using outdoor air) Light control Cogeneration	Natural lighting Natural ventilation Less chemical materials	Rainwater usage Recycle water usage Underground water usage Reduced self-load Less material usage Reduced CO ₂ emissions Recyclable building skin

In the case of membrane structures, translucent fabrics further define the character of the spaces they enclose by bringing in daylight. High reflectivity and low absorption of heat greatly moderate the interior climate. In addition, the surface geometry, together with characteristics of

the fabric or of an inner liner control the acoustics in the space. The sound dissipating geometry of tent shapes combined with the sound absorbing surface of the inner liner acts as a ‘black hole’ for internal sound (Berger 1999).



Figure 2.2-1 Eden project (Knebel et al. 2002) (left) and Great glasshouse of national botanic garden of Wales (Ali-Nezhad & Eskandari 2012) (right)

Here are introduced a few examples that incorporate the eco-friendly aspect of spatial structures. The Eden project is a series of biomes indoor gardens covered by domes that consist of hundreds of hexagonal and pentagonal, inflated, plastic cells supported by steel frames (Fig. 2.2-1 left). The foil material used in this spatial structure allows much more UV light to pass into the domes and also provides good heat insulation. Besides, it minimized the weight and amount of steel needed for the construction reducing also the amount of CO₂ emitted to the atmosphere (Knebel et al. 2002).

A similar example of energy efficiency is the great glasshouse of the national botanic garden of Wales where the aluminum glazing system and its tubular-steel supporting structure are also designed to reduce materials and maximize light transmission (Fig. 2.2-1 right). In addition, to optimize

energy usage, indoor and outdoor conditions are monitored by a computer-controlled system (Ali-Nezhad & Eskandari 2012).

In the Park dome stadium, the dome is constructed with a double pneumatic-film structure (Fig. 2.2-2 left). The design utilizes and conserves natural energy by a swirl flow natural ventilation system, underground thermal tunnel and underground heat storage air-conditioning system using reduced-rate night time electric power (Sakai et al. 1999). In the case of the Millennium Dome, the membrane is being supported by a dome-shaped cable network from twelve king posts (Fig. 2.2-2 right). A water-cycle project was developed with the roof surface of the building, becoming one of the largest recycling schemes in Europe. It is designed to supply up to 500 m³/day of reclaimed water (Hills et al. 2002) .



Figure 2.2-2 Park dome (Sakai et al. 1999) (left) and Millennium dome (Hills et al. 2002) (right)

2.3. Historical development of tensile structures

Tensile structures include a wide variety of systems that are distinguished by their reliance upon tension only members to support load. They have been employed throughout recorded history as in rope bridges and tents. However, large permanent tensile structures of bridges and buildings were generally developed during the 19th century development in bridges and the 20th century respectively.

The design of large tension membranes has been fully dependent upon the use of computers. Many of the developments in membranes have occurred in the last 30 years, precisely because of the accessibility of powerful computers. The pioneering work of Frei Otto was accomplished using physical models, which, while they well illustrated the desired form of a membrane, are not conducive to the precise determination of the membrane's structural characteristics in a manner necessary for the construction of large complex systems (Bradshaw et al. 2002).

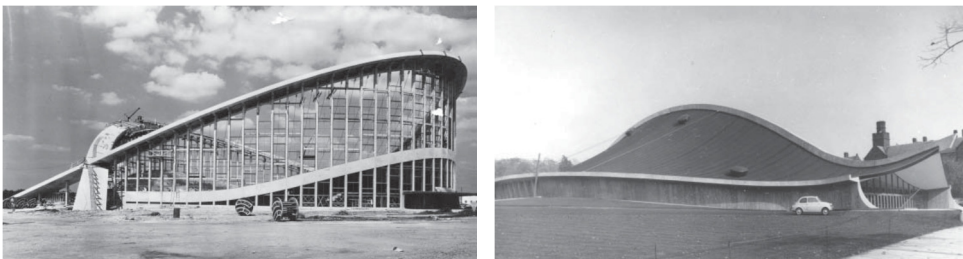


Figure 2.3-1 J. S. Dorton Arena Pavilion in Raleigh, North Carolina (left) and the Yale University hockey rink, New Haven, Connecticut (right) (Fang 2009)

Architectural membrane systems were a natural extension of tension structures of the 1950s and 1960s for long-span buildings. Fred Severud demonstrated the long-span potential of tension structures in benchmark projects such as the J. S. Dorton Arena Pavilion in Raleigh, North Carolina and the Yale University hockey rink, New Haven, Connecticut (Fig. 2.3-1). Severud's engineering practice was the incubator of membrane structure design in the United States.

In particular, the J. S. Dorton Arena, Fig. 2.3-1 (left), designed by architects William Deitrick, Matthew Nowicki, and engineer Fred Severud, is often cited as the first modern, large-scale, cable-net structure. The famous saddle-shaped roof is composed of a set of upwardly-curved cables, which intersect with perpendicular downwardly-curved cables. The upward cables span approximately 95 meters between two intersecting and inclined parabolic arches. The cable-net roof supports a more traditional roof consisting of rigid insulation and corrugated steel sheets, and creates a 30 meter diameter column-free plan. This structure is said to have inspired Frei Otto to pursue the study of cable-net structures after visiting Severud's New York office as a student (Fang 2009).

Designers of subsequent tension membranes included David Geiger, Horst Berger, Paul Gossen, Edmund Happold and Frei Otto.

Horst Berger and David Geiger worked together between 1969 and 1984. While Geiger's interest in membrane structures was for their structural efficiency and economy, Berger did much to demonstrate the aesthetic potential of tension membrane forms in architecture. Together, they

developed analysis and design tools and techniques indispensable in the design, documentation, and construction of complex tension structures.

Going through the work of Frei Otto and Horst Berger it is possible to have a broader view of the development of this kind of structures and the existing types.

2.3.1. Frei Otto and the natural forms

Frei Otto developed and built the most important basic shapes of modern tent construction: the simple four-point tent in Kassel in 1955, the peak tents in Lausanne, the arch-supported tent in Cologne in 1957, and finally the hump tents in Berlin (Otto & Rasch 1996).

The crucial factors in tent construction are the shape of the membrane surface and the type of support. The membrane must exhibit a sufficient degree of anticlastic curvature to allow the transfer of external loads such as snow and wind without causing excessive deformation. The support structure and structure of the edges must obey certain laws to avoid producing areas of excessive tension and causing the membrane to tear.

The membrane must be prestressed to allow the flexible, extremely thin material to serve as a sufficiently rigid load-bearing structure. The shape of the membrane is the primary factor. It is the shape that determines the action of the membrane and the flow of the forces.

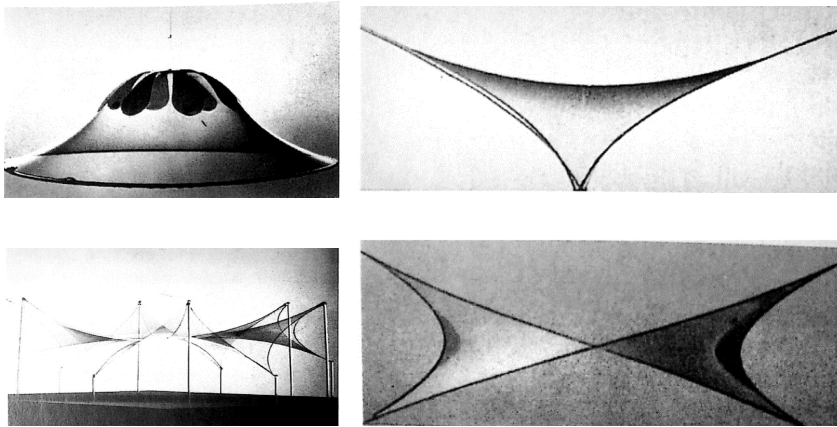


Figure 2.3-2 Frei Otto soap film experiments (Otto & Rasch 1996)

In his experiments with soap films (Fig. 2.3-2), Frei Otto discovered a method of creating membrane surfaces in his models. The resultant membrane has specific physical and geometrical properties. The forces acting between the individual molecules in the membrane always cause the soap film to assume a shape in which the surface tensions are equal at every point and in every direction. A soap film is anticlastic at every point of its surface. The two main radii of curvature are equal in magnitude at every point.

This means that the shape of the soap film represents an equilibrium form for a state of prestress which is equal in all directions and constant over the entire surface of the film. Additionally, the surface formed by a soap film is the surface which encloses the smallest possible area within a closed space curve. Thus the surface of a soap film is termed a minimal surface (Otto & Rasch 1996).

The following tent types may be distinguished according to the construction of their edges and supports. With this classification, Frei Otto defined the basic shapes of membrane structures.

2.3.1.1. The four-point tent

The four-point tent is a basic, elementary tent shape (Fig. 2.3-3 left and center). A saddle-shaped membrane is stretched between two high and two low points placed diagonally opposite each other. Edge cables absorb the forces of the membrane. The geometry of the edges forms autonomously, depending on the length of the threads.

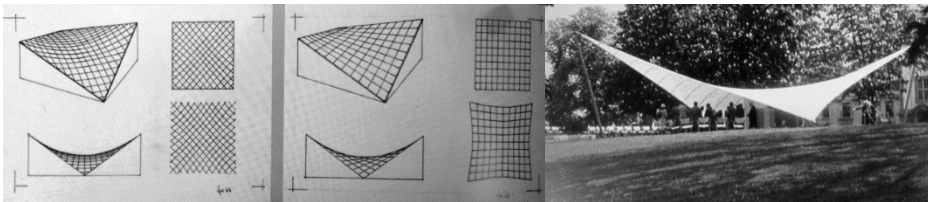


Figure 2.3-3 For-point tent, woven diagonally to the base area (left), woven parallel with the edges of the base area (center) and Music Pavilion at the 1955 Federal Exhibition in Kassel (right) (Otto & Rasch 1996)

The Music Pavilion at the 1955 Federal Exhibition in Kassel (Fig. 2.3-3 right) is one of the first tent structures that Frei Otto brought to construction. As the primary stresses and curvatures are of equal magnitude in both directions, the roof is termed a minimal surface. The fabric strips diagonally to the edges and followed the direction of maximum curvature. Two guyed masts of pinewood and two anchor bolts were used to anchor the high and low points respectively. 16 mm

steel cables sewn into the edges of the membrane created the required prestress and transferred the membrane forces into the stress points.

2.3.1.2. *The Peak tent*

The Peak tent is supported by a mast at a single point within the membrane surface. As it is impossible to support a membrane at a single point, the forces of the membrane are gathered along specific lines and then directed to the tip of the mast as it is possible to see in Frei Otto's form finding studies in Fig. 2.3-4 (left). This is done by means of valley reinforced by cables or straps, by a ridge cable, a cable loop, a so-called eye, or a series of several eyes.

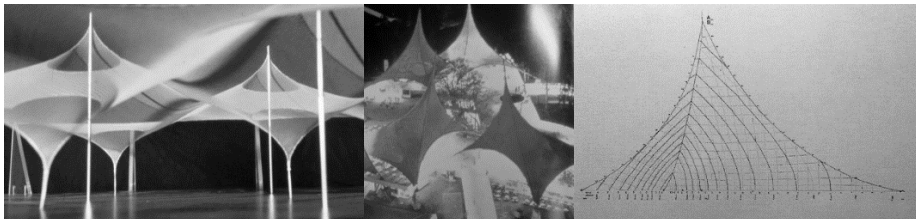


Figure 2.3-4 Form finding study, high and low points with cable loops (left), Swiss Regional expo 1964 in Lausanne (center and right) (Otto & Rasch 1996)

As a constructed example of the peak tent, Fig. 2.3-4 (center and right) illustrates the Swiss Regional expo 1964 in Lausanne “neige et rocs” tent. Each tent consists of two linked two-up, two-down saddle shapes, one of which is additionally subdivided into two triangular surfaces by a ridge cable. In order to achieve a sufficient curvature in the large tent surfaces, the cable net rises tangentially towards the tips of the masts, which are up to 24 m high. The longest ridge cables are 36 m in length and are guyed to the tops of man-high concrete bases. In this way, the

pavilion can be linked to one another without causing the visitors to trip over the guy cables.

2.3.1.3. *The arched tent*

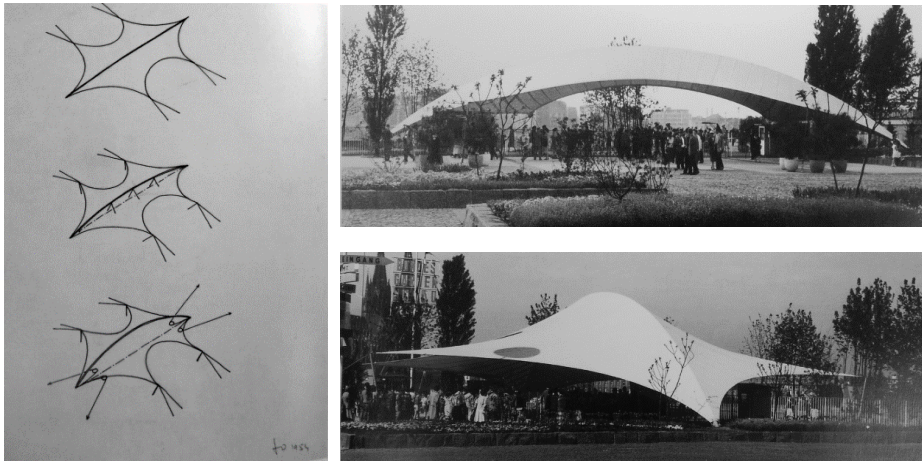


Figure 2.3-5 Arched tent and the entrance of the Federal Garden Exhibition (Otto & Rasch 1996)

The arched tent is supported by a compression arch (Fig. 2.3-5). The membrane stretches across the arch or is secured along the arch by a ridge cable or a series of eyes. The membrane can help to stabilize the arch.

The Federal Garden Exhibition in Cologne 1957 (Fig. 2.3-5) is a shallow arch spanning 34 m and supporting a PU-coated membrane made of fiber-glass. The arch consists of a steel tube with only 17 mm in diameter, which rests on hinged supports. The arch is stabilized and kept in position by the membrane. The membrane is guyed outwards by means of edge cables and mast to create a wide, spreading canopy.

2.3.1.4. *The hump tent*

The hump tent is supported by one or more hump-like high points (Fig. 2.3-6 left). The high points can be formed by mast which may have either mushroom-shaped heads or heads with flexible lamellae across which the membrane is stretched.

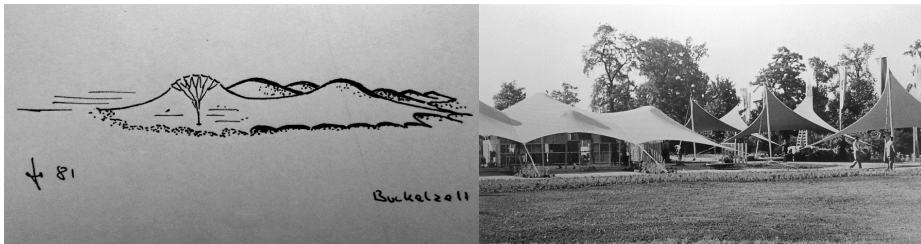


**Figure 2.3-6 Hump tent (left) and canopy of the Interbau café in Berlin (right)
(Otto & Rasch 1996)**

The canopy of the Interbau café in Berlin (Fig. 2.3-6 right) is one example of hump tent. A star-shaped wooden leaf springs form the high points which are prestressed from below against the 24 m x 28 m membrane by hydraulic presses. The membrane is guyed outwards by means of edge cables. The membrane exhibits an anticlastic curvature everywhere except in the areas above the supporting humps, where its curvature is equidirectional. The gentle curvatures make it possible to achieve an anticlastic shape simply by changing the angles between the meshes, using a cloth which was originally flat and not cut to a special pattern.

2.3.1.5. Hybrids and variations

In addition to these basic tent shapes, any combination of hybrid shapes is possible as shown in the drawings of Frei Otto in Fig. 2.3-7. Frei Otto created the Institute of Lightweight Structures in Stuttgart, Germany and dedicated his career to investigate about tensile structures and the different variations and possible hybrids.

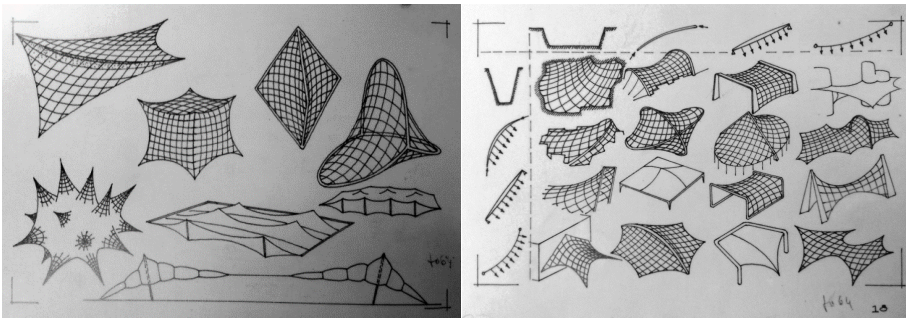


Figure 2.3-7 Studies for membranes and cable nets (left) and matrix of nets dependent on the four different shapes (Otto & Rasch 1996)

2.3.1.6. Olympic Stadium, Munich, Germany

In Fig. 2.3-8 the Olympic Stadium for the 1972 Munich Olympic Games is represented, which is considered a masterpiece project of Frei Otto; the culmination of several years of research and design with the Institute of Lightweight Structures. The scale of this project is significant for its time, covering a total area of 75,000 square meters and using over 210 kilometers of cable.

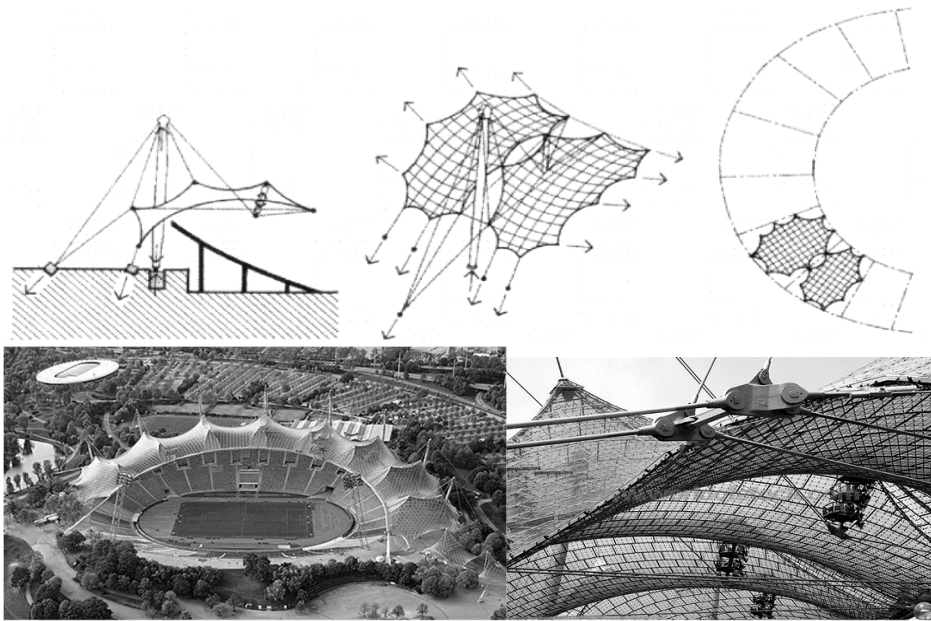


Figure 2.3-8 Olympic Stadium, Munich, Germany (Fang 2009)

2.3.2. Horst Berger

Horst Berger is considered the first person to discover the mathematical relationship that describes the soap bubble forms investigated by Frei Otto (Berger 2012). Furthermore, looking through his constructed projects it is possible to see the importance of his work for the exploration of different membrane support systems to achieve architectural spaces free of interior supports (Berger 1996).

To make a tensile surface structure work requires a minimum of four support points, one more than is needed for a rigid structural system. The most basic form, therefore, is a four point structure, and if an orthogonal grid is used, this can be used as the basic module.

Additionally, the pattern of surface stresses which is required for the stability and load carrying capacity of the structure results in horizontal forces at the anchors in addition to the customary vertical forces. This is the price to be paid for the advantages of a tensile structure. The skill and efficiency with which these horizontal forces are anchored or balanced has a large impact on the economy of the structural system. Also, because of the lack of structural weight, there need to be elements which resist upward loads from wind suction in addition to the elements which carry downward loads. In order to generate the structural surface grid which satisfies all these requirements there have to be support points at the high points of the surface, others at the low points, and still others located around all sides of the periphery. The choice of these support points defines the shape of the structure. Their geometry, combined with the stress pattern assigned to the surface, lead to the form of the structural surface (Berger 1999).

2.3.2.1. Inefficient solutions

As explained earlier, tent shapes require a support at the peak of each tent unit, but this is not always achieved in an efficient way. In the Canada Place, Vancouver (Fig. 2.3-9 left) this was resolved by moving the supports to the edge. The result is a space which is high at the ends and low in the center, and a structure which is not very efficient. Another example is the Jeddah Haj Terminal (Fig. 2.3-9 right), where the mast was placed at the corners suspending the tent units from them, again resulting in a structurally inefficient solution (Berger 1999).

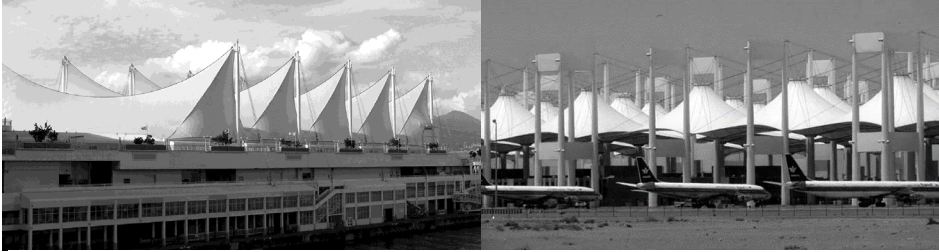


Figure 2.3-9 Canada Place (left) and Jeddah Haj Terminal (right) (Berger 1999)

The examples in the following sections explain efficient solutions for this problem.

2.3.2.2. Point-supported structures



Figure 2.3-10 Jeppesen Terminal, Denver International Airport (Berger 1999)

The Jeppesen Terminal in Denver (Fig. 2.3-10) follows the structural principles of a pole supported tensile structure. The upper supports points are formed by the masts which are spaced 46 meters apart. Ridge cables are draped over these points and anchored to the adjacent lower roofs similar to the main cables of a suspension bridge. They occur every 18.3 meters along the length of the building and are designed to carry the downward loads. Valley cables are placed between any two

ridge cables and run parallel, taking on the form of an arch. They carry the upward load from wind suction and are tied to lower roof anchors. The edges of the roof are formed by edge catenaries.

2.3.2.3. A-frame supported structures

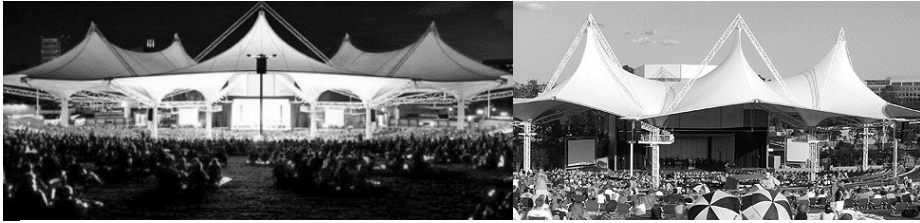


Figure 2.3-11 Cynthia Woods Mitchell Center (<http://www.eventfinda.com/>)

In the Fig. 2.3-11 the Cynthia Woods Mitchell Center of the Performing Arts at the Woodlands, Texas, is shown, which covers 3000 fixed seats. Three A-frames form the support system together with the stage house structure. Horizontal anchors are avoided by introducing compression struts which connect the support columns and edge cable anchors to the stage house, thereby balancing the horizontal components of the membrane forces. The supports of the A-frames form low points of the membrane which function as drainage locations for the rain water. The trussed columns supporting the A-frames contain the rain leaders and support platforms for the follow spot lighting of the theater.

2.3.2.4. Arch-supported structures

For spans in rectilinear structures of up to 100 m, arch-supported fabric roof systems can be highly efficient. For domes with circular, elliptic or super-elliptic edge shapes spans of more than 200 m can be also an efficient solution.

A number of structures have been built using prefabricated steel sections, often with a triangular cross-section.



Figure 2.3-12 McClain indoor practice facility (<https://www.flickr.com>)

The largest using such prefabricated steel arches is the McClain indoor practice facility at the University of Wisconsin in Madison (Fig. 2.3-12). This building covers a football practice field. It has a length of 110 m and a width of 67 m. Arches, spaced 18.3 m apart, span the full width between rigid concrete abutments. The arches are 2.1 m deep and have a triangular cross-section

2.3.3. Recent constructions

The traditional aesthetic of fabric membranes comprised highly curved surfaces reminiscent of vernacular tents. These dramatically curved structures have enjoyed continued popularity from their inception in 1955 by Frei Otto with a small bandstand for the Federal Garden Exhibition in Kassel, Germany to the present day, and have resulted in outstanding works of Architecture for sports stadia, airports and retail.

Recently there has been a significant move towards flatter forms driven by changing aesthetic criteria, not least the desire to differentiate new structures from the existing body of work.



**Figure 2.3-13 Millennium Dome (left) and London 2012 Olympic Stadium (right)
(Bridgens & Birchall 2012)**

The Millennium Dome in London (now The O2 Arena) is a prime example of this change in emphasis and aesthetic, with a synclastic surface being generated by a cable net clad in almost flat fabric panels (Fig. 2.3-13 left). More recently, the London 2012 Olympic Stadium was designed for with a fabric roof and facade, both of which are largely flat on aesthetic grounds (Fig. 2.3-13 right).

It should be noted that in both instances the spanning capability of the membrane and its ability to resist loads and provide positive drainage are still influential in the design of the complete structural system, rather than the membrane being conceived simply as flat cladding without structural utilization (Bridgens & Birchall 2012).

Other examples of current constructions are the Foshan Century Lily Stadium in Guangdong Province, and the Shenzhen Bao'an Stadium, China (Fig. 2.3-14). In the former one, the maximum span of the cantilevered canopy is 92.5 meters. Between the inner and the outer rings is the prestressed cable system composed of ridge cables, valley cables, middle radial cables and inclined cables. A skin made of PTFE (Teflon) fabric is tensioned over these cables. In the Shenzhen Bao'an Stadium, the roof structure is formed by outer ring beam and two-layer inner cable rings with interconnecting cable trusses. Fabrics are established on steel arches spanning across the trusses (Lan 2012).

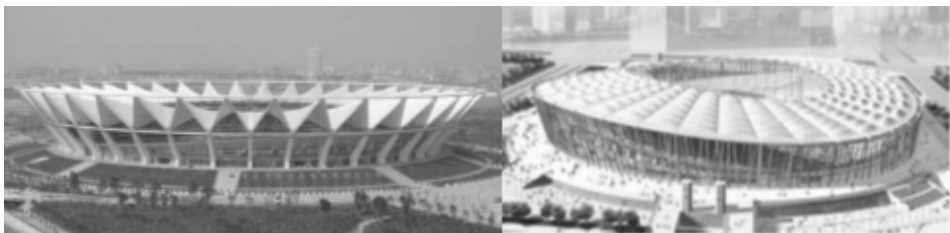


Figure 2.3-14 Foshan Century Lily Stadium (left) and Shenzhen Bao'an Stadium (right) (Lan 2012)

Chapter 3. Design Considerations for Tensile Structures

3.1. Tensile structures characteristics and properties

As explained earlier, unlike steel, concrete or timber building elements which may carry loads in bending, the principal forces in a tension structure are carried within the surface, either by membrane stress or cable tension, through to a supporting boundary structure. Architectural fabrics have negligible bending and compression stiffness, which means that fabric structures must be designed with sufficient curvature to enable environmental loads to be resisted as tensile and shear forces in the plane of the fabric.

The shape of the fabric canopy is vital to its ability to resist all applied loads predominantly in tension: to resist both uplift and down-forces (typically due to wind and snow respectively) the surface of the canopy must be double-curved and prestressed. Therefore, the detailed shape of the doubly curved surface structure is critical to its engineering performance. Coupled with the amount of installed prestress, it governs the magnitude and distribution of stresses and deflections under applied loading.

Fabric structures are prestressed to ensure that the fabric remains in tension under all load conditions and to reduce deflections. The low weight of the fabric means that gravity or self-weight loading is often negligible. Consequently, tensile fabric is frequently more structurally efficient and cost-effective for large span roofs than conventional construction methods (Gosling et al. 2013).

There must, therefore, be close interaction between architect and engineer at the initial shape determination of the structure. This is known as the form-finding stage, and iterative refinement of the form continues throughout the design process. Tension structures undergo significant surface movement in order to carry load, and any analysis must account for these relatively large displacements. This behavior is non-linear in that the actual displacements are not directly proportional to the magnitude of the applied loading and may also include on/off effects such as membrane wrinkling and cable slackening (Wakefield 1999).



Figure 3.1-1 Skysong at ASU campus, USA (FTL design engineering studio)
(<http://sgustokdesign.com>)

These basic forms or their combinations have been used to create a myriad of large structures. Tension membrane structures have been successfully combined with tensile net, truss, and dome systems to create lightweight long-span structures. The use of membranes for these cable structures has the advantage over more conventional building materials in that the membrane can well accommodate the relatively soft structures without a need for special jointing or releases. (Bradshaw et al. 2002).

An example of a hybrid tensile structure is shown in Fig. 3.1-1; a small project to provide shade to a café and restaurant area. In this project, curved trusses are hanging from tensegrity structures composed by cables and poles, supporting all together a membrane structure.

3.1.1. Tensile basic forms characteristics

For the design of tensile structures it is necessary to know the different basic forms that one can find and their properties. After reviewing the work and investigation of Frei Otto and Horst Berger it is easy to have a global idea of what these basic forms are, but for a better understanding they are summarized and explained in this section.

Regardless, any generalization of fabric forms is difficult; the appeal of fabric architecture is the ease with which unique, complex forms can be achieved. Fabric structures are also utilized across a wide range of scales, from a few meters (e.g. canopies over footpaths and bicycle racks) to hundreds of meters (sports stadia) (Bridgens & Birchall 2012).

3.1.1.1. Types of curvature

First it has to be observed that it exists two types of curvature resulting in two types of shapes: anticlastic shape and synclastic shapes (Fig. 3.1-2).

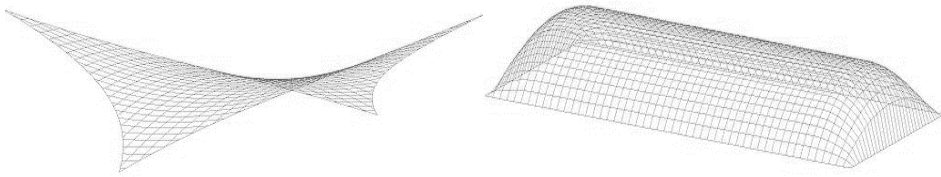


Figure 3.1-2 Example of anticlastic shape (left) and synclastic shape (right)

Anticlastic shapes are created by having the radii of the principal curvatures on opposite sides of the tension fabric surface. As a result, when loaded at a particular point, tension increases on one curve of the membrane and decreases on the opposite curve, thereby preserving equilibrium and keeping the structure stable. In order to keep anticlastic shapes, some kind of structural frame or support is necessary in the form of cables or steel beams.

Synclastic shapes are characterized by having the radii of the principal curvatures on the same side of the fabric. In order to counteract external forces, pressure within the fabric is necessary. This is why synclastic shapes are associated with air inflated structures, as the difference of pressure created by air pumped into the building is able to counteract external forces in the form of wind or snow.

3.1.1.2. Types of anticlastic shapes

Three fundamental fabric structure forms can be developed by manipulating the boundary conditions of an initially flat geometry within a square plan (Fig. 3.1-3). The shape of a tensile fabric canopy is fundamental to its ability to resist all applied loads in tension (Bridgens & Birchall 2012).

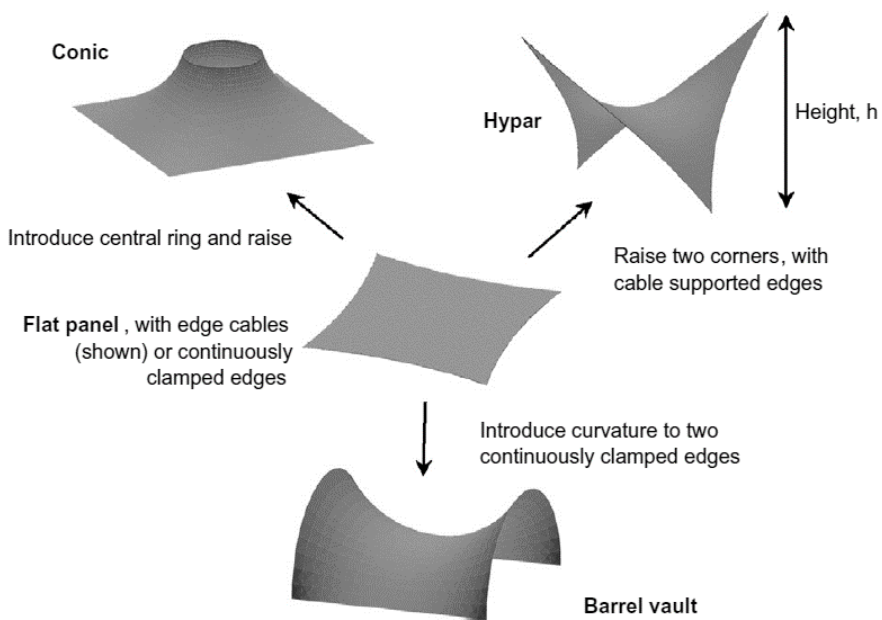


Figure 3.1-3 Three fundamental tensile forms by manipulation of boundary conditions (Bridgens & Birchall 2012)

Hypars or hyperbolic paraboloids are characterized by alternating high and low points, usually with cable-supported edges. The simplest hypar consists of two high and two low points, but more complex forms can be achieved with multiple support points. A hypar can be designed with two different fabric orientations or patterning directions. A square hypar

structure acts principally in tension between diagonally opposite corners. For the orthogonally patterned hypar this means that the fabric is acting in shear. As the shear stiffness of architectural fabrics is typically low an orthogonally patterned hypar exhibits high deflections. However, this form of construction is popular as it allows greater shear deformation during installation to achieve highly curved forms without wrinkling. This introduces a common design conflict in membrane structures where optimum properties for installation are different from those for long term performance of the structure.

In the conic, as the distance between the base and the top ring increases the minimal surface would “neck”; a point is reached where a minimal surface cannot be formed between the rings. Conic structures with a low ring height are prone to ponding, which is the formation of a hollow near the corners under snow load that leads to collection of melt-water and subsequent failure.

A rigid frame consisting of two straight sides and two curved sides provides the boundary conditions for a barrel vault with a similar double curved “saddle” shape to a hypar, but the fundamental difference is that the membrane tends to span between edges rather than between the corners.

3.1.2. Fabric material properties

Not long after its development, the light translucency of coated fiberglass became an obvious virtue, availing it as a cost-effective substitute to glazing in many commercial projects across the continent. The curved surface of a membrane structure is fabricated from flat pieces of coated woven fabric cut from rolls. Seaming is most commonly accomplished by lapped heat seals but can also be done by mechanical means such as sewing or intermittent fasteners.

Fabrics are quite different from membranes as engineering materials. Commonly used coated fabrics are composite materials whose strength is primarily provided by the woven textile and yarn: weather protection, finish, and the jointing ability are provided by the coating. This results in materials that have very low shear stiffness in relation to their tensile stiffness and are also highly nonlinear. The orthotropic behavior of coated fabrics is complex, dependent on its stress history, and is dictated by micromechanics of the weave (Bradshaw et al. 2002).

Architectural fabrics typically consist of woven glass fiber yarns with a polytetrafluoroethylene (PTFE) or Silicone coating, or woven polyester yarns with a polyvinyl chloride (PVC) coating (Fig. 3.1-4). The woven yarns provide tensile strength, whilst the coating stabilizes and protects the weave and provides waterproofing and shear stiffness (Gosling et al. 2013).

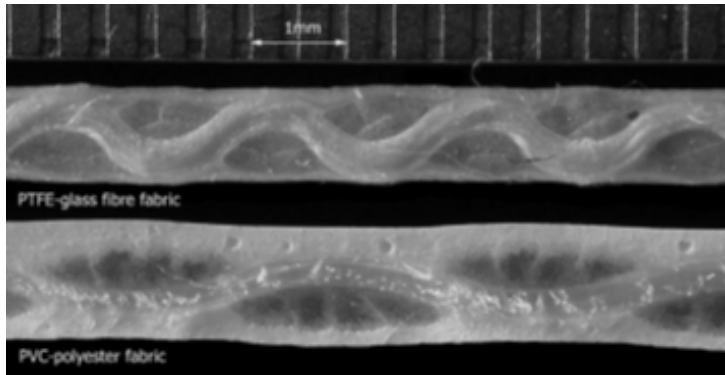


Figure 3.1-4 Architectural fabric cross-sections showing highly crimped, woven yarn bundles encased in PTFE or PVC coating (Bridgens & Birchall 2012).

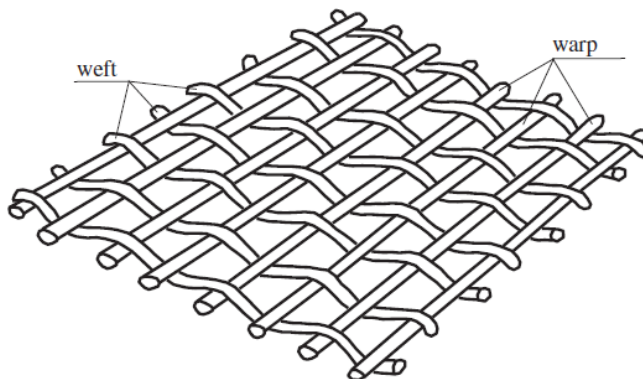


Figure 3.1-5 Base components of technical woven fabric (Ambroziak & Kłosowski 2014)

Typical technical woven fabric usually consists of two families of threads; the warp and the weft (fill) (see Fig. 3.1-5) (Ambroziak & Kłosowski 2014). Tensile strength varies greatly between the warp and fill directions, and is usually stronger in the warp (Fang 2009).

The warp is the direction of the yarns, which are spooled out lengthwise in the loom or weaving machine. The fill or weft is the yarn in the cross machine direction, which “fills” in the weave. As a curved membrane surface is fabricated from flat pieces of fabric, the warp is generally parallel to the seams. Different weaves have different mechanical qualities, which are primarily governed by the convolutions of the yarn and the initial state of crimp in the weave. Generally, the initial crimp in the warp is different from that of the fill. This results in different initial elongation properties in the warp and fill directions.

In general, elongation at service level stresses is dominated by weave crimp, rather than strain of the yarn fibers. Consequently, elongation behavior in service has more to do with the weave than yarn characteristics. The coatings employed in most structural fabric tend to attenuate this behavior, especially for transient changes in strain. This results in response to transient loads similar to membranes. However, as almost all currently employed coatings are polymeric in nature, the effects of the coating diminish with load duration as creep of the coating allows the yarn with its weave-dominated behavior to resist the loads (Bradshaw et al. 2002).

A combination of non-linear stress-strain response of the component materials (yarn and coating) with the interaction of orthogonal yarns, results in complex (non-linear, hysteretic, anisotropic) material behavior. Elastic moduli, Poisson’s ratios and shear stiffness are independent and are not constrained by conventional limits and relationships for isotropic materials (Bridgens & Birchall 2012).

As the shear modulus increases towards the value for an isotropic material (Eq. 3.1-1), the shear stiffness tends towards the elastic stiffness in warp and fill directions, and hence the displacements tend to be towards the values for the diagonally patterned structure.

$$G = \frac{E}{2(1+\nu)} \quad (3.1-1)$$

Where G is the shear modulus, E the elastic modulus and ν is the Poisson's ratio. This effect is less significant for flatter structures (i.e. as height/side lengths tends to become zero) when the fabric panel is acting primarily as a two way spanning flat panel. As the corner height and fabric curvature increases, the structure must span between diagonally opposite corners and the effect of fabric orientation and shear stiffness on deflections becomes pronounced (Bridgens & Birchall 2012).

3.2. Design procedure of tensile structures

During the design procedure, as can be seen in Fig. 3.2-1, there are several steps since the client gives the project to an architectural design company and the preliminary design is decided. An analytical step called form finding is needed where architects and engineers need to collaborate to adjust the final design corresponding to the minimal surface in equilibrium that the structure should have. In addition to satisfying the equilibrium conditions, the initial configuration must accommodate both architectural (aesthetics) and structural (strength and stability)

requirements. Further, the requirements of space and clearances should be met and the radii of the doubly-curved surfaces should be small enough to resist out-of-plane loads and to ensure structural stability. It is a very important step prior to the analysis of the structure and the cutting pattern generation made by the engineers.

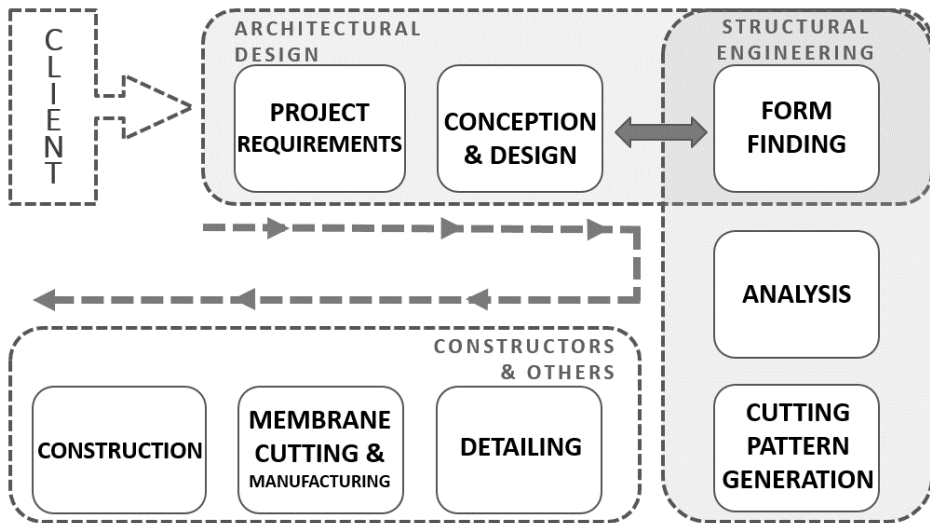


Figure 3.2-1 Design procedure of tensile structures (organized by Marta Gil Pérez)

Although physical models are still used, in particular by architects and engineers at the initial conceptual design stage, the principal design stages of form-finding, load analysis and patterning are now all undertaken by computer taking a better importance such collaboration between design and engineering (Wakefield 1999).

Along the history of tensile structures, the need for new computational structural engineering tools that can be applied to complex geometries has been highlighted by several authors (Argyris et al. 1974), (Iványi 2013), (Winslow et al. 2010), (Lienhard & Knippers 2012), and many of them have developed some computational methods to help in this early stage where engineering and architecture needs to cooperate. But there is still a lack in design guidance.

Then, it can be summarized that the modeling and analysis of membrane structures is a two stage process - form-finding followed by load analysis - requiring specialist analysis software. For the first stage, boundary conditions (support geometry, fixed or cable edges) and form-finding properties (fabric and edge cable prestress forces) are defined. Form finding is independent of the fabric material properties. A soap-film form-finding analysis provides the membrane geometry and prestress loads. A new model is created with this updated (form-found) geometry that is used for the analysis stage.

Subsequently the fabric material properties are defined, loads are applied (wind, snow, prestress) and a geometrically non-linear (large displacement) analysis is carried out using membrane elements with zero bending and compression stiffness. Due to geometric non-linearity, results from different load cases cannot be combined or factored; each combination case (e.g. prestress + wind uplift) is analyzed separately and a permissible stress approach is used to assess the required membrane strength (Bridgens & Birchall 2012).

Design of large and complex tension membrane structures is more reliant upon computers than most structural systems, as they defy classical analysis. The nonlinear behavior of these structures, coupled with the need to determine prestressed forms to meet specific design and boundary conditions as well as the loading analysis, necessitates a true “computer-aided” design and modeling technique. The procedures for prestressing the system are determined in a similar fashion. Finally, the templates used to cut and fabricate the fabric membrane surface are typically computer generated.

As with most design methodologies the process is iterative, such that anticipation of the results in the conception of a structure is expected to reduce the general effort involved in the design and engineering of the system (Bradshaw et al. 2002).

In this study a nonlinear approach for tensile membrane analysis is used where the stiffness method solves a set of equations that represent the translational and rotational equilibrium at each node of the structure (Crisfield et al. 2012). This method requires an incremental iterative process until equilibrium shape compatible with the given prestress condition is reached. At each step, a global stiffness matrix is recalculated, according to the new position of the nodes and the material properties of the membrane (Rezaiee Pajand & Moghaddasie 2009).

3.2.1. Form-finding analysis

The design process by which the shape of form-active structures and systems is determined is widely called either form-finding or shape-finding (Veenendaal & Block 2012).

Before the advent of affordable powerful computers, the design of stressed membrane surface structures had to be carried out using physical models. Frey Otto's soap film experiments to find the shape of the optimal minimal surface are the most well-known (Otto & Rasch 1996). Later, the experimental procedures have been simulated by equivalent computational methods.

The problem of finding appropriate forms of stressed membrane surface structures can be tackled in a variety of ways. Common to all approaches is the need to ensure that the resulting shape is capable of withstanding the applied loading, while satisfying the boundaries imposed by the architectural specifications. Due to the direct relationship between form and force distribution in membrane structures, compromises often need to be made between what is wanted and what is structurally possible.

From a purely philosophical point of view, it would seem reasonable to aim to provide uniform stress surfaces within the boundaries chosen by architectural constraints - thus the surface so formed would be a minimal surface, akin to a soap-film model (Forster & Mollaert 2004).

In their prestress state, fabric membranes are normally designed to have uniform or smoothly varying stresses throughout their surfaces, though not necessarily (or even usually) equal in the warp and weft directions of the weave.

The component elements may change radically in shape during this process but the stresses within them remain constant. Since the stresses correspond to the main orthogonal yarn directions, and as the shear stress for form finding is zero, the yarn directions become principal stress directions. The latter should also correspond to the principal curvatures of the surface in order to provide greater stiffness under the dominant live loadings, and also not to include high shear strains under these loads (Gosling et al. 2013).

For example, under buffeting wind loadings, a uniformly stressed surface with sufficient prestress is less likely to undergo on/off slackening of the fabric with consequently less fatigue of the yarns and their constituent fibers. Besides, in the long term prestress state there is creep of the fabric and some relaxation of the prestress. Also if the fabric is stressed in a reasonably uniform state initially there is less deformation of the form due to change in the stress ratios and perhaps in consequence less likelihood of local wrinkling.

This latter effect can occur if there is a large difference between the warp and weft stresses at the initial state which subsequently relax to become more uniform.

However, the more important issue is to ensure gradual variations in stress so as to achieve a desired form; deliberate variations in stress ratios throughout a surface can be necessary for both structural economy and increased security (Forster & Mollaert 2004).

The form-finding component of membrane structure analysis is not commonly found in other structural analysis software and has led to the development of bespoke analysis methodologies beyond the normal scope of finite element codes. The basis of the geometrically nonlinear analysis may be continuum, use of discrete elements in the form of cables, or be a combination of both approaches. Finite elements formulated on plane stress principles clearly fall in the continuum-based category, making use of orthotropic material properties including elastic moduli (axial and shear) and Poisson's ratios (Gosling et al. 2013).

Data from form-finding, typically composed of connectivity, nodal geometry and element prestress, represent a complete model description of the membrane structure and the element properties. Consequently, shape results with the addition of element properties can be employed directly in the analysis. Often, additional elements, such as struts or beams, are added to create an analysis model of a complete structural system (Bradshaw et al. 2002).

In the last five decades several methods of form-finding have been developed. Earlier methods were typically applied to discrete cable-net structures and extended by later methods to surface elements for

membrane structures (Veenendaal & Block 2012). The most widely applied methods are: the force-density method, dynamic relaxation method and nonlinear finite element method. Common to all approaches is the need to ensure that the resulting shape is capable of withstanding the applied loading, while satisfying the constraints imposed by the architectural specifications.

All of these methods idealize the surface as a network of line elements and/or a mesh of continuum orthotropic finite elements within which allowance for the shearing stiffness of the fabric and its coating are accounted for. The methods also allow for other element types such as masts, beams, cable boundaries and slip elements to be included in the complete structural model (Forster & Mollaert 2004). A further explanation of this methods and the possible variables is introduced in the following sections.

3.2.1.1. Dynamic relaxation

The dynamic relaxation method solves the geometric nonlinear problem by equating it to a dynamic problem (Barnes 1999).

The basis of the method is to iteratively calculate the movement of all nodes in a structure from their initial positions, through time steps Δt , until their equilibrium positions are found and vibrations damp out due to artificial damping. The movement of each node is caused by an out-of-balance force calculated as the sum of the forces acting in the elements adjacent to the node and the applied load. Newton's second law states that the acceleration of a body is directly proportional to the

body's net force which lay the foundation for dynamic relaxation. From the out-of balance-force and the nodal mass the acceleration can be obtained, and by stepping through time the velocity and movement of each node can consequently be calculated. Each node is moved in order to reduce the out-of-balance force, and when the total force is reached just below a certain limit value, equilibrium is assumed to be reached (Olsson 2012).

3.2.1.2. Force density method

The force density method, described originally by Scheck (Scheck 1974), uses an analytic technique to linearize the form-finding equations for a tension net. This linearization makes the method independent of the material properties of the membrane. The equations are simplified to a linear form by applying 1 quality for each element of the cable or membrane, called force density, which is the tension of that element over the length. Then, a unique solution for the state of equilibrium is obtained. Although used to date primarily with equivalent cable-net models, later research in France by Motro has extended the concept to triangular surface elements, under the name of the surface stress density method (Maurin & Motro 1998). The advantage of this method is that it provides a linearized solution to the equilibrium shape finding problem.

The main drawback of density methods is that the final distribution of stress is difficult to control. This can be overcome by iterating with updated force densities until the desired smooth stress distribution is

achieved, but this would seem to negate the advantage of a linearized solution. Once a form is found, a vector or matrix method must be used to analyze its response under load (Wakefield 1999).

A more recent research in Spain by Sanchez introduced a new method to obtain equilibrium shapes with smooth stress distribution. It is referred to as the multi-step force-density, and is an iterative process based on the original force density method (Sanchez et al. 2007).

Parallel to this one, in Japan by Miki, another method has been developed, called the extended force density method, for form-finding of tension structures (Miki & Kawaguchi 2010). In this research, the limitations of the force density method are identified when applying it to prestressed structures combined by both tension and compression members. Therefore, an extension of the original method is proposed to be able to find the forms of more complex tension structures that consist of a combination of cables, membranes, and compression members, such as tensegrity structures and suspended membranes with bars.

The most recent reviews of the force density method are the ones made by Greco in Italy (Greco & Cuomo 2012) and Ye in China (Ye et al. 2012).

3.2.1.3. Nonlinear finite element method

The finite element method provides the most versatile approach for analysis of tension structures. Owing to the greater geometric nonlinearity of membrane structures, it is preferable to use a dense mesh

of primitive elements rather than a coarse mesh made up of higher order elements (Tabarrok & Qin 1992).

It is also called matrix method and it is considered an application of more standard nonlinear structural analyses (Crisfield et al. 2012; McGuire et al. 1979; Weaver et al. 1984). Besides, for the analysis of tension structures it is necessary the use of incremental methods such as the Newton–Raphson method where the structure overall tangent stiffness matrix is solved incrementally until convergence is obtained (Rezaiee Pajand & Moghaddasie 2009). Special controls limiting the maximum incremental deflections and nodal residual forces may be required. The stress/strain relations for the individual components are coupled with the equilibrium and compatibility requirements for the complete structure (Wakefield 1999).

This method is used in the analyses of this thesis for both, the form-finding and the stress-deformation analyses. Thus, a detailed explanation of the algorithms is given in the Chapter 5 (Development of Geometrically Nonlinear Finite Element Equations).

3.2.2. Stress-deformation analysis

Once the initial equilibrium shape is determined, the behavior of the structure under a variety of loads must be investigated to ensure that the structure can withstand all the forces that it is anticipated to encounter in service (Tabarrok & Qin 1992).

As explained in the introduction of this section, general analysis of all tension-based, specifically tension membrane structures requires geometric nonlinear techniques. It is necessary to account for the change in the geometry of the structural network. It has been demonstrated that deflection terms are of first-order significance in structural networks with initial prestress.

Analysis of a form-found structure with prestress loading applied is typically carried out to assess the quality of the form-finding process for that structure. If isotropic prestress is applied and the boundary conditions allow a minimal surface to be achieved, then the stress levels should be equal to the specified prestress and be uniform throughout the membrane, and the displacements should be zero. If the boundary conditions preclude a minimal surface from being achieved, then specification of anisotropic prestress and/or accepting a poorly converged form-finding solution enables a form to be generated which has varying levels of prestress at different points on the structure. Therefore, if this structure is analyzed with prestress loading equal to the original, specified prestress values then displacements occur in order to achieve equilibrium. Or if the applied prestress values are those determined by the form-finding analysis then the structure should be also in equilibrium (Gosling et al. 2013).

Common tensile structural systems initially go through strain softening but then exhibit strain hardening once sufficient load is applied. Consequently, nonlinear solution strategies that anticipate strain hardening have been used with success to speed convergence in most

common problems. Most importantly, the principles of superposition do not apply to nonlinear systems.

Therefore, all critical load combinations must be analyzed individually. Material nonlinearity is rarely modeled, although it is inherent to most fabric materials. This is just as well, because material properties are often affected by stress history. While fabric material nonlinearity is typically not modeled, it is likely proven to be useful when the mechanics of fabric failures are better understood and utilized quantitatively in a limit states design approach.

The fabric is commonly modeled utilizing linear strain or constant strain triangle membrane finite elements or a network of string elements. These approaches have been widely used with success; each has attendant limitations that the analyst must consider (Bradshaw et al. 2002).

3.2.3. Patterning and construction

Typically the arrangement of fabric panels or "patterning" is designed such that longer term loads including snow may predominantly be carried by the warp yarns aligned with the "hanging" direction of the surface, and with shorter term dynamic wind loads (which predominantly cause suction on the surfaces) being carried by the weft yarns aligned in the "arching" direction.

Fabrication patterning has to be accounted for explicitly within the numerical models used for both form-finding and analysis of prestressed membranes. Their doubly curved surfaces are fabricated from flat unstressed panels of coated fabric with welded seams. For reasons of material economy and accuracy and to avoid wrinkling in the surface form, the centerlines (and seams) of panels should follow geodesic paths over the surface. These geodesic are the shortest distance between two points on a surface - on alternatively the trajectories which a flat tape of material could follow without shearing.

The directions of the fabric weave, with warp along the panel and weft across, are dictated by the patterning and yet pre-stresses specified in these weave directions govern the surface shape. Thus the intended weave directions for patterning must be taken into account during form-finding. The same clearly applies to modelling the stress/strain relations of the weave during load analysis. (Forster & Mollaert 2004).

3.3. Loading conditions and safety approach

By the very nature of lightweight structures, the ratio of applied loading to self-weight is usually many times larger than that of conventional building structures. Changes in the magnitude of wind and snow loading are therefore likely to have a proportionately larger impact on the size of the structural members required and the scale of deflections experienced.

Consequently the selection of suitable loading patterns for the design of membrane structures has to be carefully considered. Furthermore the codes are written for standardized building shapes and building behavior, usually making the application of a single code very difficult. As a consequence more time and effort needs to be spent in defining load cases.

Besides, for structures which exhibit strong geometric nonlinearity, in particular stiffening systems such as tensile structures, a limit stage approach (with partial safety factors applied to the loading conditions as well as material strengths) may not be appropriate since the geometry of the structure is dependent on both the magnitude and the distribution of loading; the changes in geometry being particularly significant for non-uniform loading distributions.

Another aspect that mitigates against the use of factored loadings for prestressed fabric structures is the large variation in material characteristics and the large factors which must be applied to the quoted (or ideal test) rupture strength of the virgin fabric in order to allow for aspects such as material variabilities, tear strength, degradation and local damages during erection handling (Forster & Mollaert 2004).

The two structural main performance criteria for fabric structures are stress and deflection. Large displacements and a reliance on geometric stiffness has led to the adoption of a stress factor approach as the basis of a permissible stress design methodology for tensile fabric structures.

3.3.1. Loads and load combinations

To take into account the large deflections of membrane structures, analysis has to be made using unfactored loads. It is very important that the results of a load combination are found by adding loads and then analysis, rather than analyzing each load separately and then adding the results.

The prestress and self-weight loads should be part of all load cases. Some examples of load cases to be considered could be:

- Self-weight + prestress
- Self-weight + prestress + snow
- Self-weight + prestress + wind
- Self-weight + prestress + wind (downward pressures) + snow
- Etc.

In the following sections, a further explanation of each type of load is described.

3.3.1.1. Prestress

The level of prestress in a membrane surface affects all the elements within the supporting structure (mats, frames, cables, etc.). Prestress is an inherent part of its structural behavior. The prestress levels are chosen as a result of the form-finding process, and have to be achieved and sustained during the erection and life of the structure. These forces have to be included in all other load cases. The prestress of membrane structures is a fundamental part of the shape and structural behavior.

Prestress contributes significantly to a membrane's stiffness due to its opposing curvature components interacting to constrain what would otherwise be severe deformations typical of flat or singly curved surfaces. The chosen level of prestress can normally be a compromise - low enough to reduce the work done during installation - whilst sufficiently high to maintain a sufficient prestress after losses due to "creep" of the membrane material over time. The choice of the initial boundary conditions for an anticlastic surface can often be guided by the use of the relationship expressed in Equation (3.3-1).

$$T = p \times R \quad (3.3-1)$$

Where T is the membrane tension, p is the pressure applied normal to the surface and R is the radius of curvature of the surface. This relationship has a particular relevance to the "saddle" and "hypar" shapes. Thus by knowing what the applied pressures are likely to be as well as what the membrane tensions should be limited to, the radius/radii or curvature can easily be found. This can then be fed back into the initial assumptions made about the geometry of the boundary conditions. In doing this a number of simplifying assumptions are being made, such as that the pressures are 'normal' to the deflected surface and are uniformly distributed (Forster & Mollaert 2004).

Nevertheless it can be a useful starting point for design as well as a simple means of checking the output of more elaborate computations. Where geometry constraints are placed upon design - such as to require the use of flatter and therefore larger radii of curvature - then larger values of prestress are required to control the size of the membrane's

deflection. There are practical limits to what can be safely applied and remain in the long term. In the limit where the surface becomes flat (radius = ∞), prestress and the material's stiffness (EA) are the only parameters controlling deflection.

For many structures the same quantity of prestress is applied to both directions of the textile's weave. However in cases where the magnitude of the inward and outward applied loads are markedly different to one another, it can be economically advantageous to determine the membrane's shape such that a smaller (tighter) radius of curvature carries the lower external pressure and vice-versa a larger (flatter) radius of curvature carries the lower external pressure. In this way the resulting maximum membrane tensions can be of a similar size.

Long term effects such as creep of the membrane material may alter prestress levels. Foundation settlement may also be an influence. These effects must be considered and appropriate measures taken to ensure the retention of sufficient prestress.

Generally the minimum required prestress of membrane surfaces depends on the stiffness and strength of the material and the efficiency of the membrane surface (i.e. curvature). Furthermore prestress levels lower than those given may lead to an uneven or wrinkly appearance as not all fibers in the surface may be sufficiently stretched.

3.3.1.2. *Self-weight*

The self-weight of the membrane is commonly between 0.7 and 2.0 kg/m².

It is not usual to include the self-weight in the form-finding process because this may introduce some additional mechanical freedom into the response of the membrane to wind uplift loadings. Although this is usually a trivial effect, in some cases it may be significant - for example in relatively lightly stressed membrane surfaces using heavier grade fabrics. Whether or not self-weight is included in the form-finding process (to define an initial geometrical state) it must be included in all applied load cases.

3.3.1.3. *Wind*

Wind, especially in the form of uplift, is regularly the critical case for membrane and cable stresses in lightweight membrane structures. It is generally considered as a static load case, defined by a dynamic pressure multiplied by a pressure coefficient (C_p). It is also assumed that the membrane undergoes only slight changes to its geometry such that changes to C_p factors are small enough to be safely ignored. This approach may not be appropriate if the membrane form is deflection sensitive and/or large deflections are the case.

Membrane structures are single layer elements with wind load often exerted on both faces simultaneously. The local C_p values for both internal and external surfaces can be derived using appropriate codes

and papers. The summed effects of the internal and external C_p values used are to be applied to the analysis model. Pressures need to be applied normal to the deflected surface.

Membrane structures that enclose buildings behave differently to open canopies since only the external side of the fabric is exposed directly to the dynamic wind pressure. However the internal pressure / internal suction has also to be taken into account. This may be significant when large openings in wall or roof are present. Consequently high internal C_p factors can be expected (Forster & Mollaert 2004).

3.3.1.4. Snow

Ground snow load should be investigated. For long-span structures, it is recommended that the ground snow load be investigated using available data from the local meteorological office. In areas not subjected to snow loads, a nominal uniformly distributed load of 0.3 kN/m^2 should nevertheless be considered. This figure may be reduced for structures with spans over 50 m by applying a detailed statistical investigation accounting for loading by rain, fallen leaves, sand/dirt etc.

Snow can be deposited upon roofs under calm or windy conditions. Under calm conditions an even layer tends to be deposited over the entire roof. Under windy conditions the snow tends to drift applying an uneven loading to the roof.

The nature of this uneven loading depends on the roof profile in the direction of the wind. In the case of a roof consisting of a series of ridge and valleys under windy conditions the snow drifts away from the ridges into the valleys. This effect is difficult to predict and care must be taken.

With a large snow load, the structure may develop deflections such that a downward slope becomes reversed. This can produce what is generally referred to as 'ponding' since the slope no longer allows the runoff of rain and melting snow. Due to the flexibility of the membrane, the retention of rainwater and snow leads to larger deflections. This then leads to the further attraction of rainwater and snow. Large loads are experienced and for this reason, ponding must be avoided in membrane structures (Forster & Mollaert 2004).

3.3.1.5. Temperature

Temperature effects in respect of overall structural behavior and load analysis are usually found to be less significant on fabric structures when compared with rigid construction. Temperature change manifests itself in relatively small \pm variation in prestress levels. However, temperature effects are more important for steel cable nets (Forster & Mollaert 2004).

3.3.1.6. Seismic

In general seismic loads are not a problem as membrane structures weigh so little and so would not pick up substantial acceleration forces under seismic action. Should the structure contain relatively massive components such as struts or connections, these are subject to accelerations under seismic loading (Forster & Mollaert 2004).

3.3.2. Safety factors

Due to the low shear stiffness of woven fabrics compared to their tensile stiffness, maximum stresses usually occur in the weave directions (warp and fill). Note that ‘stress’ in structural fabrics is defined as force per unit width, as fabrics do not have a consistent thickness. Stresses in warp and fill directions for each load case are compared to the fabric strip ultimate tensile strength divided by an appropriate stress factor to account for the severe reduction in fabric strength in the presence of a small tear (Bridgens & Birchall 2012).

Engineering groups across a range of countries have adopted alternative design stress factors that have been derived using a number of different approaches, with values varying from 3 to 8 (Gosling et al. 2013).

Fabric structures do not have strict deflection limits such as those imposed on conventional building structures, but limits are defined by the need to avoid ‘ponding’, and in some cases to avoid clashes between the deflected fabric form and the supporting structure or other objects.

All textiles have common attributes that are significant in structural applications. Tensile strength of fabrics is greater in uniaxial than in biaxial loading, and failure is almost always a result of tear propagation rather than tensile rupture.

This belies the fact that current design practice establishes membrane resistance solely on uniaxial strength. Tear propagation in textiles can be roughly analogous to crack propagation in metals in direct tension. Tears are initiated at cuts, abrasions, or other discontinuities and propagate when the force at the head of the tear reaches a critical value. Tear resistance is dependent on both yarn and weave properties (Bradshaw et al. 2002).

Fabric membranes are selected for a given structure based upon their strength, durability, fire performance, optical properties, and finish. Standard practice is to establish the minimum required strength in the warp and fill based upon the uniaxial dry strip tensile strength of the material in the warp and fill. Minimum strip tensile strengths during the expected life of the membrane are established as 4 times the maximum service stress due to the worst service load combination in Korea.

Other important limit state conditions to be considered are (Forster & Mollaert 2004):

- The avoidance of progressive collapse due to failure of any components
- The insurance of the security of heavy structural components in the event of the partial failure or removal of any membrane area.
- The avoidance of ponding - with the structural shaped, and remaining shaped, so that there is positive drainage from all areas.

Chapter 4. Purpose of Research

Each spatial structure is a prototype by itself, rather than a duplicate produced on an assembly line. Due to the lack of design guidance, the design of membrane structures is performed by experience, engineering judgment and pragmatism.

There are two obstacles to the more general future use of tensile membrane structures in architecture. One is the special expertise required for the design. The other is the availability of fabric which is easy to handle and has a long life span (Berger 2012).

In this research, firstly there is an attempt to put together all information about the design, modeling and analysis of tensile membrane and cable structures. For the clarity of this, two case studies with a detailed description is shown. Besides, by the analysis of those case studies, conclusions on the critical loading cases and safety is given.

As explained in the literature review, tensile membrane structures are considered to have three basic shapes: the hyper (hyperbolic paraboloid), the conic and the barrel vault. The last part of the research gives some design criteria for a specific type of module made by barrel vault shaped membrane by its parametric study. Limits on the geometry such as curvature are also specified. Besides, design application examples are

proposed. The other two basic shapes are not the scope of this research.

Specifically, this research aims to accomplish the following objectives:

- Explaining in detail the procedure for the design, modeling and analysis of tensile membrane and cable structures. Reaching this objective is important because there is a lack of guidance on the design of this type of structures.
- Describing the methodology for the geometrically nonlinear finite element analysis for cable and membrane elements and showing how this is integrating in the program used for the analysis in this thesis.
- Bringing two case studies that put into practice all the knowledge explained a priori. Illustrating every steps of the modeling and analysis with a real case example, and bringing up comparative conclusions.
- Proposing a parametric study of one of the tensile basic shapes, finding the geometry limitations of the different models, and proposing possible design applications by the combination of the different created modules.

Chapter 5. Development of Geometrically Nonlinear Finite Element Equations

For the nonlinear analysis of tension structures the principle of virtual work is used which states that the virtual work of a stress field in equilibrium vanishes.

In this thesis, a method of finite element analysis for large deformation is outlined for both the form finding and load analysis steps in the design of tension structures consisting of membranes and cables. Therefore, the nonlinear finite element equations for the membrane and cable elements are developed in the following sections.

Element coordinates and stiffness equations of those are first defined in the local axis and afterwards are shifted to the global axis of the structure by using the transformation matrices related to each element's local coordinates.

Besides, tension structures cannot resist any compressive stresses. Wrinkling occurs when the external loads give rise to compressive stresses larger than the initial tensile stresses. A procedure to treat element wrinkling should also be included in the load analysis.

5.1. Cable element equations

In this section, the tangential stiffness matrix of the cable/truss element are driven in order to analyze spatial structures which have geometrical nonlinearity. The cable element type is composed of 2 nodes and 3 degrees of freedom as seen in Figure 5.1-1 where the element coordinate system and the global coordinate system is also represented.

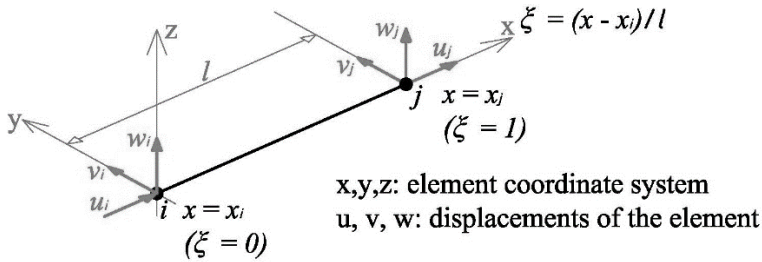


Figure 5.1-1 Local coordinates system and displacements of a cable element.

5.1.1. Coordinate system and displacement function

The displacement and force vectors of each node are defined in Equations (5.1-1) and (5.1-2) in the local coordinate system.

$$\underline{d} = \begin{Bmatrix} \underline{d}_i \\ \underline{d}_j \end{Bmatrix} = [u_i \quad v_i \quad w_i \quad u_j \quad v_j \quad w_j]^T \quad (5.1-1)$$

$$\underline{f} = \begin{Bmatrix} \underline{f}_i \\ \underline{f}_j \end{Bmatrix} = [f_{xi} \quad f_{yi} \quad f_{zi} \quad f_{xj} \quad f_{yj} \quad f_{zj}]^T \quad (5.1-2)$$

In Equation (5.1-3), the displacement of the 2 node element is assumed as a function of x for the tridimensional directions.

$$\begin{aligned} u(x) &= N_i u_i + N_j u_j \\ v(x) &= N_i v_i + N_j v_j \\ w(x) &= N_i w_i + N_j w_j \end{aligned} \quad (5.1-3)$$

In equations (5.1-4) and (5.1-5) the shape function is defined. N_i and N_j are the Lagrangian interpolation function.

$$\begin{aligned} N_i &= 1 - \xi \\ N_j &= \xi \end{aligned} \quad (5.1-4)$$

$$\xi = \frac{x - x_i}{x_j - x_i} \quad (5.1-5)$$

5.1.2. Displacement-strain relationship

The displacement-strain relationship of the element is chosen as expressed in Equation (5.1-6) to include the second order geometrical nonlinearity.

$$\varepsilon_x = \frac{\partial u}{\partial x} + \frac{1}{2} \left[\left(\frac{\partial u}{\partial x} \right)^2 + \left(\frac{\partial v}{\partial x} \right)^2 + \left(\frac{\partial w}{\partial x} \right)^2 \right] \quad (5.1-6)$$

Substituting Equation (5.1-3) into Equation (5.1-6), Equation (5.1-7) is obtained, where the strain is written in relationship with the shape function.

$$\varepsilon_x = \frac{\partial N_i}{\partial x} u_i + \frac{\partial N_j}{\partial x} u_j + \frac{1}{2} \left[\left(\frac{\partial N_i}{\partial x} u_i + \frac{\partial N_j}{\partial x} u_j \right)^2 + \left(\frac{\partial N_i}{\partial x} v_i + \frac{\partial N_j}{\partial x} v_j \right)^2 + \left(\frac{\partial N_i}{\partial x} w_i + \frac{\partial N_j}{\partial x} w_j \right)^2 \right] \quad (5.1-7)$$

Equation (5.1-8) is the matrix form of Equation (5.1-7).

$$\varepsilon_x = \underline{A}_1 \underline{d} + \frac{1}{2} \underline{d}^T \underline{B}^T \underline{B} \underline{d} \quad (5.1-8)$$

Where,

$$\underline{A}_1 = \begin{bmatrix} \frac{\partial N_i}{\partial x} & 0 & 0 & \frac{\partial N_j}{\partial x} & 0 & 0 \end{bmatrix} \quad (5.1-9)$$

$$\underline{B} = \begin{bmatrix} \frac{\partial N_i}{\partial x} & 0 & 0 & \frac{\partial N_j}{\partial x} & 0 & 0 \\ 0 & \frac{\partial N_i}{\partial x} & 0 & 0 & \frac{\partial N_j}{\partial x} & 0 \\ 0 & 0 & \frac{\partial N_i}{\partial x} & 0 & 0 & \frac{\partial N_j}{\partial x} \end{bmatrix} \quad (5.1-10)$$

5.1.3. Stress-strain relationship

The stress-strain relationship is defined in Equation (5.1-11) in the incremental domain where E is the stiffness constant of the element or Young's modulus.

$$\sigma_x = E \varepsilon_x \quad (5.1-11)$$

5.1.4. Equation of equilibrium using the principle of virtual work

When a structure with body force and surface tension is in equilibrium, virtual external work (∂W) caused by arbitrary virtual displacement and virtual strain energy (∂U) stored in the structure are equal.

Equation (5.1-12) represents this fact called the principle of virtual work.

$$\partial U = \partial W \quad (5.1-12)$$

Replacing the values of ∂W and ∂U in the Equation (5.1-12), Equation (5.1-13) is driven.

$$\int_V \sigma_x \partial \varepsilon_x dV = \underline{f}^T \partial \underline{d} \quad (5.1-13)$$

When incremental methods are used, the principle of virtual work can be presented as described in Equation (5.1-14) including the initial conditions.

$$\int_V [(\sigma_x^{(0)} + \sigma_x) \partial \varepsilon_x] dV = (\underline{f}^{(0)} + \underline{f})^T \partial \underline{d} \quad (5.1-14)$$

From the Equation (5.1-8), the differential of the strain can be calculated as shown in Equation (5.1-15).

$$\partial \varepsilon_x = \underline{A}_1 \partial \underline{d} + \underline{d}^T \underline{B}^T \underline{B} \partial \underline{d} = (\underline{A}_1 + \underline{d}^T \underline{B}^T \underline{B}) \partial \underline{d} \quad (5.1-15)$$

Then, replacing Equation (5.1-15) in Equation (5.1-14), and at the same time, having a constant cross area A , it is also possible to replace dV with the area A times the length L , so it becomes Equation (5.1-16).

$$AL\left[(\sigma_x^{(0)} + \sigma_x)(\underline{A}_1 + \underline{d}^T \underline{B}^T \underline{B})\right] \partial \underline{d} = (\underline{f}^{(0)} + \underline{f})^T \partial \underline{d} \quad (5.1-16)$$

In Equation (5.1-16), $\partial \underline{d}$ represents the arbitrary virtual displacement and it can be eliminated from both sides resulting on Equation (5.1-17).

$$AL\left[(\sigma_x^{(0)} + \sigma_x)(\underline{A}_1 + \underline{d}^T \underline{B}^T \underline{B})\right] = (\underline{f}^{(0)} + \underline{f})^T \quad (5.1-17)$$

Substituting Equation (5.1-8) into Equation (5.1-11), Equation (5.1-18) can be obtained.

$$\sigma_x = E \varepsilon_x = E \left(\underline{A}_1 \underline{d} + \frac{1}{2} \underline{d}^T \underline{B}^T \underline{B} \underline{d} \right) = E \underline{A}_1 \underline{d} + \frac{1}{2} E \underline{d}^T \underline{B}^T \underline{B} \underline{d} \quad (5.1-18)$$

After that, Equation (5.1-18) can be substituted into Equation (5.1-17) resulting in Equation (5.1-19).

$$\begin{aligned} (\underline{f}^{(0)} + \underline{f})^T = \\ AL \left\{ \left(\sigma_x^{(0)} + E \underline{A}_1 \underline{d} + \frac{1}{2} E \underline{d}^T \underline{B}^T \underline{B} \underline{d} \right) x (\underline{A}_1 + \underline{d}^T \underline{B}^T \underline{B}) \right\} \end{aligned} \quad (5.1-19)$$

In Equation (5.1-19) higher order terms can be eliminated and by transposing both sides, Equation (5.1-20) can be obtained.

$$\begin{aligned} \underline{f}^{(0)} + \underline{f} = AL (\underline{A}_1^T \sigma_x^{(0)}) + \\ AL (\sigma_x^{(0)} \underline{B}^T \underline{B}) \underline{d} + AL E (\underline{A}_1^T \underline{A}_1) \underline{d} + \text{higher order terms} \end{aligned} \quad (5.1-20)$$

Equation (5.1-21) represents the residual forces caused by eliminated higher order terms.

$$\underline{r} = AL \underline{A}_1^T \sigma_x^{(0)} - \underline{f}^{(0)} \quad (5.1-21)$$

Substituting Equation (5.1-21) into Equation (5.1-20), the tangential

stiffness equation of the element is driven as shown in Equation (5.1-22).

$$\underline{f} - \underline{r} = A L E \left(\underline{A}_1^T \underline{A}_1 \right) \underline{d} + A L \left(\sigma_x^{(0)} \underline{B}^T \underline{B} \right) \underline{d} = (\underline{k}_E + \underline{k}_G) \underline{d} \quad (5.1-22)$$

Where Equation (5.1-23) is the elastic stiffness matrix and Equation (5.1-24) is the geometric stiffness matrix of the element.

$$\underline{k}_E = A L E \left(\underline{A}_1^T \underline{A}_1 \right) \quad (5.1-23)$$

$$\underline{k}_G = A L \left(\sigma_x^{(0)} \underline{B}^T \underline{B} \right) \quad (5.1-24)$$

5.1.5. Coordinate transformation

In Equation (5.1-25) the force vector for each node is defined in the global coordinate system of the structure. In the same way, residual force vector and displacement vector are also shown in Equations (5.1-26) and (5.1-27), respectively.

$$\underline{F} = \left\{ \begin{matrix} \underline{F}_i \\ \underline{F}_j \end{matrix} \right\} \quad \underline{F}_{i(or j)} = \left\{ \begin{matrix} F_x \\ F_y \\ F_z \end{matrix} \right\}_{i(or j)} \quad (5.1-25)$$

$$\underline{R} = \left\{ \begin{matrix} \underline{R}_i \\ \underline{R}_j \end{matrix} \right\} \quad \underline{R}_{i(or j)} = \left\{ \begin{matrix} R_x \\ R_y \\ R_z \end{matrix} \right\}_{i(or j)} \quad (5.1-26)$$

$$\underline{D} = \begin{Bmatrix} \underline{D}_i \\ \underline{D}_j \end{Bmatrix} \quad \underline{D}_{i(or j)} = \begin{Bmatrix} D_x \\ D_y \\ D_z \end{Bmatrix}_{i(or j)} \quad (5.1-27)$$

Using the transformation matrix T the relation between the local and the global coordinate systems for the above vectors is described in Equation (5.1-28).

$$\underline{f} = \underline{T}F, \quad \underline{r} = \underline{T}R, \quad \underline{d} = \underline{T}D \quad (5.1-28)$$

Being the transformation matrix T as in Equation (5.1-29).

$$\underline{T} = \begin{bmatrix} \underline{T}_0 & 0 \\ 0 & \underline{T}_0 \end{bmatrix} \quad (5.1-29)$$

Where,

$$\underline{T}_0 = \begin{bmatrix} l & m & n \\ -\frac{m}{\sqrt{l^2 + m^2}} & \frac{l}{\sqrt{l^2 + m^2}} & 0 \\ -\frac{ln}{\sqrt{l^2 + m^2}} & -\frac{mn}{\sqrt{l^2 + m^2}} & \sqrt{l^2 + m^2} \end{bmatrix} \quad (5.1-30)$$

And,

$$l = \frac{1}{\Delta} (X_j - X_i), \quad m = \frac{1}{\Delta} (Y_j - Y_i), \quad n = \frac{1}{\Delta} (Z_j - Z_i) \\ \Delta = \sqrt{(X_j - X_i)^2 + (Y_j - Y_i)^2 + (Z_j - Z_i)^2} \quad (5.1-31)$$

5.1.6. Stiffness equation

Substituting Equation (5.1-28) into Equation (5.1-22), Equation (5.1-32) can be obtained.

$$\underline{T}(\underline{F} - \underline{R}) = [\underline{k}_E + \underline{k}_G] \underline{T} \underline{D} \quad (5.1-32)$$

Therefore, the stiffness matrix of the incremental domain in the global coordinate system is described in Equation (5.1-33)

$$\underline{F} - \underline{R} = [\underline{K}_E + \underline{K}_G] \underline{D} \quad (5.1-33)$$

Where the elastic stiffness matrix and geometric stiffness matrix in the global coordinate system are defined in Equations (5.1-34), (5.1-35) and (5.1-36).

$$\begin{aligned} \underline{K}_E &= \underline{T}^T \underline{k}_E \underline{T} \\ \underline{K}_G &= \underline{T}^T \underline{k}_G \underline{T} \end{aligned} \quad (5.1-34)$$

Where,

$$\underline{K}_E = A I E \begin{bmatrix} b_1^2 l^2 & b_1^2 l m & b_1^2 l n & b_1 b_2 l^2 & b_1 b_2 l m & b_1 b_2 l n \\ b_1^2 l m & b_1^2 m^2 & b_1^2 m n & b_1 b_2 l m & b_1 b_2 m^2 & b_1 b_2 m n \\ b_1^2 l n & b_1^2 m n & b_1^2 n^2 & b_1 b_2 l n & b_1 b_2 m n & b_1 b_2 n^2 \\ b_1 b_2 l^2 & b_1 b_2 l m & b_1 b_2 l n & b_2^2 l^2 & b_2^2 l m & b_2^2 l n \\ b_1 b_2 l m & b_1 b_2 m^2 & b_1 b_2 m n & b_2^2 l m & b_2^2 m^2 & b_2^2 m n \\ b_1 b_2 l n & b_1 b_2 m n & b_1 b_2 n^2 & b_2^2 l n & b_2^2 m n & b_2^2 n^2 \end{bmatrix}$$

where,

$$b_1 = \frac{\partial N_i}{\partial x}, \quad b_2 = \frac{\partial N_j}{\partial x} \quad (5.1-35)$$

And,

$$\underline{K}_G = A l \sigma_x^{(0)} \begin{bmatrix} K_{11} & K_{12} & K_{13} & K_{14} & K_{15} & K_{16} \\ K_{21} & K_{22} & K_{23} & K_{24} & K_{25} & K_{26} \\ K_{31} & K_{32} & K_{33} & K_{34} & K_{35} & K_{36} \\ K_{41} & K_{42} & K_{43} & K_{44} & K_{45} & K_{46} \\ K_{51} & K_{52} & K_{53} & K_{54} & K_{55} & K_{56} \\ K_{61} & K_{62} & K_{63} & K_{64} & K_{65} & K_{66} \end{bmatrix} \quad (5.1-36)$$

Where,

$$\begin{aligned} K_{11} &= b_1^2 \left(l^2 + \frac{m^2}{\Delta^2} + \frac{l^2 n^2}{\Delta^2} \right); & K_{12} &= b_1^2 \left(l m - \frac{l m}{\Delta^2} - \frac{l m n^2}{\Delta^2} \right) \\ K_{13} &= K_{16} = K_{34} = K_{46} = 0; & K_{14} &= b_1 b_2 \left(l^2 + \frac{m^2}{\Delta^2} + \frac{l^2 n^2}{\Delta^2} \right) \\ K_{15} &= b_1 b_2 \left(l m - \frac{l m}{\Delta^2} - \frac{l m n^2}{\Delta^2} \right); & K_{22} &= b_1^2 \left(m^2 + \frac{l^2}{\Delta^2} + \frac{m^2 n^2}{\Delta^2} \right) \\ K_{23} &= 2b_1^2 m n; & K_{25} &= b_1 b_2 \left(m^2 + \frac{l^2}{\Delta^2} + \frac{m^2 n^2}{\Delta^2} \right) \\ K_{26} &= K_{35} = 2b_1 b_2 m n; & K_{33} &= b_1^2 (n^2 + \Delta^2) \\ K_{36} &= b_1 b_2 (n^2 + \Delta^2); & K_{44} &= b_2^2 \left(l^2 + \frac{m^2}{\Delta^2} + \frac{l^2 n^2}{\Delta^2} \right) \\ K_{45} &= b_2^2 \left(l m - \frac{l m}{\Delta^2} - \frac{l m n^2}{\Delta^2} \right); & K_{55} &= b_2^2 \left(m^2 + \frac{l^2}{\Delta^2} + \frac{m^2 n^2}{\Delta^2} \right) \\ K_{56} &= 2b_2^2 m n; & K_{66} &= b_2^2 (n^2 + \Delta^2) \end{aligned}$$

5.1.7. Wrinkling of cable element

Wrinkling problem in the cable is treated. When an element with negative stress appears, it is modified as in Equations (5.1-37) and (5.1-38), so only tension occurs in the cable.

$$\sigma_{x'} = 0 \quad (5.1-37)$$

$$E' = 0 \quad (5.1-38)$$

5.2. Membrane element equations

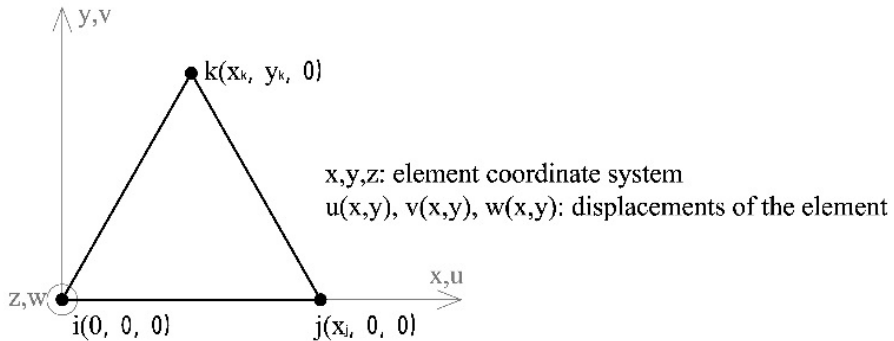


Figure 5.2-1: Local coordinates system and displacements of a membrane element.

Membrane elements are defined as 3 node elements. Figure 5.2-1 shows a typical triangular element in the local coordinate system (x, y, z) . As also shown in the Figure, each node is named i, j and k . The node i is always considered as the local origin of each element with coordinates $(0, 0, 0)$, and the node j defines the direction of the local axis x . In this way, the nodal displacements are defined in the local plane x - y as $u(x, y)$, $v(x, y)$ and $w(x, y)$.

5.2.1. Shape function

The displacements and force vectors in each local direction for the 3 nodes are defined in Equations (5.2-1) and (5.2-2) respectively.

$$\{\underline{d}_x\} = \begin{pmatrix} d_{xi} \\ d_{xj} \\ d_{xk} \end{pmatrix}, \quad \{\underline{d}_y\} = \begin{pmatrix} d_{yi} \\ d_{yj} \\ d_{yk} \end{pmatrix}, \quad \{\underline{d}_z\} = \begin{pmatrix} d_{zi} \\ d_{zj} \\ d_{zk} \end{pmatrix} \quad (5.2-1)$$

$$\{\underline{f}_x\} = \begin{pmatrix} f_{xi} \\ f_{xj} \\ f_{xk} \end{pmatrix}, \quad \{\underline{f}_y\} = \begin{pmatrix} f_{yi} \\ f_{yj} \\ f_{yk} \end{pmatrix}, \quad \{\underline{f}_z\} = \begin{pmatrix} f_{zi} \\ f_{zj} \\ f_{zk} \end{pmatrix} \quad (5.2-2)$$

Expressing the global displacements $u(x, y)$, $v(x, y)$ and $w(x, y)$ linearly over the element, the displacement functions are assumed as in Equation (5.2-3) where the nine coefficients α, β, γ are unspecified at this stage.

$$\begin{aligned} u(x, y) &= \alpha_1 + \alpha_2 x + \alpha_3 y \\ v(x, y) &= \beta_1 + \beta_2 x + \beta_3 y \\ w(x, y) &= \gamma_1 + \gamma_2 x + \gamma_3 y \end{aligned} \quad (5.2-3)$$

Then, it is possible to find the relationship between local and global displacements by applying the boundary conditions defined in Fig. 5.2-1. In this way, the displacement vector in the x direction \underline{d}_x can be written as a function of $\alpha_1, \alpha_2, \alpha_3$ as expressed in Equation (5.2-4).

$$\begin{aligned} d_{xi} &= u(0, 0) = \alpha_1 \\ d_{xj} &= u(x_j, 0) = \alpha_1 + \alpha_2 x_j \\ d_{xk} &= u(x_k, y_k) = \alpha_1 + \alpha_2 x_k + \alpha_3 y_k \end{aligned} \quad (5.2-4)$$

Equation (5.2-5) is the matrix form of Equation (5.2-4).

$$\begin{pmatrix} d_{xi} \\ d_{xj} \\ d_{xk} \end{pmatrix} = \begin{bmatrix} 1 & 0 & 0 \\ 1 & x_j & 0 \\ 1 & x_k & y_k \end{bmatrix} \begin{pmatrix} \alpha_1 \\ \alpha_2 \\ \alpha_3 \end{pmatrix} \quad (5.2-5)$$

From Equation (5.2-5), the geometry matrix $\underline{\Phi}$ is defined as the relationship between the local displacement vector in the x direction \underline{d}_x and the coefficient vector $\underline{\alpha}$ as shown in Equation (5.2-6).

$$\{\underline{d}_x\} = [\underline{\Phi}]\{\underline{\alpha}\} \quad (5.2-6)$$

By applying the boundary conditions for vectors \underline{d}_y and \underline{d}_z , the same relationship can be obtained using the geometry matrix $\underline{\Phi}$ (Equations (5.2-7) and (5.2-8)).

$$\{\underline{d}_y\} = [\underline{\Phi}]\{\underline{\beta}\} \quad (5.2-7)$$

$$\{\underline{d}_z\} = [\underline{\Phi}]\{\underline{\gamma}\} \quad (5.2-8)$$

The geometry matrix determinant has the property to be equal to 2 times the area of the triangle element as in Equation (5.2-9) due to the local coordinate definition shown in Fig. 5.2-1.

$$|\underline{\Phi}| = 2A_m = x_j y_k \quad (5.2-9)$$

Using Cramer's method the inverse of the geometry matrix can be obtained as illustrated in Equation (5.1-10).

$$[\underline{\Phi}]^{-1} = \begin{bmatrix} 1 & 0 & 0 \\ -\frac{1}{x_j} & \frac{1}{x_j} & 0 \\ \frac{x_k - x_j}{x_j y_k} & -\frac{x_k}{x_j y_k} & \frac{x_j}{x_j y_k} \end{bmatrix} \quad (5.2-10)$$

To simplify the terms of the inverse, they are named with roman letters as in Equation (5.2-11), and this letters are just equivalent as each term (Equation (5.2-12)).

$$[\underline{\Phi}]^{-1} = \begin{bmatrix} a_1 & 0 & 0 \\ b_1 & b_2 & 0 \\ c_1 & c_2 & c_3 \end{bmatrix} \quad (5.2-11)$$

$$\begin{aligned} a_1 &= 1 \\ b_1 &= -\frac{1}{x_j}, \quad b_2 = \frac{1}{x_j} \\ c_1 &= \frac{x_k - x_j}{x_j y_k}, \quad c_2 = -\frac{x_k}{x_j y_k}, \quad c_3 = \frac{x_j}{x_j y_k} \end{aligned} \quad (5.2-12)$$

Now, the values of the variables $\underline{\alpha}$, $\underline{\beta}$ and $\underline{\gamma}$ can be found by multiplying the displacement vectors in each direction by the inverse of the geometry matrix as shown in Equation (5.2-13).

$$\begin{aligned} \{\underline{\alpha}\} &= [\underline{\Phi}]^{-1} \{\underline{d}_x\} \\ \{\underline{\beta}\} &= [\underline{\Phi}]^{-1} \{\underline{d}_y\} \\ \{\underline{\gamma}\} &= [\underline{\Phi}]^{-1} \{\underline{d}_z\} \end{aligned} \quad (5.2-13)$$

In Equation (5.2-14), the values obtained for $\underline{\alpha}$, $\underline{\beta}$ and $\underline{\gamma}$ are replaced in the displacement assumption equation that was made (Equation (5.2-3)) to obtain the final displacement function.

$$\begin{aligned} u(x, y) &= a_1 d_{xi} + (b_1 d_{xi} + b_2 d_{xj})x + (c_1 d_{xi} + c_2 d_{xj} + c_3 d_{xk})y \\ v(x, y) &= a_1 d_{yi} + (b_1 d_{yi} + b_2 d_{yj})x + (c_1 d_{yi} + c_2 d_{yj} + c_3 d_{yk})y \\ w(x, y) &= a_1 d_{zi} + (b_1 d_{zi} + b_2 d_{zj})x + (c_1 d_{zi} + c_2 d_{zj} + c_3 d_{zk})y \end{aligned} \quad (5.2-14)$$

Besides, organizing the terms of Equation (5.2-14) as shown in Equation (5.2-15), the shape function \underline{N} is obtained as in Equation (5.2-16).

$$\begin{aligned} u(x, y) &= [\underline{N}] \{ \underline{d}_x \} \\ v(x, y) &= [\underline{N}] \{ \underline{d}_y \} \\ w(x, y) &= [\underline{N}] \{ \underline{d}_z \} \end{aligned} \quad (5.2-15)$$

$$[\underline{N}] = \begin{bmatrix} N_1 \\ N_2 \\ N_3 \end{bmatrix}, \quad \text{where} \quad \begin{cases} N_1 = a_1 + b_1 x + c_1 y \\ N_2 = b_2 x + c_2 y \\ N_3 = c_3 y \end{cases} \quad (5.2-16)$$

5.2.2. Displacement-strain relationship

The small-deflection theory of linear elasticity is inapplicable as in the cable element, and the quadratic terms in the displacement-strain relations must be taken into account. The nonlinear displacement-strain relations may be expressed as in Equation (5.2-17).

$$\begin{aligned} \varepsilon_x &= \frac{\partial u}{\partial x} + \frac{1}{2} \left[\left(\frac{\partial u}{\partial x} \right)^2 + \left(\frac{\partial v}{\partial x} \right)^2 + \left(\frac{\partial w}{\partial x} \right)^2 \right] \\ \varepsilon_y &= \frac{\partial v}{\partial y} + \frac{1}{2} \left[\left(\frac{\partial u}{\partial y} \right)^2 + \left(\frac{\partial v}{\partial y} \right)^2 + \left(\frac{\partial w}{\partial y} \right)^2 \right] \\ \gamma_{xy} &= \frac{\partial v}{\partial x} + \frac{\partial u}{\partial y} + \frac{\partial u}{\partial x} \frac{\partial u}{\partial y} + \frac{\partial v}{\partial x} \frac{\partial v}{\partial y} + \frac{\partial w}{\partial x} \frac{\partial w}{\partial y} \end{aligned} \quad (5.2-17)$$

Substituting the displacement function from Equation (5.2-14) into Equation (5.1-17), Equation (5.1-18) is obtained.

$$\begin{aligned}
\varepsilon_x &= b_1 d_{xi} + b_2 d_{xj} \\
&+ \frac{1}{2} \left[(b_1 d_{xi} + b_2 d_{xj})^2 + (b_1 d_{yi} + b_2 d_{yj})^2 + (b_1 d_{zi} + b_2 d_{zj})^2 \right] \\
\varepsilon_y &= c_1 d_{yi} + c_2 d_{yj} + c_3 d_{yk} + \frac{1}{2} (c_1 d_{xi} + c_2 d_{xj} + c_3 d_{xk})^2 \\
&+ \frac{1}{2} (c_1 d_{yi} + c_2 d_{yj} + c_3 d_{yk})^2 + \frac{1}{2} (c_1 d_{zi} + c_2 d_{zj} + c_3 d_{zk})^2 \\
\gamma_{xy} &= (b_1 d_{yi} + b_2 d_{yj}) + (c_1 d_{xi} + c_2 d_{xj} + c_3 d_{xk}) \\
&+ (b_1 d_{xi} + b_2 d_{xj}) (c_1 d_{xi} + c_2 d_{xj} + c_3 d_{xk}) \\
&+ (b_1 d_{yi} + b_2 d_{yj}) (c_1 d_{yi} + c_2 d_{yj} + c_3 d_{yk}) \\
&+ (b_1 d_{zi} + b_2 d_{zj}) (c_1 d_{zi} + c_2 d_{zj} + c_3 d_{zk})
\end{aligned} \tag{5.2-18}$$

To simplify this relationship, it can be written in its matrix form as in Equation (5.2-19).

$$\begin{Bmatrix} \varepsilon_x \\ \varepsilon_y \\ \gamma_{xy} \end{Bmatrix} = [\underline{A}] \{ \underline{d} \} + \begin{Bmatrix} \frac{1}{2} \underline{d}^T \underline{B}^T \underline{B} \underline{d} \\ \frac{1}{2} \underline{d}^T \underline{C}^T \underline{C} \underline{d} \\ \underline{d}^T \underline{B}^T \underline{C} \underline{d} \end{Bmatrix} \tag{5.2-19}$$

Where \underline{d} is the total displacement and is rearranged as in Equation (5.2-20), \underline{A} is the strain-displacement matrix corresponding to the small deflection and can be divided into the rows \underline{A}_1 , \underline{A}_2 , and \underline{A}_3 as shown in Equation (5.2-21) for later calculations, and \underline{B} and \underline{C} are the strain-displacement matrices due to the change in geometry for large displacement (Equation (5.2-22)).

$$\{ \underline{d} \} = \begin{Bmatrix} \underline{d}_i \\ \underline{d}_j \\ \underline{d}_k \end{Bmatrix}, \quad \{ \underline{d}_i \} = \begin{Bmatrix} d_{xi} \\ d_{yi} \\ d_{zi} \end{Bmatrix}, \quad \{ \underline{d}_j \} = \begin{Bmatrix} d_{xj} \\ d_{yj} \\ d_{zj} \end{Bmatrix}, \quad \{ \underline{d}_k \} = \begin{Bmatrix} d_{xk} \\ d_{yk} \\ d_{zk} \end{Bmatrix} \tag{5.2-20}$$

$$[\underline{A}] = \begin{bmatrix} b_1 & 0 & 0 & b_2 & 0 & 0 & 0 & 0 & 0 \\ 0 & c_1 & 0 & 0 & c_2 & 0 & 0 & c_3 & 0 \\ c_1 & b_1 & 0 & c_2 & b_2 & 0 & c_3 & 0 & 0 \end{bmatrix} \equiv \begin{Bmatrix} \underline{A}_1 \\ \underline{A}_2 \\ \underline{A}_3 \end{Bmatrix} \quad (5.2-21)$$

$$[\underline{B}] = \begin{bmatrix} b_1 & 0 & 0 & b_2 & 0 & 0 & 0 & 0 & 0 \\ 0 & b_1 & 0 & 0 & b_2 & 0 & 0 & 0 & 0 \\ 0 & 0 & b_1 & 0 & 0 & b_2 & 0 & 0 & 0 \end{bmatrix}$$

$$[\underline{C}] = \begin{bmatrix} c_1 & 0 & 0 & c_2 & 0 & 0 & c_3 & 0 & 0 \\ 0 & c_1 & 0 & 0 & c_2 & 0 & 0 & c_3 & 0 \\ 0 & 0 & c_1 & 0 & 0 & c_2 & 0 & 0 & c_3 \end{bmatrix} \quad (5.2-22)$$

5.2.3. Stress-strain relationship

The stress-strain relationship is defined in Equation (5.2-23) for the 3 directions where E_m is the Young's modulus of the membrane and ν is the Poisson's ratio.

$$\begin{Bmatrix} \sigma_x \\ \sigma_y \\ \tau_{xy} \end{Bmatrix} = \frac{E_m}{1-\nu^2} \begin{bmatrix} 1 & \nu & 0 \\ \nu & 1 & 0 \\ 0 & 0 & \frac{1-\nu}{2} \end{bmatrix} \begin{Bmatrix} \epsilon_x \\ \epsilon_y \\ \gamma_{xy} \end{Bmatrix} \quad (5.2-23)$$

With the previous relationship, \underline{E} will be defined as the elastic matrix (Equation (5.2-24)).

$$\{\underline{\sigma}\} = [\underline{E}] \{\underline{\epsilon}\} \quad (5.2-24)$$

5.2.4. Equation of equilibrium using the principle of virtual work

The equilibrium equations for a single element in the local coordinate system may now be obtained following the principle of virtual work as in Equation (5.2-25). Similarly to the case of the cable element, initial conditions have to be included such as the initial stress, $\sigma_x^{(0)}$, $\sigma_y^{(0)}$, $\tau_{xy}^{(0)}$, and the initial force vector $\underline{f}^{(0)}$.

$$\begin{aligned} \iiint_V \left[(\sigma_x^{(0)} + \sigma_x) \partial \varepsilon_x + (\sigma_y^{(0)} + \sigma_y) \partial \varepsilon_y + (\tau_{xy}^{(0)} + \tau_{xy}) \partial \gamma_{xy} \right] dV \\ = (\underline{f}^{(0)} + \underline{f})^T \partial \underline{d} \end{aligned} \quad (5.2-25)$$

From Equation (5.2-19), the differential of the strains $\partial \varepsilon_x$, $\partial \varepsilon_y$, $\partial \gamma_{xy}$ can be calculated as shown in Equation (5.2-26).

$$\begin{aligned} \partial \varepsilon_x &= [\underline{A}_1] \partial \underline{d} + [\underline{d}^T \underline{B}^T \underline{B}] \partial \underline{d} \\ \partial \varepsilon_y &= [\underline{A}_2] \partial \underline{d} + [\underline{d}^T \underline{C}^T \underline{C}] \partial \underline{d} \\ \partial \gamma_{xy} &= [\underline{A}_3] \partial \underline{d} + \underline{d}^T [\underline{C}^T \underline{C} + \underline{B}^T \underline{C}] \partial \underline{d} \end{aligned} \quad (5.2-26)$$

Then, the strain differentials of Equation (5.2-26) can be replaced in Equation (5.2-25), obtaining Equation (5.2-27). Besides, the virtual displacement $\partial \underline{d}$ can be eliminated from both sides of the equation and the volume of the membrane can be replaced by the area times the height of the triangular element ($A_m h_m$).

$$\begin{aligned}
& A_m h_m (\sigma_x^{(0)} + \sigma_x) \left([\underline{A}_1] + [\underline{d}^T \underline{B}^T \underline{B}] \right) \\
& + A_m h_m (\sigma_y^{(0)} + \sigma_y) \left([\underline{A}_2] + [\underline{d}^T \underline{C}^T \underline{C}] \right) \\
& + A_m h_m (\tau_{xy}^{(0)} + \tau_{xy}) \left([\underline{A}_3] + \underline{d}^T [\underline{C}^T \underline{B} + \underline{B}^T \underline{C}] \right) = (\underline{f}^{(0)} + \underline{f})^T
\end{aligned} \tag{5.2-27}$$

Equation (5.2-27) can be simplified and rearranged as shown in Equation (5.2-28).

$$\begin{aligned}
\underline{f}^{(0)} + \underline{f} &= A_m h_m \left(\underline{A}^T \underline{\sigma}^{(0)} \right) \\
& + A_m h_m \left[\sigma_x^{(0)} \underline{B}^T \underline{B} + \sigma_y^{(0)} \underline{C}^T \underline{C} + \tau_{xy}^{(0)} (\underline{C}^T \underline{B} + \underline{B}^T \underline{C}) \right] \underline{d} \\
& + A_m h_m \left[\underline{A}^T \underline{E} \underline{A} \right] \underline{d}
\end{aligned} \tag{5.2-28}$$

Where $\underline{\sigma}^{(0)}$ is defined as the initial stress vector (Equation (5.2-29)).

$$\left\{ \underline{\sigma}^{(0)} \right\} = \begin{Bmatrix} \sigma_x^{(0)} \\ \sigma_y^{(0)} \\ \tau_{xy}^{(0)} \end{Bmatrix} \tag{5.2-29}$$

By eliminating higher order terms, in Equation (5.2-30) the residual force \underline{r} vector is defined.

$$\underline{r} = A_m h_m \cdot \underline{A}^T \underline{\sigma}^{(0)} - \underline{f}^{(0)} \tag{5.2-30}$$

Substituting Equation (5.2-30) into Equation (5.2-28), the tangential stiffness equation of the element is driven as shown in Equation (5.2-31).

$$\underline{f} - \underline{r} = [\underline{k}_E + \underline{k}_G] \underline{d} \tag{5.2-31}$$

Where \underline{k}_E represent the local elastic stiffness matrix as in Equation (5.2-32) and \underline{k}_G the local geometric stiffness matrix as in Equation (5.2-33).

$$\underline{k}_E = A_m h_m \left[\underline{A}^T \underline{E} \underline{A} \right] \quad (5.2-32)$$

$$\underline{k}_G = A_m h_m \left[\sigma_x^{(0)} \underline{B}^T \underline{B} + \sigma_y^{(0)} \underline{C}^T \underline{C} + \tau_{xy}^{(0)} \left(\underline{C}^T \underline{B} + \underline{B}^T \underline{C} \right) \right] \quad (5.2-33)$$

The global stiffness equation represented in Equation (5.2-34) can be obtained by using the transformation matrix \underline{T} . Furthermore, this transformation matrix can be also used to drive the relationship between the global and local elastic and geometric matrix is as in Equation (5.2-35).

$$\underline{F} - \underline{R} = \left[\underline{K}_E + \underline{K}_G \right] \underline{D} \quad (5.2-34)$$

$$\begin{aligned} \underline{K}_E &= \underline{T}^T \underline{k}_E \underline{T} \\ \underline{K}_G &= \underline{T}^T \underline{k}_G \underline{T} \end{aligned} \quad (5.2-35)$$

5.2.5. Coordinate transformation and global stiffness equation

To drive the transformation matrix \underline{T} , a transformation from the local axis (x, y, z as shown in Fig. 5.2-1) to the global axis (X, Y, Z) is needed. For that reason, firstly the coordinates of the nodes i, j, k have to be defined in the global axis. As shown in Equation (5.2-36), the vector \underline{X}_i will represent the coordinates of the node i in the global coordinates systems X, Y, Z , and in the same way \underline{X}_j and \underline{X}_k will represent j and k .

$$\underline{X}_i = \begin{Bmatrix} X_i \\ Y_i \\ Z_i \end{Bmatrix}, \quad \underline{X}_j = \begin{Bmatrix} X_j \\ Y_j \\ Z_j \end{Bmatrix}, \quad \underline{X}_k = \begin{Bmatrix} X_k \\ Y_k \\ Z_k \end{Bmatrix} \quad (5.2-36)$$

Next step is defining the vectors \underline{a} and \underline{b} in the global axis as in

Equation (5.2-37) that represent the geometry of the membrane triangular element with the vectors \vec{ij} and \vec{ik} respectively.

$$\underline{a} = X_j - X_i, \quad \underline{b} = X_k - X_i \quad (5.2-37)$$

Now it is possible to drive each unit vector of the three directions of the local axis in the global axis using the geometry of \underline{a} and \underline{b} as explained in Equation (5.2-38).

$$\underline{i} = \frac{\underline{a}}{|\underline{a}|}, \quad \underline{k} = \frac{\underline{a} \times \underline{b}}{|\underline{a} \times \underline{b}|}, \quad \underline{j} = \underline{k} \times \underline{i} \quad (5.2-38)$$

Using a unit vector \underline{e} in the global axis, Equation (5.2-39) and (5.2-40) show the rewritten vectors \underline{a} and \underline{b} with all the terms in each direction.

$$\underline{a} = (X_j - X_i)e_x + (Y_j - Y_i)e_y + (Z_j - Z_i)e_z \quad (5.2-39)$$

$$\underline{b} = (X_k - X_i)e_x + (Y_k - Y_i)e_y + (Z_k - Z_i)e_z \quad (5.2-40)$$

After that, the calculations of the Equation (5.2-38) can be carried out as in Equations (5.2-41), (5.2-42) and (5.2-43).

$$\underline{a} \times \underline{b} = \begin{bmatrix} e_x & e_y & e_z \\ (X_j - X_i) & (Y_j - Y_i) & (Z_j - Z_i) \\ (X_k - X_i) & (Y_k - Y_i) & (Z_k - Z_i) \end{bmatrix} = \Delta_x e_x + \Delta_y e_y + \Delta_z e_z \quad (5.2-41)$$

$$\begin{aligned} \Delta_x &= (Y_j - Y_i)(Z_k - Z_i) - (Y_k - Y_i)(Z_j - Z_i) \\ \Delta_y &= (X_k - X_i)(Z_j - Z_i) - (X_j - X_i)(Z_k - Z_i) \\ \Delta_z &= (X_j - X_i)(Y_k - Y_i) - (X_k - X_i)(Y_j - Y_i) \end{aligned} \quad (5.2-42)$$

$$\begin{aligned} l_{ij} &= \sqrt{(X_j - X_i)^2 + (Y_j - Y_i)^2 + (Z_j - Z_i)^2} \\ \Delta &= \sqrt{\Delta_x^2 + \Delta_y^2 + \Delta_z^2} \end{aligned} \quad (5.2-43)$$

Substituting and operating in Equation (5.2-38), Equations (5.2-44), (5.2-45) and (5.2-46) are obtained.

$$\underline{i} = \frac{(X_j - X_i)}{l_{ij}} = \lambda_x e_x + \lambda_y e_y + \lambda_z e_z \quad (5.2-44)$$

$$\underline{k} = \frac{(a \times b)}{\Delta} = v_x e_x + v_y e_y + v_z e_z \quad (5.2-45)$$

$$\underline{j} = \underline{k} \times \underline{i} = u_x e_x + u_y e_y + u_z e_z \quad (5.2-46)$$

Equation (5.2-47), along with Equation (5.2-48), represents the combination of the previous equations into its matrix form.

$$\begin{Bmatrix} X_i \\ Y_i \\ Z_i \end{Bmatrix} = \begin{bmatrix} \lambda_x & \lambda_y & \lambda_z \\ u_x & u_y & u_z \\ v_x & v_y & v_z \end{bmatrix} \begin{Bmatrix} e_x \\ e_y \\ e_z \end{Bmatrix} \quad (5.2-47)$$

Where,

$$\lambda_x = \frac{X_j - X_i}{l_{ij}}, \quad \lambda_y = \frac{Y_j - Y_i}{l_{ij}}, \quad \lambda_z = \frac{Z_j - Z_i}{l_{ij}}$$

$$v_x = \frac{\Delta_x}{\Delta}, \quad v_y = \frac{\Delta_y}{\Delta}, \quad v_z = \frac{\Delta_z}{\Delta}$$

$$u_x = \lambda_z v_y - \lambda_y v_z, \quad u_y = \lambda_x v_z - \lambda_z v_x, \quad u_z = \lambda_y v_x - \lambda_x v_y \quad (5.2-48)$$

In this way, the unit vector \underline{i} in the local x direction is transformed into the global coordinate system, and \underline{T}_n is defined as the transformation of one single direction or node (Equation (5.2-49)).

$$\{\underline{i}\} = [\underline{T}_n] \{\underline{e}\} \quad (5.2-49)$$

Using the transposed matrix of \underline{T}_n , the unit vector of the global coordinate system can be also transformed into the local coordinate system as in Equation (5.2-50).

$$\{\underline{e}\} = [\underline{T}_n]^T \{\underline{i}\} \quad (5.2-50)$$

Then, as shown in Equation (5.2-51), the whole transformation matrix \underline{T} is a 9 by 9 matrix with the \underline{T}_n terms in the diagonal that will transform each node vector from the global to the local axis or vice versa.

$$[\underline{T}] = \begin{bmatrix} \underline{T}_n & 0 & 0 \\ 0 & \underline{T}_n & 0 \\ 0 & 0 & \underline{T}_n \end{bmatrix} \quad (5.2-51)$$

Equations (5.2-52), (5.2-53) and (5.2-53) define the force, residual force and displacement in the global coordinate system respectively.

$$\underline{F} = \begin{Bmatrix} \underline{F}_i \\ \underline{F}_j \\ \underline{F}_k \end{Bmatrix} \quad \underline{F}_{i(or\ j\ or\ k)} = \begin{Bmatrix} F_x \\ F_y \\ F_z \end{Bmatrix}_{i(or\ j\ or\ k)} \quad (5.2-52)$$

$$\underline{R} = \begin{Bmatrix} \underline{R}_i \\ \underline{R}_j \\ \underline{R}_k \end{Bmatrix} \quad \underline{R}_{i(or\ j\ or\ k)} = \begin{Bmatrix} R_x \\ R_y \\ R_z \end{Bmatrix}_{i(or\ j\ or\ k)} \quad (5.2-53)$$

$$\underline{D} = \begin{Bmatrix} \underline{D}_i \\ \underline{D}_j \\ \underline{D}_k \end{Bmatrix} \quad \underline{D}_{i(or\ j\ or\ k)} = \begin{Bmatrix} D_x \\ D_y \\ D_z \end{Bmatrix}_{i(or\ j\ or\ k)} \quad (5.2-54)$$

Then, the transformation matrix \underline{T} is used to relate the global vectors of Equations (5.2-52), (5.2-53) and (5.2-53) to the local vectors as shown in Equation (5.2-55).

$$\underline{f} = [\underline{T}] \underline{F}, \quad \underline{r} = [\underline{T}] \underline{R}, \quad \underline{d} = [\underline{T}] \underline{D} \quad (5.2-55)$$

And the local stiffness equilibrium equation calculated in the previous section can be also transformed as explained in Equations (5.2-56) and (5.2-57) using the transformation matrix.

$$\underline{T}(\underline{F} - \underline{R}) = [\underline{k}_E + \underline{k}_G] \underline{T} \underline{D} \quad (5.2-56)$$

$$\underline{F} - \underline{R} = \underline{T}^T [\underline{k}_E + \underline{k}_G] \underline{T} \underline{D} = [\underline{K}_E + \underline{K}_G] \underline{D} \quad (5.2-57)$$

With \underline{K}_E and \underline{K}_G as the global elastic stiffness matrix and the global geometric stiffness matrix respectively, having a relationship with the local matrices as shown in Equation (5.2-58).

$$\begin{aligned} \underline{K}_E &= \underline{T}^T \underline{k}_E \underline{T} \\ \underline{K}_G &= \underline{T}^T \underline{k}_G \underline{T} \end{aligned} \quad (5.2-58)$$

Chapter 6. Nonlinear Analysis and Modeling of Tensile Structures

The fundamental basis of most computational systems used for the design of surface structures is some form of equilibrium modeling. In such systems the structure is discretized to form a finite element mesh with fixed topology but, with the exception of the fixed points, only approximate nodal coordinates. Depending on the particular finite element type used, element's internal forces can be determined and then summed at the node. Once external loads are applied, the residual out-of-balance nodal forces may be determined. Equilibrant nodal coordinate values can then be approached through a directed perturbation of the mesh based on these residual forces. One of the main advantages of using such a computational approach to form finding is that the subsequent prediction of member forces under both prestress and applied load is facilitated (Forster & Mollaert 2004).

In this chapter, the non-commercialized program used for the geometrically nonlinear analysis is described. Additionally, the modeling procedure for tensile structures is also explained including the factors to take into account in each step.

6.1. Nonlinear Analysis of Spatial Structures program (NASS)

NASS (Nonlinear Analysis of Spatial Structures) program is a non-commercialized program written in FORTRAN and developed by Professor Kim Seung Deog at Semyung University for the complete numerical analysis of spatial structures.

It uses geometrically nonlinear finite element analysis and includes the stiffness matrix calculation for the possible different elements that a spatial structure can present. At the same time, it offers the possibility to perform different types of analysis from the beginning (form-finding, stress-deformation and so on), and by the used of the Newton-Raphson method, a solution can be obtained for the type of analysis required.

As the program is coded in FORTRAN, a text data file is required for the input and the same type of data file is obtained after running the program for the output results.

In the following sections, the different charts for the general flow of the program are presented. Besides, as the analysis of this thesis is focused on cable and membrane elements, the charts of those elements are explained more in detail, as well as for the nonlinear analysis steps. Besides, general information about the input data required and output data obtained are also presented.

6.1.1. General chart

Figure 6.1-1 shows the synthesized general chart for the use of the program. Looking at it from a general perspective, it is possible to see the main flow that an analysis follows when running the program.

In this way, for a concrete input data file, firstly initial calculations take place to determine and allocate the strain and residual forces vectors as well as the control vector required for the connectivity between global and local axis. After that, a loop begins where one by one other important information is calculated; force vectors, stiffness matrix, displacements, reactions and strain and stress. Therefore, the sum of incremental values are completed and the new residual forces are calculated. After that, if the current step is lower than the number of steps inputted, the process is repeated as shown in Fig. 6.1-1. Otherwise, the residual force is compared with the allowed error, if this is not smaller than the error, then the loop is also repeated. But if the value is small enough, then the output data is written and the program stops.

However, to understand more in detail how the program works including the different element stiffness matrix calculations, a more detailed chart is presented in Fig. 6.1-2, which shows how each subroutine is called and what the exact flow of the program is. The main subroutines of the chart are labeled with letters. The first subroutines are for creating the matrices that are used during the analysis and clear the system. In subroutine C, all the data from the data file is read. Then, subroutine D defines the width of the band matrix and subroutine E

does the renumbering considering the boundary conditions input. In the subroutine F, the input data is written in the output file. But the most important subroutines are subroutines G and K.

Subroutine G is the one in charge of driving the stiffness matrix of the elements. Inside this subroutine different element subroutines can be called depending on the type of elements that the analysis model has. This includes plane, asymmetric, truss or cable, beam, membrane and shell elements. When this subroutine is completed the total stiffness matrix of the structure, including all elements, will be store in the global matrix. Further explanation about how the element stiffness subroutine work is in Section 6.1.2 of this thesis, for the target elements of cable and membrane, and Figs. 6.1-3 and 6.1-4 represent those element charts.

Subroutine K is the one that performs the static analysis of the structure. The program gives also the option of performing dynamic analysis, but this is not the scope of this research. For the static analysis, there is also the option of performing linear or nonlinear analysis.

Additionally, during the analysis, the stiffness subroutine G is called several times to modify the total stiffness matrix depending on the calculations, and to recalculate the residual forces or obtain the new stress.

In Section 6.1.3 and Fig. 6.1-5, the chart for the nonlinear static analysis is developed more in detail.

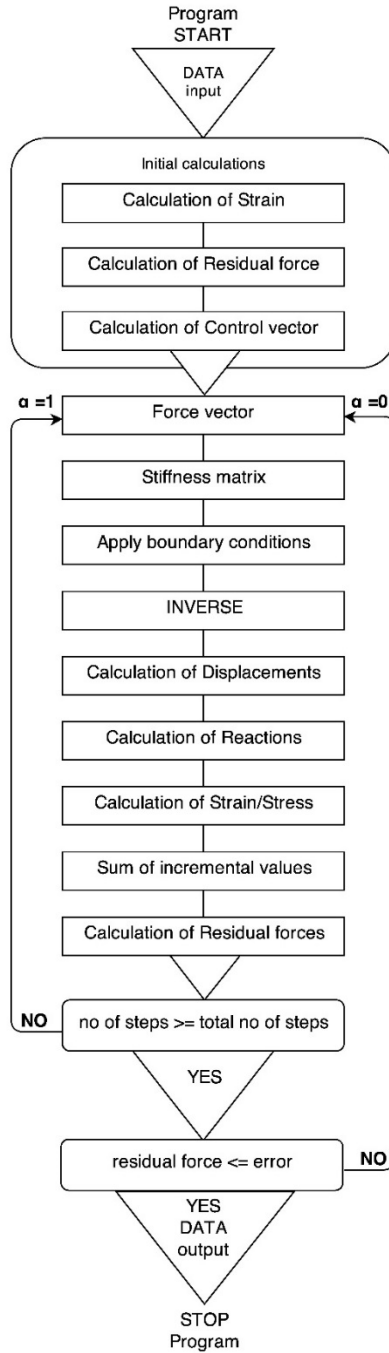


Figure 6.1-1 Synthesized general chart of NASS program

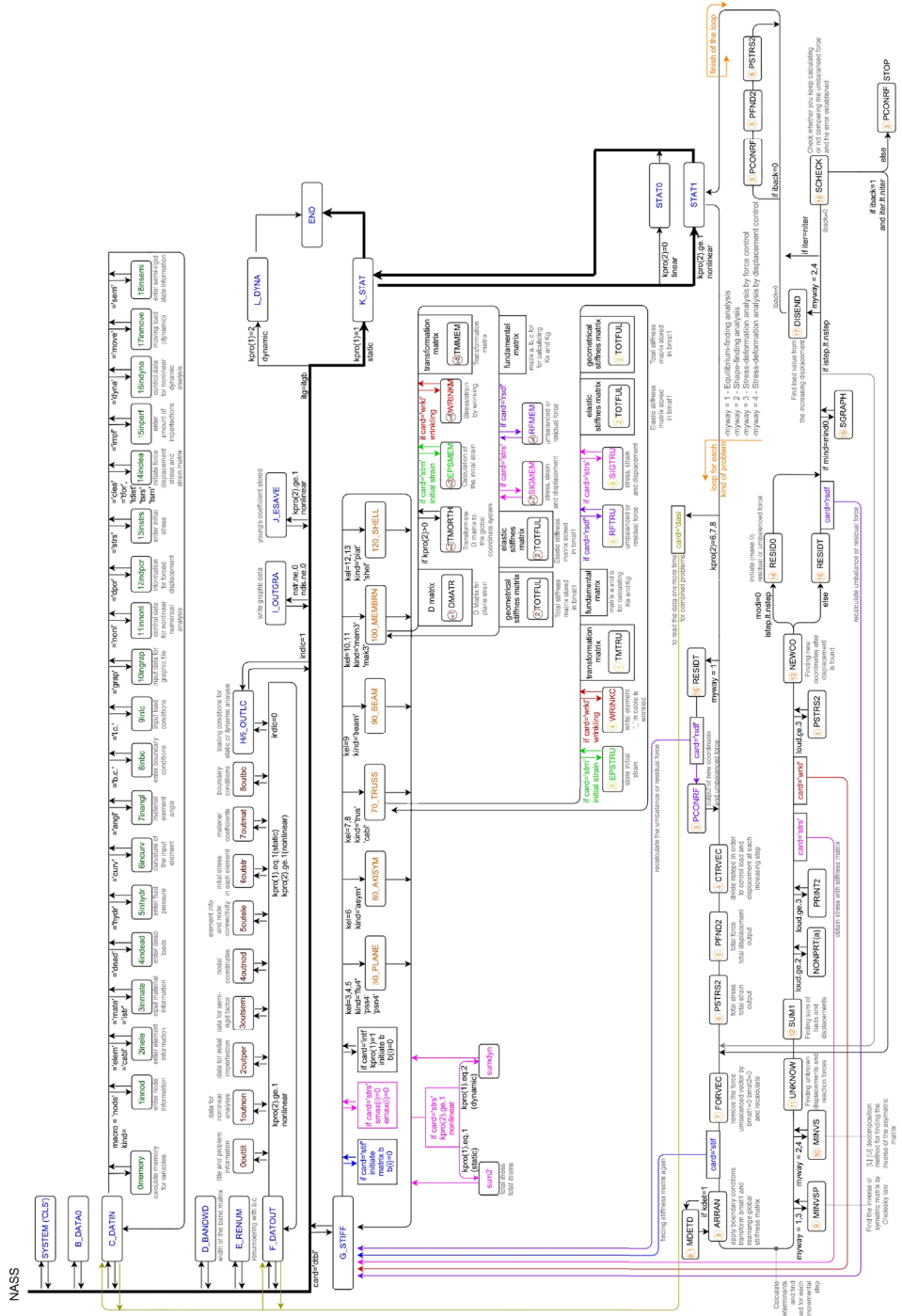


Figure 6.1-2 Extended general chart of NASS program (organized by Marta Gil Pérez)

6.1.2. Element charts

Figures 6.1-3 and 6.1-4 show the chart for the stiffness matrix calculation of the cable element and the membrane element, respectively.

They are a zoom into the general chart, explaining only about the flow of the target element (cable or membrane) and comparing it with the equations needed for the calculation of the stiffness matrix of that element. At the same time, for a better understanding of this charts, a zoom into the explanations can be found in Tables 6.1-1 and 6.1-2 linked by numbers to the respective figures.

Both of them follow a similar path of calculation but as the cable (or truss) elements are simpler than membranes, the subroutine is also simplified.

From a general view, the element subroutines are composed of other subroutines following this course: defining the young's modulus and D matrix for isotropic or orthotropic materials, initial strains and stress/strain by wrinkling, calculation of the transformation matrix, calculation of residual forces, displacements, strain and stress, and finally calculation of the elastic stiffness matrix, geometrical stiffness matrix and storage if those in the total stiffness matrix.

Table 6.1-1 Zoom into the cable element stiffness matrix chart (organized by Marta Gil Pérez)

<p>1 Define Young's modulus $E = ec = \text{young}(1, ic)$</p>	<p>4 Calculation of the transformation matrix</p> $gili = ss = \sqrt{(x_j - x_i)^2 + (y_j - y_i)^2 + (z_j - z_i)^2}$ $sl = \frac{(x_j - x_i)^2}{ss}$ $sl = \frac{(y_j - y_i)^2}{ss}$ $sl = \frac{(z_j - z_i)^2}{ss}$ $slm = \sqrt{sl^2 + sm^2}$ <p>when $slm \neq 0$</p> $t = \begin{pmatrix} sl & sm & sn \\ -\frac{sm}{slm} & \frac{sl}{slm} & 0 \\ -\frac{sl*sn}{slm} & -\frac{sl*sn}{slm} & slm \end{pmatrix}$ <p>when $slm = 0$</p> $t = \begin{pmatrix} 0 & 0 & 1 \\ 0 & 1 & 0 \\ -1 & 0 & 0 \end{pmatrix}$
<p>2 Store initial strain $\varepsilon = \frac{\sigma}{E} \rightarrow \text{tEPS}(1, ic) = \frac{\text{tsig}(1, ic)}{ec}$</p>	
<p>3 Stress/strain by wrinkling INITIAL STRESS $\sigma_x^{(0)} = sx = \text{tsig}(1, ic)$ if $(ss < 0)$ then (length of the element) young = 0 tsig = 0 teps = 0 write : element () in cable is wrinkled</p>	
<p>5 Total transformation matrix</p> $tm = \begin{pmatrix} t & o \\ o & t \end{pmatrix}$ <p>Compose total transformation matrix (tm) using the matrix (t) calculated in the subroutine TMTRU</p>	
<p>6 $b_1 = \frac{-1}{ss}$ $b_2 = \frac{1}{ss}$ $a = (b_1 \ 0 \ 0 \ b_2 \ 0 \ 0)$ $b = \begin{pmatrix} b_1 & 0 & 0 & b_2 & 0 & 0 \\ 0 & b_1 & 0 & 0 & b_2 & 0 \\ 0 & 0 & b_1 & 0 & 0 & b_2 \end{pmatrix}$ Calculate matrix (a) and (b) that will be used later for the calculation of the stiffness matrix and the stress and strain</p>	
<p>7 Calculation of residual force Residual force in the local coordinate system $d1(1^{st} \text{row}) = r = \text{arca} * l * a^T * \sigma_x^{(0)}$ Residual force in the global coordinate system $d1(2^{nd} \text{row}) = R = d1(2, i) + tm(j, i) * d1(1, i)$ Total residual force $rfor = rfor + d1(2, i)$</p>	<p>8 Displacement: dis(ntdof) Displacement in the local coordinate system $u1 = \text{dis}(ntdof)$ Displacement in the global coordinate system $u2 = u2 + tm * u1$ Strain (eps-x) Strain in the global coordinate system because it is using already u2, the displacement in the global axis $\text{eps0} = \text{eps0} + a * u2$ $\text{eps1} = \text{eps1} + \frac{1}{2} * u2^T * b^T * b * u2$ $\varepsilon_x = \text{eps}(1) = \text{eps0} + \text{eps1}$ Stress (sig-x) $\sigma_x = \varepsilon_x * E \rightarrow \text{sig}(1) = \text{eps}(1) * ec$</p>

<p>9 Elastic stiffness matrix</p> <p>Elastic stiffness matrix in the local axis</p> $st1(i, j) = k_E = area * l * E(a^T * a)$ <p>Elastic stiffness matrix in the global axis</p> $K_E = st2 = st2 + tm^T * st1 * tm$	<p>10 Storing total elastic stiffness matrix</p> $K_E = st2 \rightarrow bmat1$
<p>11 Geometrical stiffness matrix</p> <p>Geometrical stiffness matrix in the local axis</p> $st1(i, j) = k_G = st1(i, j) + area * l(\sigma_x^{(0)} * b^T * b)$ <p>Geometrical stiffness matrix in the global axis</p> $K_G = st2 = st2 + tm^T * st1 * tm$	<p>13 Sum total stress and total strain</p> <p>for truss/cable</p> $kcl = 7, 8 \rightarrow kend = 1 \text{ (x direction)}$ $tsig(1, ie) = tsig(1, ie) + sig(1) \text{ (total stress)}$ $teps(1, ie) = teps(1, ie) + eps(1) \text{ (total strain)}$ <p>Adding the stress and strain calculated in the subroutine SIGTRU (sig and eps) to the total stress and strain of each element (tsig and teps)</p> <p>Store:</p> $a(ka(16))=tsig$ $a(ka(17))=teps$
<p>12 Storing total geometrical stiffness matrix</p> $K_G = st2 \rightarrow bmat1$ <p style="text-align: center;">↓ TOTAL STIFFNESS MATRIX</p> <p>bmat 1 already contained the elastic stiffness matrix, with the addition of the geometrical stiffness, bmat1 becomes the total stiffness matrix</p>	

Table 6.1-2 Zoom into the membrane element stiffness matrix chart (organized by Marta Gil Pérez)

<p>1 Young's modulus</p> <p>If pro(2) = 0 (linear) change1 = -1 ; change2 = -1</p> <p>If pro(2) > 0 (nonlinear) change1 = young(1, ie) ; change2 = young(2, ie)</p> <p style="text-align: right;">DMATR 2</p> <p>Specifications for making D matrix for different situations</p> <p>For plane stress</p> <p>Type = isotropic material</p> $d1 = \frac{e1}{1 - \nu_1^2} ; d2 = \frac{e1 * \nu_1}{1 - \nu_1^2} ; d3 = G_{12}$ $change1 = -1 ; change2 = -1$ <p>Type = orthotropic material</p> $d1 = \frac{e1}{1 - \nu_{12} * \nu_{21}} ; d2 = \frac{e1 * \nu_{12}}{1 - \nu_{12} * \nu_{21}} ; d3 = G_{12}$ <p>It is also defined the values of d1, d2 and d3 for other cases: fluid, plane strain and thin axymmetric shell</p>	<p style="text-align: center;">TMORTH 4</p> <p>Transformate D matrix to the global coordinate system</p> <p>Converse degrees to Radians</p> $\theta = th = \frac{theta * \pi}{180}$ <p>Element transformation matrix</p> $t = \begin{pmatrix} \cos^2\theta & \sin^2\theta & \sin\theta * \cos\theta \\ \sin^2\theta & \cos^2\theta & -\sin\theta * \cos\theta \\ -2 * \sin\theta * \cos\theta & 2 * \sin\theta * \cos\theta & \cos^2\theta - \sin^2\theta \end{pmatrix}$ <p>Transform D matrix to the global coordinate system</p> $tm = tm + t^T * dm * t$ <p>Store new transformed D matrix in dm</p> $dm(i, j) = tm(i, j)$ <p>EPSMEM</p> <p>5 Initial strain</p> <p>Call MINVSP to calculate the inverse of D matrix by Cholesky decomposition</p> <p>Make dm symmetric matrix</p> $dm(i, j) = dm(j, i)$ <p>Calculate the initial strain</p> $teps(i, ie) = teps(i, ie) + dm(i, j) * tsig(j, ie) \quad \epsilon = \frac{\sigma}{E}$
---	---

3 Storing final D matrix

if change1 & change 2 < 0 (linear)

$$dm = \begin{pmatrix} d1 & d2 & 0 \\ d2 & d1 & 0 \\ 0 & 0 & d3 \end{pmatrix}$$

if change1 & change 2 > 0 (nonlinear)

$$dm = \begin{pmatrix} d1 & d2 & 0 \\ \text{change1} & \text{change2} & 0 \\ 0 & 0 & d3 \end{pmatrix}$$

$\theta = \text{angl}(ie)$

then, we will have the following D matrix for isotropic materials

$$dm = \begin{pmatrix} \frac{e1}{1-\nu1^2} & \frac{e1*\nu1}{1-\nu1^2} & 0 \\ \frac{e1*\nu1}{1-\nu1^2} & \frac{e1}{1-\nu1^2} & 0 \\ 0 & 0 & G_{12} \end{pmatrix}$$

for orthotropic materials

$$dm = \begin{pmatrix} \frac{e1}{1-\nu12*\nu21} & \frac{e1*\nu12}{1-\nu12*\nu21} & 0 \\ \frac{e1*\nu12}{1-\nu12*\nu21} & \frac{e1}{1-\nu12*\nu21} & 0 \\ 0 & 0 & G_{12} \end{pmatrix}$$

D matrix

WRINKM 6

Stress/strain by wrinkling

Initial stresses

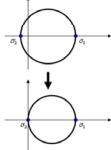
$$s1 = \text{tsig}(1, ie) = \sigma_x \quad s2 = \text{tsig}(2, ie) = \sigma_y \quad s3 = \text{tsig}(3, ie) = \tau_{xy}$$

call PRINCP to calculate principal stresses

1. if s2 (minimum principal stress) > 0 return

2. if s2 (minimum principal stress) < 0 and s1 (maximum principal stress) > 0

input s2 = 0 and recalculate



$$\sigma'_x = s_x = \frac{\sigma_{max} * (1 + \cos 2\theta)}{2}$$

$$\sigma'_y = s_y = \frac{\sigma_{max} * (1 - \cos 2\theta)}{2}$$

$$\tau'_{xy} = t_{xy} = \frac{\sigma_{max} * \sin 2\theta}{2}$$

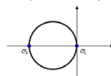
Store sx, sy and txy in tsig

Calculate modified Young's Modulus

$$young(1, ie) = \frac{young(1, ie) * s1}{(s1 - s2)} \quad E' = E * \frac{\sigma_1}{\sigma_1 - \sigma_2}$$

$$young(2, ie) = \frac{young(2, ie) * s1}{(s1 - s2)}$$

3. if s1 (maximum principal stress) < 0 return



$young = 0$
 $tsig = 0$
 $tpps = 0$

Write:
 Element '...' is wrinkled
 in membrane

PRINCP Principal stresses bt Mohr's circle

$$smean = \frac{(\sigma_x + \sigma_y)}{2} \quad sroot = \sqrt{\left(\frac{\sigma_x - \sigma_y}{2}\right)^2 + \tau_{xy}^2}$$

Store maximum principal stress $s1 = smean + sroot$

Store minimum principal stress $s2 = smean - sroot$

Radius of Mohr's circle $flow = \frac{(\sigma_x - \sigma_y)}{2}$

$$\text{if } flow < 10^{16} \rightarrow s3 = \frac{\pi}{4}$$

$$\text{else} \rightarrow s3 = \frac{1}{2} * \tan^{-1} \left(\frac{2 * \tau_{xy}}{\sigma_x - \sigma_y} \right)$$

7 TMMEM

Calculation of the transformation matrix from local axis to global axis

Store node numbers for each element ii, jj, kk

Store coordinates of each node/element $\begin{cases} x_i, y_i, z_i \\ x_j, y_j, z_j \\ x_k, y_k, z_k \end{cases}$

Unit vectors in local axis: i, k, j

$$i = \frac{a}{|a|}; k = \frac{a \times b}{|a \times b|}; j = k \times i$$

Unit vectors in global axis: e_x, e_y, e_z

Relation between local and global vectors

$$a \times b = \begin{vmatrix} e_x & e_y & e_z \\ x_j - x_i & y_j - y_i & z_j - z_i \\ x_k - x_i & y_k - y_i & z_k - z_i \end{vmatrix} = \Delta_x * e_x + \Delta_y * e_y + \Delta_z * e_z$$

$$l_{ij} = ss = \sqrt{(x_j - x_i)^2 + (y_j - y_i)^2 + (z_j - z_i)^2}$$

$$\Delta_x = dx = (y_j - y_i) * (z_k - z_i) - (y_k - y_i) * (z_j - z_i)$$

$$\Delta_y = dy = (z_j - z_i) * (x_k - x_i) - (z_k - z_i) * (x_j - x_i)$$

$$\Delta_z = dz = (x_j - x_i) * (y_k - y_i) - (x_k - x_i) * (y_j - y_i)$$

$$\Delta = dd = \sqrt{(dx)^2 + (dy)^2 + (dz)^2}$$

Transformation matrix from the relation of the vectors

$$T = \begin{pmatrix} t_{11} & t_{12} & t_{13} \\ t_{21} & t_{22} & t_{23} \\ t_{31} & t_{32} & t_{33} \end{pmatrix} = \begin{pmatrix} \lambda_x & \lambda_y & \lambda_z \\ u_x & u_y & u_z \\ v_x & v_y & v_z \end{pmatrix} =$$

$$T = \begin{pmatrix} \frac{x_j - x_i}{ss} & \frac{y_j - y_i}{ss} & \frac{z_j - z_i}{ss} \\ (t_{13} * t_{32} - t_{12} * t_{33}) & (t_{11} * t_{33} - t_{13} * t_{31}) & (t_{12} * t_{31} - t_{11} * t_{32}) \\ \frac{dx}{dd} & \frac{dy}{dd} & \frac{dz}{dd} \end{pmatrix}$$

Vectors \vec{a} and \vec{b} define the membrane in the global axis

$$\vec{a} = X_j - X_i \rightarrow \begin{pmatrix} a_1(1) \\ a_1(2) \\ a_1(3) \end{pmatrix} = \begin{pmatrix} x_j - x_i \\ y_j - y_i \\ z_j - z_i \end{pmatrix}$$

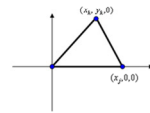
$$\vec{b} = X_k - X_i \rightarrow \begin{pmatrix} a_2(1) \\ a_2(2) \\ a_2(3) \end{pmatrix} = \begin{pmatrix} x_k - x_i \\ y_k - y_i \\ z_k - z_i \end{pmatrix}$$

And the vectors in the local axis will be

$$b1 = t * a1 = (x_j, 0, 0)$$

$$b2 = t * a2 = (x_k, y_k, 0)$$

$$area = \frac{x_j * y_k}{2}$$



8 Total transformation matrix

$$tm = \begin{pmatrix} t & 0 & 0 \\ 0 & t & 0 \\ 0 & 0 & t \end{pmatrix}_{9 \times 9}$$

transformation

10 Calculation of residual force

Residual force in the local coordinate system

$$d1(1, i) = d1(1, i) + area * thick * a^T * \sigma^{(i)}$$

Residual force in the global coordinate system

$$d2(1, i) = d2(1, i) + tm^T * d1(1, i)$$

Total residual force

$$rfor = rfor + d2$$

RFMEM

9 fundamental matrix

Calculate matrix [A], [B], and [C] that will be used for the calculation of the stiffness matrix and stress/strain

$$a1 = 1$$

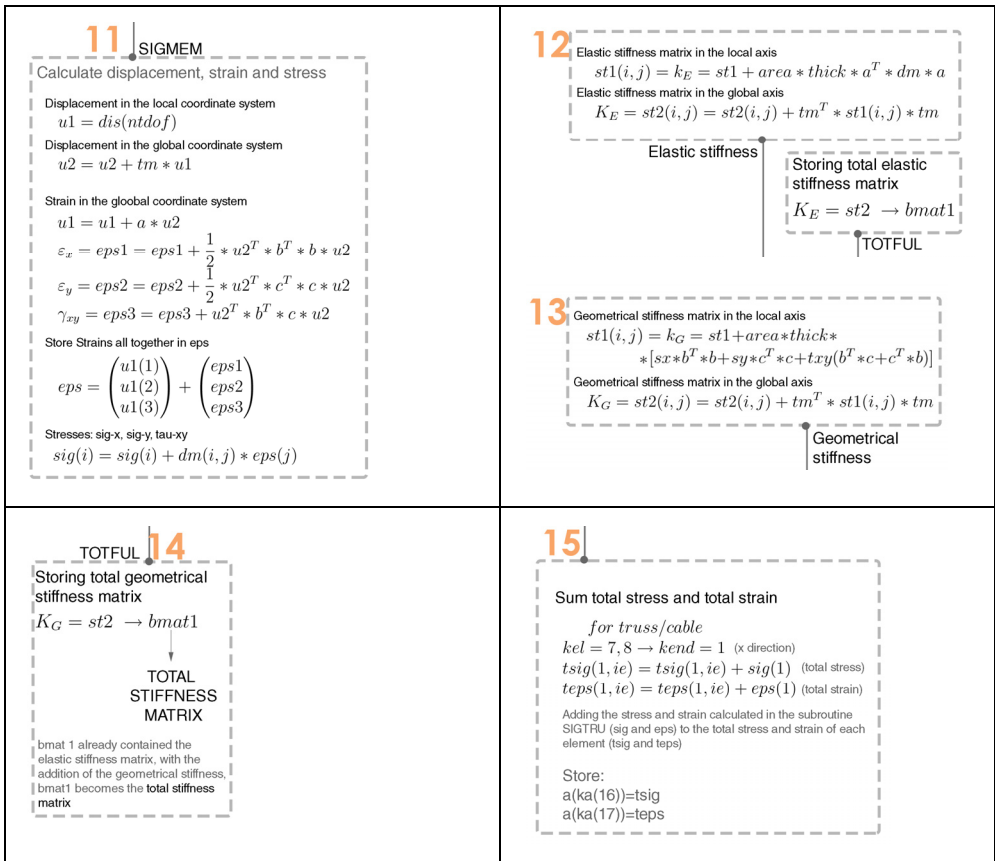
$$b1 = \frac{-1}{xj}; b2 = \frac{1}{xj}$$

$$c1 = \frac{xk - xj}{xj * yk}; c2 = \frac{-xk}{xj * yk}; c3 = \frac{xj}{xj * yk}$$

$$[A] = a = \begin{pmatrix} b1 & 0 & 0 & b2 & 0 & 0 & 0 & 0 & 0 \\ 0 & c1 & 0 & 0 & c2 & 0 & 0 & c3 & 0 \\ c1 & b1 & 0 & c2 & b2 & 0 & c3 & 0 & 0 \end{pmatrix}$$

$$[B] = b = \begin{pmatrix} b1 & 0 & 0 & b2 & 0 & 0 & 0 & 0 & 0 \\ 0 & b1 & 0 & 0 & b2 & 0 & 0 & 0 & 0 \\ 0 & 0 & b1 & 0 & 0 & b2 & 0 & 0 & 0 \end{pmatrix}$$

$$[C] = c = \begin{pmatrix} c1 & 0 & 0 & c2 & 0 & 0 & c3 & 0 & 0 \\ 0 & c1 & 0 & 0 & c2 & 0 & 0 & c3 & 0 \\ 0 & 0 & c1 & 0 & 0 & c2 & 0 & 0 & c3 \end{pmatrix}$$



6.1.3. Nonlinear analysis chart

Figure 6.1-5 shows the chart for the nonlinear analysis chart and Table 6.1-3 zooms into the explanations of this chart. For the static nonlinear analysis this program provides 4 types of analysis:

1. Equilibrium-finding analysis,
2. Shape-finding analysis
3. Stress-deformation analysis by force control
4. Stress-deformation analysis by displacement control.

Basically, analysis types 1 and 2 are to find the perfect shape of the structure. The first one, equilibrium-finding analysis, only utilizes the initial stresses and geometry to balance the forces and find the equilibrium shape.

In the second one, a displacement is input in one of the nodes, so the rest of the nodes attempts to find their optimal position to obtain a balanced stress distribution. Types 3 and 4 are analysis under loading conditions. The difference is that in the fourth a displacement control factor is also included. In this thesis, analyses 1 and 3 are only used.

In Fig. 6.1-5 the chart for the analysis can be read. Comparing it with the general chart of Fig. 6.1-2 the whole procedure can be understood. The incremental steps and iterations are controlled in this loop depending on the input data and the error check obtained. Rest of the procedure is explained in Table 6.1-3.

Table 6.1-3 Zoom into the nonlinear analysis chart (organized by Marta Gil Pérez)

<p>1 Types of problems</p> <pre> if (kpro(2)=1) then mind0 = 1 kim(1) = 1 if (kpro(2)=2) then mind0 = 1 kim(1) = 2 kim(2) = 1 if (kpro(2)=3) then mind0 = 1 kim(1) = 3 if (kpro(2)=4) then mind0 = 1 kim(1) = 4 if (kpro(2)=5) then mind0 = 2 kim(1) = 1 kim(2) = 3 if (kpro(2)=6) then mind0 = 2 kim(1) = 1 kim(2) = 4 if (kpro(2)=7) then mind0 = 2 kim(1) = 2 kim(2) = 3 if (kpro(2)=8) then mind0 = 2 kim(1) = 2 kim(2) = 4 </pre> <div style="border: 1px dashed orange; padding: 5px; margin: 10px 0;"> <pre> mind0 = 1 for doing only 1 loop (1 kind of problem) mind0 = 2 for doing 2 loops (1 for the 1st kind of problem and another one for the 2nd kind) kim(1) first kind of problem kim(2) second kind of problem kim = 1 → myway = 1 - Equilibrium-finding analysis kim = 2 → myway = 2 - Shape-finding analysis kim = 3 → myway = 3 - Stress-deformation analysis by force control kim = 4 → myway = 4 - Stress-deformation analysis by displacement control steps + iterations → myway = 1,3 only steps → myway = 2,4 </pre> </div>	<p>2 Write type of problem title depending on myway</p> <pre> graph TD A[DATA0 DATIN] --> B[card='dasi'] B --> C{if mind0 > 1 kpro(2)=6,7,8} C --> A C --> D[] </pre> <p>When we enter in the second loop (to calculate the second kind of problem if there is) it takes the initial data again for the second problem</p>
<p>3 Write coordinates and residual force for 3D problem with 3 DOF/node and calculate sum of forces</p> $fsum = s fsum + rfor(\text{of each node})$ <pre> graph TD PCONRF --> card["card='rsdf'"] card --> RESIDT RESIDT --> rfor["rfor(i) = -tfor(i) make residual force equal to the negative total force"] rfor --> G_STIFF G_STIFF --> PCONRF G_STIFF --> calc["Calculate residual force again for each degree of freedom"] </pre> <p>output of new coordinates and unbalanced force</p> <p>myway = 1 ↑ Equilibrium-finding</p>	<p>4 For force control</p> <p>my way = 1 (Equilibrium-finding analysis)</p> $cntrl(i) = \frac{-rfor(i)}{nstep} \quad \text{control} = \text{residual force divided by nsteps}$ $tfor(i) = rfor(i) \quad \text{Pass residual force to total force and initiate residual force}$ $rfor(i) = 0$ <p>my way = 3 (Stress-deformation by force control)</p> $cntrl(i) = \frac{for(i)}{nstep} \quad \text{Control} = \text{loading condition divided by nsteps}$ <p>For displacement control</p> <p>my way = 2 (Shape-finding analysis) = 4 (Stress-deformation analysis by displacement control)</p> $cntrl(i) = for(i) \quad \text{Control} = \text{loading condition in each DOF}$
<p>5</p> <pre> 300 ← alpha = alpa 200 alpha = 0 iter = iter + 1 iteration number increasing by 1 100 alpha = 1 istep = istep + 1 step number increasing by 1 </pre>	<p>6 Modify residual force and force vector</p> <p>when we are inside a step (alpha = 1)</p> $for(i) = cntrl(i) - rfor(i)$ <p>when we are inside an iteration (alpha = 0)</p> $for(i) = -rfor(i)$ <p>Initiate stiffness matrix</p> $bmat(1) = 0$ $bmat(2) = 0$

7 Arrange of stiffness matrix by boundary conditions

Store stiffness matrix in **bmat2**

$bmat2 = bmat1$

Take renumbering from **indbc** (3rd row)

$ii = indbc(3, i) \quad jj = indbc(3, j)$

Rearrange total stiffness matrix in **bmat1**

$bmat1(i, j) = bmat2(ii, jj)$

For **myway = 2, 4**

displacement control analysis

$kpivot = (ktrnod - 1) * mdj + ktrdof$

$kkk = indbc(2, kpivot)$

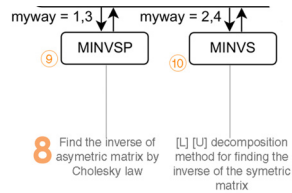
Find load for each incremental step in displacement control problems

$for(ii) = -bmat1(i, kkk) * \frac{ctrdis}{nstep}$

$$f = [K] * d$$

for (ii) = loading condition corresponding with the free DOF

$bmat1(i, kkk) = -for(ii)$



8 Find the inverse of asymmetric matrix by Cholesky law [L][U] decomposition method for finding the inverse of the symmetric matrix

10 Sum of total forces and displacements

$tfor(i) = tfor(i) + for(i) + rfor(i)$

$tdis(i) = tdis(i) + dis(i)$

If **myway = 1** (equilibrium-finding analysis)
= 3 (stress-deformation by force control)

when $i \neq j$ make stiffness matrix symmetric for the values corresponding with free displacement conditions (1,nfree)

$bmat1(i, j) = bmat1(j, i)$

$dis(ii) = dis(ii) + bmat1(i, j) * for(jj)$
initiate displacement corresponding with free conditions (1, nfree) and recalculate.

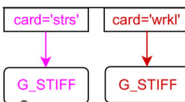
If **myway = 2** (shape-finding analysis)
= 4 (stress-deformation by displacement control)

$ramda = \frac{dis(kpivot)}{nstep}$ Ramda = steps of forced displacement
Dividing forced displacement values in nsteps

$for(ii) = ramda * cntrl(ii)$ Control force from subroutine CTRVEC
 $cntrl(i) = for(i)$

$for(ii) = for(ii) + bmat1(i, j) * dis(jj)$
For fixed degrees of freedom (nfree + 1, ntdof)
initiate force (force=0) and recalculate

9



11 Recalculate displacement, strain and stress with the total stiffness matrix

Find new coordinates after displacement have been found

12 $xyzco = xyzco + dis$

13

Error check

$gama = abs(rf/tf)$
if $gama > error \rightarrow iback = 1$

Check whether you keep calculating or not comparing the unbalanced force and the error established

14 CONTROL DATA FOR NONLINEAR ANALYSIS
 nstep = total incremental steps in load incremental method and displacement incremental method
 niter = total iteration number of Newton-Raphson method
 error = allowed error for Newton-Raphson iteration
 kdet = decide calculation of tangential stiffness matrix in each step (on=1)

CONTROL DATA FOR INCREASING DISPLACEMENT METHOD
 ktrnod = nodes corresponding with forced displacement
 ktrdof = contro DOF of forced displacement
 ctrdis = forced displacement value

6.1.4. Input and output data

For the input of the data a text file (.dat) is needed. In this file 3 types of data could be recognized: the title data, control data and macro data. An example of an input and output data file can be found in the appendices, corresponding to the basic model of the parametric analysis described in Chapter 8.

The title data is found in the first line of the document, and as the name indicates, it contains the title of the analysis to be performed.

Then, the control data is written in the next four lines. Table 6.1-4 explains all the data that is contained in these four lines to specify how the analysis should be performed.

Table 6.1-4 Control data for the input data file

1 st line	<p>Dimension of the problem</p> <ul style="list-style-type: none"> • 2 for 2D • 3 for 3D 	<p>Static/dynamic problem</p> <ul style="list-style-type: none"> • 1 for static • 2 for dynamic 	<p>Type of problem</p> <ul style="list-style-type: none"> • 0 for linear problem • 1 for equilibrium-finding by force control • 2 for shape-finding by displacement control • 3 for stress-deformation by force control • 4 for stress deformation by displacement control • 5 for 1+3 • 6 for 1+4 • 7 for 2+3 • 8 for 2+4
2 nd line	<p>Maximum DOF of each node</p>	<p>Maximum nodes of each element</p>	<p>Output level</p> <ul style="list-style-type: none"> • 1 for getting output data for only final results • 2 for getting output of the steps of displacement, load, coordinates and residual forces • 3 for getting output of the steps of strain and stress
3 rd line	<p>Total nodes</p>	<p>Total elements</p>	
4 th line	<p>Integrating points for in-plane and bending</p>	<p>Integrating points for shear</p>	

As shown in the table, in the first line, the dimension of the problem, the choice of a static or a dynamic problem and the type of problem are defined.

In the second line, the maximum degrees of freedom of each node and maximum nodes of each element are specified. This is needed because, as explained earlier, the same problem can have different types of elements, so in this way computer space is prepared depending on the biggest element that is to be utilized. Besides, also in this second line, the output level is defined. With it, it is specified how much information the output file is expected to contain.

The third line defines the total number of nodes of the model and the total elements, no matter if those are from a different type.

Finally, in the fourth line, the integrating points for in-plane and bending and for shear are defined.

For the last data type, the macro data defines the rest information of the model. For the macro data, a key word has to be written to introduce the type of data that is read. For example, to input the data of the node coordinates, the word “node” should be written first. The order to introduce the macro data is changeable and depends on this first key word. A detailed list of the possible macro data to use is explained in Table 6.1-5. However, not all the project analysis use all the macro data information, so it can be just omitted.

Table 6.1-5 Macro data for the input data file

Macro data	Line	Data required
Nonlinear data Control data for nonlinear analysis	1 st	Input “ nonl ”
	2 nd	Total incremental steps in load incremental method and displacement incremental method Total iteration number of Newton-Raphson Allowed error for Newton-Raphson iteration Modified Newton-Raphson control (off=0) Decide calculation of tangential stiffness matrix in each step (on=1)
Node Decide coordinate values for each node	1 st	Input “ node ”
	2 nd and repeat for each node	Node number x-coordinate y-coordinate z-coordinate Increasing value of node number
	Final	0,,,,,,,,,
Element Decide values for element number	1 st	Input “ elem ” Input type of element. For example: • “trus” for truss element • “cabl” for cable element • “beam” for beam element • “mak3” for membrane element • “plat” for plate element • “shel” for shell element Input number of nodes in the element
	2 nd and repeat for each element	Element number Node numbers (connectivity) Number for material type Input 0 for dead load Increasing value of element number
	Final	0,,,,,,,,,

<p>Material Decide material types and properties</p>	1 st	<p>Input “mate”</p> <p>Input type of material:</p> <ul style="list-style-type: none"> • “istr” for isotropic material • “ortr” for orthotropic material
	2 nd and repeat for each different material	<p>If isotropic material</p> <ul style="list-style-type: none"> • im: material number • tora: area in lineal material or thickness in surface material • rho: density (for dynamic analysis) • e11: Young’s modulus • v12: Poisson’s ratio • secmy : inertia modulus I_y • secmz : inertia modulus I_z • polar : polar inertia modulus $I_p = I_y + I_z$ <p>If orthotropic material</p> <ul style="list-style-type: none"> • im: material number • tora: area in lineal material or thickness in surface material • rho: density (for dynamic analysis) • e11: Young’s modulus in x-direction • e22: Young’s modulus in y-direction • v12: Poisson’s ratio in y-direction when load is applied in x-direction • v21: Poisson’s ratio in x-direction when load is applied in y-direction • g12: shear factor in x-y surface
	Final	0,,,,,,,,,
<p>Angle Needed when it is orthotropic material. Decide the angle between the main direction of fibers and the local coordinate system in element.</p>	1 st	Input “ angl ”
	2 nd and repeat for each element	<p>Element number</p> <p>Angle between direction of fibers in element (X1) and direction in local coordinate system (X)</p> <p>Increasing element number</p>
	Final	0,,,,,,,,,

Boundary conditions Define boundary conditions for the model	1 st	Input “ b.c. ”
	2 nd and repeat for each node	Node number Boundary conditions for each DOF of the node · 0 for free condition · 1 for fix condition Increasing node number
	Final	0,,,,,,,,,
Loading conditions Decide loading conditions for the model	1 st	Input “ l.c. ”
	2 nd and repeat for each node	Node number Loading condition for each DOF of the node in global coordinate system Increasing node number
	Final	0,,,,,,,,,
Displacement control data Increasing displacement method control data	1 st	Input “ dpcr ”
	2 nd	Decide nodes corresponding with forced displacement; designate node number for forced displacement Control DOF of forced displacement Forced displacement value
Initial stress Initial stress for each element	1 st	Input “ strs ”
	2 nd And repeat for each element	Element number initial stress in x , y (for 2D) or x , y and z (for 3D) Incremental element number
	Final	0,,,,,,,,,
Clear matrices total force, total displacement, total stress, total strain clearing	1 st	Input “ clea ” Input “ tfor ” for total force clear, “ tdis ” for total displacement clear, “ tsrs ” for total stress clear, and “ tsrn ” for total strain clear
Initial imperfection Initial imperfection control data	1 st	Input “ impf ”
	2 nd	Amount of initial imperfection Applied eigen-mode

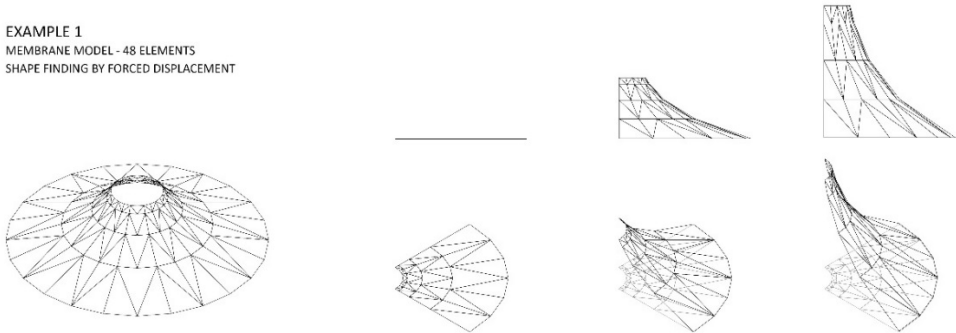
Semi-rigid Semi-rigid control data	1 st	Input “ semi ”
	2 nd	Semi-rigid efficiency (for steel structures)
End For Macro data ending	1 st	Input “ end ” (It should be placed at the end of the input data file, and it should be always used in all the analysis)

The resulting output data depends on the level of output decided and the type of analysis selected. In general terms, all analyses include a first section where the general initial data information is described. This is followed by the results of the selected analysis type, including the sum of forces and displacements, the sum of stress and strain, and the new coordinates and residual forces. The number of steps and iterations that the program has performed to obtain the results is also shown. If the level of output is designated higher, then more information can be obtained.

6.1.5. Application examples

Two examples are shown in Fig. 6.1-6. The first one is corresponding to the analysis type 2, shape-finding analysis. As explained, a forced displacement is inputted to this type of analysis to obtain the perfect shape where the stress is equally distributed. In the right side of the Figure the evolution from a flat model to a conic model is shown with two different forced displacements, so two different shapes found.

EXAMPLE 1
MEMBRANE MODEL - 48 ELEMENTS
SHAPE FINDING BY FORCED DISPLACEMENT



EXAMPLE 2
HYBRID MODEL - 25 MEMBRANE ELEMENTS / 15 CABLE ELEMENTS
SHAPE FINDING AND STRESS DEFORMATION BY FORCE

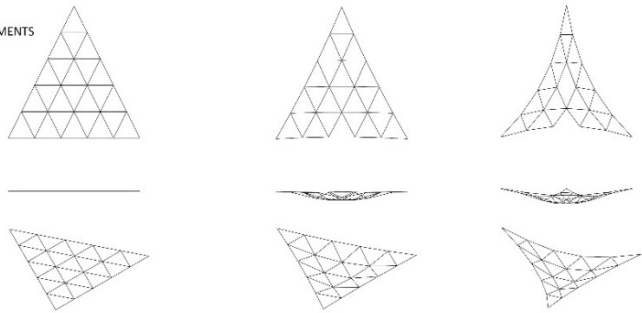


Figure 6.1-6 Membrane application examples of the program NASS

In the second analysis a membrane and cable model is shown. The model is a triangle made of membrane elements that has cables in the edges and it is only supported by the corners. First, the model is subjected to form-finding analysis and then to stress-deformation analysis under a simple loading condition. The first figure on the left shows the initial shape, while second and third show the deformed shapes under the same loading conditions but different initial stresses.

6.2. Modeling of membrane and cable elements

Before preparing the input data file for the analysis of a particular project, it is very important to model the design in the most simple and organized way. Firstly, it is important to identify symmetries or modules that are repeated along the project. In this way, the most representative parts of the project can be chosen for the modeling, saving time and effort.

6.2.1. Fabric weave orientation

First of all, it is necessary to define the weave orientation and also the warp and fill directions. This is needed when numbering the membrane triangular elements as explained in the next section.

Ideally the fabric weave directions should coincide with the directions of principal curvature of the surface (for example, the radial patterning of a simple conic tent, or the high point to high point seam trajectory of a parabolic four-point sail).

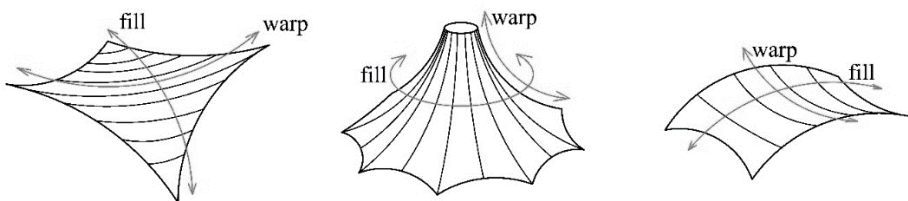


Figure 6.2-1 Typical wave (warp and fill) directions for the three basic tensile structure shapes.

This optimizes the stiffness of a given form, enabling easier initial stressing of the membrane and reducing surface deflections under load.

The actual practical choice as to whether the material warp or fill direction follows a particular direction of principal curvature is governed by requirements of strength, installation strategy and fabrication economics (Wakefield 1999). Figure 6.2-1 shows the typical wave directions, both warp and fill, for the three basic tensile structure shapes.

6.2.2. Nodes and elements

Once it is decided which representative part is going to be modeled for the analysis and which the fabric warp and fill directions are, the division into nodes and elements have to be done. For tensile structures, normally only cable and membrane elements are considered. The presence of other type of elements, like for example truss elements when arches are holding the membrane, can be just considered as fixed nodes.

These elements have to be analyzed separately as they are much more rigid than the tensile members and the objective of the analysis is to evaluate the safety of the fabric.

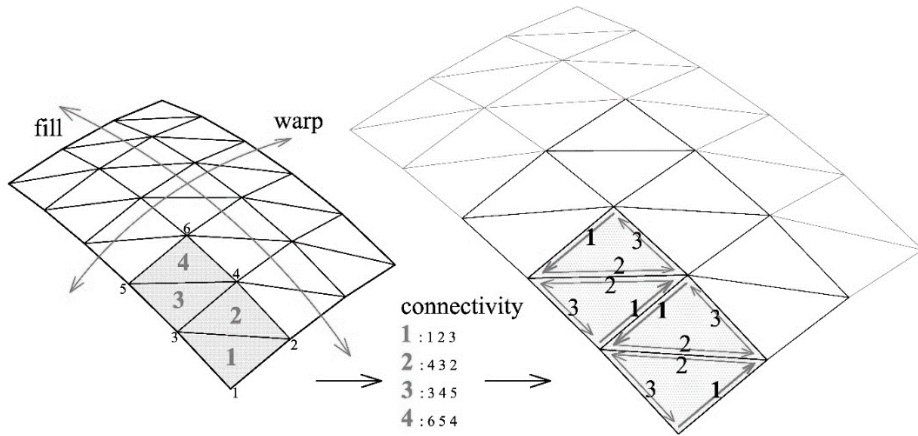


Figure 6.2-2 Example of membrane elements connectivity order

Nodes and elements should be numbered in an organized way. For membrane elements, the numbering connectivity of the nodes should follow always in the warp direction of the fabric as shown in Fig. 6.2-2. Besides, the well organization of the node and element numbers would save time and make the results easier to interpret.

6.2.3. Material properties

The material properties should be assigned separately for cables and membranes according to the project requirements. For an easier calculation, for both membranes and cables, the thickness is taken as a unit and the value is considered together with the Young's modulus. That is why the Young's modulus in membranes is given as kN/m and in cables the value EA is given instead of only E .

6.2.4. Initial stresses

Prestressing of the surface contributes significantly to its stiffness. The work done by applied loads causes deformation which is balanced by the change in strain energy within the surface, and this is both a function of the increasing strain in the load carrying direction and the decreasing strain in the opposing/orthogonal weave direction. The prestress should not be smaller than 2 kN/m. The currently strongest membrane, PTFE (Polytetrafluoroethylene) -coated glass fiber membrane, is often prestressed to typically 5 kN/m (and for very flat surfaces perhaps up to 10 kN/m) (Forster & Mollaert 2004).

The satisfactory long-term behavior of a membrane structure requires either a uniform or smoothly varying distribution of stress within the warp and fill directions of the fibers. This minimizes the chances of the development of wrinkles or local stress concentrations under load (Wakefield 1999). However, if the membrane is not bi-axially prestressed, the membrane is subject to wrinkles. Wrinkles degrade the surface reflectivity and modify the dynamic characteristics of the membrane. Thus, the design challenge here is to apply prestress to a membrane as uniformly as possible, without increasing the structural mass and volume significantly (Sakamoto et al. 2007).

6.2.5. Loading conditions

Critical load cases for fabric structures are usually the cases with snow and wind loads (Figs. 6.2-3 and 6.2-4). In general, seismic loads are not a problem as the membrane structures weigh little and thus do not create substantial inertial forces under seismic action.

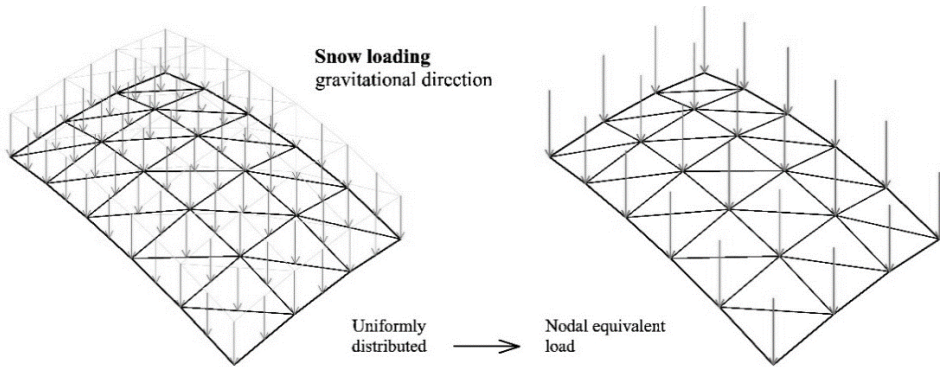


Figure 6.2-3 Example of the equivalent nodal loads for the snow loading

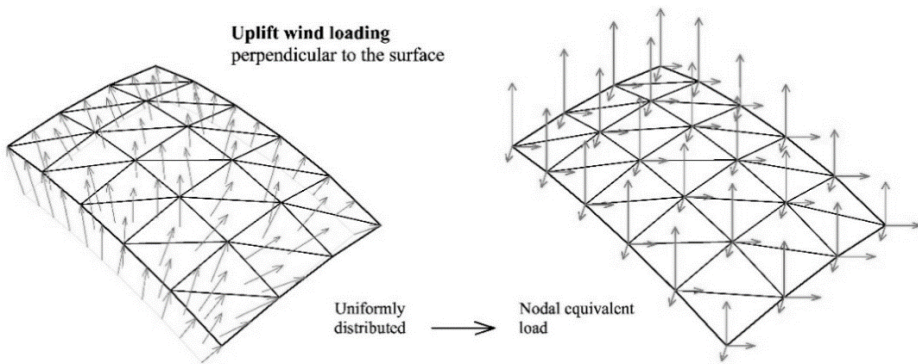


Figure 6.2-4 Example of the equivalent nodal loads for the uplift wind loading

Both loadings, snow and wind, are normally given as uniformly distributed forces, and need to be transfer to equivalent nodal loads. Besides, the way to apply these forces is different. The wind load is applied as a suction force that acts perpendicular to the fabric surface, so the local coordinates should be used as shown in Fig. 6.2-4. The snow load is applied as uniform downward force acting on the projected plan area of the membrane as in Fig. 6.2-3.

Chapter 7. Case Studies

For a better understanding of the modeling and analysis of tensile structures, in this Chapter two case studies are developed.

The first one is the dome of the Seoul Southwestern Baseball Stadium and the second one the dome of the Jeju World Cup Stadium. Both of them are sport stadiums covered by barrel vault shaped membrane structures supported by steel arches. Individual analysis, results and conclusions are given in each case study, and the differences between them are also underlined during the description of the second case study.

7.1. Seoul Southwestern Baseball Stadium dome

The Seoul Southwestern Baseball Stadium is the first of its kind in Korea, located at the heart of a busy commercial area in the south-west district of Seoul. With a gross area of 62,443 m², the stadium features 22,258 seats for baseball games or performances. As seen in Fig. 7.1-1, the dome has an irregular shape that is symmetric to major axis due to the characteristics of the site and the architectural design represents the dynamic waves of the baseball and the nation (Kim et al. 2010).

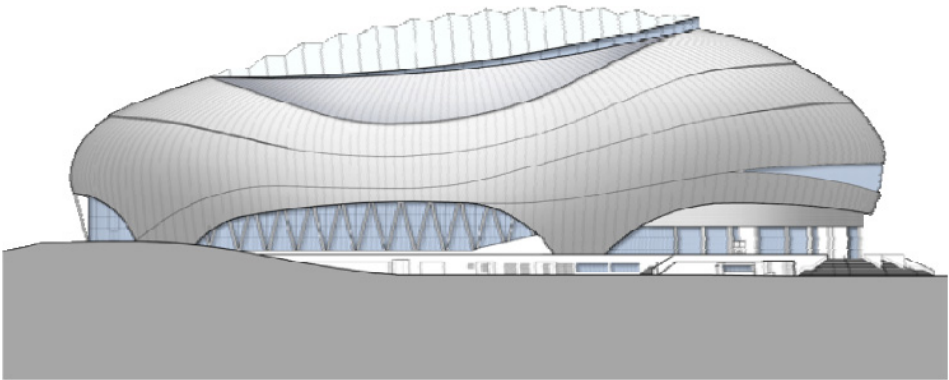


Figure 7.1-1: 3D view and elevation of the stadium (Kim et al. 2010).

The size of the dome is 157 meters wide, 214 meters long and 30 meters high. The superstructure is composed of a spatial steel frame covered in the center by a membrane with valley cables supported by steel arches (Fig. 7.1-2).

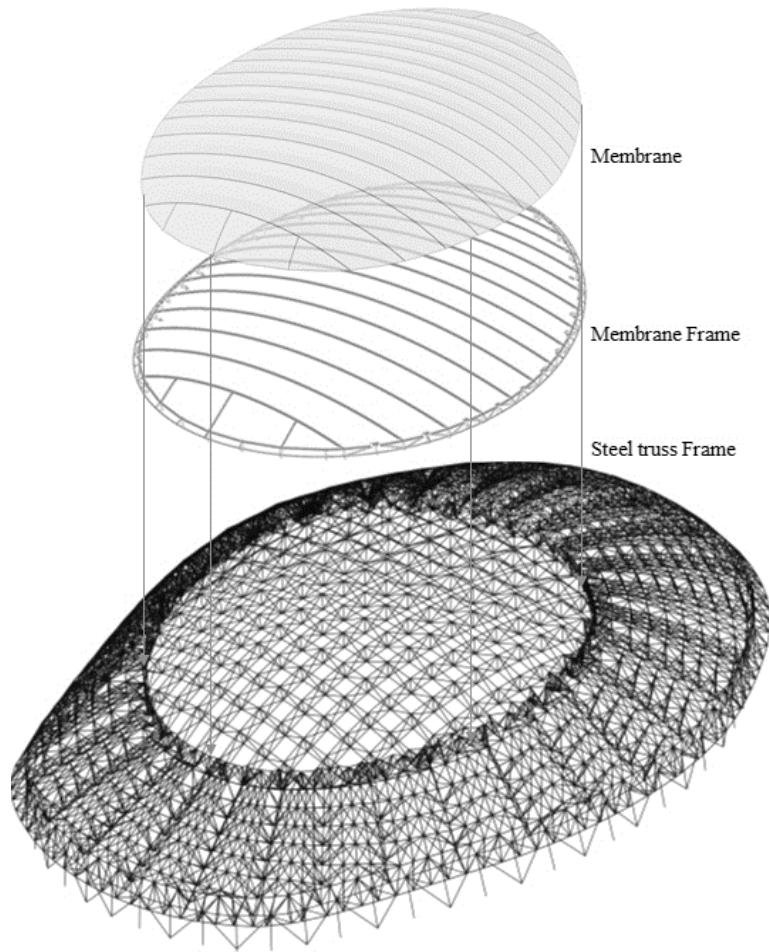


Figure 7.1-2 Structural system of the dome

This membrane dome comprises 16 panels of a width of 7.4 meters, and it has a total size of 100 meter width by 120 meter length with a maximum height of 12 meters at the center.

Currently this stadium is under construction and it is planned to be completed in 2005. In Fig. 7.1-3 some pictures of the construction stage are shown.

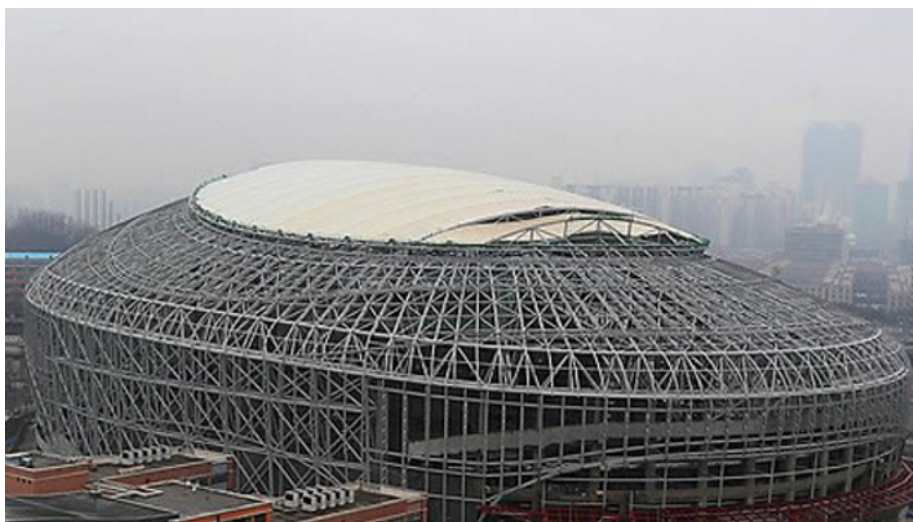
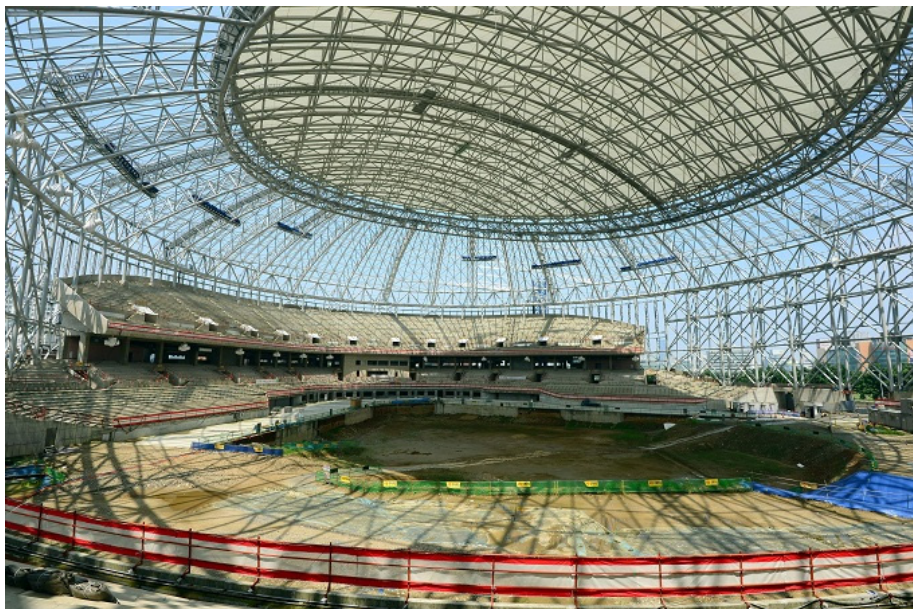


Figure 7.1-3 Interior and exterior of the Seoul Southwestern Baseball Stadium construction

7.1.1. Membrane model

7.1.1.1. Models and panels for analysis

For this study, two different models are designed (Fig. 7.1-4). Model A has membrane fabric in between the arches without cables, whereas in Model B a valley cable tenses the membrane of each panel at the center in the longitudinal direction.

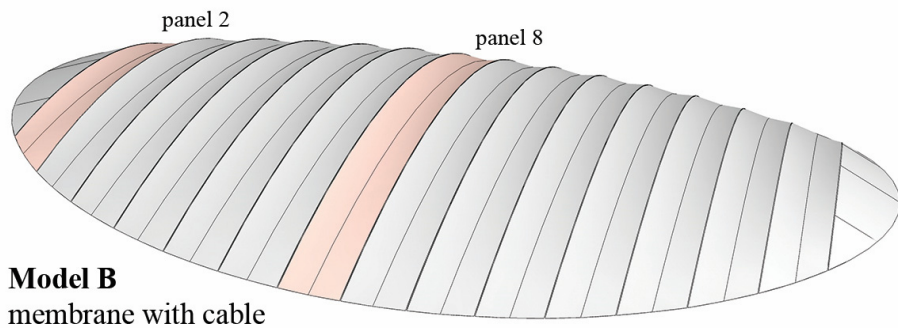
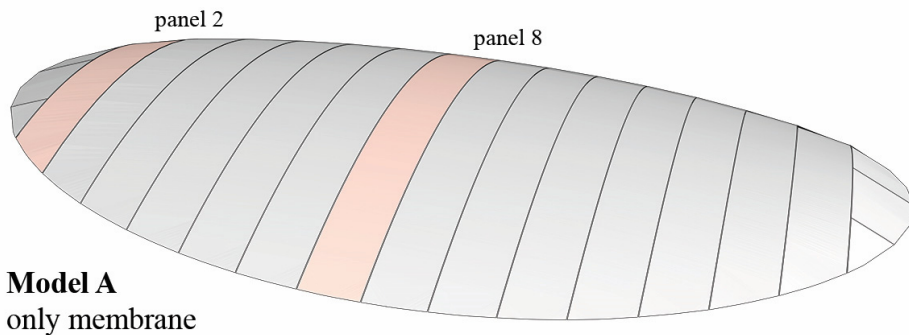


Figure 7.1-4: Models A and B of the membrane structure and panels chosen for the analysis

Additionally, for the analysis, the most two representative panels are chosen in each model (panel 1 and panel 2; see Fig. 7.1-4). The panel 2 is the shortest, with the most irregular shape and the most pronounced curvature. Its size is 58 meters long and 3 meters high on center. The panel 8 is the longest with 100 meters and it has the maximum height of 12 meters on center, but it is also the most regular in terms of curvature and symmetry.

Both panels for each Model will be divided into triangular membrane elements following the weave directions, warp and fill, as shown in Fig. 7.1-5. The connectivity of the triangular elements follows first the warp direction as explained in the Chapter 6, Nonlinear Analysis and Modeling of Tensile Structures.

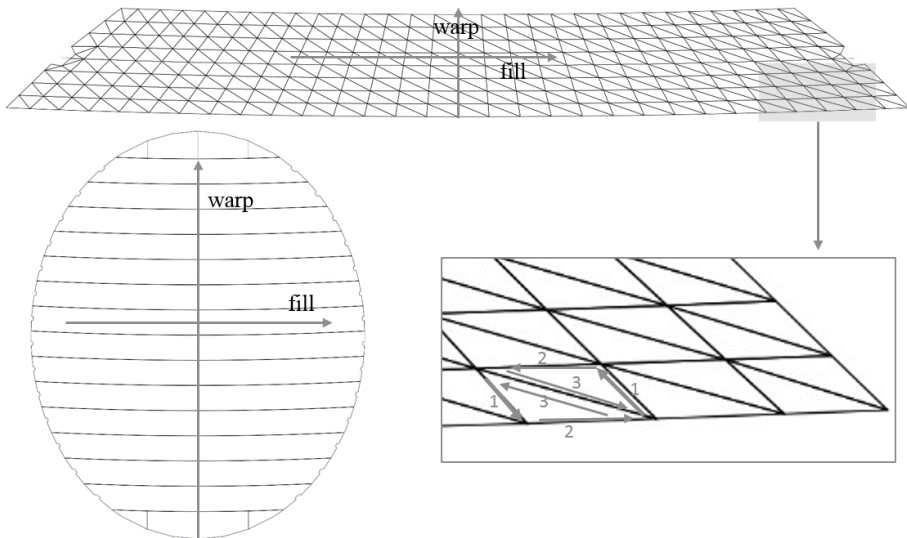


Figure 7.1-5 Definition of the warp and fill directions and connectivity of the triangular elements.

7.1.1.2. Material properties

The membrane properties used for this dome are indicated in Table 7.1-1, and the material properties for the valley cables in Table 7.1-2. Note that the stress and elastic modulus of structural fabrics are defined as force per unit width, as fabrics do not have a consistent thickness, and thus thickness is taken as a unit (Bridgens & Birchall 2012).

Table 7.1-1 Membrane properties for the dome

E_{11} (kN/m)	E_{22} (kN/m)	V_{12}	V_{21}	G (kN/m)
1230	950	0.804	0.62	96.26

Table 7.1-2 Valley cable properties for the dome

A (cm ²)	E (kN/m ²)	EA (kN)
15.2	1.4×10^8	212800

7.1.1.3. Initial stress conditions

In the Seoul Southwestern dome, an initial uniform stress condition of 3 kN/m in both warp and fill directions is applied for the membrane. In the case of the cable, the prestressing force varies with the length of the panel, being 140 kN for the shortest panel (panel 2) up to 170 kN for the longest panel (panel 8) as it is shown in Fig. 7.1-6.

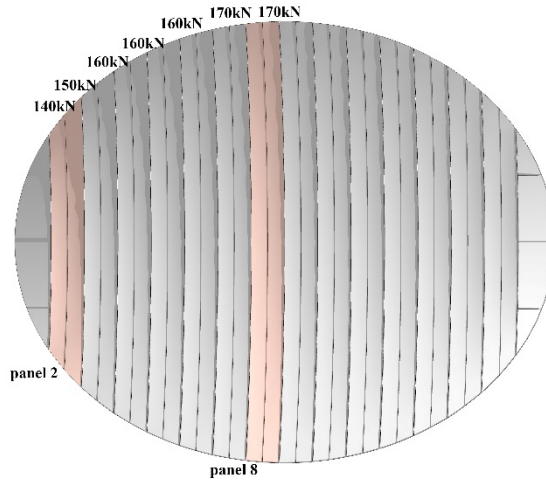


Figure 7.1-6 Prestressing of the cable for Model B

7.1.2. Form finding analysis

For the first stage, boundary conditions (support fixed geometry) and form-finding properties (fabric and edge cable prestress forces) are defined. Each panel is divided into triangular membrane elements, and both elements and nodes are numbered accordantly.

In Fig. 7.1-7, two different options are shown for each panel: Model A without valley cable and Model B with it. These models represent the initial shape but they are just an approximation of the optimal shape for the membrane. A form finding analysis is required to obtain the new coordinates that allow for the uniform initial stress for the membrane and also for the cables.

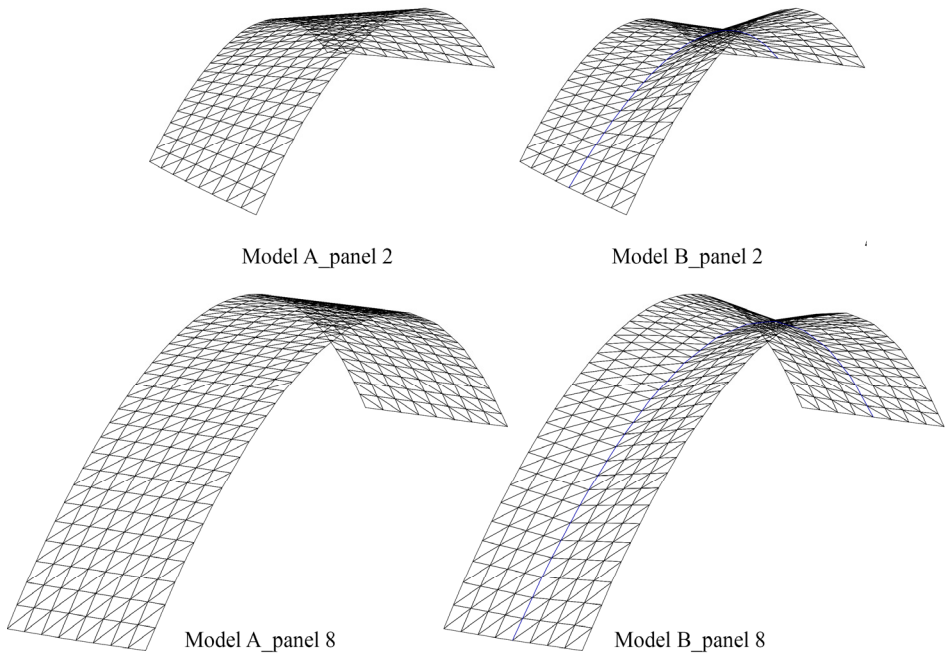


Figure 7.1-7 Initial shapes of panels 2 and 8 (Models A and B)

7.1.2.1. Initial stress balance

The form finding analysis provides the membrane geometry for the initial prestress conditions. It would seem reasonable to aim to provide uniform stress surfaces within the boundaries chosen by architectural constraints; thus, the surface so formed would be a minimal surface.

After performing each analysis, new coordinates can be obtained and the stresses resulting from the analysis tend to be the initial stress that needs to be input. Furthermore, the residual forces can be reduced significantly with the number of analyses performed.

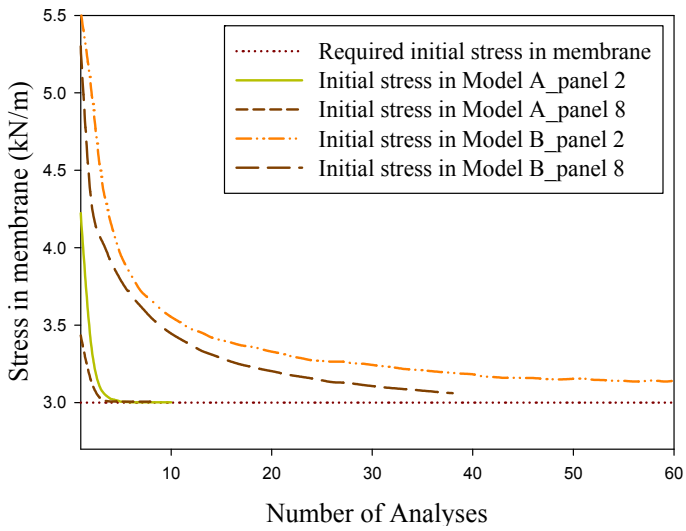
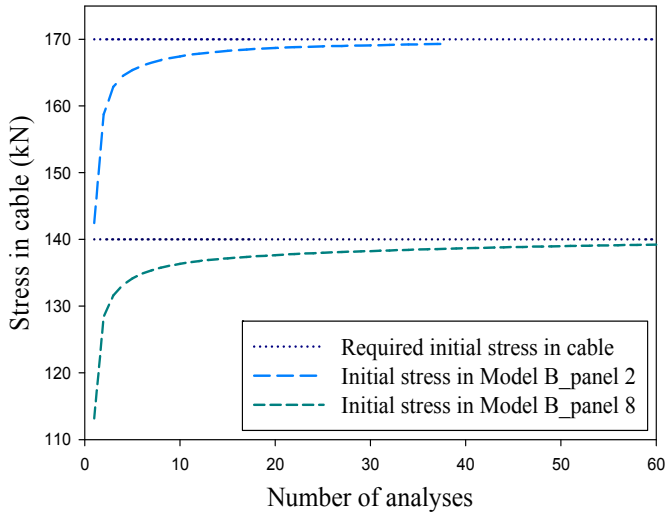


Figure 7.1-8 Balance of initial stress in cable and membrane for panels 2 and 8 and Models A and B.

Figure 7.1-8 presents the comparison of the number of analyses versus the resulting stress in the cables and membranes for each panel and each model.

As observed, for Model A in both panels (membrane without cable) a much small number of analyses is required to reach the shape corresponding to the uniformly distributed initial stress.

In the case of Model B, a much larger number of analyses is needed due to the required stress balance between the cables and the membranes. It is also observable that more analyses are required for panel 2 than for panel 8 because the geometry of the latter is more regular despite the greater length.

7.1.2.2. Perfect shape

After balancing the initial stress a new model is created with this updated ‘form-found’ geometry that is to be used for the stress deformation analysis. Figure 7.1-9 shows the comparison of the shapes found after the first analysis and the last analysis.

In Model A, for both panels, the shape of the first analysis is almost the same as the one obtained from the last analysis, and the resulting shape has an anticlastic curvature instead of the flat original model. In the case of Model B, because of the same balance phenomenon between membrane and cables explained earlier, the first analysis shape is not so close to the last analysis shape. It confirms that a large number of analyses is necessary.

Additionally, there is also a significant difference between the panel 2 and panel 8 in Model B. The variation of the displacements of the panel 8 is less than in panel 2 because of the more regular and symmetric geometry of the panel.

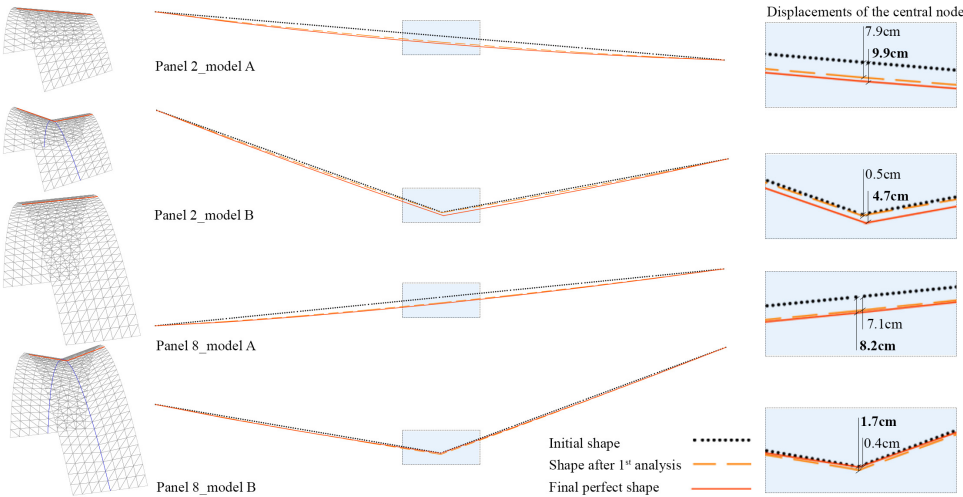


Figure 7.1-9 Comparison of transverse displacements at the central section from the shape finding analysis

7.1.3. Stress deformation analysis

In this stage, loads are applied (wind, snow, prestress) and a geometrically nonlinear (large displacement) analysis is carried out using membrane elements with zero bending and compression stiffness.

7.1.3.1. Design loading cases

Due to geometric nonlinearity, results from different load cases cannot be combined or factored: each combination case is analyzed separately, and the prestress and self-weight loads should be part of all loading cases. Then, for this analysis the two most critical cases are chosen as described in Table 7.1-3.

Table 7.1-3 Load combinations for the analysis

Case 1	Downward loading	Self-weight + prestress + snow + wind (downwards)
Case 2	Uplift loading	Self-weight + prestress + wind (uplift)

7.1.3.2. Displacement results of the deformed shape

Figure 7.1-10 compares the displacement for each loading case, model and panel at the nodes corresponding to the central longitudinal section of the panel. The first thing to observe is that in most of the cases the displacements of the Model B for both cases and both panels are smaller than in the Model A. This happens because the prestressing cable restrains the movement of the membrane, making it more stable.

Another noticeable issue is the difference in displacement pattern between panel 2 and panel 8, particularly that of y direction of Case 2 (uplift loading) and Model A (only membrane). Having a more regular and symmetrical shape, the panel 8 is also more regular in its displacement pattern. The arches of panel 2 are located with different heights (because it is an edge panel) so the membrane is inclined, making the displacement patterns more unpredictable.

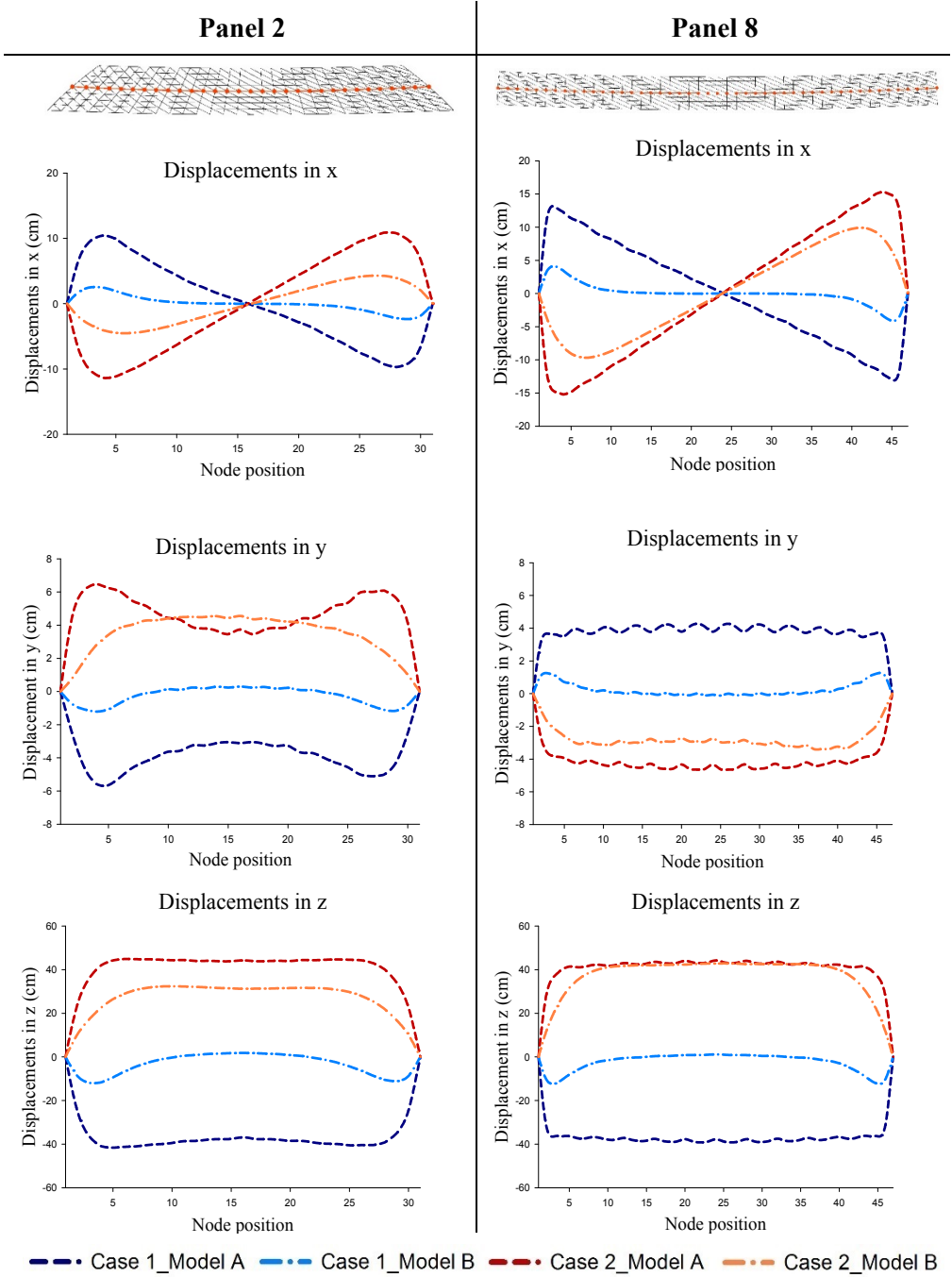


Figure 7.1-10 Displacements of panel 2 and panel 8 at the central longitudinal section

7.1.3.3. Stress, deformed shape and safety factor

Stresses in warp and fill directions for each load case are compared in terms of the fabric strip ultimate tensile strength. In this dome, the used fabric is Sheerfill II which has an ultimate strength of 137.5 kN/m in warp direction and 98.1 kN/m in fill direction. Typically in Korea, a minimum safety factor of 4 for the fabric strength is used in both warp and fill directions: each in relation to the rupture strength.

In Tables 7.1-4 and 7.1-5, a detailed comparison of each case, model and panel is made with respect to the deformed shape, stress distribution in the panel, maximum stress and safety factor. In both panels, the Model B (with cable) is safe for both loading cases (all safety values are higher than 4).

However, in the case of Model A (without cable), some unsafe situations are found. As noted in Tables 7.1-4 and 7.1-5, the cable increases the stiffness of the structure and makes the structure more stable especially for the uplift loading (Case 2), where the difference between stresses obtained for the Models A and B is much greater than the difference in the Case 1 with downward loading.

It is also worth mentioning that in the panel 2 (Table 7.1-5), the most unsafe cases are found from Model A. Even though this panel is shorter, its geometry is more irregular, which makes the panel to reach higher stresses under the same loading condition.

Table 7.1-4 Deformed shape, stress distribution in warp and fill directions, maximum stress and safety factor (γ) of panel 8

Stress distribution in membrane (kN/m)		panel 8			
		σ_x (warp)		σ_y (fill)	
Model A membrane	Case 1 downwards loading (snow + wind)				
	Max γ	25.2	5.5	16.8	5.8
	Case 2 upwards loading (uplift wind)				
Max γ	25.1	5.5	20.8	4.7	
Model B Membrane + cable	Case 1 downwards loading (snow + wind)				
	Max γ	21.1	6.5	14.4	6.8
	Case 2 upwards loading (uplift wind)				
Max γ	15.6	8.8	14.0	7.0	

Table 7.1-5 Deformed shape, stress distribution in warp and fill directions, maximum stress and safety factor (γ) of panel 2

Stress distribution in membrane (kN/m)		panel 2			
		σ_x (warp)		σ_y (fill)	
Model A membrane	Case 1 downwards loading (snow + wind)				
	Max γ	29.8	4.6	26.5	3.7
	Case 2 upwards loading (uplift wind)				
Max γ	26.4	5.2	29.4	3.3	
Model B Membrane + cable	Case 1 downwards loading (snow + wind)				
	Max γ	21.7	6.3	20.5	4.8
	Case 2 upwards loading (uplift wind)				
Max γ	18.2	7.6	19.7	5.0	

In Figs. 7.1-11 and 7.1-12, the final deformed shape of each case is shown. As explained with Figs. 7.1-9 and 7.1-10, the influence of the cable on the stability of the membrane for the downward loading is not so significant, and this also can be seen from the deformed shapes.

On the other hand, when the uplift loading is applied, the influence of the cable on the stability of the membrane is more crucial.

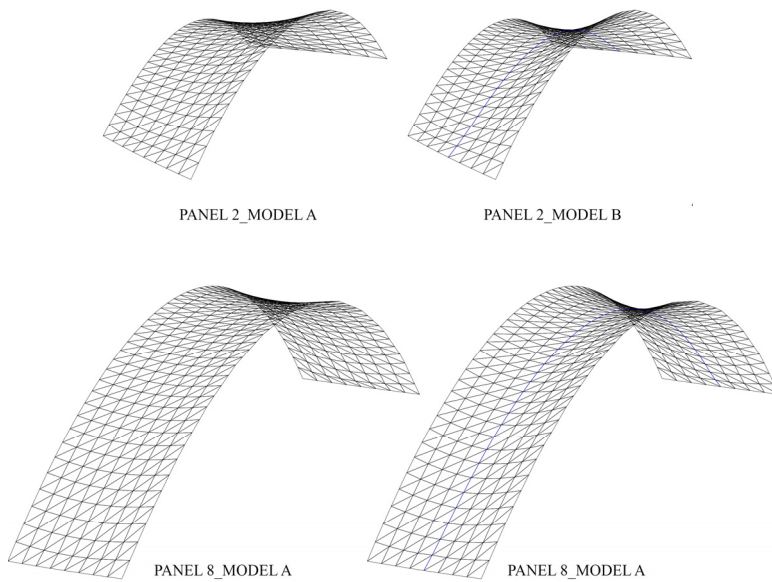


Figure 7.1-11 Final deformed shape under downward loading

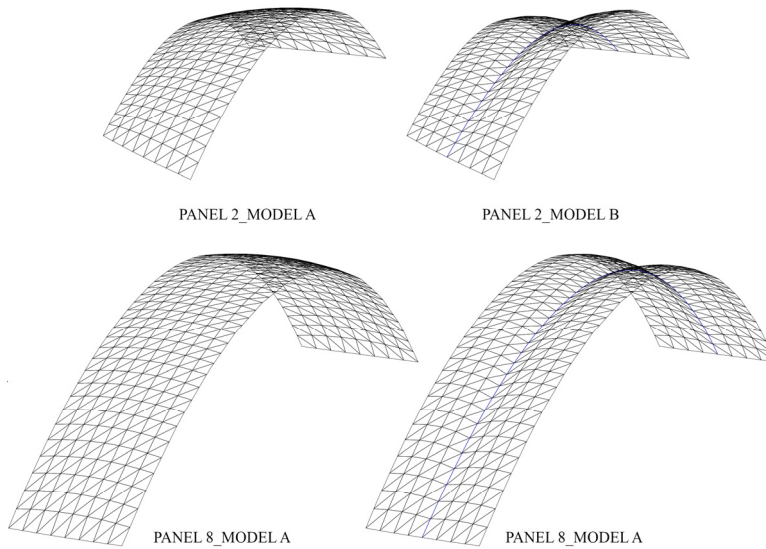


Figure 7.1-12 Final deformed shape under uplift loading

7.1.4. Conclusion

This study demonstrates how the implementation of cables can strengthen the membrane structures, especially in the most critical loading case (uplift wind). From the comparison of panels 2 and 8 it is understood that a more regular geometry helps to have a more stable response under various loading conditions.

Not only the consideration of cables or other restraining conditions are important but the form finding step also has a great significance on the stiffness of the structure. Without finding a balance initial stress and a minimal surface, the membrane behavior is unpredictable, and the limit stress could be reached much faster, potentially producing the collapse of the structure.

7.2. Jeju World Cup Stadium dome

The Jeju World Cup Stadium, located in the city of Seogwipo, in Jeju Island (Korea), is a multipurpose sports facility with a maximum capacity of 40,000 spectators that was designed to host the 2002 FIFA World cup.



Figure 7.2-1 Original dome of Jeju Stadium (up) (<http://ojakgyoo.com.ne.kr>), new dome of the Stadium (down)

The design of the stadium represents the shape of the crater volcano, inspired by the natural environment of Jeju Island. Besides, the roof of Jeju World Cup Stadium has the form of nets of traditional fishing boats of Jeju.

The dome, a mast-supported membrane structure, was collapsed due to uplift wind loading. In Fig. 7.2-1 both the original design and the new design of the dome after the collapse are shown. In this second case study, the analysis of the new design of the Jeju World Cup Stadium dome is explained.

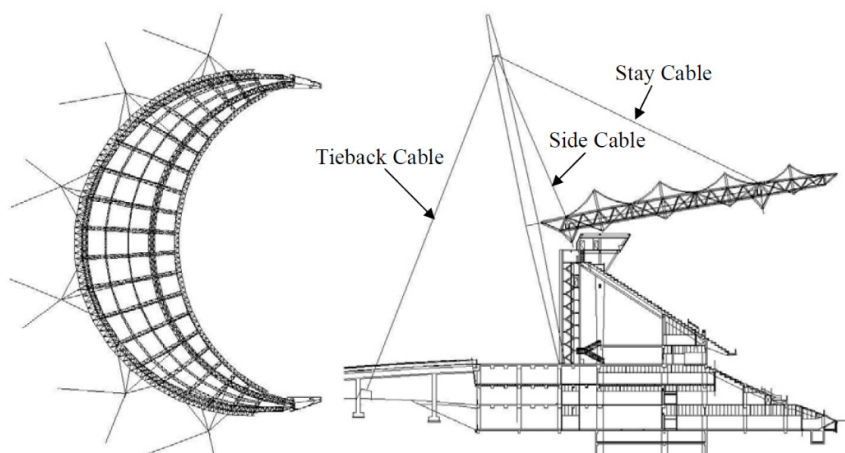


Figure 7.2-2 Plan view (left) and section (right) of the structure of the dome (Brzozowski et al. 2005)

The structural system of the dome features a unique spatial steel trussed frame suspended from six masts by stay, side and tieback cables as shown in Fig. 7.2-2. It has twenty triangular radial trusses, diamond shaped front and rear trusses, and planar tie trusses, all made of steel pipes. Between each radial truss, spans a teflon-coated fiberglass membrane supported by steel cables (Brzozowski et al. 2005).

The frame structural system with a width of 20 meters between supports was not changed after the collapse and just the membrane was redesigned. Figure 7.2-3 shows the redesign of one strip in between the framing system. As it is observable in the figure, the span between the transverse arches that supported the original membrane was much larger than in the new design; from 14 meters span it was reduced to 3.5 meters.

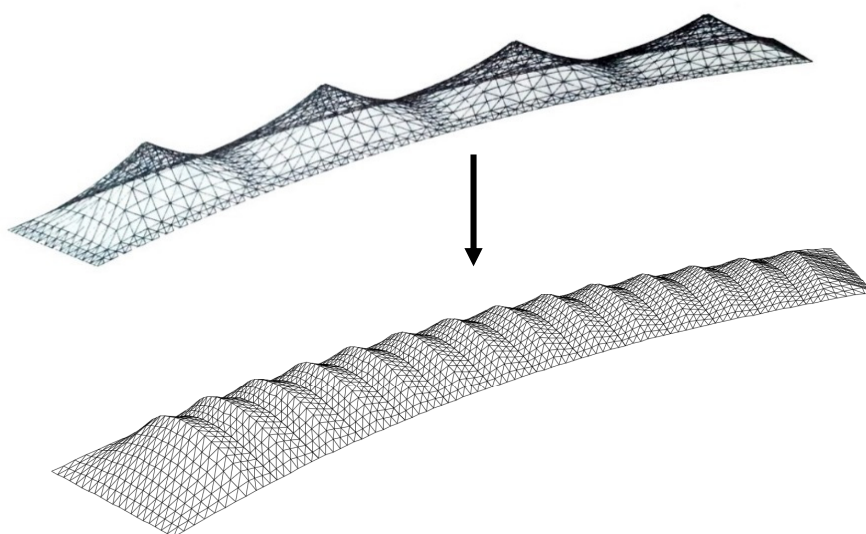


Figure 7.2-3 Original model of one strip of Jeju dome (left), new model of the same strip (right)

Besides, the canopy shape of the membrane was changed for a membrane supported between arches and prestressed with cables in their central section in a similar way as the dome of Seoul Southwestern Stadium explained in the previous section.

7.2.1. Membrane model

7.2.1.1. Models and panels for the analysis

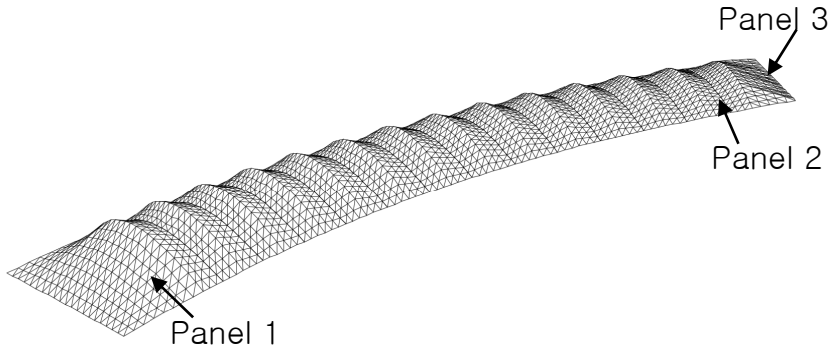
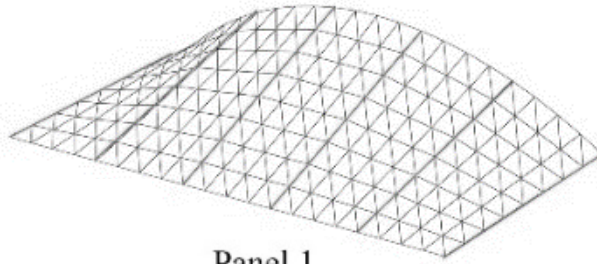


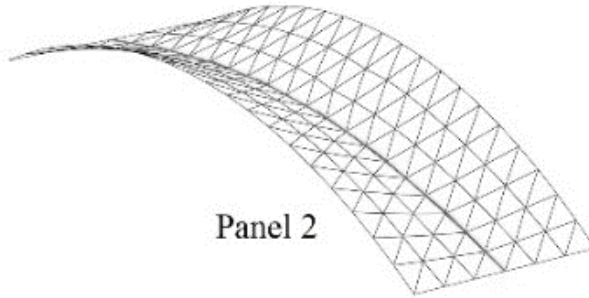
Figure 7.2-4 Representative panels chosen for the analysis

For this analysis, the more representative 3 panels more are chosen as shown in Fig. 7.2-4. Panel 1 and Panel 3 are the border panels and are supported by trusses, and panel 2 is a membrane supported between arches with a prestressed cable in the center. This type of panel is repeated through all the strip.

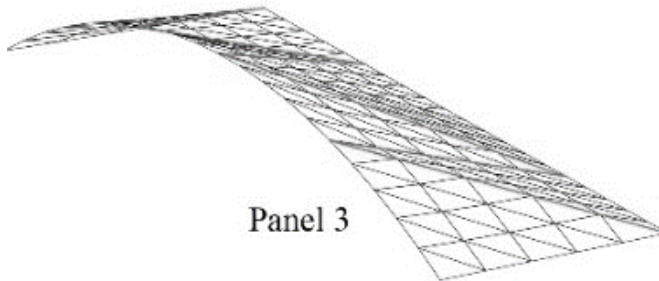
Models for the 3 panels are constructed with triangular membrane elements and cable elements when needed (Fig. 7.2-5). The size of the panels 1 and 2 are 20 meters long and 3.5 meters wide, while panel 1 has 7 meters width. This double width is possible because panel 1 is located in the lower point of the dome strip, while panel 3 is in the higher point. Panel 2 is also chosen from the higher point so the uplift wind is stronger and more representative for the analysis.



Panel 1



Panel 2



Panel 3

Figure 7.2-5 Initial models of the panels chosen for the analysis

7.2.1.2. Material properties

Membrane and cable properties are shown in Table 7.2-1 and 7.2-2 respectively.

Table 7.2-1 Membrane properties for the dome

E_{11} (kN/m)	E_{22} (kN/m)	ν_{12}	ν_{21}	G (kN/m)
1362	975	0.9	0.64	94.4

Table 7.2-2 Valley cable properties for the dome

A (cm ²)	E (kN/m ²)	EA (kN)
6.9	1.38×10^8	95220

7.2.1.3. Initial stress conditions

The initial stress for the membrane was increased from 3 kN/m used in the original design to 5.25 kN/m in the new design, and the cable in the panel 2 is prestressed with 120 kN.

7.2.2. Analysis results

The analysis procedure of these models is the same as explained in the first case study. Firstly, a form-finding analysis is realized to find the proper balance shape where stresses are equally distributed, and then, a stress-deformation analysis is performed to check if the design is sufficiently safe under the loading conditions.

As the form-finding step was explained in detail for the Seoul Southwestern Stadium dome, in this study, the analysis results are shown, focusing on the stress-deformation step and the safety confirmation under the uplift wind loading condition.

7.2.2.1. Design loading cases

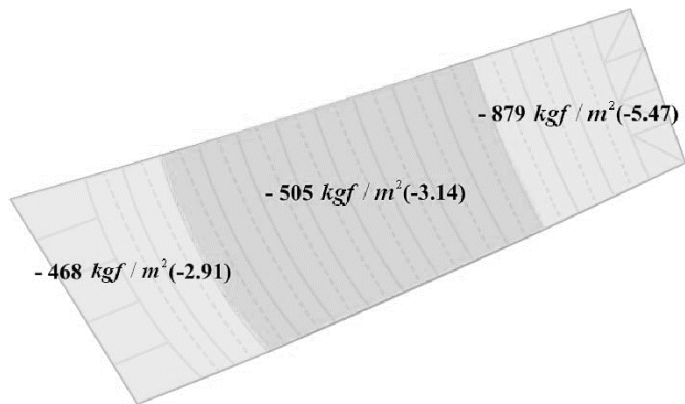


Figure 7.2-6 Uplift wind loading condition

When an open stadium with membrane dome is presented, the most dangerous loading condition is the one created by the uplift wind. A special care has to be taken and detailed analysis should be performed to ensure that in any condition the uplift wind does not make the dome to collapse.

Particularly, the loading condition should not be underestimated in an island like Jeju where the strong monsoon winds hit during the raining season. However, this was not considered in the original design and the dome collapsed.

Figure 7.2-6 shows the new stricter uplift wind loading conditions that were considered for the current design. As the dome is inclined, higher values are taken depending on the height of the location of the panel.

7.2.2.2. Results of the deformed shape and displacements

In Fig. 7.2-7, the displacements of the surface of each panel in the z direction are shown. The behavior of panel 1 and panel 3 is linked with the trust support system that is provided for each edge panel.

Panel 1, located in the lower height of the dome, presents a parallel support system that restricts the movement.

However, as panel 3 is in the higher point of the dome strip, a triangular support system was required to overcome the stronger uplift winds. In the case of panel 2, the behavior is similar as the one described in the case study 1 as the panel is supported between arches with a prestress cable in the central section.

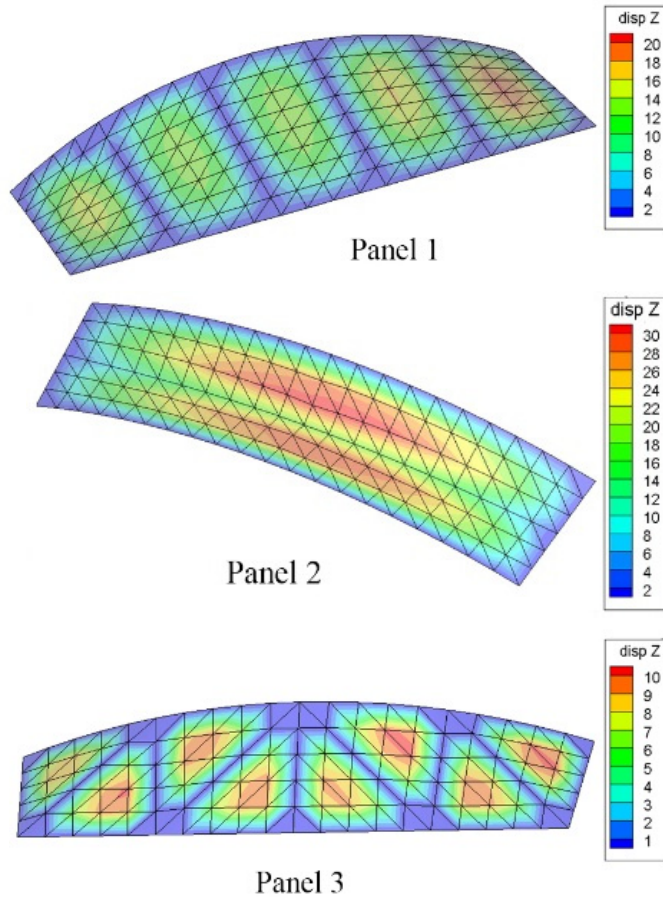


Figure 7.2-7 Comparison of displacement of panels 1, 2 and 3 of the surface in the z direction

Displacements of the central longitudinal section of each panel are described in Fig. 7.2-8. The incline geometry and boundary conditions are the reason for the diverse behavior patterns represented in the graphs.

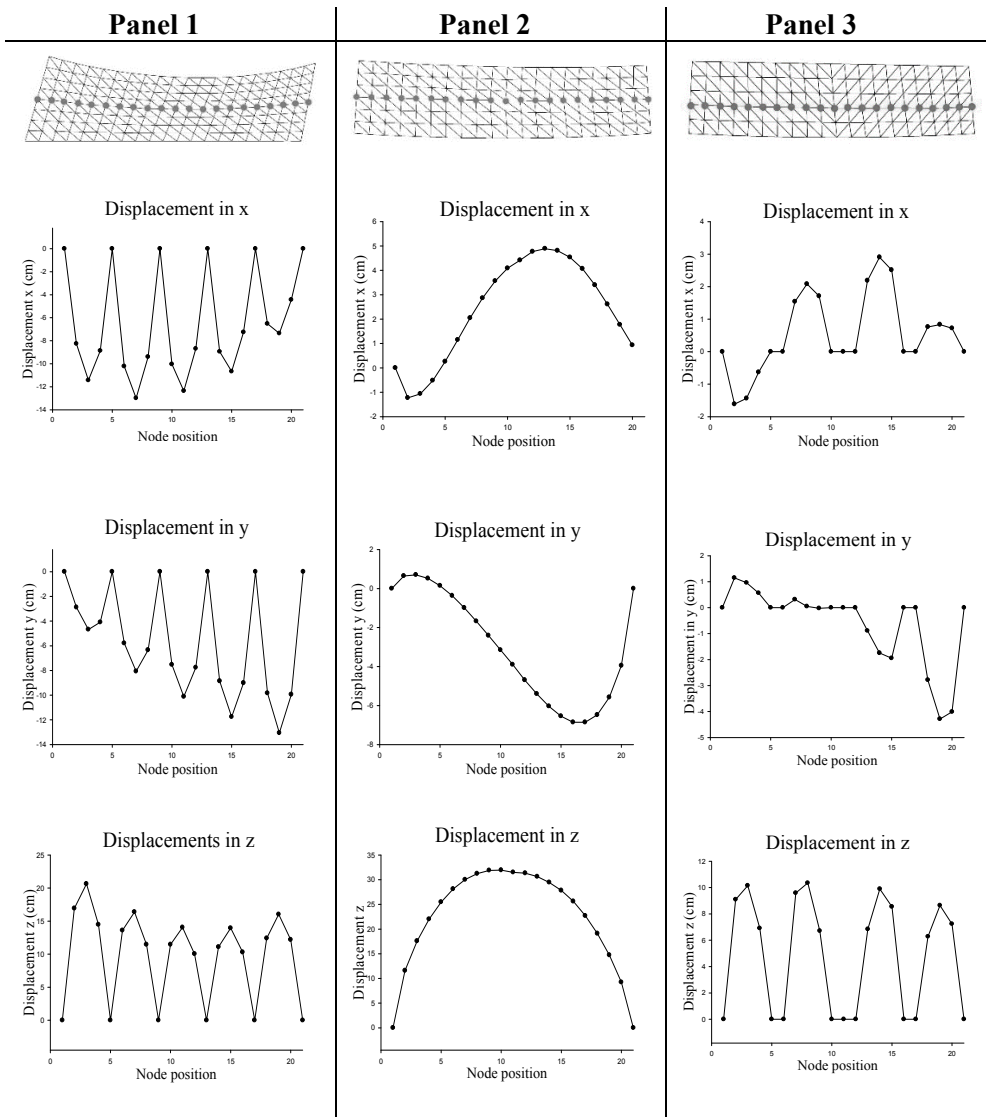


Figure 7.2-8 Displacements of panels 1, 2 and 3 at the nodes of the central longitudinal section

The most restricted panel, panel 3, reaches a maximum displacement of 10 cm in the z direction. In the case of panel 1, the value is near 20 cm. The higher values are found in the case of panel 2 where the

displacement exceeds 30 cm in the center of the section.

However, these values are not that high compared to the displacements of the dome of the case study 1, where the same type of panel reached 40 cm in the center.

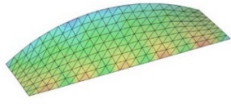
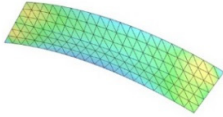
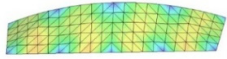
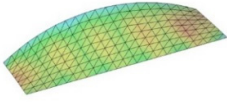
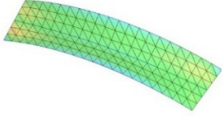
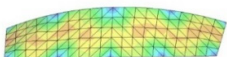
The difference between the panels of the dome in the case study 1 and 2 is that even though the uplift wind loading is much greater in the case of Jeju dome, the size of the panels in the Seoul dome is 5 times longer and 2 times wider. That is why displacements in the case of the dome of the Seoul Southwestern Stadium are greater although, as shown later in this thesis, stresses are smaller due to stricter loading conditions.

7.2.2.3. Stress, deformed shape and safety factor

Table 7.2-3 shows the stress distribution and maximum stress values in the warp and fill directions. It is observable that even these panels are much smaller than the ones in the Seoul Southwestern dome, the values of the maximum stress are much higher. In the Seoul dome, any value of any case and panel reached even 30 kN/m of maximum stress while in this dome, almost all values are around 35 kN/m or higher.

For this reason, the normal fabric used for stadium domes, Sheerfill-II (also used in the Seoul Southwestern dome) could not be used for the Jeju dome because the safety factors were too low due to the high stresses.

Table 7.2-3 Stress distribution and maximum values of each panel in the warp and fill directions

Stress distribution (kN/m)	Panel 1	Panel 2	Panel 3
Maximum in warp direction			
	37.62	36.72	36.43
Maximum in fill direction			
	34.72	34.75	32.31

Then, a much stronger fabric, normally used for the military purpose was finally chosen, Sheerfill-I, and as shown in Table 7.2-4, for this fabric the minimum safety factor of 4 was finally obtained.

Table 7.2-4 Factor of safety for wind up loading for the two types of fabric, Sheerfill-II and Sheerfill-I

Panel	Sheerfill-II		Sherfill-I	
	Warp	Fill	Warp	Fill
1	3.66	2.83	4.54	4.54
2	3.74	2.82	4.65	4.54
3	3.77	3.04	4.69	4.88

Figure 7.2-9 represents the deformed shapes of the three panels under the uplift loading condition. Each of them respond to the boundary conditions imposed; panels 1 and 3 with the edge trusses and panel 2 with the cable between arches.

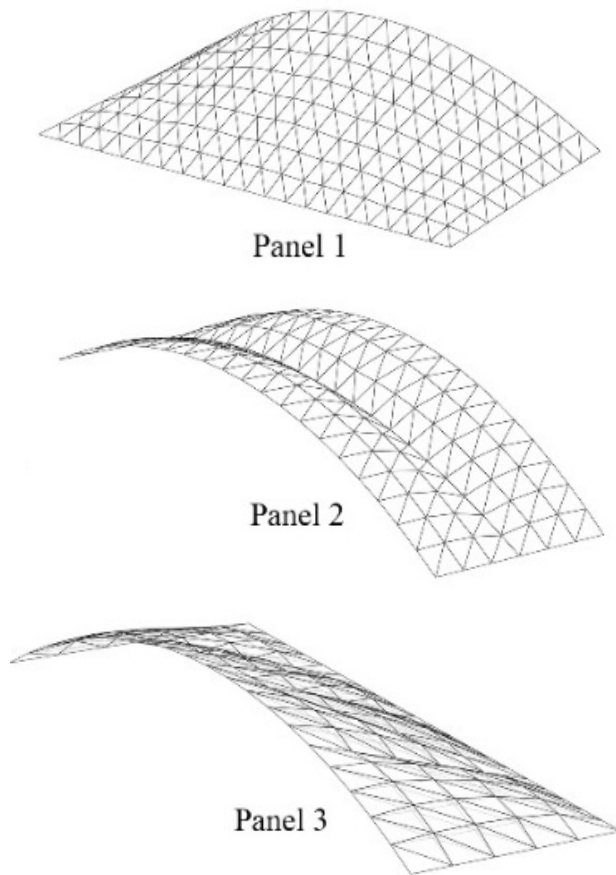


Figure 7.2-9 Deformed shapes of the 3 panels under uplift wind loading condition

7.2.3. Conclusion

With this case study, the importance of the correct consideration of loading conditions is emphasized. Especially, in the case of open stadiums where the uplift wind is much stronger and very high stress could be reached easily.

Besides, several comparisons have been made between the Seoul Southwestern Stadium dome and the Jeju World Cup Stadium dome, concluding that the size of the panels is not as important as the loading conditions and the geometry.

Chapter 8. Parametric Study and Design of Barrel Vault Shaped Membranes

In the previous chapters, after the study of the Seoul Southwestern Baseball Stadium dome and the Jeju World Cup Stadium dome, some general behavior of barrel vault shaped membrane structures was disclosed. For example, it was proved that the geometry of the structure is one of the most influential factors for the performance.

The motivation for this part of the thesis comes from the need of understanding the structural behavior of such structures and the willingness of finding some design limitations to help in the first stages of the project proposal. For this reason, a detailed study is made for the different parameters that participate in the geometry of barrel vault shaped membranes, and procedure and results are explained in this chapter.

8.1. Assumptions for the models

The barrel vault shaped membranes are considered to be supported between steel arches, keeping the double curvature characteristic from tensile structures as shown in Fig. 8.1-1

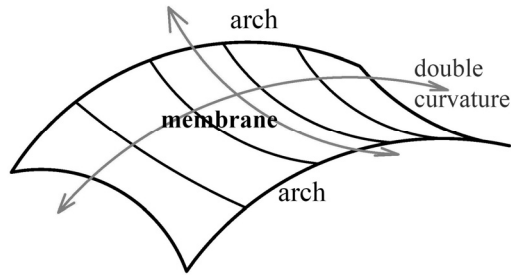


Figure 8.1-1 Barrel vault shaped membrane structures

The following assumptions are the base for this study, and are chosen considering that this study is made in Korea.

8.1.1. Material properties, loading conditions and initial stress

For the simplification of the study, the assumptions are made based on the case studies. Material properties and loading conditions are taken from the Seoul Southwestern Baseball Stadium dome (Tables 8.1-1 and 8.1-2). The membrane material used for the Seoul dome is commonly used in Korea, and at the same time, taking the loading conditions for Seoul (wind and snow) can provide a general idea of the design limitations in this country. However, future research should include other loading conditions and material properties for a more generalized conclusion.

Table 8.1-1 Membrane properties for the models

E_{11} (kN/m)	E_{22} (kN/m)	ν_{12}	ν_{21}	G (kN/m)
1230	950	0.804	0.62	96.26

Table 8.1-2 Load combinations for the analysis

Case 1	Downward loading	Self-weight + prestress + snow + wind (downwards)
Case 2	Uplift loading	Self-weight + prestress + wind (uplift)

The initial stress is set to 5 kN/m in both the warp and fill directions.

8.1.2. Maximum stress and safety factors

In the same way, the safety factors are taken as the ones used for membrane structures in Korea. Each country has a different regulation regarding safety factors for membrane structures. While in other countries the factor can be very moderate, getting to values greater than 6 or 7, the Korean approach set the value to 4 for any membrane structure.

Having this into account and considering the ultimate tensile strength of the Sherfill II fabric for this study (the most commonly used membrane fabric in Korea), the maximum stresses for the warp and fill directions can be set as in Table 8.1-3.

Table 8.1-3 Membrane properties for the models

Direction	Safety factor	Sherfill II (kN/m) Ultimate tensile strength	Maximum stress allowed (kN/m)
Warp	4	137.5	34.38
Fill	4	98.1	24.53

8.1.3. Barrel vault shaped membrane parameters for the study

In this study, regular barrel vault shaped membranes are the main focus. However, one grade of irregularity is also introduced to have a wider range of design possibilities. The parameters for the study are described in this section.

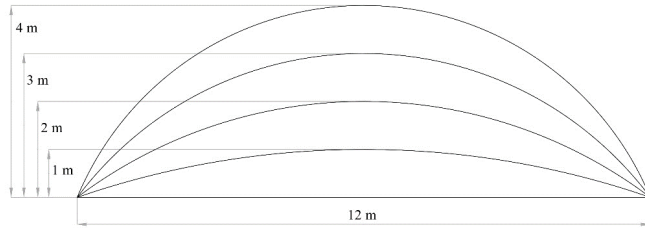
8.1.3.1. Regular barrel vault shaped membranes

The geometry of regular barrel vault shaped membranes can be divided into 3 different parameters: the arch curvature, the width between arches and the span of the arches. These 3 parameters are described in Fig. 8.1-2. The arch curvature parameter considers the same span with different heights; the width parameter also considers the same span and different width between the arches of the membrane; and the scale parameter keeps the same arch curvature and width of the panels, and by increasing the scale, covers different spans.

With these 3 parameters all the possible regular barrel vault shaped membranes can be defined. For this reason, all these parameters are studied in detail including all possible combinations between them.

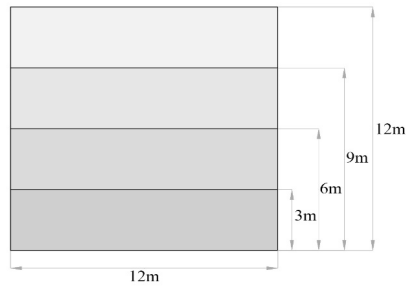
ARCH CURVATURE

Same span
Different height



WIDTH

Same span
Different width



ARCH SCALE

Same arch curvature and width
Different span

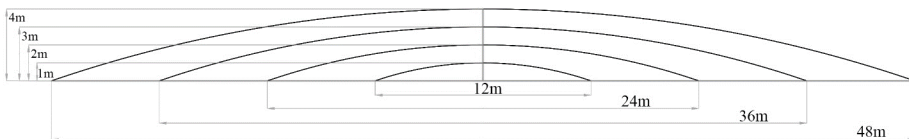


Figure 8.1-2 Regular barrel vault shaped membrane's parameters

8.1.3.2. One grade of irregularity for barrel vault shaped membranes

For a wider range of design possibilities, one grade of irregularity is introduced. From the regular shaped panels that are symmetric about the two axis, one of the symmetries is removed.

In this way, two new parameters are introduced as described in Fig. 8.1-3: asymmetry about the transversal axis and asymmetry about the longitudinal axis.

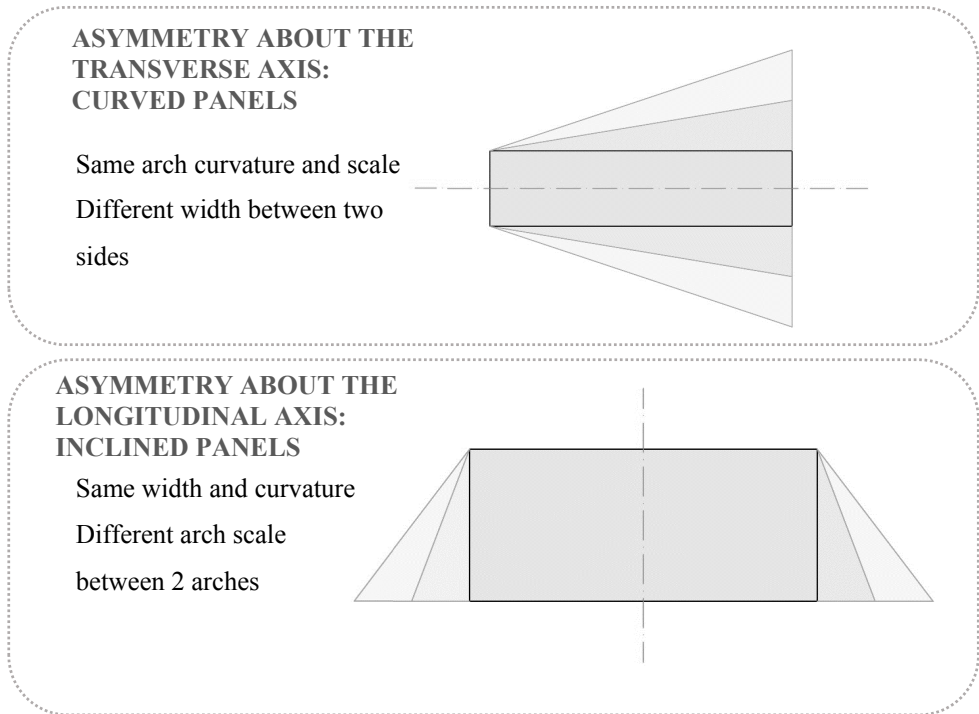


Figure 8.1-3 One grade of irregularity barrel vault shaped membrane parameters

In the case of asymmetry about the transverse axis, the same curvature and scale in the arches are maintained but a different width ratio is introduced creating an angle in between the arches. This results in panels that can be used in curved situations. In the second parameter, asymmetry about the longitudinal axis, the width in the panel and the curvature of the arches are maintained, but each arch has a different scale creating an angle between the arches in section, which means that the panels are inclined. Further explanation about the parameter is given in the following sections.

8.1.4. Design and analysis procedure

For this study different models are designed investigating the different parameters explained earlier. Then, the two step analysis is performed. Firstly, form-finding analysis is made to find the proper coordinates of the model that correspond to a balanced initial stress. The capacity of the shape to obtain a proper balanced stress is also considered as a factor for the design limitations.

After obtaining the form-found models, those are used to perform the stress-deformation analysis under both loading conditions; downwards and upwards loading. From the results, two limitations are considered: the excess of the maximum stress allowed, which means that the model is not safe; and the existence of negative stresses after the analysis, which indicates wrinkle in the membrane and thus the possibility of ponding.

8.1.4.1. Modeling of the panels for the analysis

To simplify the representation of the results as much as possible, the same element division and numbering is used. Figure 8.1-3 represents a basic panel with the node and element numbers used.

137	138	139	140	141	142	143	144	145	146	147	148	149	150	151	152	153
120	121	122	123	124	125	126	127	128	129	130	131	132	133	134	135	136
103	104	105	106	107	108	109	110	111	112	113	114	115	116	117	118	119
86	87	88	89	90	91	92	93	94	95	96	97	98	99	100	101	102
69	70	71	72	73	74	75	76	77	78	79	80	81	82	83	84	85
52	53	54	55	56	57	58	59	60	61	62	63	64	65	66	67	68
35	36	37	38	39	40	41	42	43	44	45	46	47	48	49	50	51
18	19	20	21	22	23	24	25	26	27	28	29	30	31	32	33	34
1	2	3	4	5	6	7	8	9	10	11	12	13	14	15	16	17

Node numbers (total 153)

226	228	230	232	234	236	238	240	242	244	246	248	250	252	254	256	
225	227	229	231	233	235	237	239	241	243	245	247	249	251	253	255	
194	196	198	200	202	204	206	208	210	212	214	216	218	220	222	224	
193	195	197	199	201	203	205	207	209	211	213	215	217	219	221	223	
162	164	166	168	170	172	174	176	178	180	182	184	186	188	190	192	
161	163	165	167	169	171	173	175	177	179	181	183	185	187	189	191	
130	132	134	136	138	140	142	144	146	148	150	152	154	156	158	160	
129	131	133	135	137	139	141	143	145	147	149	151	153	155	157	159	
98	100	102	104	106	108	110	112	114	116	118	120	122	124	126	128	
97	99	101	103	105	107	109	111	113	115	117	119	121	123	125	127	
66	68	70	72	74	76	78	80	82	84	86	88	90	92	94	96	
65	67	69	71	73	75	77	79	81	83	85	87	89	91	93	95	
34	36	38	40	42	44	46	48	50	52	54	56	58	60	62	64	
33	35	37	39	41	43	45	47	49	51	53	55	57	59	61	63	
1	2	4	6	8	10	12	14	16	18	20	22	24	26	28	30	32
	3	5	7	9	11	13	15	17	19	21	23	25	27	29	31	

Element numbers (total 256)

Figure 8.1-4 Node and element numbers for the base model

8.2. Regular barrel vault shaped membranes

To define the design limitations for the regular shaped membranes, each parameter related to the geometry should be studied. The three parameters that defined the regular shapes introduced earlier are described and analyzed in detail in this section.

8.2.1. Arch curvature

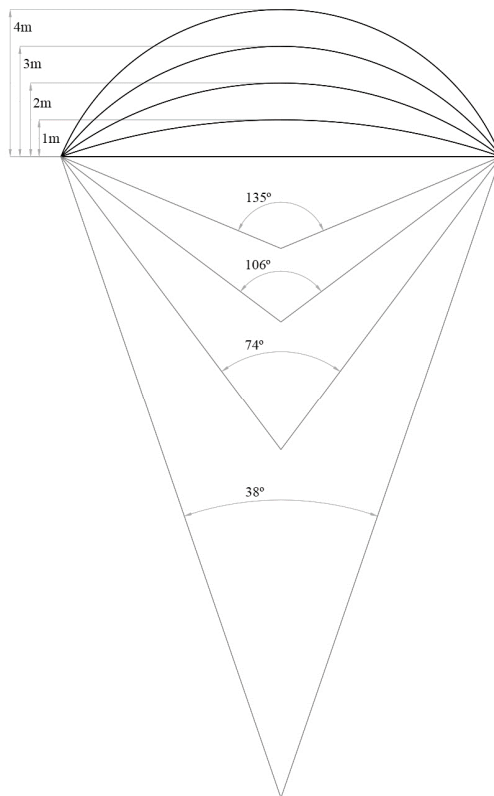


Figure 8.2-1 Angle subtended by the arch

The arch curvature is studied by keeping the same span and changing the height of the arch. To define the parameter, the angle subtended by the arch is used as shown in Fig. 8.2-1.

Four initial curvatures are studied: 38° , 74° , 106° and 135° . All these models are created with the same span and width of 12 m and 6 m respectively, and with the node and element numbering shown earlier in Fig. 8.1-3. The selection of these parameters is based on experience, and they are just initial values. Other ratios are studied in later sections. Figure 8.2-2 represents the four models that are initially analyzed.

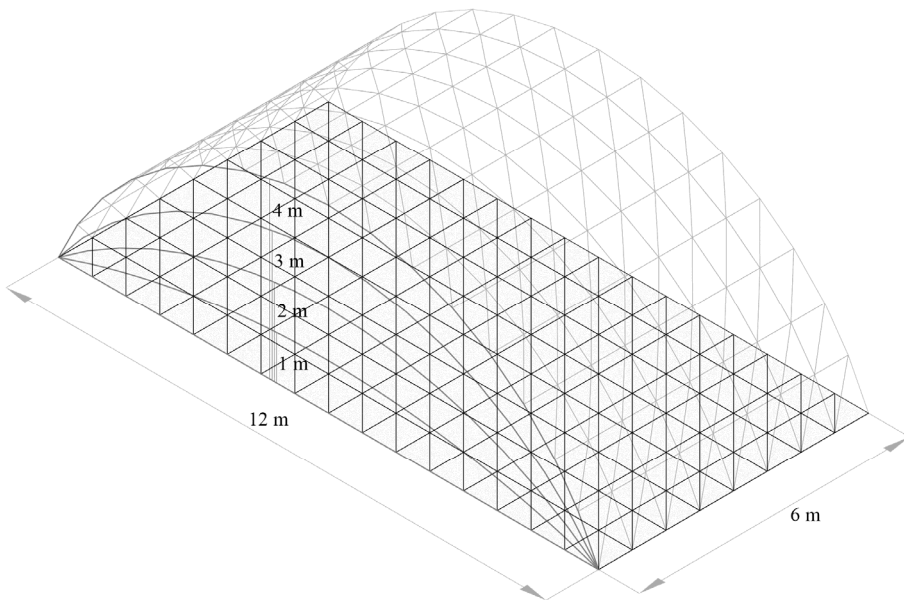


Figure 8.2-2 Arch curvature initial models

8.2.1.1. Form-finding analysis for various arch curvatures

Figure 8.2-3 represents the initial models that were designed for the four different curvatures, and the final shapes determined from the form-finding analysis. In the figure it is shown how the double curvature is obtained after performing the analysis and how with the increment of the arch curvature, the transverse curvature in the final shape is also increased.

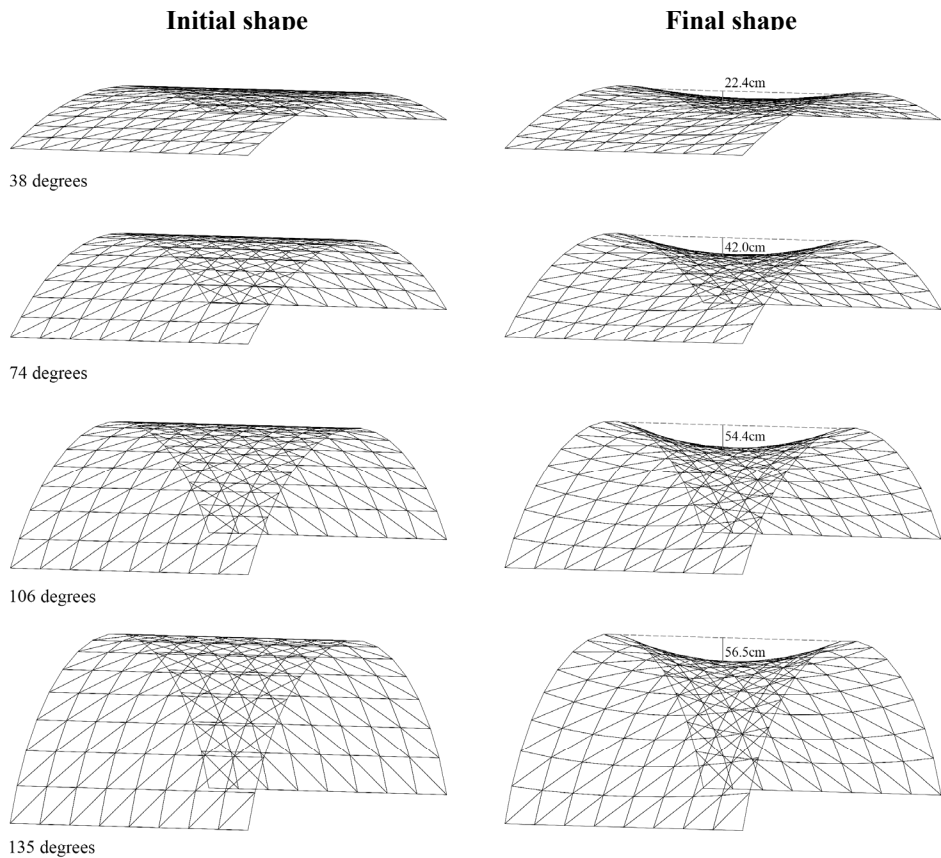
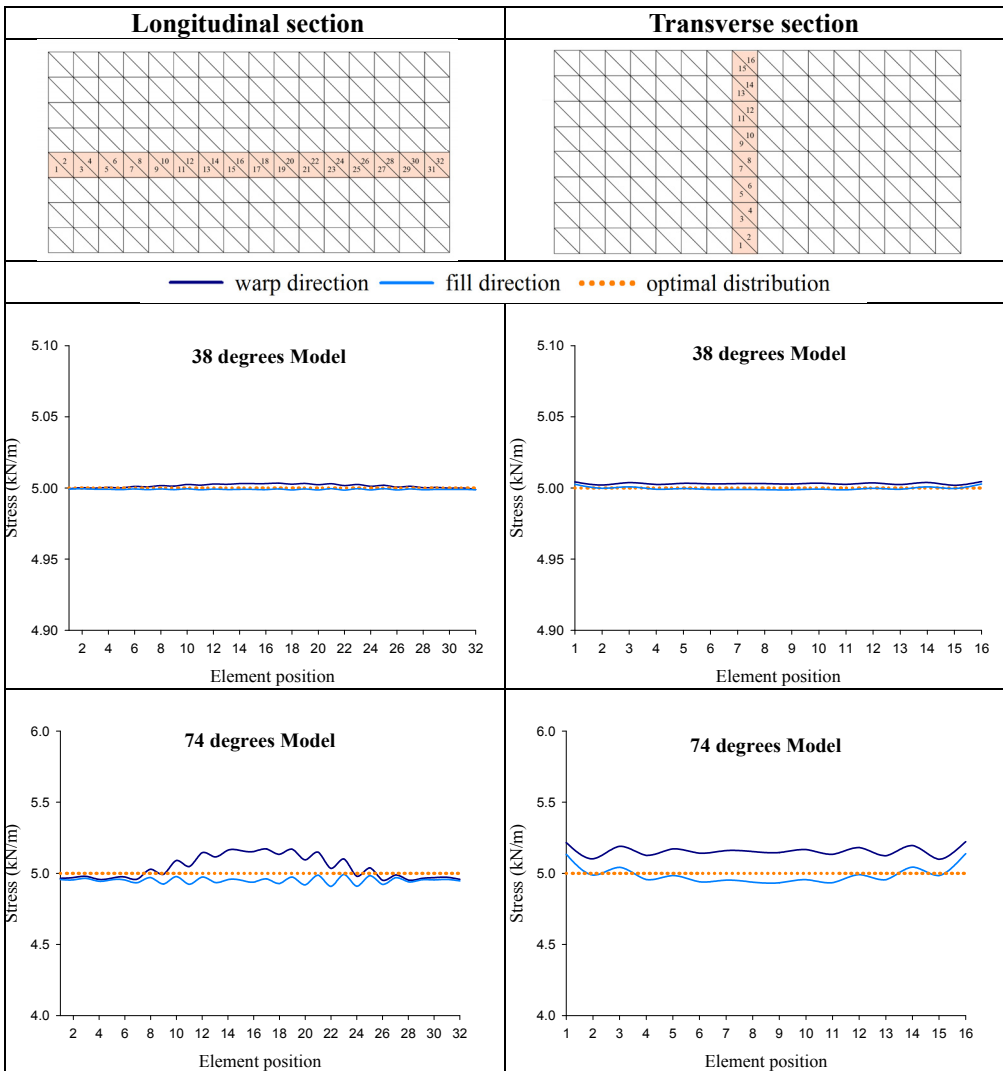
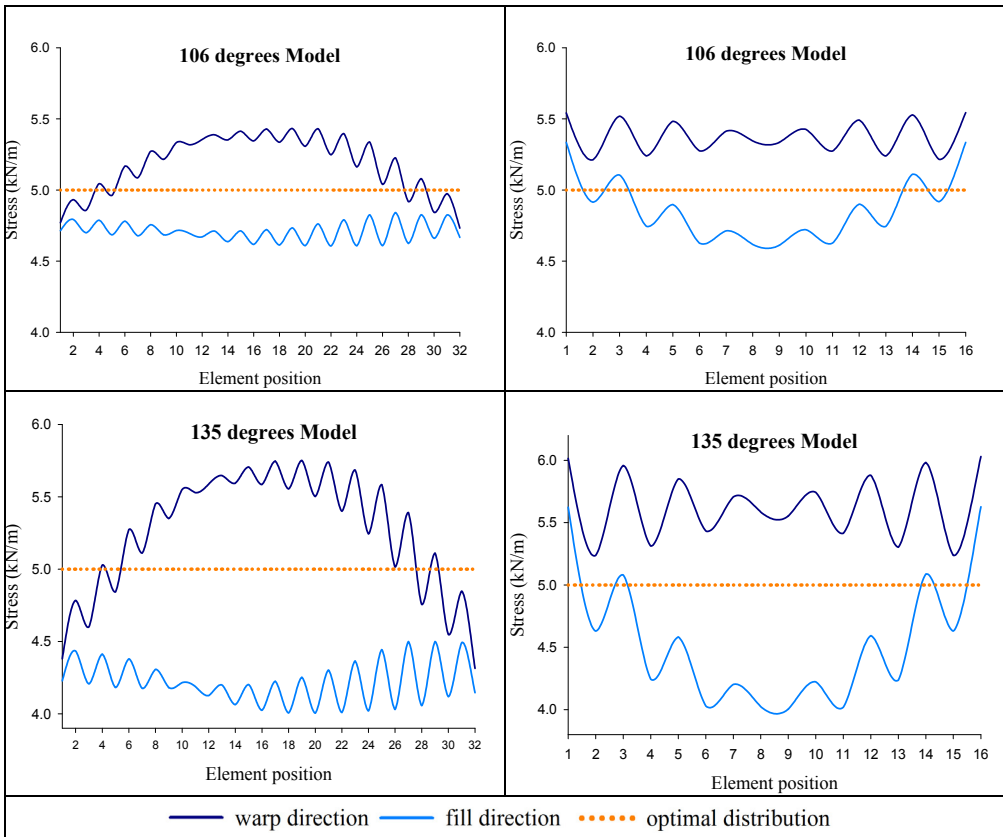


Figure 8.2-3 Arch curvature initial shape and final shape after form-finding analysis

The initial stress distribution in the elements of the longitudinal and transverse sections after the form-finding analysis can be read from Table 8.2-1. As explained earlier, the distribution of the initial stresses should intend to be balanced between both warp and fill directions and along all elements.

Table 8.2-1 Initial stress distribution after form-finding analysis





The initial stress is set to be 5 kN/m in both directions; however, when looking at the initial stress distribution graphs in Table 8.2-1, it is noticed that as the curvature increases in the arches, the uniformly distributed stress is more difficult to reach. Only 38 and 74 degrees models seem to reach an appropriate balanced distribution.

As studied earlier, if the initial stress is not balanced in the form-finding process, the structure could have an unpredictable behavior, reaching maximum allowable stresses or negative values after the stress-deformation analysis.

It is for that reason, that the stress-deformation analysis should be performed to check the performance of these models before having a clear conclusion

8.2.1.2. Stress-deformation analysis for various arch curvatures

After having found the perfect shapes from the form-finding analysis, the stress-deformation analysis is performed under both loading conditions, downwards and upwards loadings.

Figure 8.2-4 represents the maximum stresses obtained in the different arch curvature models for both loading conditions and in both warp and fill directions. Limitations were given by the ratio between the fabric strip's ultimate tensile strength and the safety factor, being 34.38 kN/m for the warp direction and 24.53 kN/m for the fill direction.

As the behavior was not very clear in the area underlined on Fig. 8.2-4 graphs, more intermediate models are also analyzed corresponding to 10, 19, 29 and 56 degrees. However, in any case the maximum allowable stress is reached, and a decrease of the stresses is observed when the arch curvature increases. From these criteria, it can be said that all models are safe.

Nevertheless, when looking at the full stress distribution in the panels resulting from the stress-deformation analysis under upward loading condition (Fig. 8.2-5), negative values are found in the arch curvature models of 74, 106 and 135 degrees. When this happens, wrinkle in the membrane can occur and thus ponding problems too.

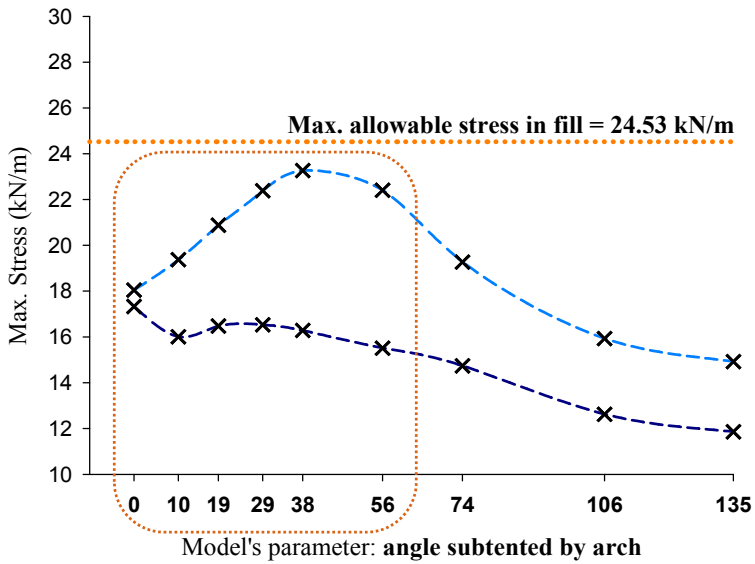
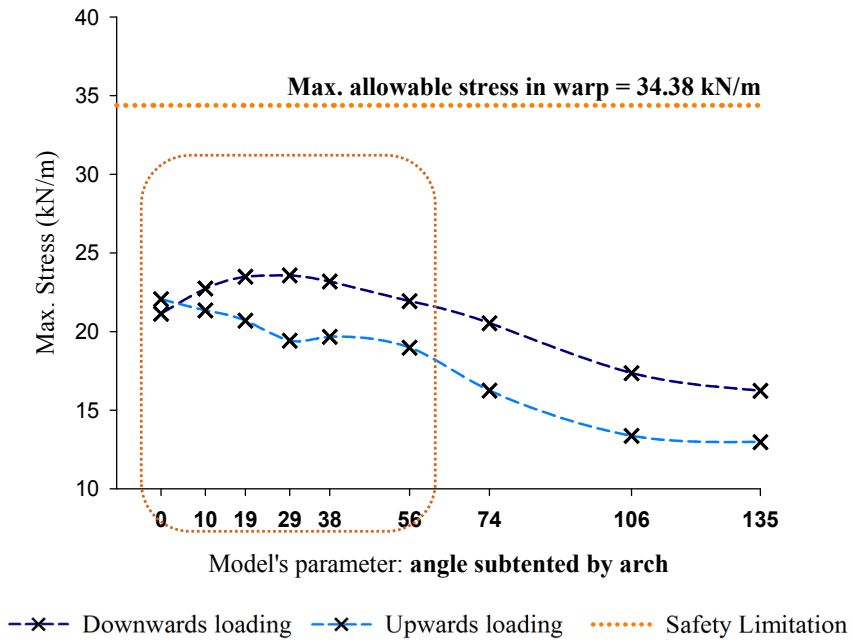


Figure 8.2-4 Maximum stresses in warp and fill directions for the different arch curvature models

For all those reasons and considering also the initial stress distribution problems found in the form-finding analysis, curvatures from 0 to 74 degrees can be considered more proper for the design.

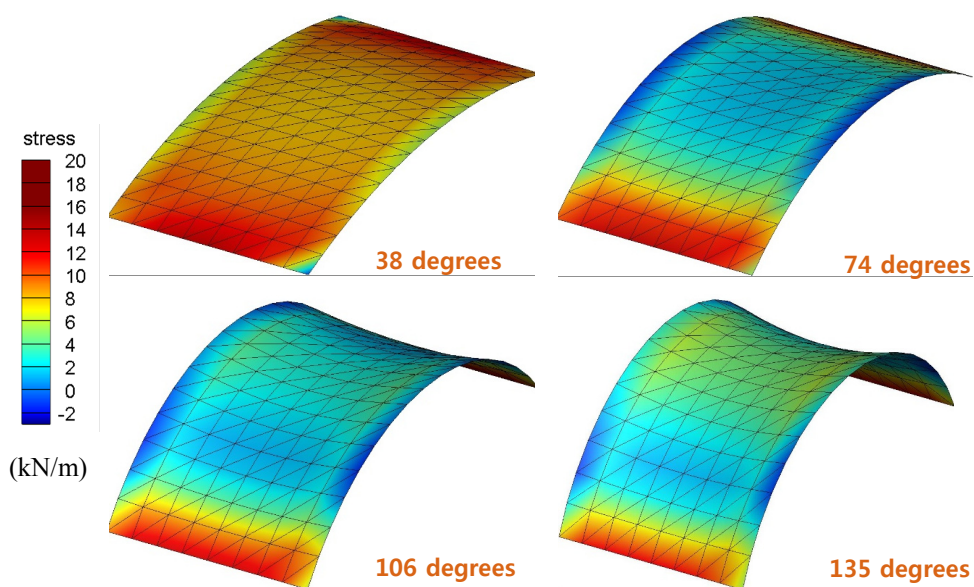


Figure 8.2-5 Stress distribution in the warp direction under upwards loading condition

8.2.2. Width

For the panel width parameter, 4 different spans between arches are studied: 3, 6, 9 and 12 meters, while the span in the longitudinal direction remains as 12 meters (Fig. 8.2-6). These four width values are modeled for the most relevant arch curvatures found in the previous section: 19, 38, 56 and 74 degrees.

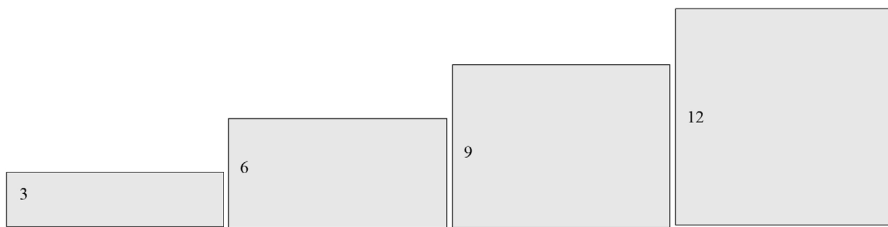


Figure 8.2-6 Width parameter models

8.2.2.1. Form-finding analysis for various widths

In Fig. 8.2-7 the final shapes of the width models for the different arch curvatures studied earlier are represented. As in the previous section with the arch curvature parameter, the balance of the initial stresses in both directions can be studied after the form-finding analysis. While there is a great influence when increasing the arch curvature in the models to reach a uniformly distributed initial stress, the influence of the width increase is much smaller. In moderate arch curvature models with 19, 38 and 56 degrees, the influence is almost imperceptible. Still, in the most curved model studied for the width parameter, that is 74 degrees, the influence of the width is not that relevant as shown in Fig. 8.2-8.

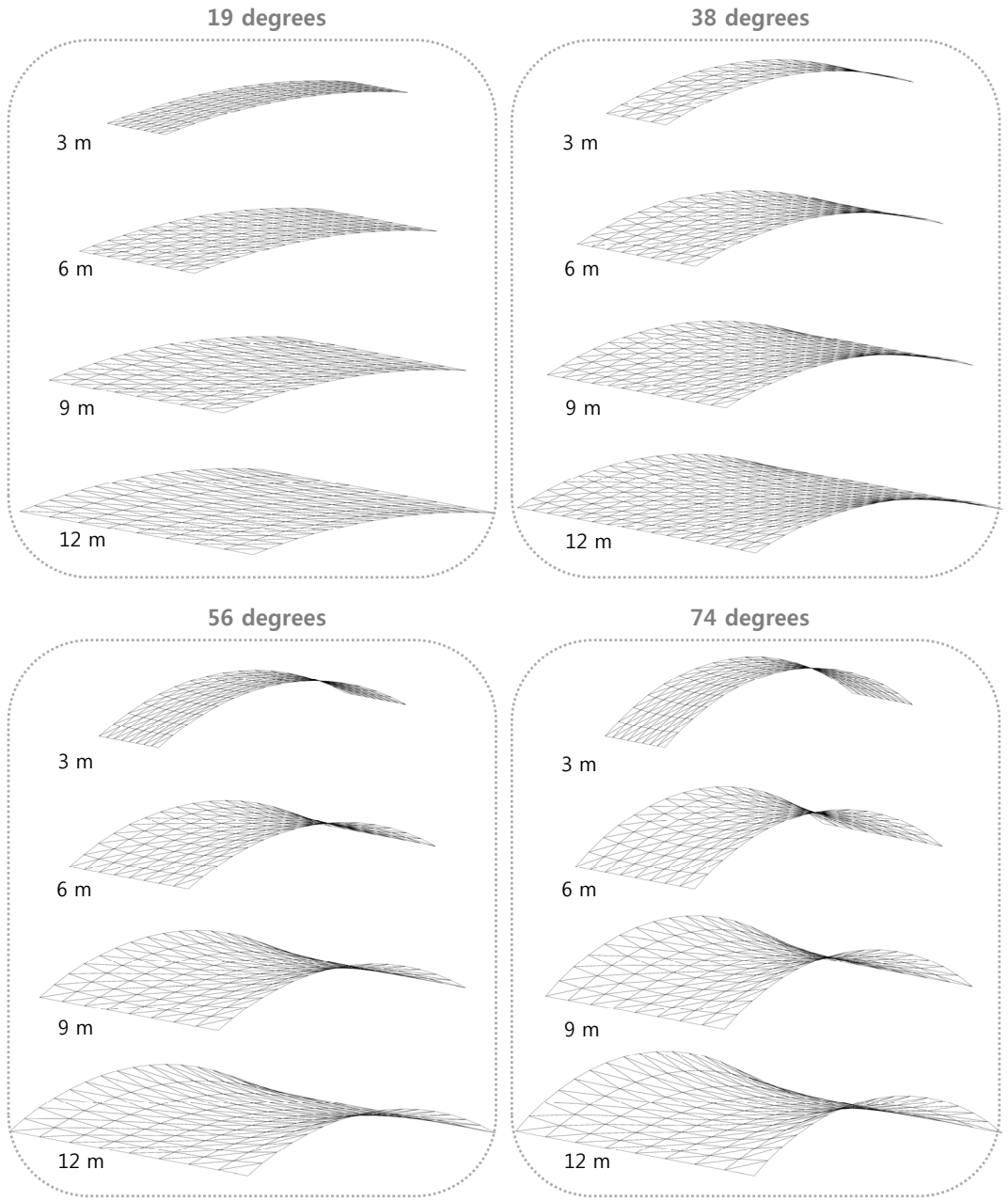


Figure 8.2-7 Final shapes of width models for different arch curvatures

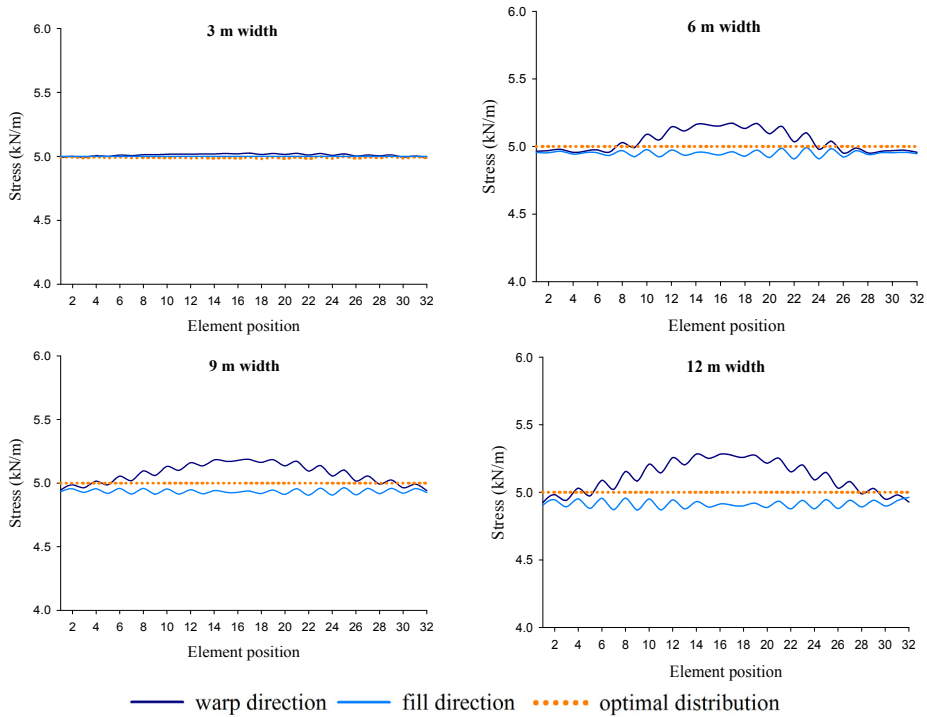


Figure 8.2-8 Initial stress distribution after form-finding analysis in the elements of the longitudinal section for 74 degree arch curvature and variable width models

8.2.2.2. Stress-deformation analysis for various widths

When the stress-deformation analysis is performed under both loading conditions, downwards and upwards loading, maximum stresses can be obtained for each model. Resulting values are compared for the width variation in each arch curvature studied as represented in Fig. 8.2-9.

In this figure, the left column graphs correspond to the maximum stresses in the warp direction, while in the right column the maximum stresses in the fill direction can be found. Here it is appreciable that the maximum stress in the warp direction corresponds always to the values obtained after the analysis with the downward loading condition. However, it is the upwards loading condition that produces the maximum stresses in the fill direction.

When warp and fill directions are compared for the same arch curvature models, it is noticeable that the maximum stress limitation (dotted orange line in Figure 8.2-9) is always reached in the fill direction before in the warp direction. This means that the limitations of width for each arch curvature are given by the fill direction results under the upwards loading condition. As shown in Fig. 8.2-9, the maximum allowed width for 19 degree curvature is 8.1 m. In the same way, for 38 degree is 6.8 m, for 56 degree is 8.8 m and for 74 degree is 12.7 m.

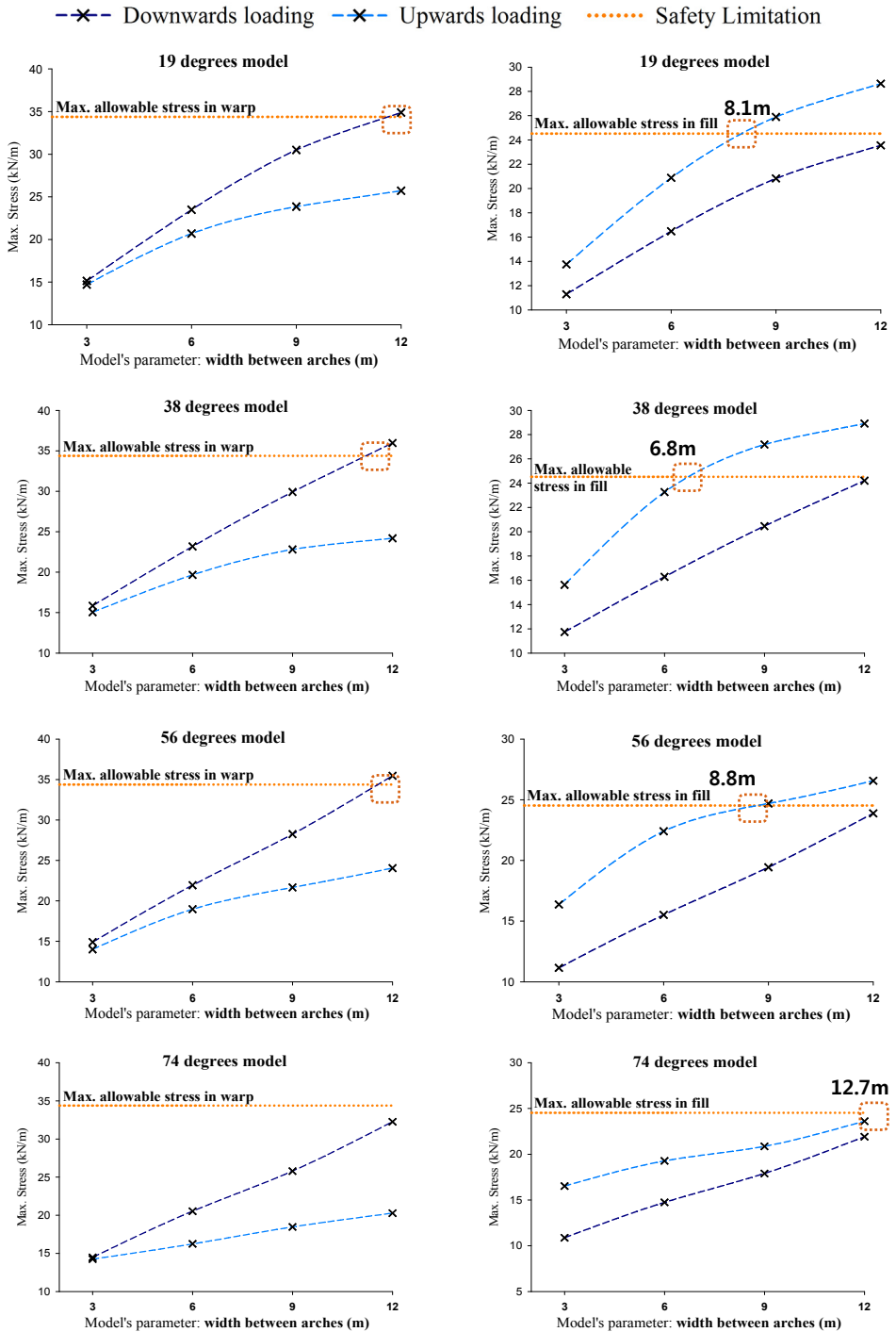


Figure 8.2-9 Maximum stress of width models for the different arch curvature

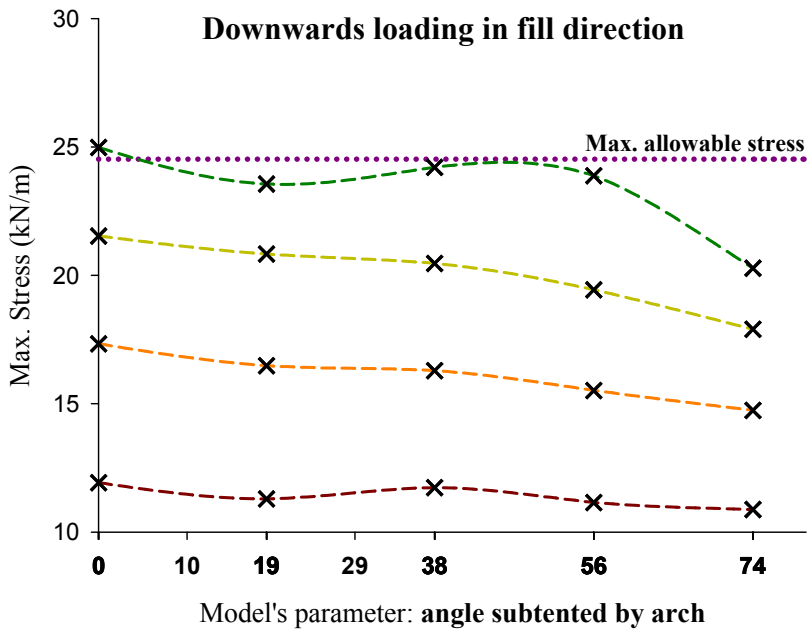
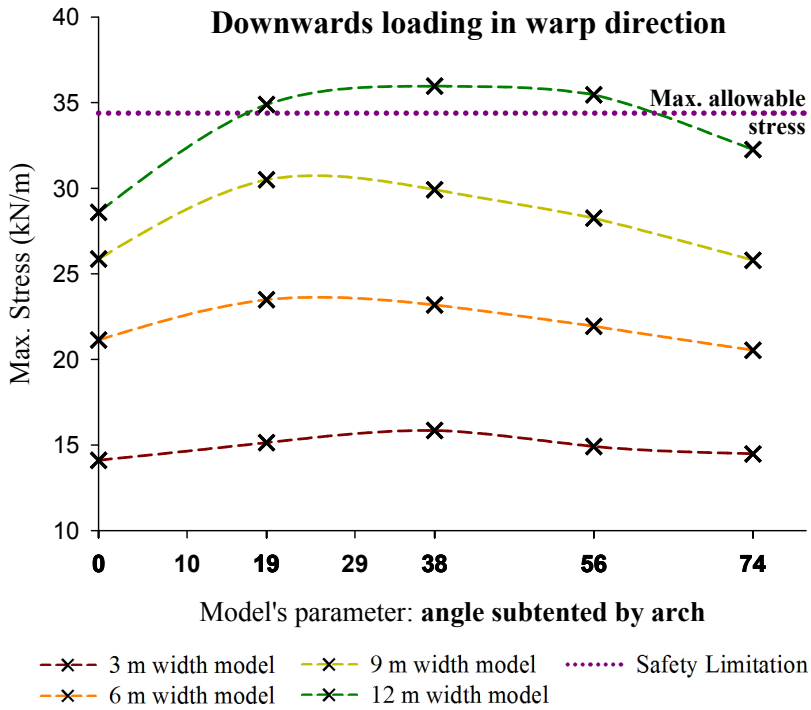


Figure 8.2-10 Behavior with respect to width models under downwards loading

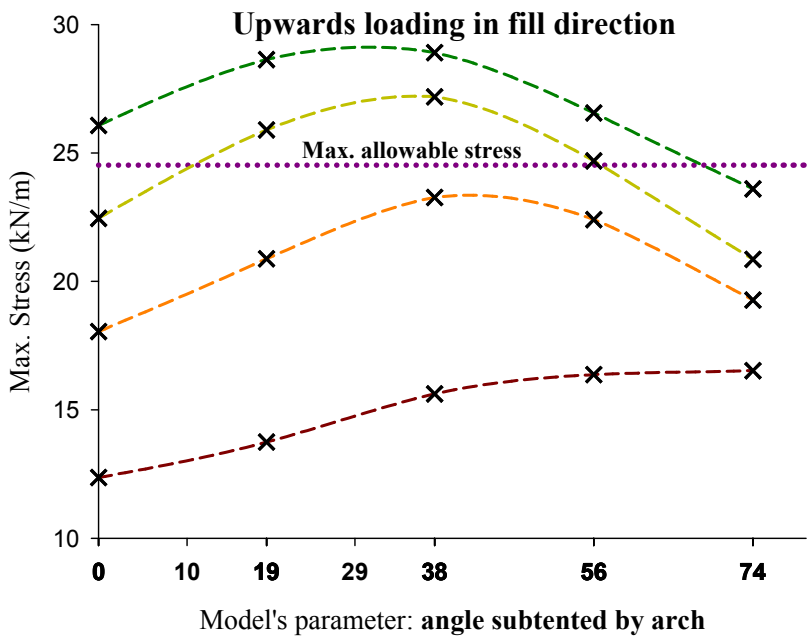
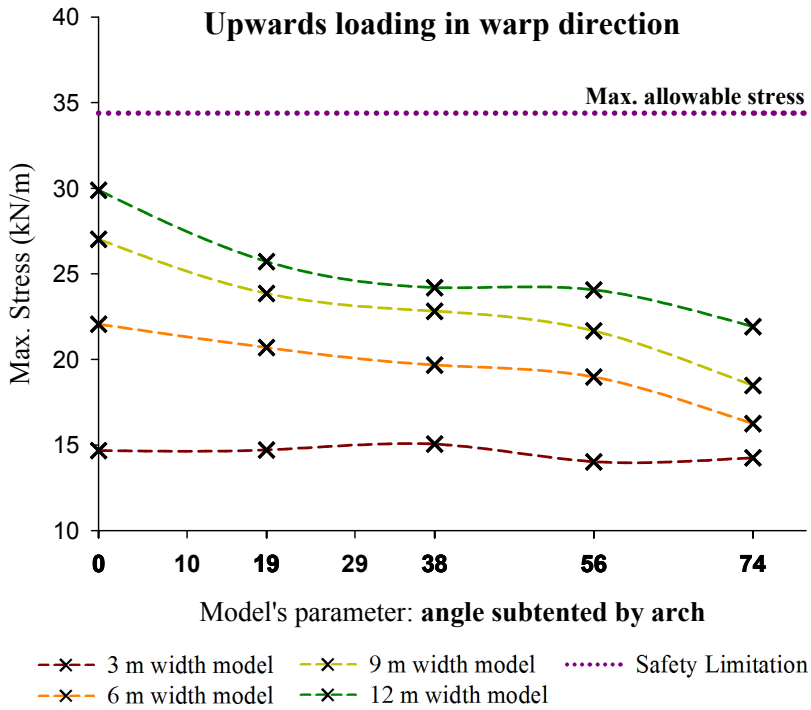


Figure 8.2-11 Behavior with respect to width models under upwards loading

Figures 8.2-10 and 8.2-11 show the behavior with respect to width models under downwards loading and upwards loading, respectively. The most singular behavior is found in the fill direction under upwards loading (Fig. 8.2-11 down) where there is an increase in stress when the curvature is increasing from 0 to about 30 degrees, and after that, the maximum stress decreases again. This behavior is accentuated with the increase of the width.

The reason can be explained with Fig. 8.2-12 where the stress distribution of the panels corresponding to 6 m width in the fill direction under upwards loading is represented. Here it is shown how the stress increments from the 19 to the 38 degrees model, but after the 38 degrees model, because of the double curvature of the panel that is opposite to the deflection direction, the stresses began to decrease.

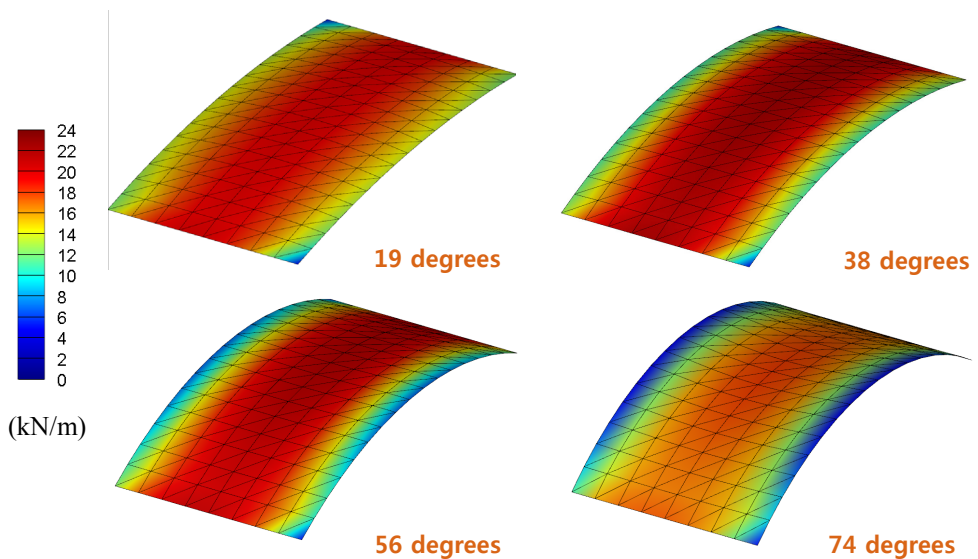


Figure 8.2-12 Stress distribution in the fill direction under upwards loading condition for 6 meter width models

8.2.3. Arch scale

For the scale parameter, the width of the panels and arch curvature is maintained, changing the scale of the arch to cover greater spans.

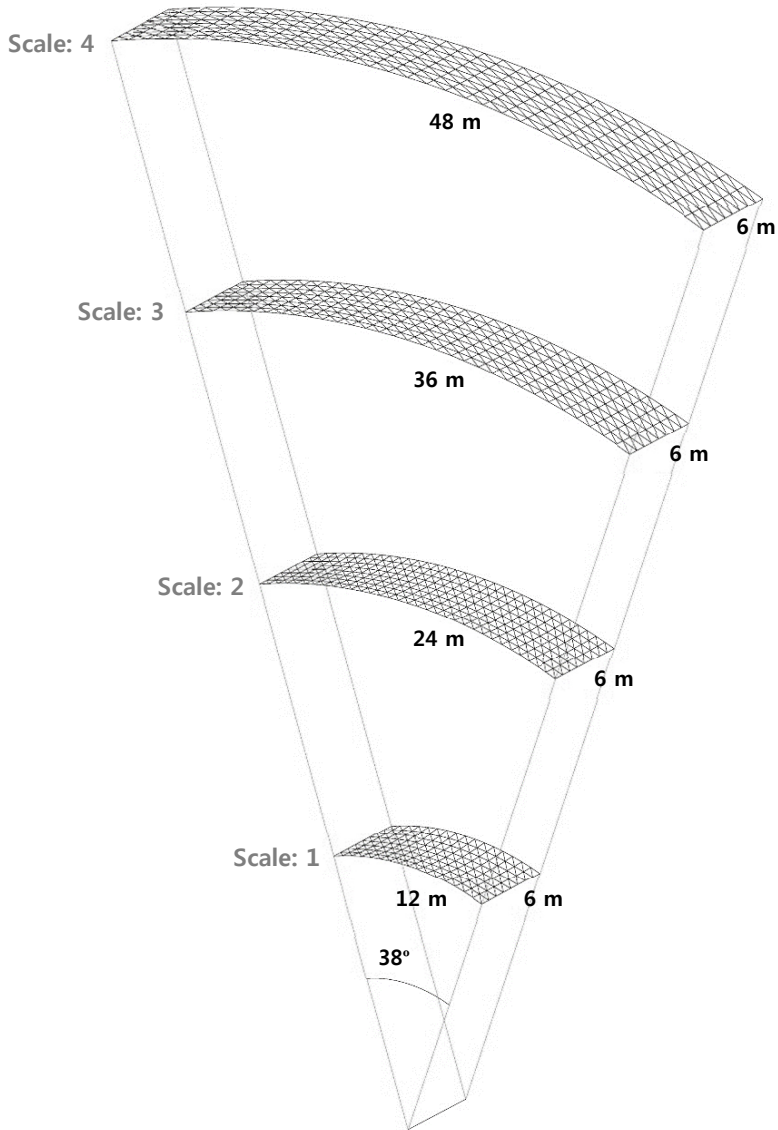


Figure 8.2-13 Scale parameter models

8.2.3.1. Form-finding and stress-deformation analysis for various arch scales

Figure 8.2-13 shows the models of the 6 meter width and 38 degree arch curvature, scaled 2, 3 and 4 times bigger than the original model of 12 m by 6 m.

Results for the stress-deformation analysis performed after the equilibrium shapes are found are shown in Fig. 8.2-14, where the maximum stresses obtained for all these models are represented.

These graphs show how the maximum stress due to downwards loading remains almost equal despite the scale is incremented. However, the maximum stress due to upwards loading in the warp direction increases and in the fill direction decreases. In both cases, it tends to be linear and the variation in value is very small. Additionally, similar behavior is found when checking other scaled models if width and curvature are kept constant.

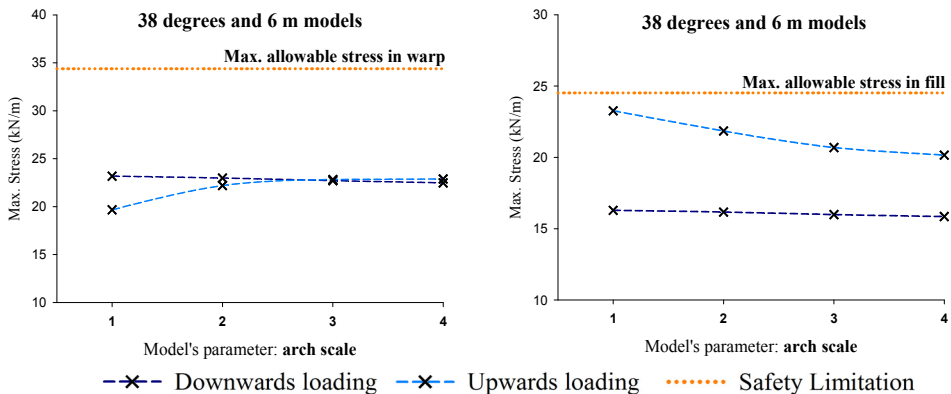


Figure 8.2-14 Maximum stress of scale models for 38 degree curvature and 6 m width

Then, as explained earlier, the upwards loading in the fill direction is the most critical case when increasing width or curvature, and as in the scale model cases the maximum stress decreases, the scale parameter can be neglected.

8.2.4. Parametric study for regular barrel vault shaped membranes

When comparing the regular parameter for barrel vault shaped membranes, maximum stress limitations and wrinkle possibilities are taken into account.

Figure 8.2-15 summarizes all the results from this study. The graph compares the arch curvature in the x axis and the width of the panels in the y axis. Additionally, as the scale can be neglected, this combination results can be applied for any span with the safety of at least 4..

The limit line with orange numbers represents the width limitations caused by upwards loading in the fill direction shown in Fig. 8.2-9. Besides, the limit line in the right side with blue numbers represents the width eliminating the possibility of wrinkle in the models as explained in Fig. 8.2-5. With these two safety boundaries, the maximum arch curvature with the maximum panel width is defined as 50 degrees and 7.8 m, and all the combinations below this lines are considered safe for the design.

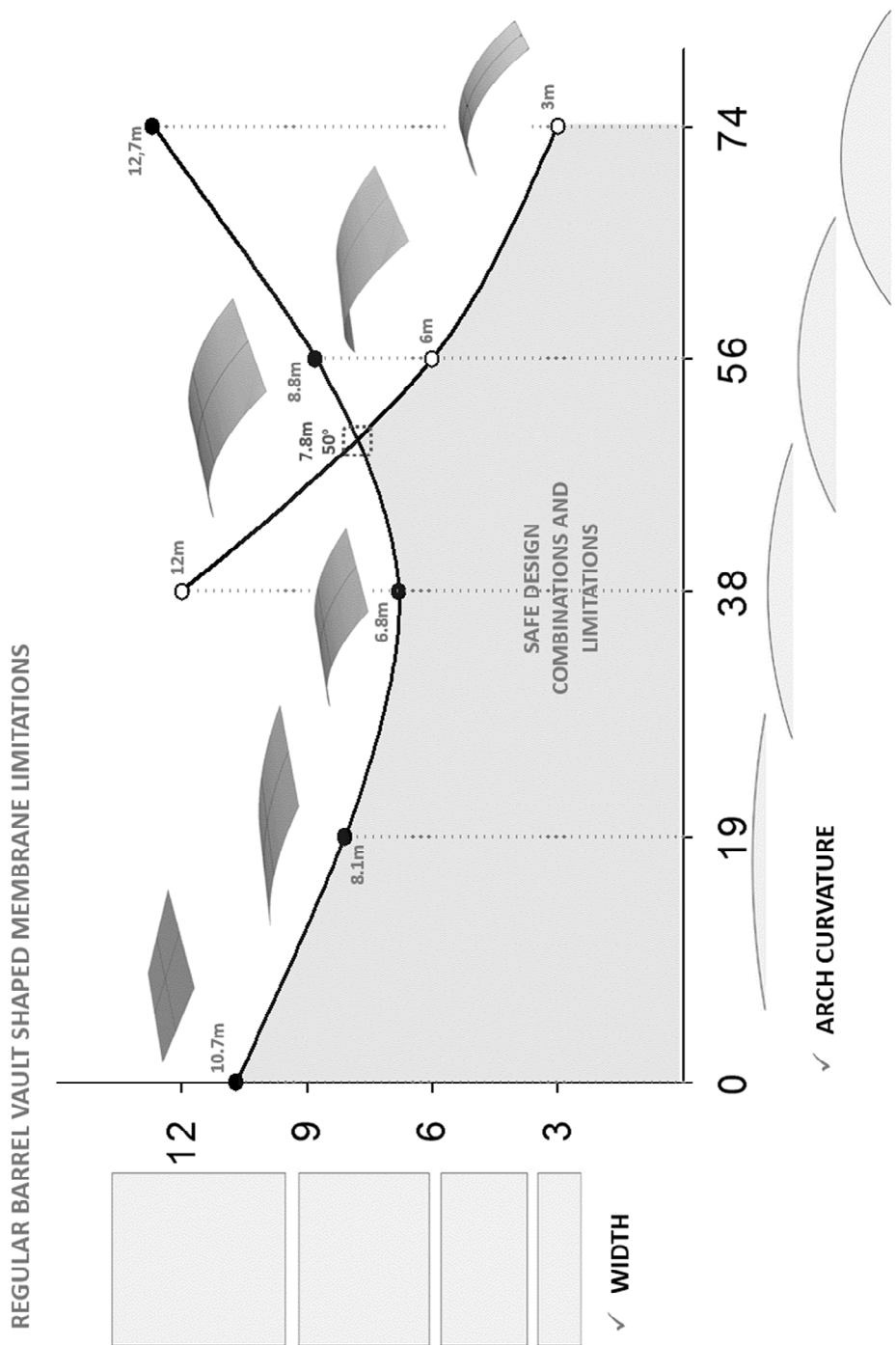


Figure 8.2-15 Regular barrel vault shaped membrane limitations

8.3. Curved barrel vault shaped membranes

By introducing asymmetry about the transverse axis to the regular barrel vault shaped membranes, curved panels are created and more range of designs can be modeled as illustrated in this section. Figure 8.3-1 explains the parameters used for the definition of this type of panels. An initial width is defined followed by an opening angle in both sides of the panel.

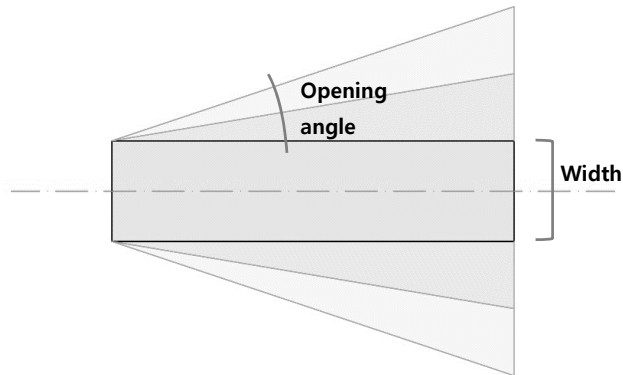


Figure 8.3-1 Parameters to define the curved barrel vault shaped membrane panels

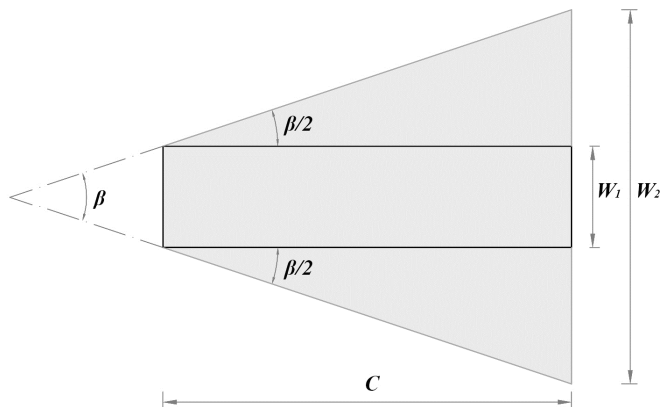


Figure 8.3-2 Parameter nomenclature for curved panels

Even though only the initial width and the opening angle are needed to define this type of curved panels, there are other parameters that need to be known for the design. In Fig. 8.3-2 all measurements are named, having C as the span chosen for the panel, W_1 the initial width, β the sum of the opening angle in each side, and W_2 the resulting width on the larger side when applying the opening angle for a chosen panel span.

$$W_2 = W_1 + 2C \tan\left(\frac{\beta}{2}\right) \quad (8.3-1)$$

With Equation (8.3-1), the width W_2 on the larger side of the panel for a chosen span C , initial width W_1 , and angle β can be calculated.

8.3.1. Initial model design and analysis for curved panels

To begin the analysis of this type of panels, an arch curvature for both arches of 38° and an initial width of 3 m (W_1) is chosen. With that constant parameters, four different models are designed with 10° , 20° , 30° and 40° opening angles (β), and those are compared with the regular panel of 38° curvature and 3 m width. Figure 8.3-3 shows the initial shape in plan and final shape after form-finding analysis of those described curved panels.

**38° arch curvature
3 m initial width**

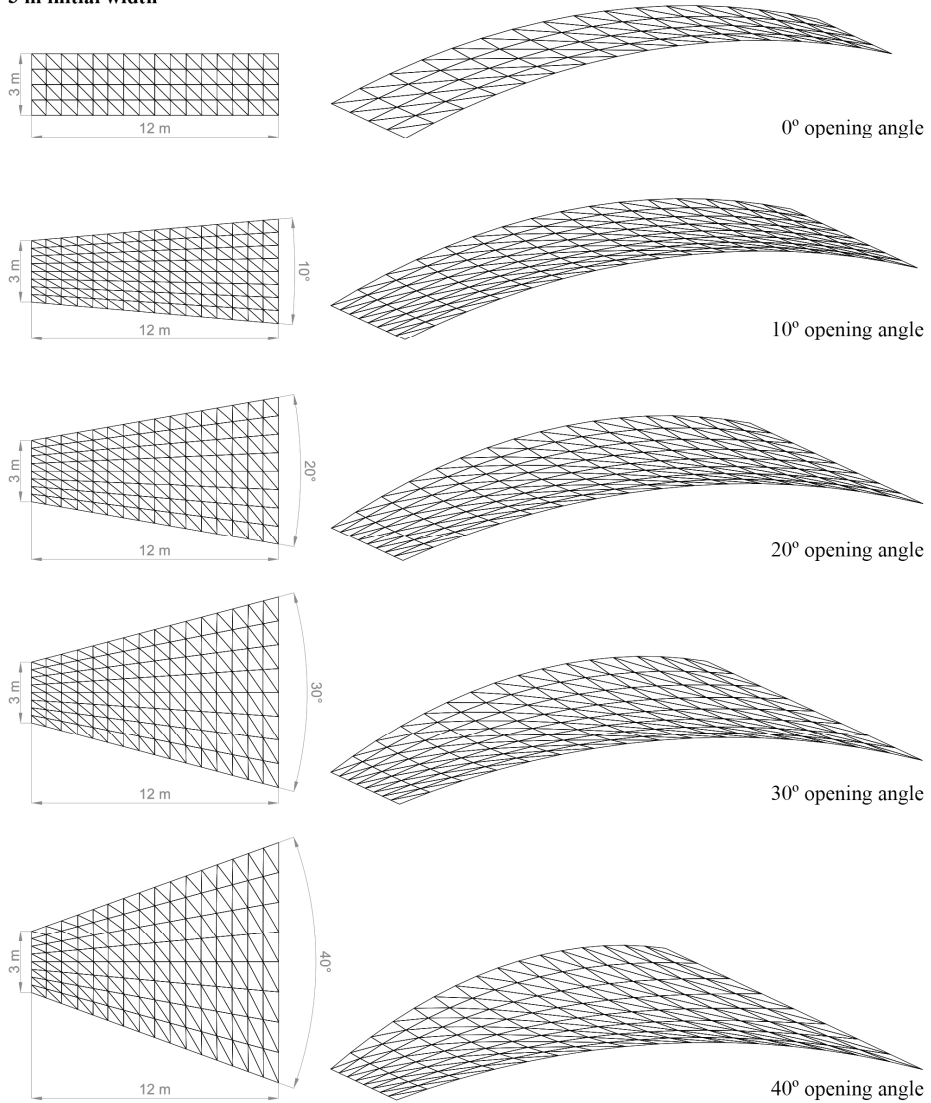


Figure 8.3-3 Initial shape in plan and final shape of curved panels with 38° of curvature, 12 m span (C), 3 m of initial width (W_I) and different opening angles (β).

38° curvature and $W_I = 3$ m

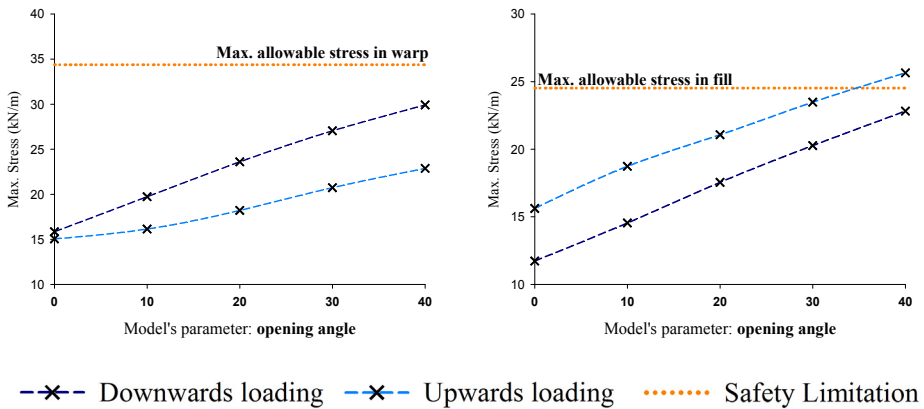


Figure 8.3-4 Maximum stress in the warp and fill directions for the different opening angles (β) in panels with 38° of curvature and 3 m of initial width (W_I)

Figure 8.3-4 represents the results of the maximum stress in the warp and fill directions for the different opening angles (β) of the curved panels shown in Fig. 8.3-3. In these graphs, it can be read that the stress increments almost linear with the opening angle regardless of the type of loading condition or the fabric direction. Once more, as it happened with previous analyses for the regular barrel vault shaped membrane, the limits are reached first under the upward loading in the fill direction.

However, the behavior discovered from the results is also interesting. When looking at the model with an opening angle of 30°, the maximum stress in that critical condition (upward loading in the fill direction) is almost equal to the one found for a panel of 6 m width. The condition that they have in common is that the 30° opening angle model has 6.22 m of width in its central section.

8.3.1.1. Comparison of a regular panel with 6 m width and a curved panel with the same width in the central section

To check these results, a model of exactly 6 m width in the central section is made and compared in detail with the regular one with the same width along the panel. The models for the analysis comparison are represented in Fig. 8.3-5.

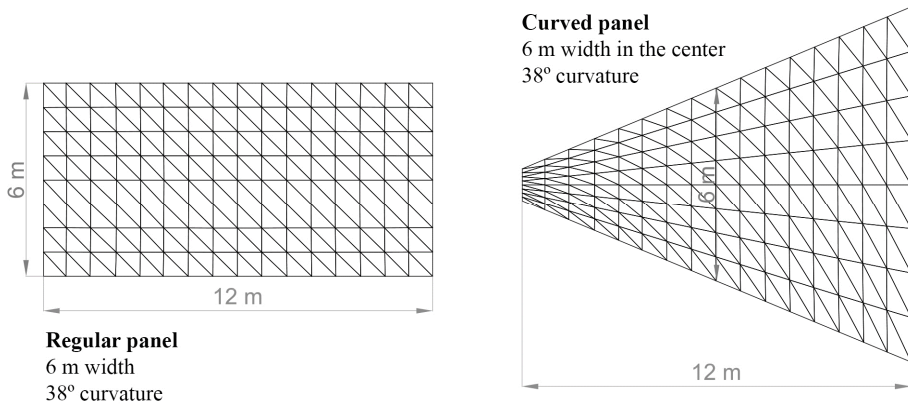


Figure 8.3-5 Regular panel with 6 m width and 38° curvature and curved panel with the same curvature and 6 m width in the central section of the panel

Figure 8.3-6 represents the stress distribution for those panels in the warp and fill directions under downwards and upwards loadings, as well as the maximum values of each case. Looking at the most critical case, upwards loading in the fill direction, it is recognizable that the maximum stress is obtained from the central section of the panel. It is for that reason that the maximum values are almost the same. An almost same situation occurs with the upwards loading in the warp direction, having a comparable behavior and same maximum stress in both panels.

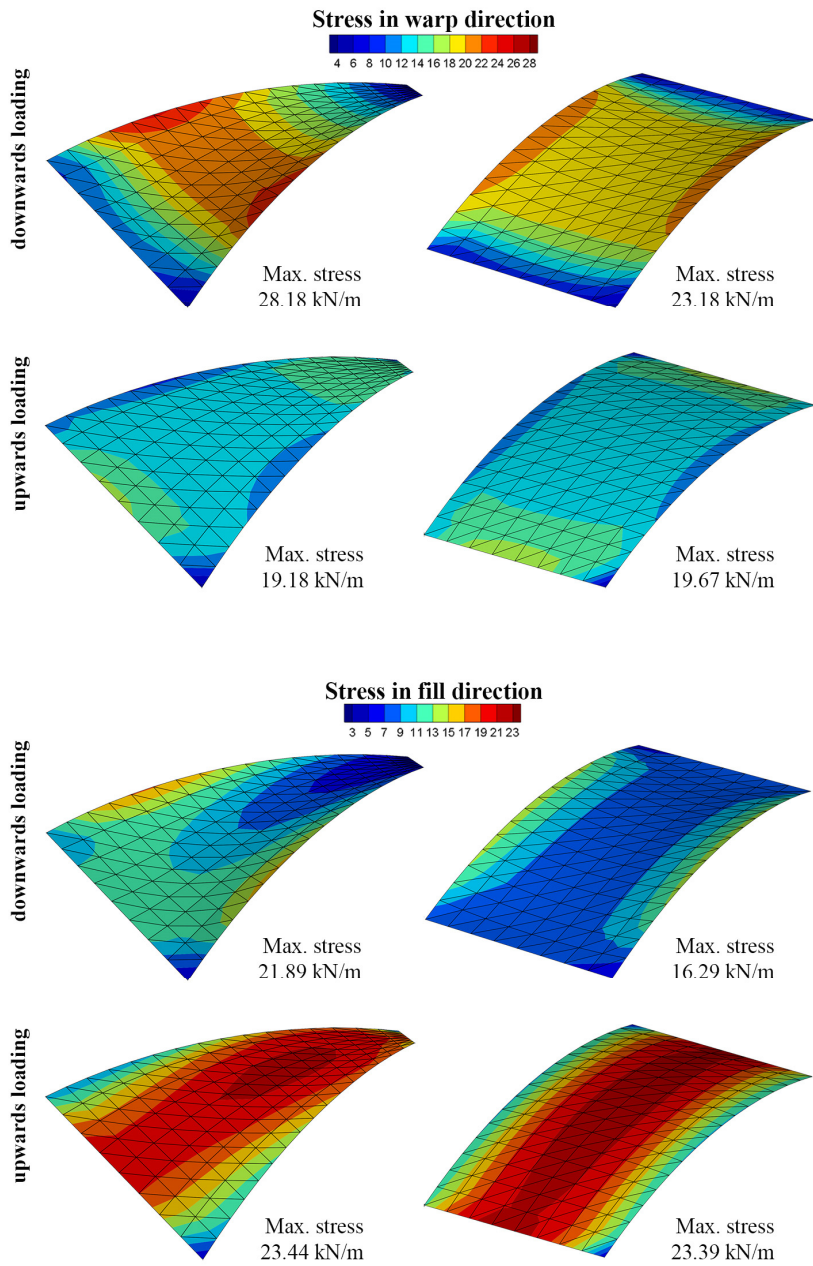


Figure 8.3-6 Comparison of stress distribution, maximum stress and deformed shape under downwards and upwards loadings between a regular panel of 6 m width and a curved panel with the same width in the central section

The cases of the downwards loading in the warp and fill directions are a bit different. In both cases the maximum stress is greater for the curved panel than for the regular one. For both panels, these maximum values are obtained near the edges. However, in the case of the curved panel, they occur about one third distance from the larger side while in the regular panel it happens in the center in a more distributed way.

After obtaining this results, it is possible to equate the behavior of the curved panel with the regular panel when the first one has the same width in the central section than the second one. But this assumption can be only made for the upward loading in both warp and fill direction. Due to this fact, it is necessary to evaluate the influence of the opening angle when assessing in downwards loading.

8.3.1.2. *New parameters defining curved panels*

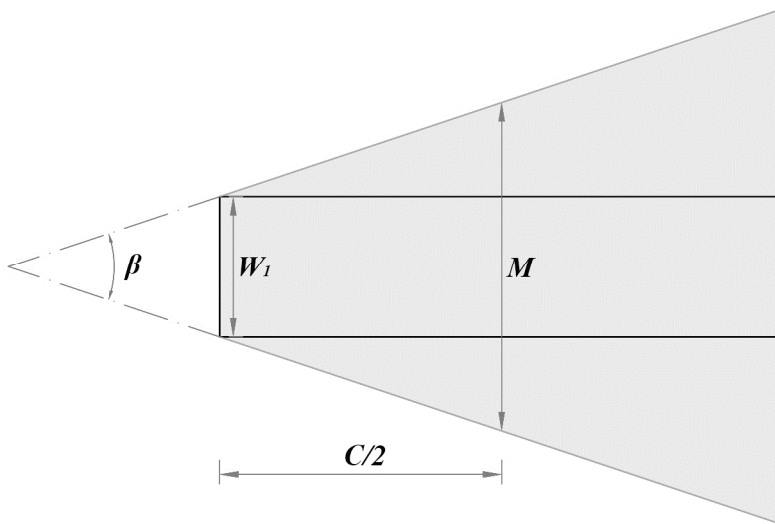


Figure 8.3-7 New parameters defining curved panels

As shown in the previous section, a new approach is needed to define curved barrel vault shaped membranes. Figure 8.3-6 shows the parameters that define this type of panel from this section. In this way, the width of the panel at the central section ($C/2$) is named as M , and along with the opening angle β and the initial width W_1 , are the main parameters for the design and analysis of curved panels.

In addition, when designing these panels, 3 parameters have to be chosen. The span to be covered C , and the width in the center M , are the first parameters to decide. Afterwards, if the initial width W_1 is chosen, the opening angle can be determined as shown in Equation (8.3-2). Conversely, if the chosen parameter is the opening angle β , the initial width can be calculated with Equation (8.3-3).

$$\beta = 2 \arctan \left(\frac{M - W_1}{C} \right) \quad (8.3-2)$$

$$W_1 = M - C \tan \left(\frac{\beta}{2} \right) \quad (8.3-3)$$

Finally, to calculate the width on the larger side W_2 , Equation (8.3-1) shown in the previous section can be used, or by the use of the parameter M , the simpler relationship shown in Equation (8.3-4) can be also applied.

$$W_2 = 2M - W_1 \quad (8.3-4)$$

8.3.2. Analysis of curved panels with same width in the center and different opening angle

56° arch curvature
 $M = 6$ m width in the center

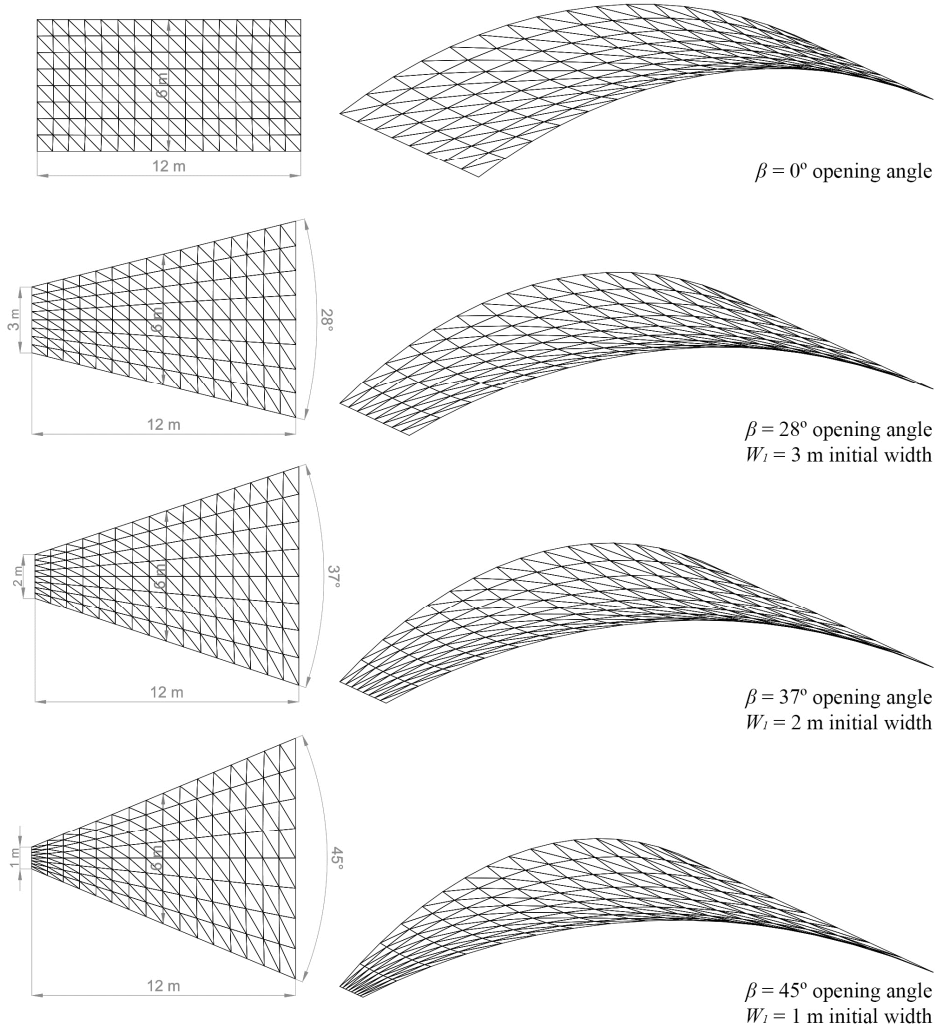


Figure 8.3-8 Initial shape in plan and final shape of curved panels with 56° curvature, 12 m span (C), 6 m width in the center (M), and different opening angles (β) and initial widths (W_1).

To check if the maximum stress under the upwards loading is maintained when increasing the opening angle β and the width in the center M is kept equal, 4 new models are analyzed. Figure 8.3-8 shows the initial shape in plan and final shape of these models after the form-finding analysis.

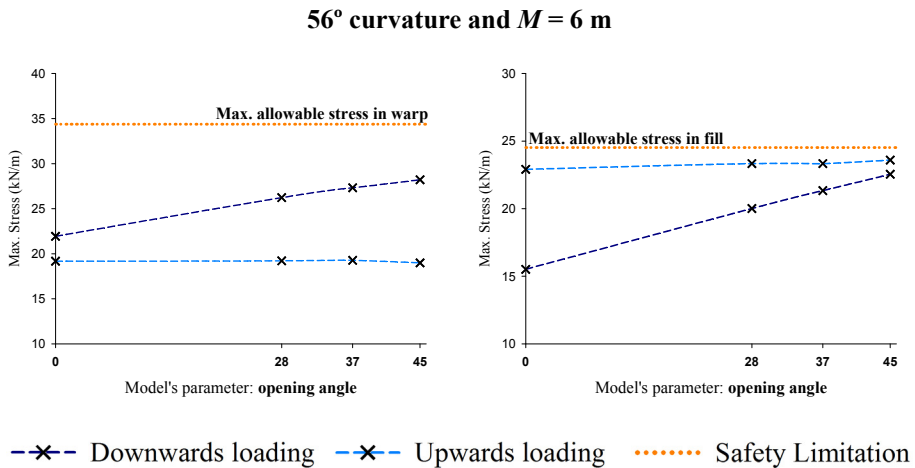


Figure 8.3-9 Maximum stress in the warp and fill directions for the different opening angles (β) in panels with 56° curvature and 6 m width in the center (M)

Figure 8.3-9 represents the values for the maximum stress after the stress-deformation analysis in the warp and fill directions for the different opening angles β in panels with 56° curvature and 6 meter width in the center (M). It is verified that under upwards loading the stress is kept constant for both warp and fill directions. However, in the case of the downwards loading, the increment of the stress is linear with the increase of the opening angle. In addition, it is again in the fill direction where the downwards loading reaches first the safety limitation.

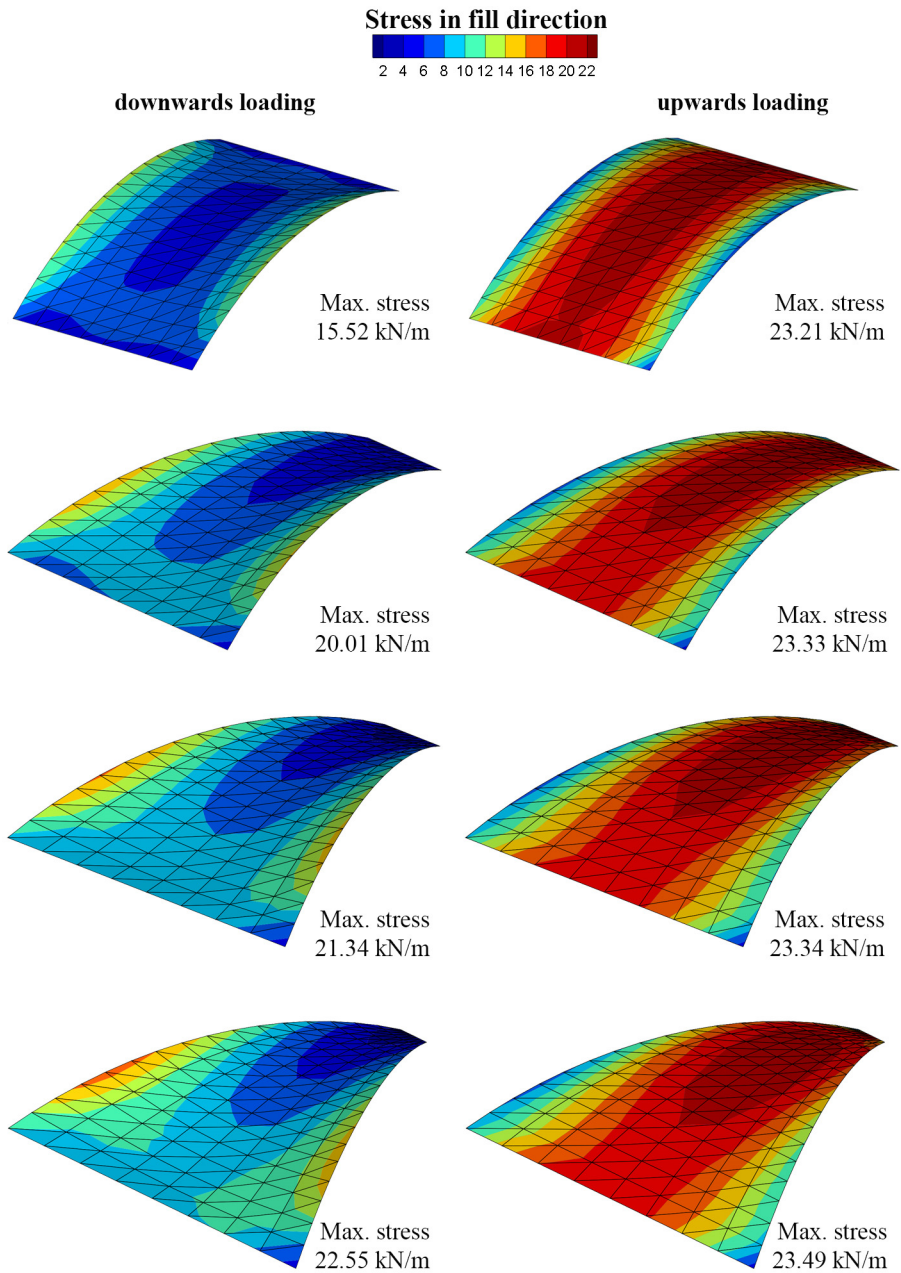


Figure 8.3-10 Stress distribution in the fill direction, maximum stress and deformed shape of curved panels with 56° curvature, 12 m span (C), 6 m width in the center (M), and different opening angles (β) and initial widths (W_i).

To understand the influence of the opening angle (β) with both loading conditions it is better to look into the stress distribution over the whole panel (Fig. 8.3-10). Here it is easy to see how the distribution is very similar for the upwards loading, having the maximum stress in the center of the panel, where the section is M . When looking at the left column, corresponding to the downwards loading in the fill direction, it is observable how maximum stress values are higher when the opening angle is increased, and they appear about 1/3 distance from the longer side W_2 .

When checking for different arch curvatures, the maximum stress in the fill direction under upwards loading is kept same regardless of the opening angle. Then, it can be assumed that the limitations found for the regular barrel vault shaped membranes can be applied to the curved panels if instead of the width of the whole panel, the M value is used.

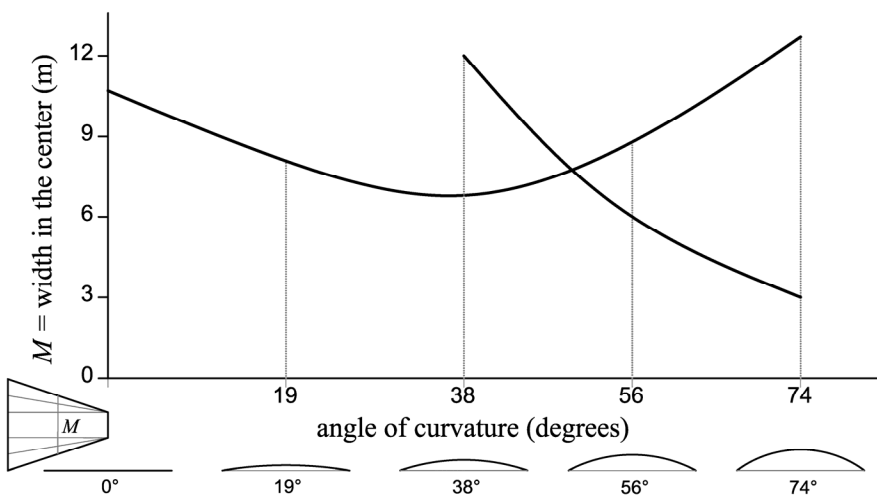


Figure 8.3-11 Limitations for curved barrel vault shaped membranes considering the arch curvature and the width in the center of the panel (M).

Figure 8.3-11 represents the adaptation of the limitations explained in Fig. 8.2-15 for regular panels. In this graph any safe combination between the width in the center of the panel (M) and the arch curvature can be found. However, for each of these combinations, the maximum opening angle is still not known, and more analyses are needed to find those limitations.

8.3.3. Analysis of curved panels with same arch curvature and different width in the center.

In the previous section, it was disclosed that the stress in the fill direction under upwards loading is constant with the increase of the opening angle. Besides, maximum stress under downwards loading in the fill direction is the one that limits the opening angle. From the analysis made for 38° arch curvature and 56° arch curvature it was shown that the increment of the stress when increasing the opening angle is linear. However, when comparing each other, the incrementing stress lines result not to be parallel for the different curvatures. For example, the slope of the stress increment for 38° curvature is a bit smaller than the one for 56°.

Knowing this, there is a need to check whether these slopes are equal for all types of panels if the curvatures are the same or they are different. Figure 8.3-12 shows the panels analyzed for this comparison. Panels with the same arch curvature and different M values are chosen and compared with the equivalent regular panel with same width as M .

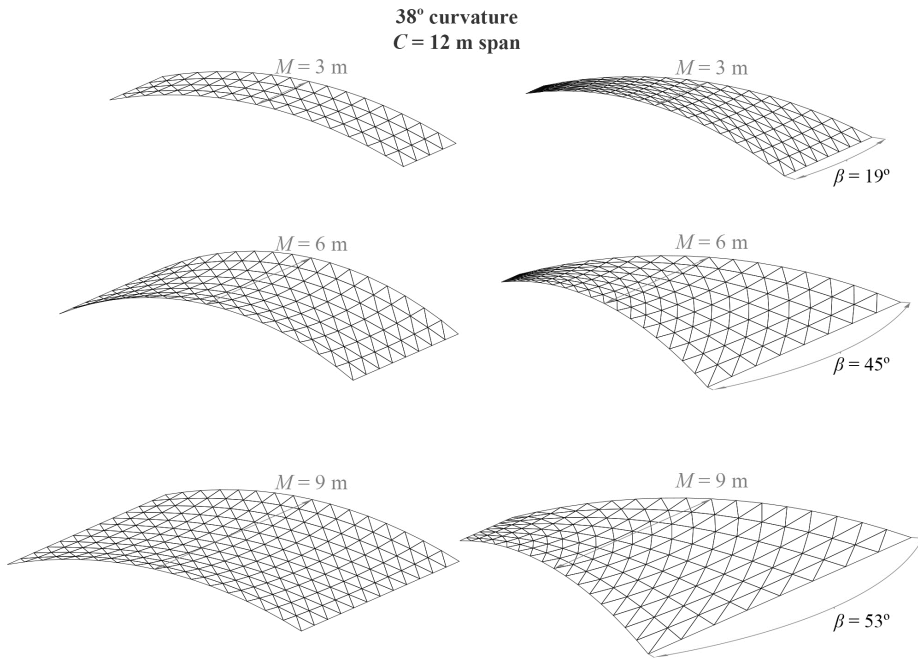


Figure 8.3-12 Comparison of regular and curved panels with the same curvature of 38°, span of 12 m (C), and width in the center M of 3 m, 6 m and 9 m.

Figure 8.3-13 shows the results after stress-deformation analysis of the panels explained in Fig. 8.3-12 with respect to their opening angle. Here it is remarkable that the linear increase of the stress is parallel regardless of the M value chosen. This means that for the same arch curvature the increase of the stress under downwards loading in the fill direction is linear and parallel; thus, it has the same slope. Besides, the ordinate in the origin for a panel with M width in the center is the value corresponding to the maximum stress of a regular panel with same M width along the whole panel.

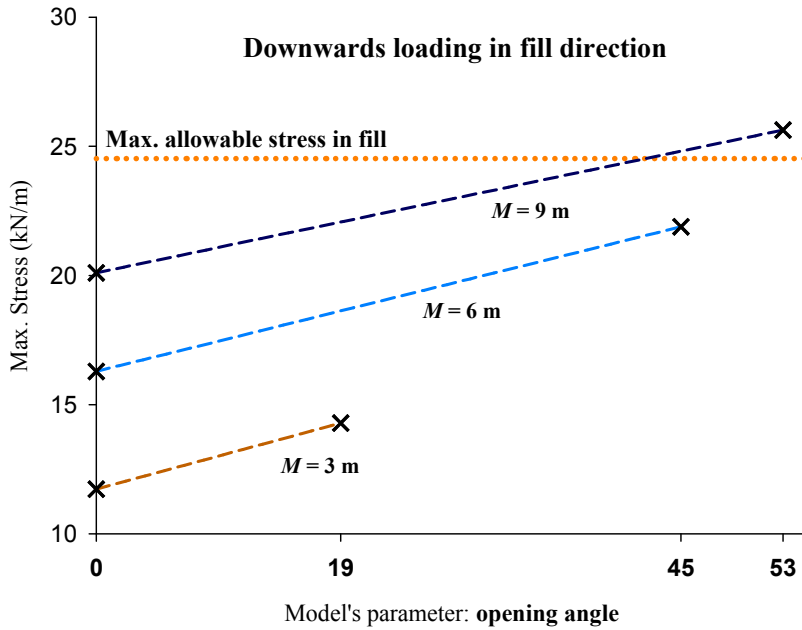


Figure 8.3-13 Maximum stress in the fill direction under downwards loading for models with the same curvature of 38° and different width in the center (M) when increasing the opening angle (β)

After the analysis of other arch curvatures, different slopes for each of the curvatures are found as expressed in Fig. 8.3-14.

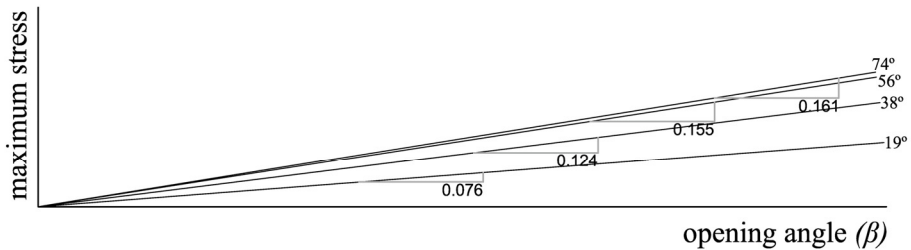


Figure 8.3-14 Increase of maximum stress slope for models with different arch curvatures when increasing the opening angle (β)

8.3.4. Parametric study for curved barrel vault shaped membranes

In the previous sections the different parameters that participate in the curved panels' definition were analyzed. To define numerically and graphically the limitations for the curved barrel vault shaped membranes, each of the loading conditions, downwards loading and upwards loading, gives different limitations in the fill direction.

As expressed in Fig. 8.3-11, the stress behavior under upwards loading is equivalent to the one found for regular panels when these have the same width as the M value. With that, width limitations of the curved panels are found.

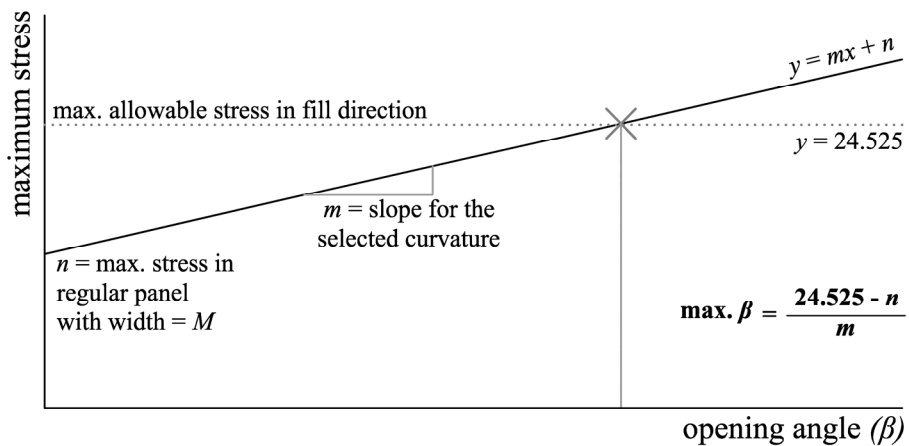


Figure 8.3-15 Explanation of how to obtain the maximum opening angle for the selected model

The opening angle limitations are given by the increase of the stress produced by downwards loading. As different slopes were found for each curvature, the limit can be easily calculated as explained in Fig. 8.3-15.

By the intersection of the limit line that defines the maximum stress in the fill direction ($y = 22.525 \text{ kN/m}$) and the inclined line that represents the increment of the stress when the opening angle increases under downwards loading ($y = mx + n$), the maximum opening angle can be calculated. This inclined line has the slope defined by the selected arch curvature of the panel (m) and the ordinate in the origin n is the maximum stress found in a regular panel with the same width as M . With all of this, Equation (8.3-5) is defined as explained in the figure.

$$\max. \beta = \frac{24.525 - n}{m} \quad (8.3-5)$$

For the use of this formula with any parameter combination, two more graphs are created regarding the two values that need to be used, m and n .

In Fig. 8.3-14 different slopes for different curvatures are shown. To be able to use any other curvature, these slopes are plotted in another graph expressed in Fig. 8.3-16, where the increment of the slope with the arch curvature can be read. By reading this graph, any curvature can be designed by selecting the corresponding m value.

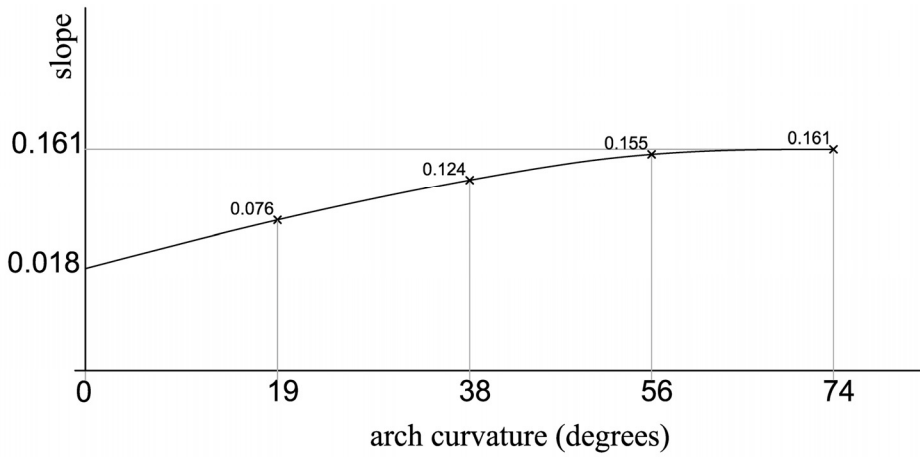


Figure 8.3-16 Slope values m for the increase of maximum stress in models with different arch curvature when increasing the opening angle

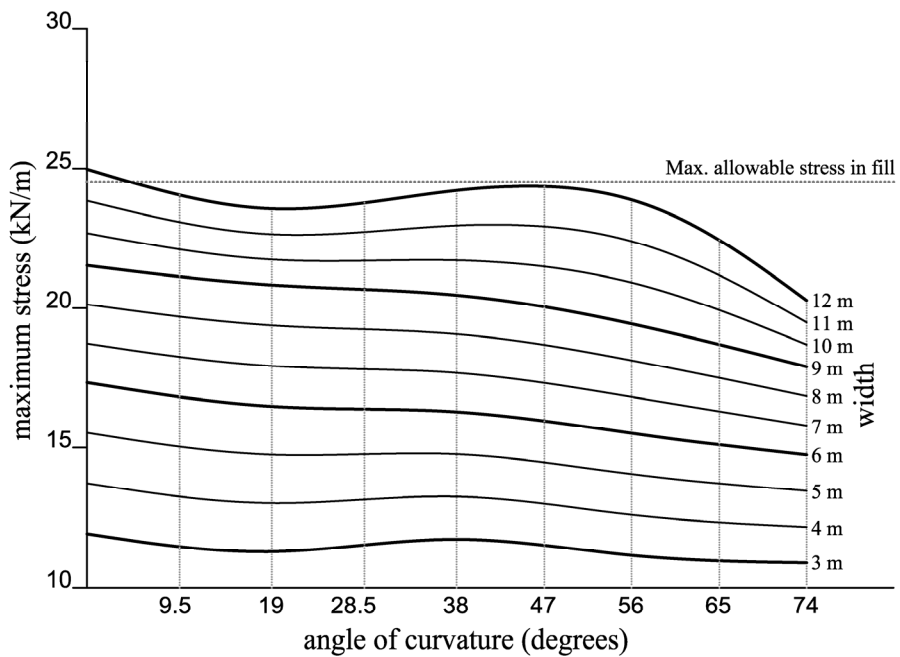


Figure 8.3-17 Maximum stress under downwards loading in the fill direction with the increase of the curvature of the arch for different widths in regular panels (n)

To find the n values corresponding to the maximum stress under downwards loading in the fill direction for the regular panels with M width, the graph represented in Fig. 8.2-10 can be interpolated so all possible M values are represented as shown in Fig. 8.3-17.

Then, once a determined arch curvature and width in the central section M are chosen, by selecting the corresponding slope m for that arch curvature and maximum stress in the regular panel with M width (Fig. 8.3-16 and Fig. 8.3-17 respectively), and using all those values in Equation (8.3-5), the maximum opening angle can be checked.

Table 8.3-1 shows some of the values that have been found following the explained method.

Table 8.3-1 Maximum width in the center M for different combinations of opening angles β and arch curvature

Curvature (degrees)		0	19	38	56	74
$m = \text{slope}$		0.018	0.076	0.124	0.155	0.161
Max. β (degrees)						
$n = \text{max. stress with } \beta = 0^\circ$ (kN/m)	90	22.905	17.685	13.365	10.575	10.035
	80	23.085	18.445	14.605	12.125	11.645
	70	23.265	19.205	15.845	13.675	13.255
	60	23.445	19.965	17.085	15.225	14.865
	50	23.625	20.725	18.325	16.775	16.475
	40	23.805	21.485	19.565	18.325	18.085
	30	23.985	22.245	20.805	19.875	19.695
Max. width in the center M (m)	90	10.2	6.8	4.1	2.85	2.75
	80	10.35	7.35	4.9	3.67	3.6
	70	10.5	7.88	5.71	4.74	4.84
	60	10.65	8.4	6.58	5.8	6.12
	50	10.8	8.93	7.47	6.96	7.65
	40	10.95	9.72	8.35	8.15	9.24
	30	11.1	10.55	9.28	9.3	11.27

The values found in Table 8.3-1 can be now plotted for the different arch curvatures and M values as represented in Fig. 8.3-18. Here it is possible to see how the width M varies for each opening angle along the different arch curvatures depending on the slope found previously.

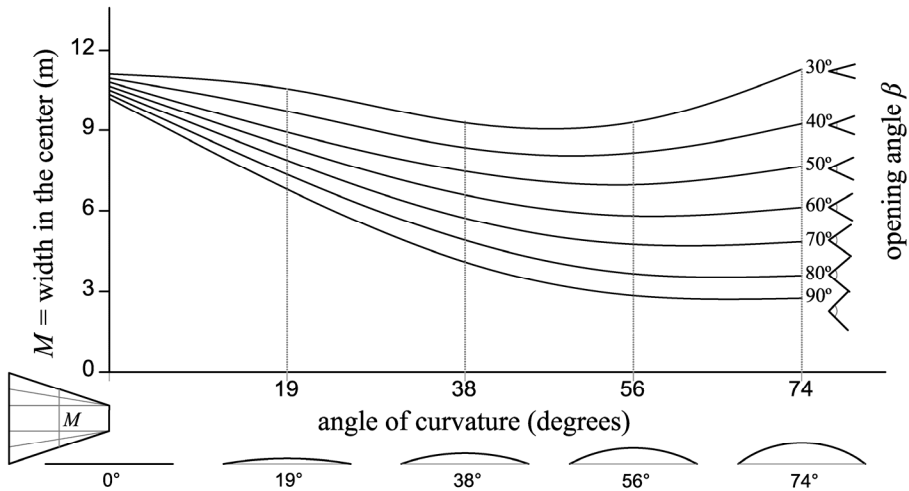


Figure 8.3-18 Maximum width in the center M for different opening angles β when increasing the arch curvature

However, these limitations are only related to the results found for the downwards loading condition in the fill direction, and the limitations in width M respecting the upwards loading said a priori need to be considered too. For that reason, in Fig. 8.3-19 the limitations from both loading conditions are overlapped combining the graphs represented in Fig. 8.3-11 and Fig. 8.3-18.

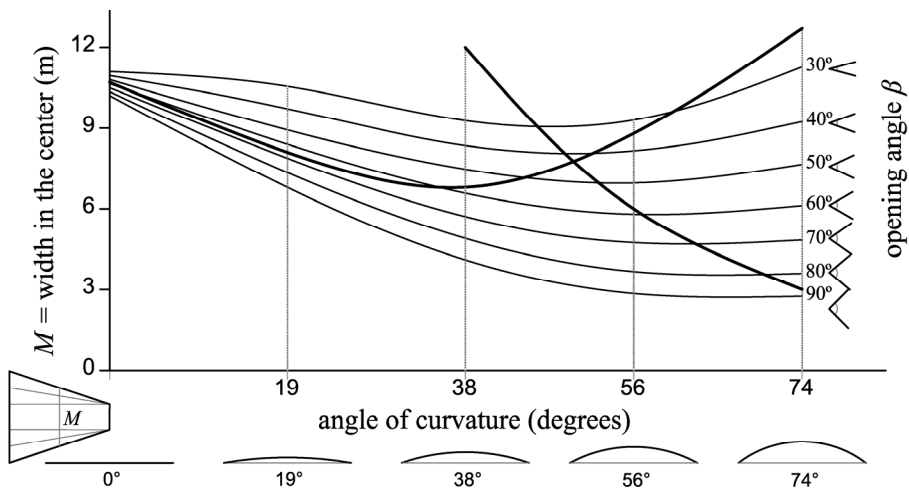


Figure 8.3-19 Combination of the M and β limitations found under downwards loading and upwards loading

Then, as the limitations related to the upwards loading conditions were independent from the opening angle, they determine the maximum M regardless of the maximum β , so the limiting graph can be simplified as represented in Fig. 8.3-20. With the combinations shown in that graph, any curvature can be combined with a width M inside the limited area, and the maximum opening angle can be checked following the curved lines. In addition, for a more exact solution, the procedure explained earlier to apply Equation (8.3-5) can be also used.

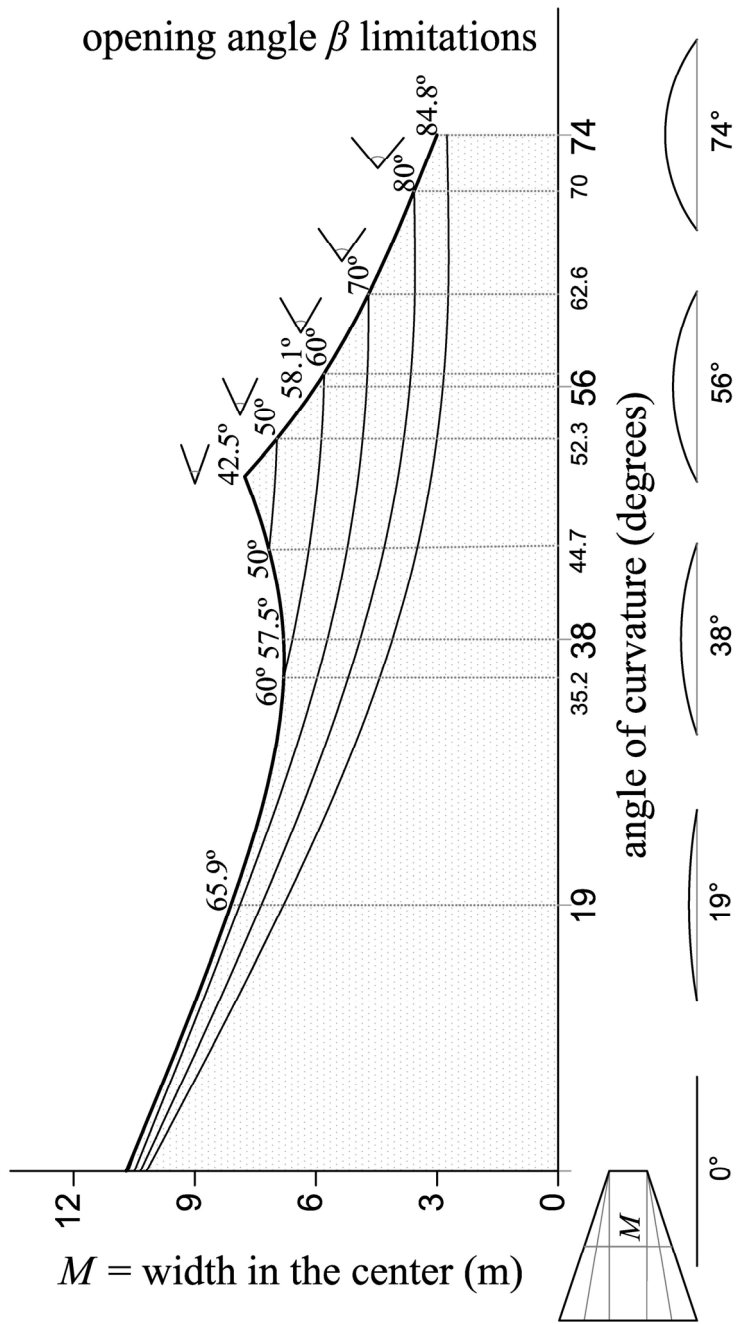


Figure 8.3-20 Final design chart for arch curvature, width in the center M , and opening angle β of curved barrel vault shaped membrane panels.

8.4. Inclined barrel vault shaped membranes

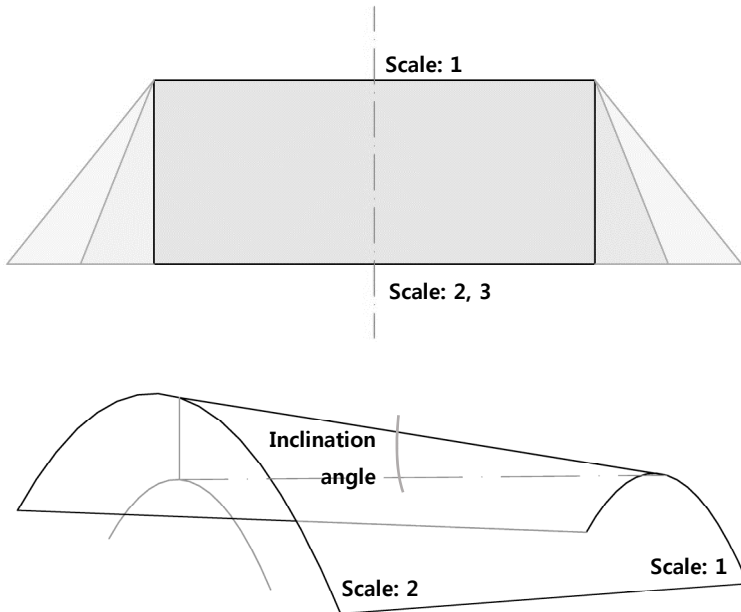


Figure 8.4-1 Parameters to define the asymmetry about the longitudinal axis models

Figure 8.4-1 shows the parameters to define the asymmetry about the longitudinal axis models. Having a different scale in the arches and keeping the width of the panel, the parameter is defined by the inclination angle between the horizontal line and the 2 arches in the section. It is for that reason that these panels are named as inclined barrel vault shaped membranes.

The resulted geometry of these inclined panels is a bit more complicated than the one related to the curved panels. Then, a detailed explanation is needed to find the relationships between the parameters that are needed for the design.

8.4.1. Parameters defining the inclined barrel vault shaped membranes

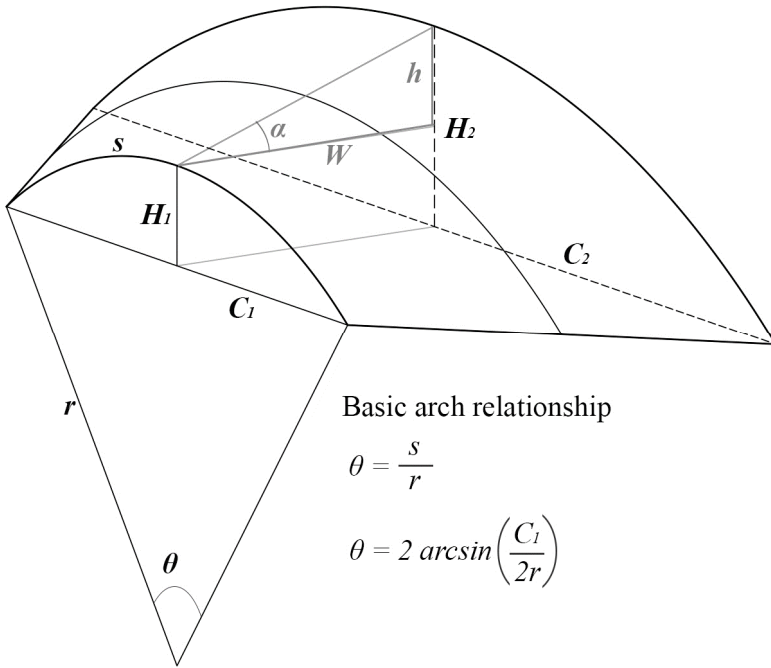


Figure 8.4-2 Parameters defining the scale of the second arch with consideration of the inclination between the arches

The parameters that participate in the design of the inclined barrel vault shaped membranes are represented in Fig. 8.4-2. As explained earlier, the arch curvature named as θ is equal for both arches and they are separated from a chosen width W . Each arch covers a span C , which for the smaller arch is called C_1 and for the larger arch is named C_2 . And at the same time, these arches have a height H_1 and H_2 in relation with the curvature angle θ and the spans C_1 and C_2 .

The inclination between the arches is defined by the inclination angle α , so in this way, a relationship between the selected panel width W and this angle α can be expressed as in Equation (8.4-1).

$$h = \tan(\alpha) \times W \quad (8.4-1)$$

For the design of these inclined panels, if a determined width W , arch curvature θ , and inclination angle α are chosen, the resulting scale of the second arch needs to be known. For this purpose, if the smaller arch is considered to have a scale equal to one, the scale of the larger arch is named as S , and the relationship between both is driven by the arches' height proportions as expressed in Equation (8.4-2).

$$S = \frac{h + H_1}{H_1} \quad (8.4-2)$$

Then, by substituting Equation (8.4-1) into Equation (8.4-2), Equation (8.4-3) can be obtained.

$$S = \frac{\tan(\alpha) \times W + H_1}{H_1} \quad (8.4-3)$$

In Equation (8.4-3) the scale of the larger arch S is written in relationship of the inclination angle α , the width of the panel W , and the height of the smaller arch H_1 . However, the height of the arch is not a relevant parameter, and when designing these inclined panels, the choice of the span to cover C_l and arch curvature θ are more proper. It is for that reason that the relationship among H_1 , C_l , and θ needs to be found.

As shown in Fig. 8.4-2, a basic arch relationship between the arch curvature θ , arch length s , and radius of curvature r can be written as shown in Equation (8.4-4). Besides, this expression can be also related to the span of the arch C_1 as driven in Equation (8.4-5).

$$\theta = \frac{s}{r} \quad (8.4-4)$$

$$\theta = 2 \arcsin \left(\frac{C_1}{2r} \right) \quad (8.4-5)$$

To find the relationship among the height H_1 , the span C_1 and the arch curvature θ , the intersecting chord theorem can be applied with the arch parameters as in Equation (8.4-6). Then, substituting Equation (8.4-6) into Equation (8.4-5), the relationship among these three parameters is found as shown in Equation (8.4-7).

$$r = \frac{C_1^2}{8H_1} + \frac{H_1}{2} \quad (8.4-6)$$

$$\theta = 2 \arcsin \left(\frac{C_1}{2 \left(\frac{C_1^2}{8H_1} + \frac{H_1}{2} \right)} \right) \quad (8.4-7)$$

Now, Equation (8.4-7) needs to be solved for H_1 to substitute its value into Equation (8.4-3) and find in this way the relationship that is needed for the design of inclined panels. For this purpose, Equation (8.4-7) can be rearranged as shown in Equation (8.4-8).

$$4H_1^2 - \frac{4C_1}{\sin(\theta/2)} H_1 + C_1^2 = 0 \quad (8.4-8)$$

The resulting equation can have two solutions, but in practice there should be only one. It is for that reason that the function of this equation needs to be investigated. Written the function and its first derivative as in Equation (8.4-9), the value of the horizontal tangent for the parabolic function can be found when equalizing the first derivative to 0. The resulting value that is named as H_1^0 is close to half of the span C_l as shown in Equation (8.4-10). Besides, when inserting it into the function of H_l , the result is negative. All of this is represented in Fig. 8.4-3 where it can be observed that the solution of Equation (8.4-8) should be the smaller one, because the value of H_l , which represents the height of the arch, can never be larger than the value of H_1^0 , which is close to half of the span of the arch C_l .

$$f(H_1) = 4H_1^2 - \frac{4C_l}{\sin(\theta/2)}H_1 + C_l^2; \quad f'(H_1) = 8H_1 - \frac{4C_l}{\sin(\theta/2)} \quad (8.4-9)$$

$$f'(H_1) = 0 \rightarrow H_1^0 = \frac{C_l}{2\sin(\theta/2)} > 0; \quad f(H_1^0) < 0 \quad (8.4-10)$$

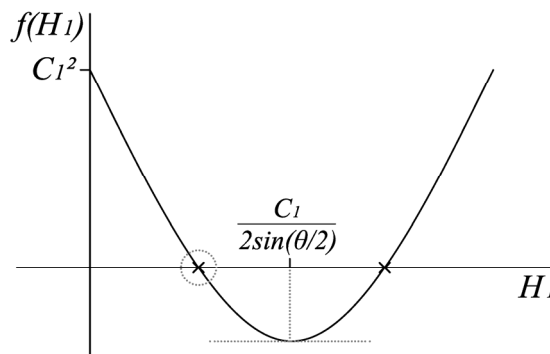


Figure 8.4-3 Representation of the H_l function and its solution

Then, Equation (8.4-8) can be solved as shown in Equation (8.4-11), and rearranging Equation (8.4-12) is obtained.

$$H_1 = \frac{\frac{2C_1}{\sin(\theta/2)} - \sqrt{\frac{4C_1^2}{\sin^2(\theta/2)} - 4C_1^2}}{4} \quad (8.4-11)$$

$$H_1 = \frac{C_1}{2\sin(\theta/2)} \left(1 - \sqrt{1 - \sin^2(\theta/2)} \right) \quad (8.4-12)$$

With that the scale of the second arch S can be written in relationship with the inclination angle α , span of the smaller arch C_1 , arch curvature θ , and panel width W that are selected for the design as expressed in Equation (8.4-13).

$$S = \frac{(\tan(\alpha) \times W) + \frac{C_1}{2\sin(\theta/2)} \left(1 - \sqrt{1 - \sin^2(\theta/2)} \right)}{\frac{C_1}{2\sin(\theta/2)} \left(1 - \sqrt{1 - \sin^2(\theta/2)} \right)} \quad (8.4-13)$$

On the contrary, if the selected parameter is the scale of the second arch S , to cover a determined span C_2 , the inclination angle α can be found with Equation (8.4-14)

$$\alpha = \arctan \left[\left[\frac{S \times \left(\frac{C_1}{2\sin(\theta/2)} \left(1 - \sqrt{1 - \sin^2(\theta/2)} \right) \right)}{\left(\frac{C_1}{2\sin(\theta/2)} \left(1 - \sqrt{1 - \sin^2(\theta/2)} \right) \right)} \right] \div W \right] \quad (8.4-14)$$

8.4.2. Analysis of inclined panels with same arch curvature and different inclination angle for two different widths

As explained in the previous section, three main parameters influence on the design of inclined barrel vault shaped membranes: the arch curvature θ , the inclination angle α , and the width of the panel W .

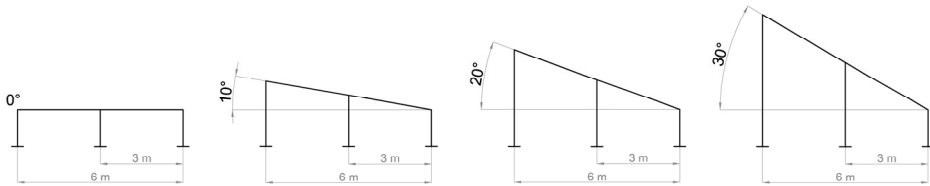
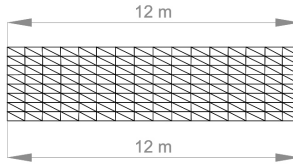


Figure 8.4-4 Different inclination angles α for 3 and 6 m width W inclined panels

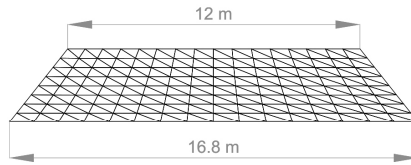
For the first investigation of this kind of panels, three increasing inclination angles ($\alpha = 10^\circ, 20^\circ, 30^\circ$) are studied and compared to a panel without inclination. This is made for 2 different widths, keeping the same inclination ratio as shown in Fig. 8.4-4.

The main difference between the models with different widths W is that for maintaining the same inclination α and same arch curvature θ , the scale of the second arch S is smaller when the width W is narrower. In this first analysis, panels with 50° curvature and 3 m and 6 m width are chosen and investigated for the different inclination angles explained earlier. The scale of the second arch for all these models is calculated with Equation (8.4-13). Resulting scale values and plan of the models for the analysis are shown in Fig. 8.4-5 for 3 m width and in Fig. 8.4-6 for 6 m width.

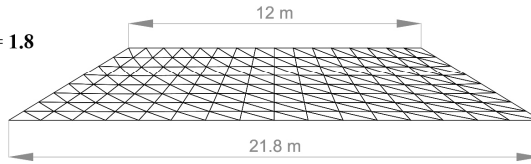
0° Inclination
Second arch scale = 1



10° Inclination
Second arch scale = 1.4



20° Inclination
Second arch scale = 1.8



30° Inclination
Second arch scale = 2.3

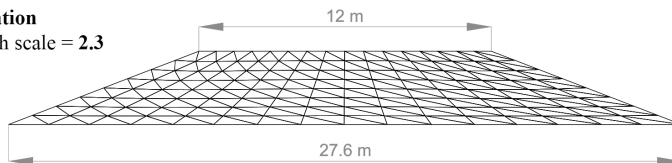
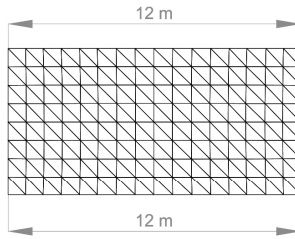
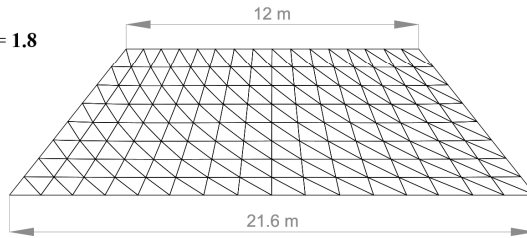


Figure 8.4-5 Plan of the models with 50° curvature and 3 m width for the various inclination angles α and corresponding scale of the second arch S

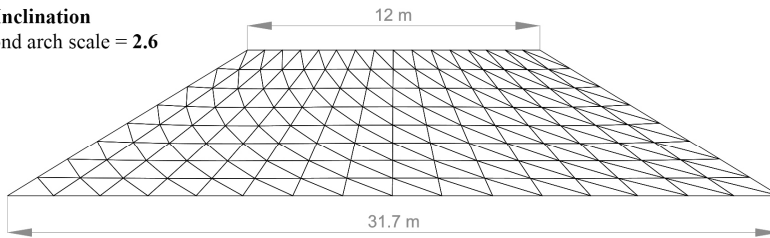
0° Inclination
Second arch scale = 1



10° Inclination
Second arch scale = 1.8



20° Inclination
Second arch scale = 2.6



30° Inclination
Second arch scale = 3.6

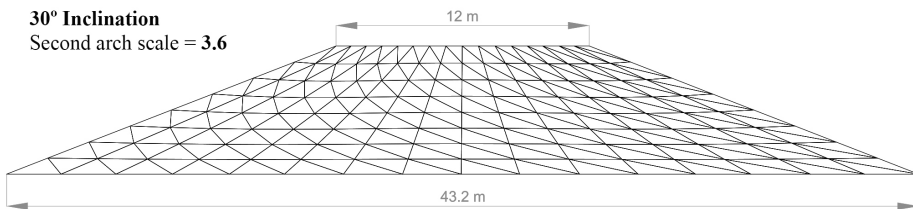


Figure 8.4-6 Plan of the models with 50° curvature and 6 m width for the various inclination angles α and corresponding scale of the second arch S

Figure 8.4-7 shows the final shape after form-finding analysis for the 50° curvature models with 3 and 6 m width for the various inclination angles ($\alpha = 10^\circ, 20^\circ$ and 30°) in comparison with a regular panel with the same width and no inclination.

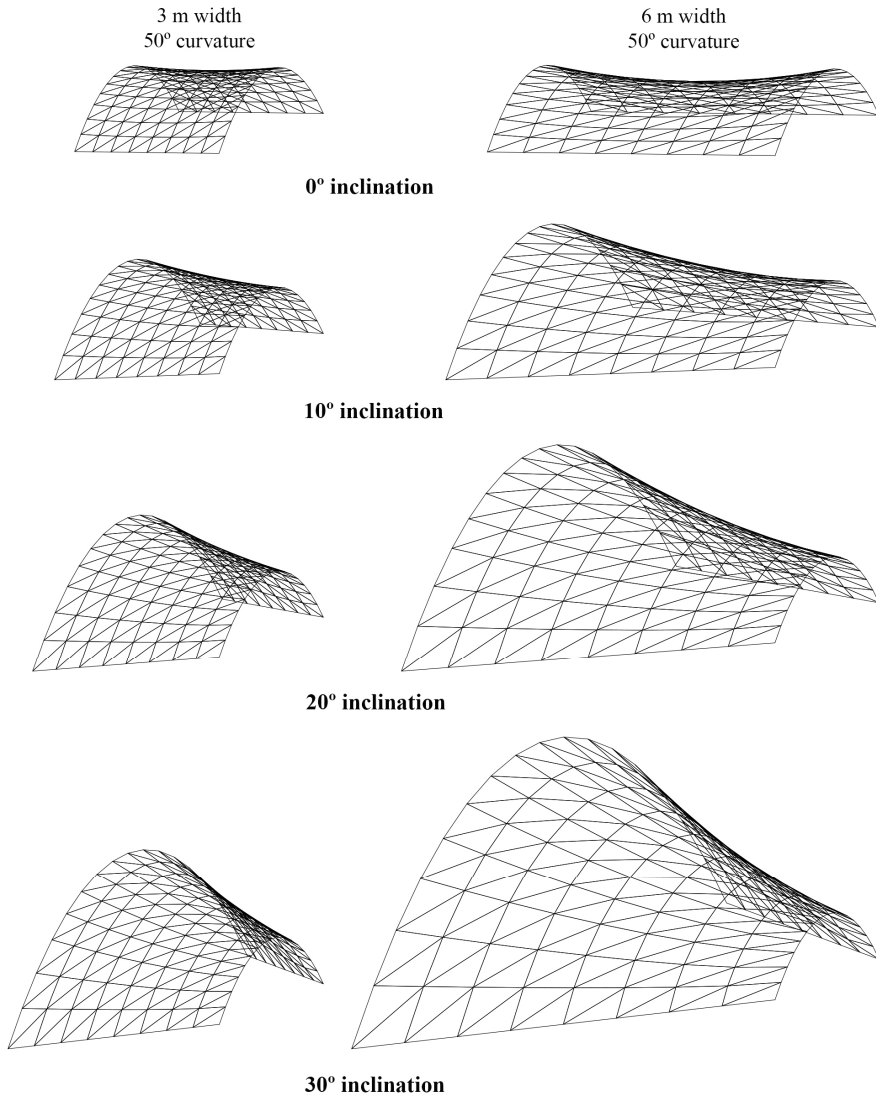


Figure 8.4-7 Final shape for 50° curvature models with 3 and 6 m width for the various inclination angles α

Figure 8.4-8 represents the results after the stress-deformation analysis for the maximum stress in the warp and fill directions under the upwards and downwards loadings when the inclination angle is increased for the models represented earlier in Fig. 8.4-7.

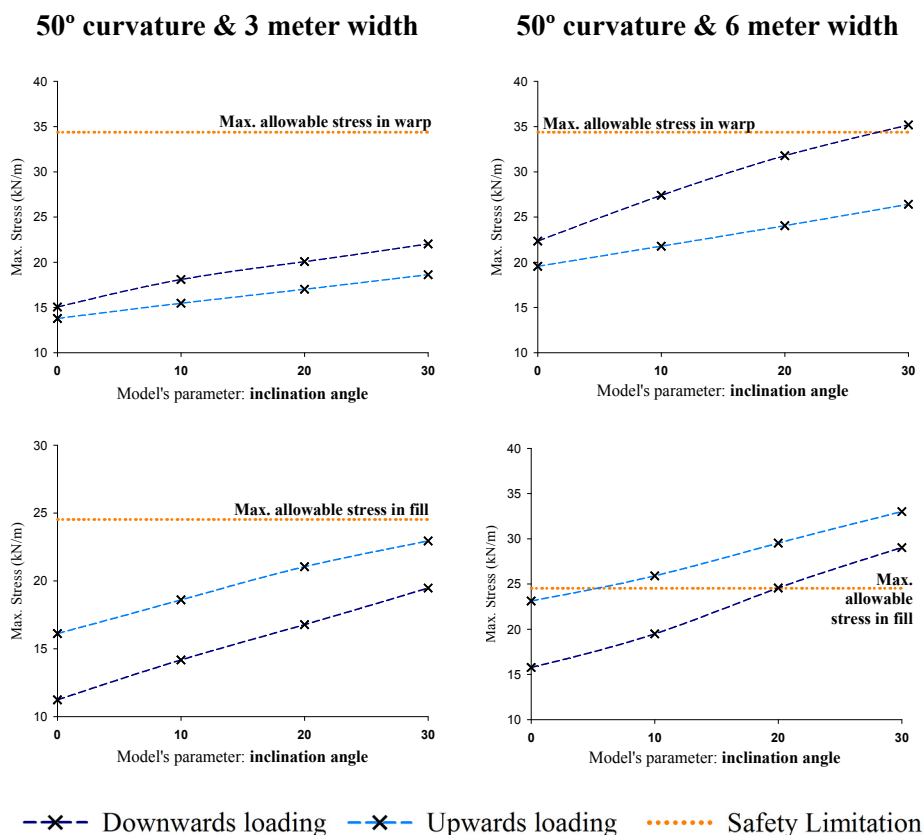


Figure 8.4-8 Maximum stresses in the warp and fill directions for the different inclinations angles between arches with 3 and 6 m width

Here it is observable that in all the cases the stress increases with the inclination angle. However, some details are different. Firstly, the most critical case is still happening in the fill direction under upwards loading.

Then, it is also remarkable that the increase of the stress under upwards loading tends to be almost linear but in the case of the downwards loading, it is slightly curved. And the third observation is that the increment of the stress for the 3 m width models and the 6 m width models is not parallel as it happened with the curved barrel vault shaped membranes.

To better understand the behavior of this type of panels, the stress distribution along the model for the downwards and upwards loading, as well as the maximum stress values obtained from the stress-deformation analysis, are represented in Fig. 8.4-9 for the warp direction and Fig. 8.4-10 for the fill direction.

In the case of the warp direction, higher stresses occur under downwards loading. In Fig. 8.4-9 it is observable that while in the regular panel without inclination the stress is distributed regularly through the central section of the panel, and in the case of the inclined models the stress increases around the central area near the lower arch. So as the inclination increases, the stress near this smaller arch also increases. Similar behavior happens for the upwards loading, but near the larger arch and with a lower stress.

In the case of the fill direction, as shown in Fig. 8.4-10, the downwards loading causes stress near both arches. But it is the upwards loading that makes the panel to reach the highest stresses, and these values are found in the central transverse section of the panel as it happened with the curved and regular panels.

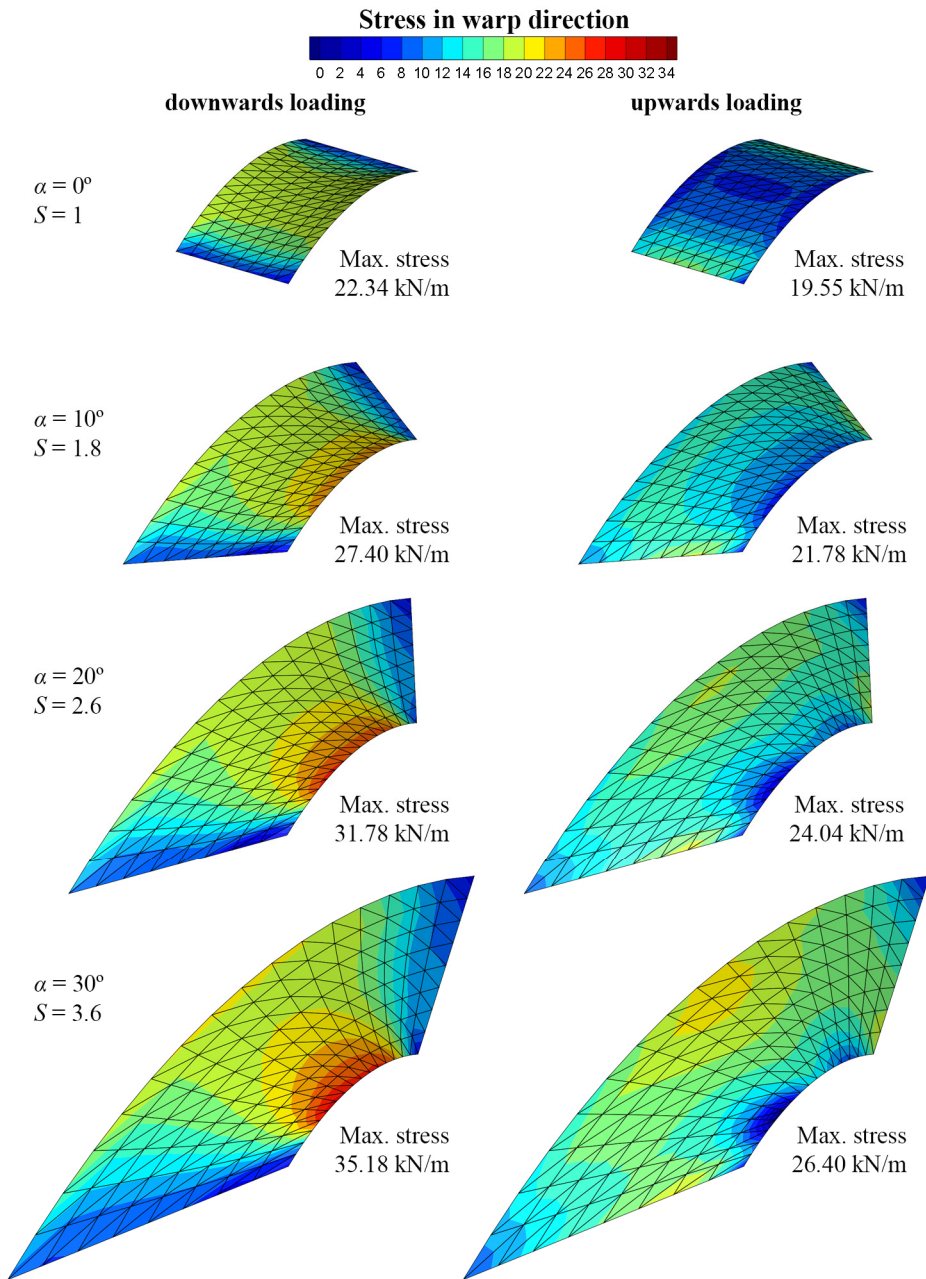


Figure 8.4-9 Stress distribution in the warp direction and deformed shape under downwards and upwards loadings for inclined panels with 6 m width and 50° curvature and various inclinations between arches (α)

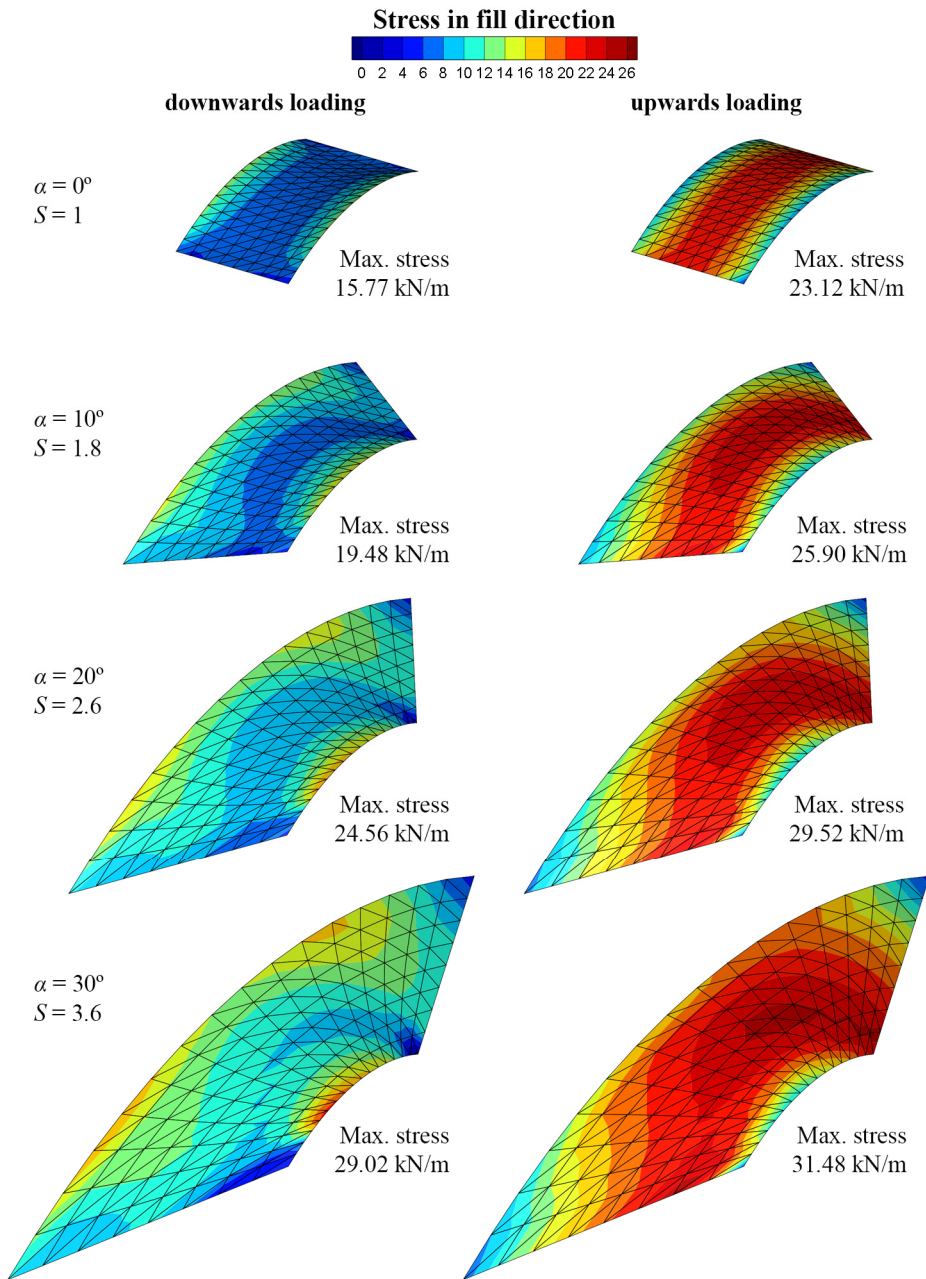


Figure 8.4-10 Stress distribution in the fill direction and deformed shape under downwards and upwards loadings for inclined panels with 6 m width and 50° curvature and various inclinations between arches (α)

8.4.3. Analysis of inclined panels with same inclination angle and same width but different arch curvatures

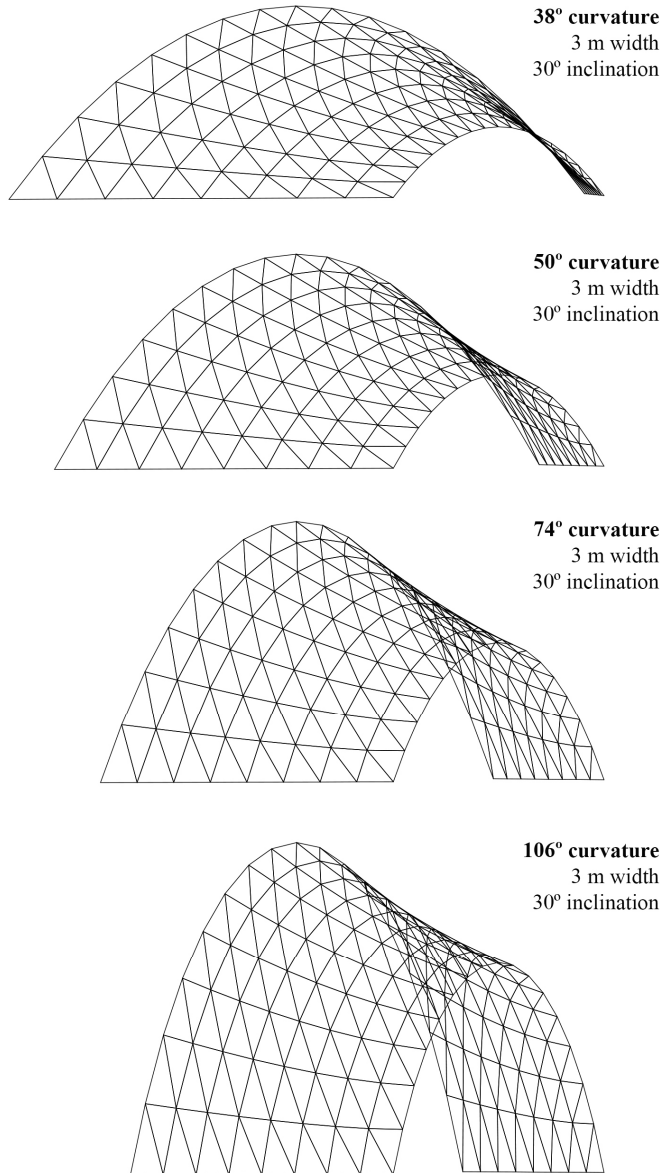


Figure 8.4-11 Final shape for models with different arch curvatures θ , with the same width of 3 m and the same inclination angle of 30°

In the previous section it was shown that the increase of the stress in the fill direction under upwards loading is not parallel for the same arch curvature and different widths. In this section, different arch curvatures are investigated for the same width. Figure 8.4-11 represents the final shape after the form-finding analysis for models with different arch curvatures ($\theta = 38^\circ, 50^\circ, 74^\circ,$ and 106°) but with the same width of 3 m and same inclination angle of 30° .

To see how the stress increase with the inclination angle in the stress-deformation analysis, these models are compared with a regular panel of the same curvature but with no inclination, and the results are shown in Fig. 8.4-12.

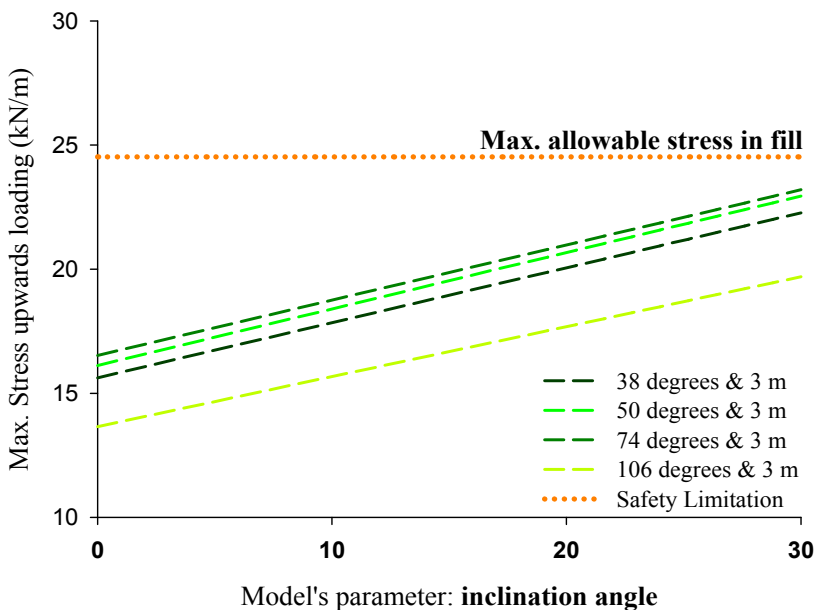


Figure 8.4-12 Comparison of maximum stress in the fill direction under upwards loading between models with different arch curvatures, but with the same width and inclination angles

As it is observable, the increasing rate of the stress in the fill direction under upwards loading is parallel for all the models analyzed regardless of the arch curvature. This is possible because as shown in the previous section with Fig. 8.4-10, the maximum stress in this case (upwards loading in the fill direction) occurs in the central section of the panel.

When looking at the transverse sections of the models analyzed (Fig. 8.4-13), it is easy to realize that the inclination angle is not related to the arch curvature but the width of the panel. While H_I is different for each arch curvature, h remains equal to achieve a determined inclination angle for a chosen width, where H_I and h are defined in Fig. 8.4-2.

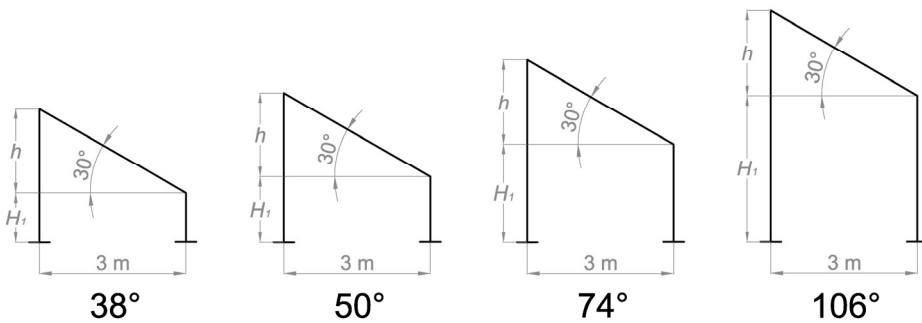


Figure 8.4-13 Central transverse section of the models with different arch curvatures θ , but with same width and inclination angle

Knowing this, the slopes of the linearly increasing stress in the fill direction under upwards loading for different panel widths can be found and are represented in Fig. 8.4-14.

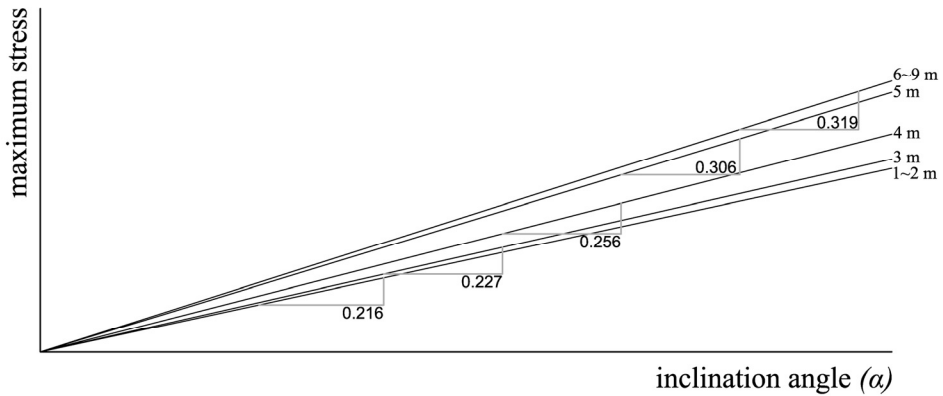


Figure 8.4-14 Increase of maximum stress slope for models with different widths for the increasing of inclination angle between arches

8.4.4. Parametric study for inclined barrel vault shaped membranes

After having analyzed all the parameters that influence on the design of inclined barrel vault shaped membranes; arch curvature θ , inclination angle α , and width of the panel W , limitations of this type of panel can be found.

Earlier in previous sections, it was shown that it is always in the fill direction under upwards loading where the maximum stress reaches first the safety limitation boundary. Because of that, and in a similar way that it was shown with the curved panels, the limit can be easily calculated as explained in Fig. 8.4-15.

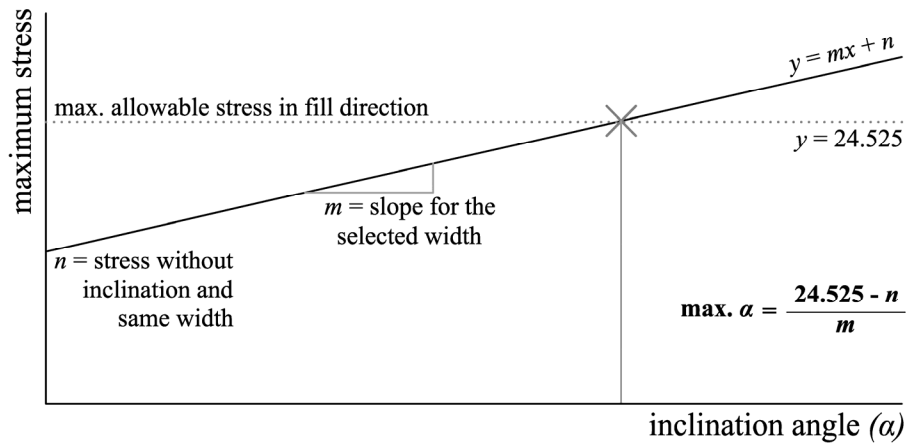


Figure 8.4-15 Explanation of how to obtain the maximum inclination between arches for the selected model

By the intersection of the limit line that defines the maximum stress in the fill direction ($y = 22.525 \text{ kN/m}$) and the inclined line that represents the increment of the stress when the inclination angle increases under upwards loading ($y = mx + n$), the maximum inclination angle can be calculated. This inclined line has the slope defined by the selected panel width (m) and the ordinate in the origin n is the maximum stress found in a regular panel with the same width but no inclination. With all of this, Equation (8.4-15) is defined as explained in the figure.

$$\text{max. } \alpha = \frac{24.525 - n}{m} \quad (8.4-15)$$

For the use of this formula with any parameter combination, two more graphs are created regarding the two values that need to be used (m and n).

In Fig. 8.4-14 different slopes for different panel widths are shown. For any other intermediate width, these slopes are plotted in another graph expressed in Fig. 8.4-16, where the increment of the slope with the increased width can be read and intermediate values are found. By reading this graph, any panel width can be designed by selecting the corresponding m value.

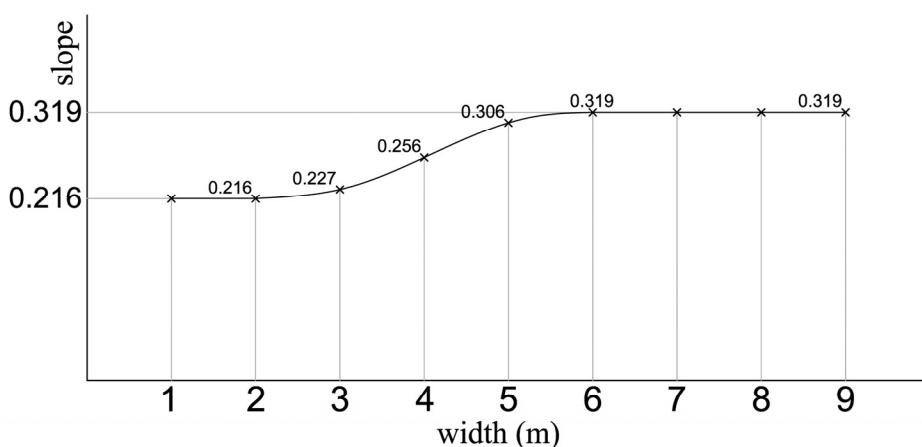


Figure 8.4-16 Slope m values for the increase of maximum stress in models with different widths when increasing the inclination angle between arches

To find the n values corresponding to the maximum stress under upwards loading in the fill direction for the regular panels without inclination, the graph represented in Fig. 8.2-11 can be interpolated so all possible panel widths for the different arch curvatures are represented as shown in Fig. 8.4-17.

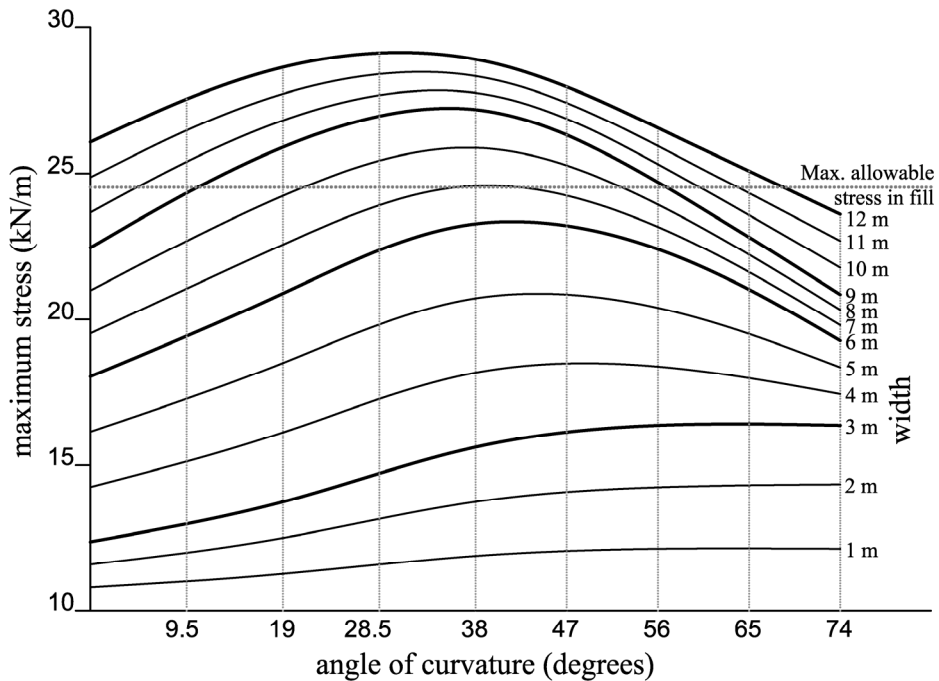


Figure 8.4-17 Maximum stress under upwards loading in the fill direction with the increase of the curvature of the arch for different widths

Then, once a determined panel width and arch curvature are chosen, by selecting the corresponding slope m for that width and maximum stress in a regular panel with same width and arch curvature but no inclination n (Fig. 8.4-16 and Fig. 8.4-17 respectively), and using all those values in Equation (8.4-15), the maximum inclination angle can be checked.

Table 8.4-1 shows the values that have been found following the explained method for the different panel width and arch curvature combinations,

Table 8.4-1 Maximum inclination between arches for different combination of arch curvatures and width

Width (m)	2	3	4	5	6	7	8	9	
$m = \text{slope}$	0.216	0.227	0.256	0.306	0.319	0.319	0.319	0.319	
Arch curvature									
$n = \text{max. stress inclination } \theta^\circ$ (kN/m)	9.5	11.99	12.98	15.13	17.27	19.43	21.05	22.69	24.33
	19	12.49	13.74	16.12	18.51	20.89	22.56	24.23	25.9
	28.5	13.15	14.72	17.27	19.82	22.37	23.91	25.44	26.96
	38	13.75	15.62	18.17	20.72	23.27	24.58	25.88	27.18
	47	14.09	16.14	18.49	20.85	23.21	24.24	25.28	26.32
	56	14.25	16.37	18.38	20.39	22.41	23.17	23.93	24.7
	65	14.31	16.42	17.99	19.5	21.02	21.62	22.22	22.82
	74	14.34	16.37	17.44	18.36	19.27	19.8	20.33	20.85
Max. inclination angle α (degrees)	9.5	58.0	50.9	36.7	23.7	16.0	10.9	5.8	0.6
	19	55.7	47.5	32.8	19.7	11.4	6.2	0.9	-4.3
	28.5	52.7	43.2	28.3	15.4	6.8	1.9	-2.9	-7.6
	38	49.9	39.2	24.8	12.4	3.9	-0.2	-4.2	-8.3
	47	48.3	36.9	23.6	12.0	4.1	0.9	-2.4	-5.6
	56	47.6	35.9	24.0	13.5	6.6	4.2	1.9	-0.5
	65	47.3	35.7	25.5	16.4	11.0	9.1	7.2	5.3
	74	47.2	35.9	27.7	20.1	16.5	14.8	13.2	11.5

As shown in the table, some combinations result in a negative inclination angle α , this means that for that combination, inclined panels are not safe. The plot of the resulting values results in a limitation graph in 3D where the 3 parameters are combined as shown in Fig. 8.4-14. For an exact value or other intermediate solution the formula and graphs explained earlier can be used.

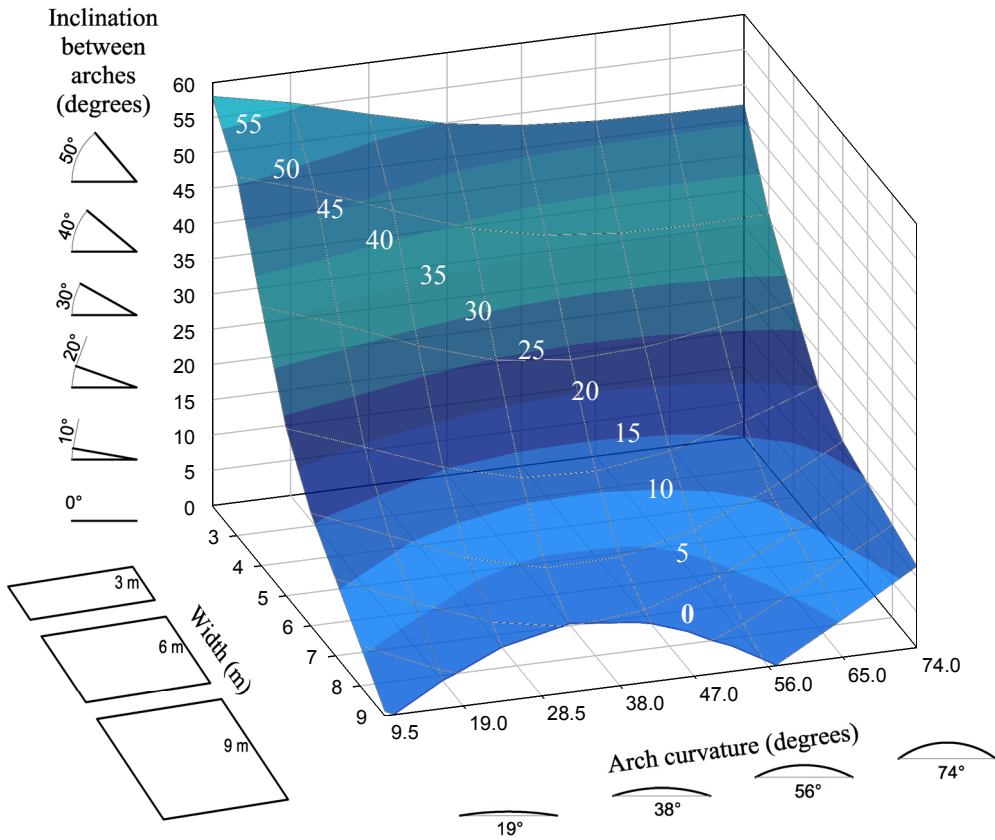


Figure 8.4-18 Maximum inclination between arches α for various combination of arch curvatures and panel widths

Still the models that result in wrinkle need to be removed from the safe combination cases. As was done for the regular panels, models with negative values appear for more pronounced curvatures and wider panels. Figure 8.4-18 represents the maximum inclination angles α for various combination of arch curvatures and panel widths, excluding the combinations where wrinkle appears.

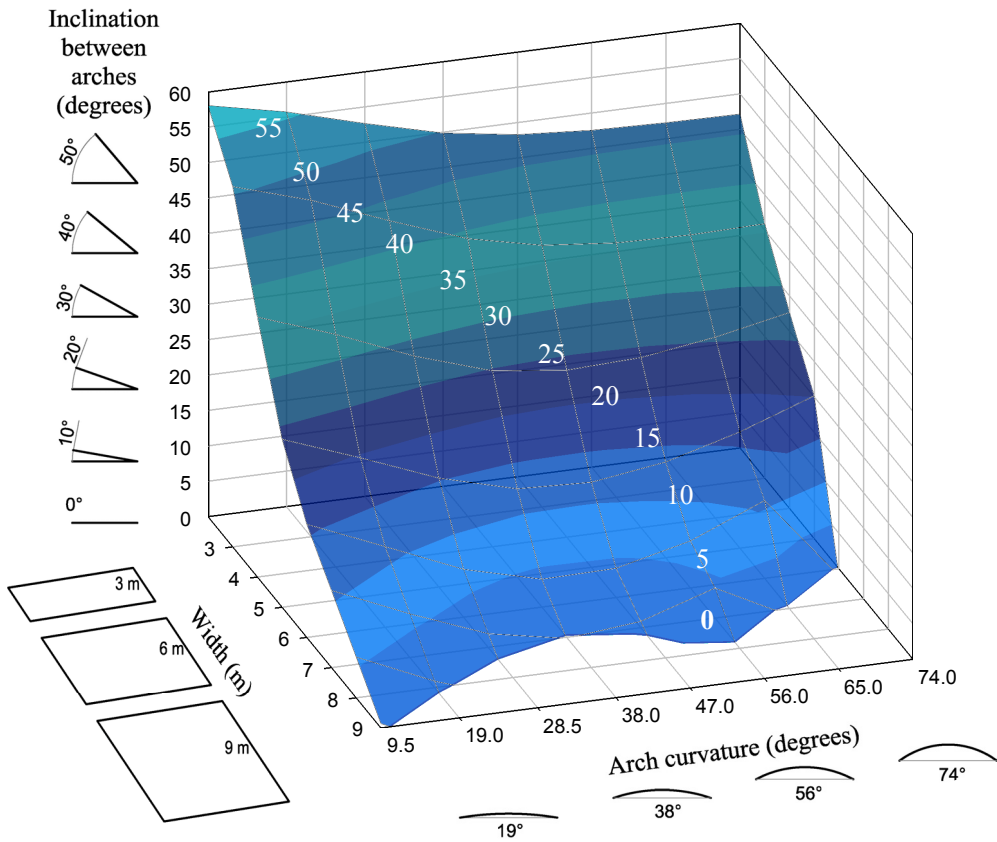


Figure 8.4-19 Maximum inclination between arches α for various combinations of arch curvatures and panel widths excluding combinations where wrinkle appears

8.5. Design application examples

In this section some simple design applications are shown for the three types of barrel vault shaped membranes analyzed: the regular panels, the curved panels and the inclined panels. The aim is to illustrate with the most basic examples the used of the limitation graphs and formulas developed in the previous sections. More complicated designs can be also created using the same approach, but that is not the scope of this thesis.

8.5.1. Regular barrel vault shaped membranes

One of the possible applications for simple regular barrel vault shaped membranes can be a cover for market streets. With the lightness of these structures and transparency quality, they result a proper solution for shading in a street market as shown in Fig. 8.5-1.



Figure 8.5-1 Membrane roof of Hatikva Market in Tel Aviv, Israel

8.5.1.1. Example 1: Regular panels for street market with low buildings

Figure 8.5-2 shows the regular panels chosen for the first example. By choosing two different curvatures with the same width and span, a space between the arches is created allowing for a good ventilation but at the same time also protecting from the sun and rain.

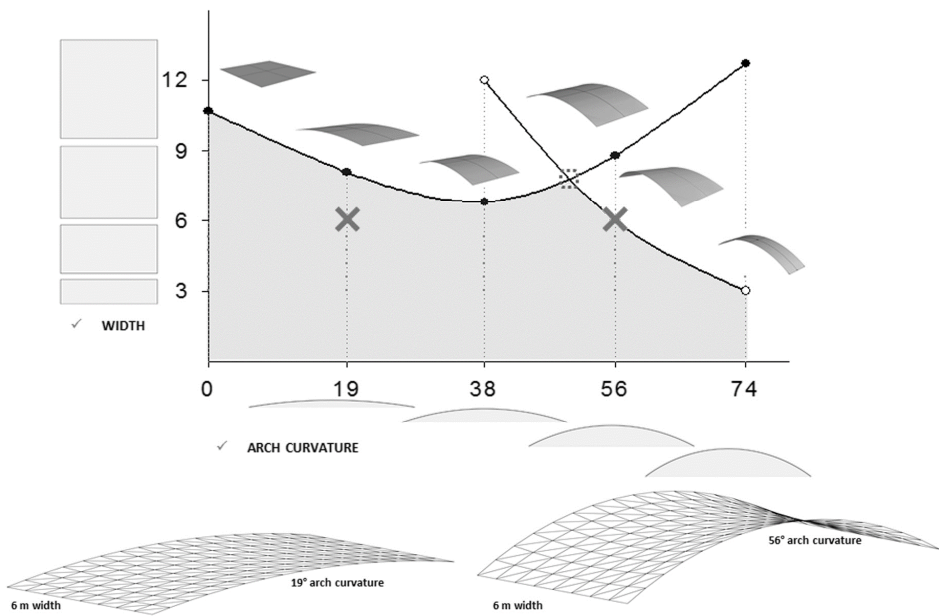


Figure 8.5-2 Regular panels used for the design example 1

Figure 8.5-3 illustrates the 3D view of the example 1 where the regular panels with different curvature rhythm can be appreciated. Figure 8.5-4 represents a possible interior view of the design example.

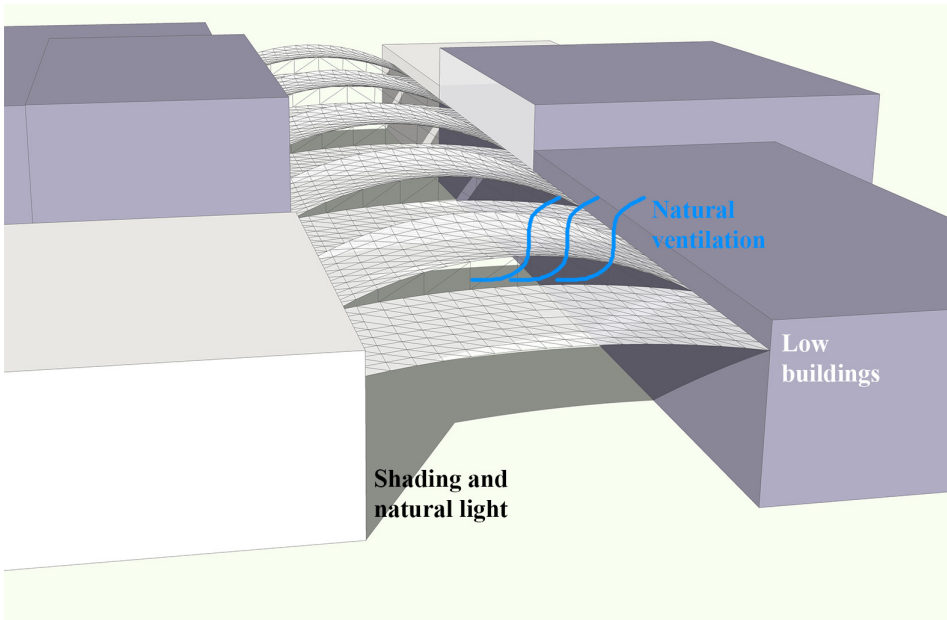


Figure 8.5-3 Example 1: 3D view



Figure 8.5-4 Example 1: interior view

8.5.1.2. Example 2: Regular panels for street market with higher buildings

For the second example, a different combination of regular panels is chosen. Supposing that the project is similar to the example 1, but in this case the building are higher than the ones in the previous example. Then, the needs of the design are also different. To create wider spaces between the arches, other two different curvatures are chosen. Besides, to make the rhythm of spaces more frequent, the panel with the most pronounced curvature is chosen with a narrower width. Figure 8.5-5 shows the panels chosen for the example 2.

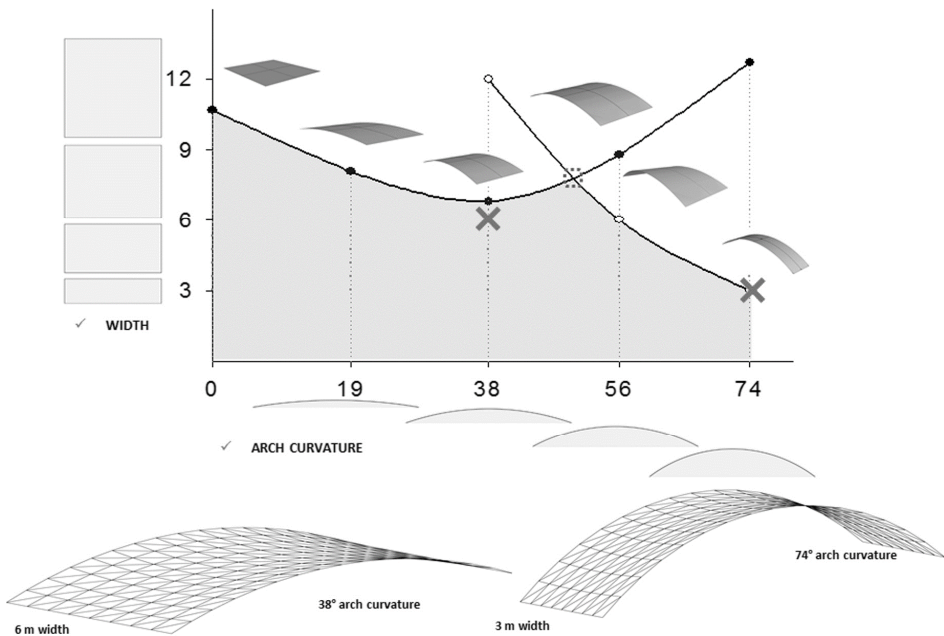


Figure 8.5-5 Regular panels used for the design example 2

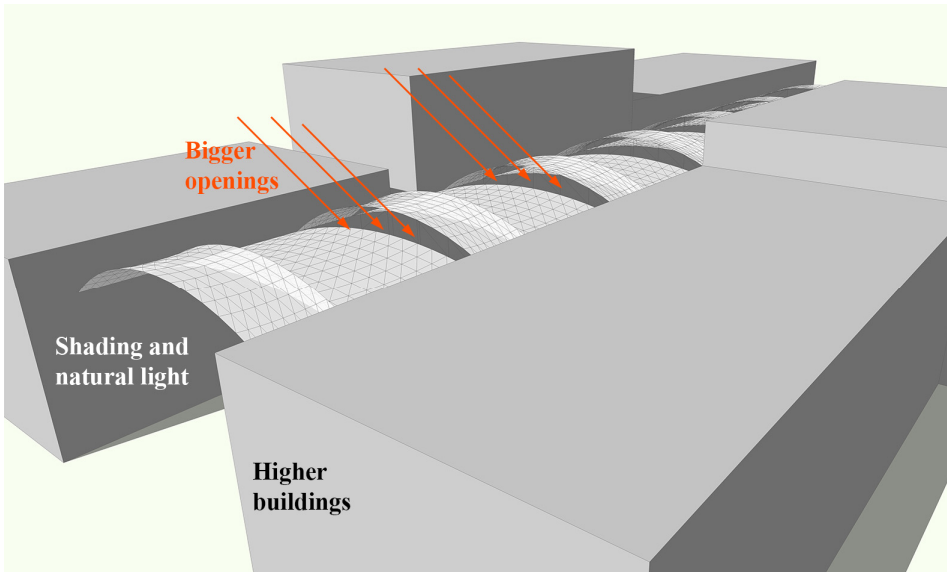


Figure 8.5-6 Example 2: 3D view

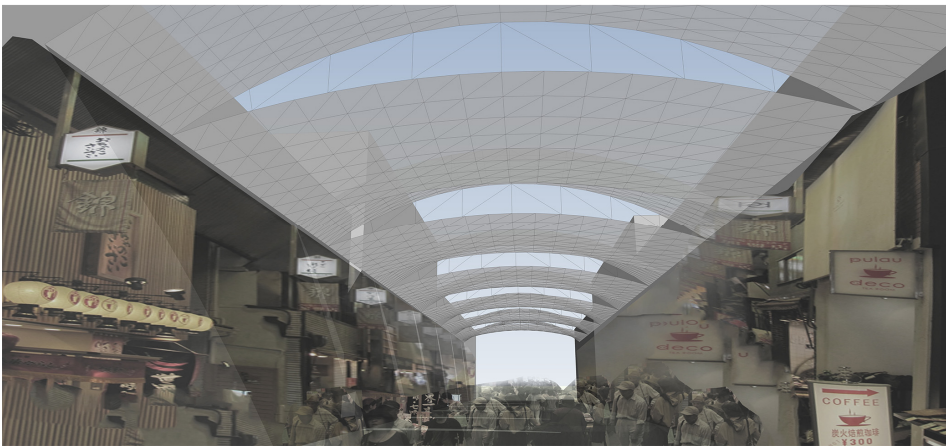


Figure 8.5-7 Example 2: interior view

Figure 8.5-6 represents the 3D view of this example, where the bigger opening and the narrower rhythm of the panels can be observed. In Fig. 8.5-7 the interior view is illustrated, assuming this to be a more busy market with higher covering roof and more people.

8.5.2. Curved barrel vault shaped membranes

When introducing one more type of panel, the design combinations can be wider. Basically, the curved panel is similar to the regular one, but it gives the possibility to adapt to more organic situations following different angles. Two simple designs are illustrated in this section and for both of them the same panels shown in Fig. 8.5-8 are used.

For the curved panel, a curvature of 56° and a width in the center of 6 m are chosen. Looking at the graph, the maximum opening angle β is determined to be 58.1° , but for this example only 45° are used, indicating that the panel is totally safe.

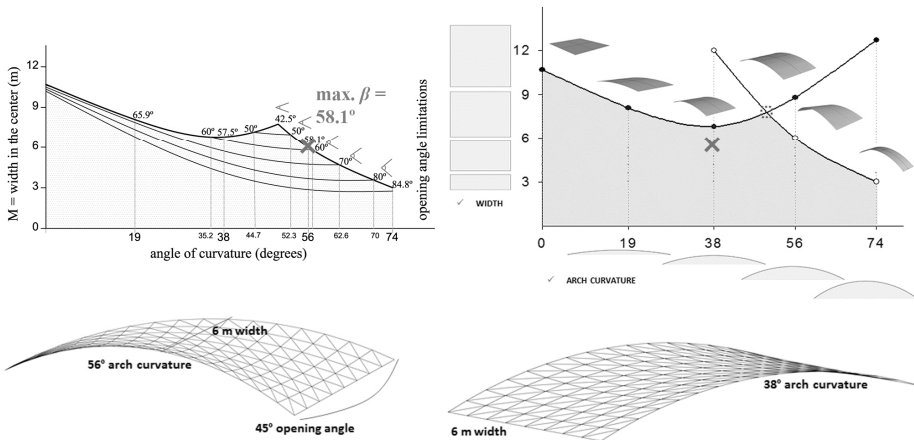


Figure 8.5-8 Regular and curved panels used for examples 3 and 4

8.5.2.1. Example 3: Regular and curved panels for irregular street market

The example 3 is the same type of project as examples 1 and 2, but in this case the membrane structure has to adapt itself to an irregular street as shown in Fig. 8.5-9. Given that the street has another shape, different opening angles for the curved panels could be chosen adapting to each curve of the street. With this example the flexibility and adaptation of this type of structures is demonstrated. Besides, the image of this kind of structure curving with the street results in a very organic and attractive situation for the observer (Fig. 8.5-10)

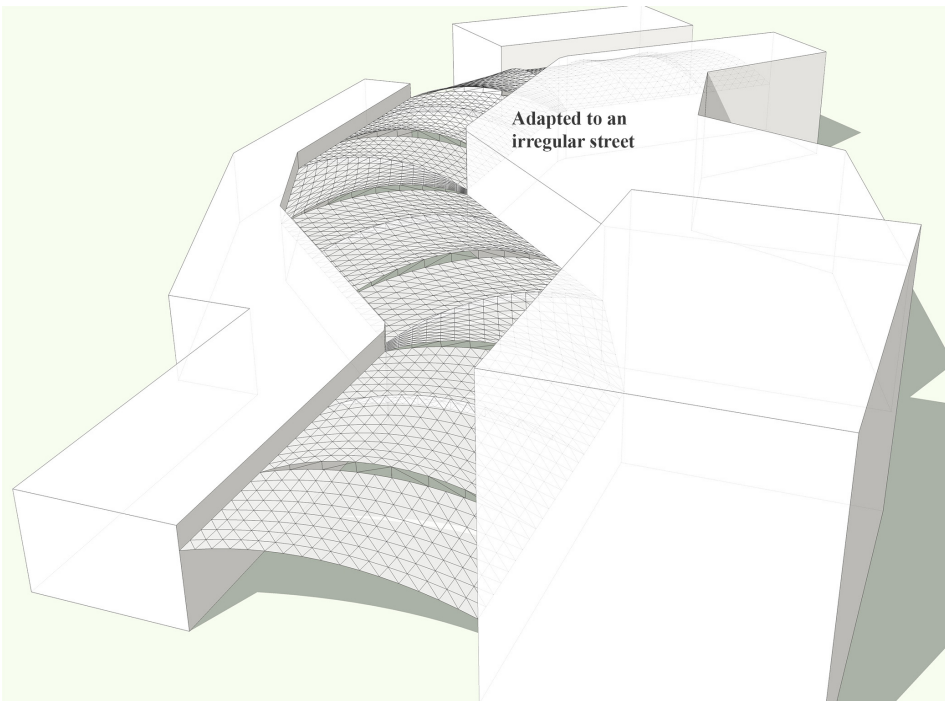


Figure 8.5-9 Example 3: 3D view

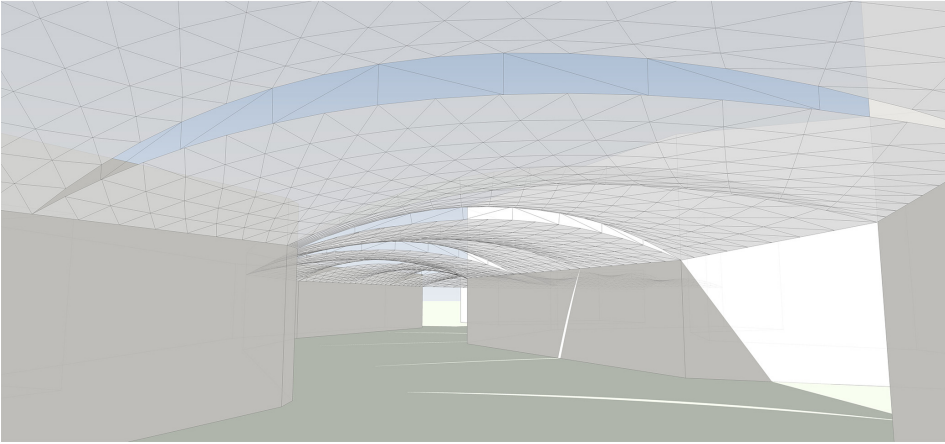


Figure 8.5-10 Example 3: interior view

8.5.2.2. Example 4: Regular and curved panels for a green walking path

Example 4 represented in Fig. 8.5-11 shows how this structure can be also adapted organically to the landscape in a park respecting the natural environment and vegetation, looking light and integrated, and producing the necessary shade for a walking path.

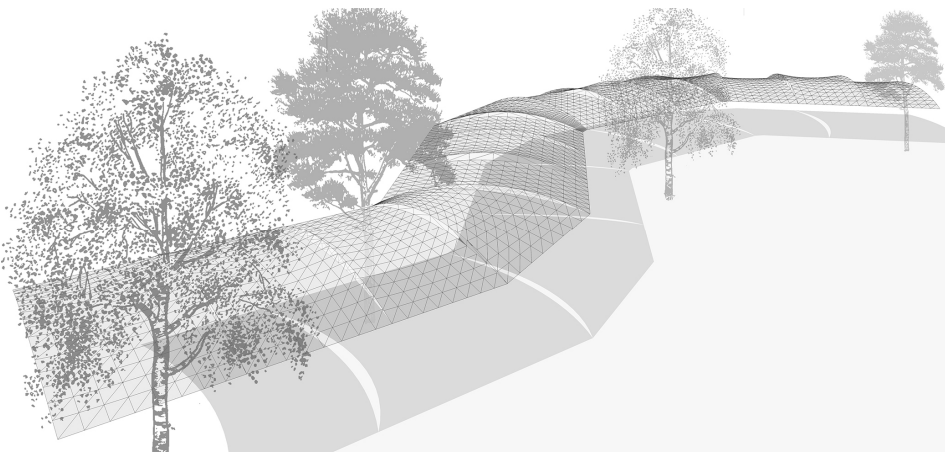


Figure 8.5-11 Example 4: 3D view

8.5.3. Inclined barrel vault shaped membranes

In the case of the inclined barrel vault shaped membranes, the applications can be various, but perhaps the most common one is the domed membrane roof. In this section a situation is given to cover a determined span with a dome, and the way to use the previously investigated inclined panels is explained.

8.5.3.1. Example 5: Regular and inclined panels for domed roofs

As shown in Fig. 8.5-12 a sphere with a diameter of 54 m is assumed to be covered by a dome, and a curvature of 40° is chosen for the design. After that, the width of the panels needs to be decided depending on the maximum inclination angle α .

In the center of the dome a regular panel can be chosen, and then from the center to the both sides in a symmetrically way the panels are inclined. As a result, the most inclined panels would be the ones on the edges.

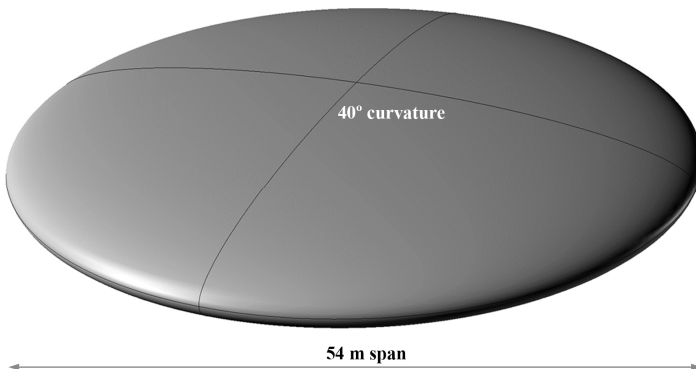


Figure 8.5-12 Assumptions for the example 5

In a first attempt, all panels were chosen to have 6 m width. However, when calculating the maximum inclination angle for 40° curvature with 6 m width using the formulas explained in previous sections, the result was only 3.73°, which was not enough for the side panels. Finally, a 6 m wide regular panel was chosen for the center, and 5 m wide inclined panels for the rest of the dome, having those a maximum inclination of 12.14° as shown in Fig. 8.5-13.

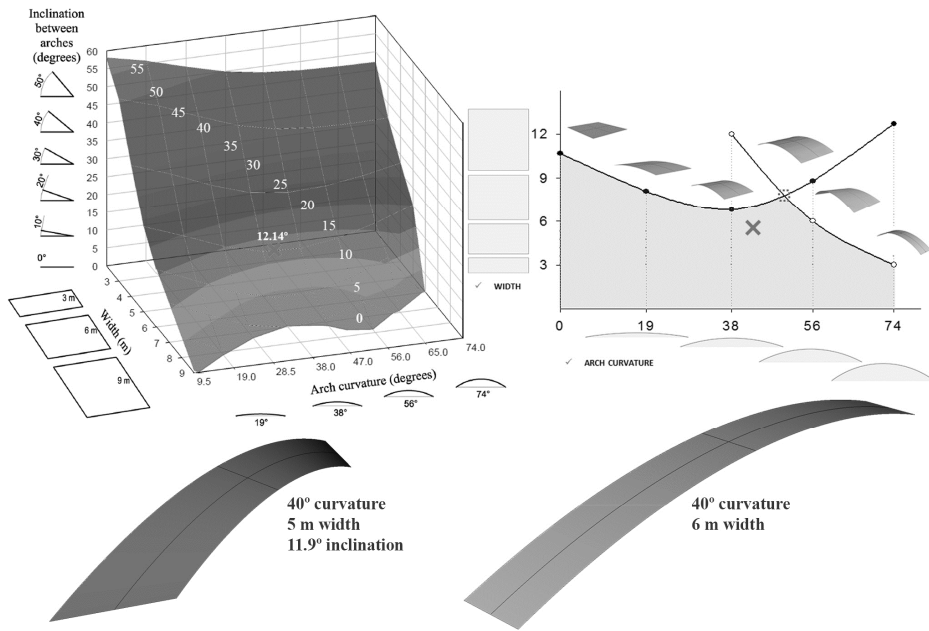


Figure 8.5-13 Panels chosen for the design example 5

Having made the choice of the maximum inclined panel for the dome, the rest of them are known to be safe as they are less inclined than the first one. Figure 8.5-14 shows the representation of this dome with its corresponding panel division.

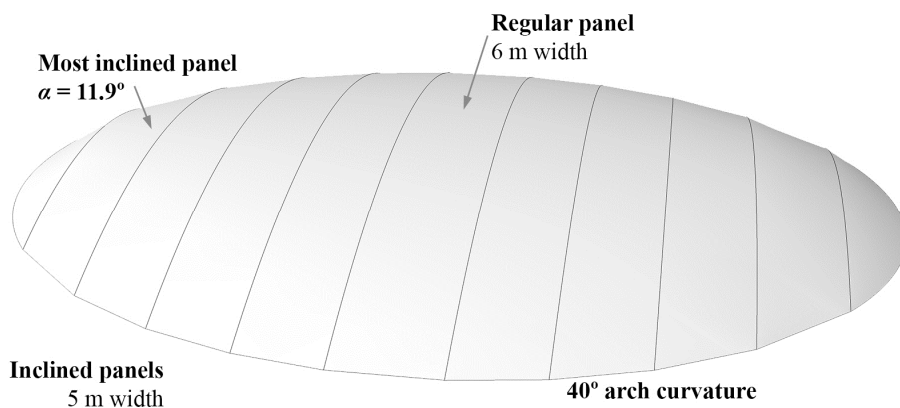


Figure 8.5-14 Example 5: 3D view of the dome

As mentioned at the beginning of this section, all of the examples illustrated in this thesis are just simple and basic applications. More complex designs can be made using the same procedure for each type of panel.

Chapter 9. Conclusion

After the two case studies, some characteristics were found about the behavior of barrel vault shaped membranes:

- In the case study 1, regarding the Seoul Southwestern Baseball Stadium dome, it is shown that the most critical loading case is the uplift wind.
- It is also demonstrated how the implementation of cables can strengthen the membrane structures, especially in that critical loading condition.
- From the comparison of panels 2 and 8 in the Seoul Southwestern dome it is understood that a more regular geometry helps to have a more stable response under various loading conditions.
- At the same time, it is also disclosed that not only the consideration of cables or other restraining conditions are important but the form-finding step also has a great significance on the stiffness of the structure. Without finding a balance initial stress and a minimal surface, the membrane behavior is unpredictable and the limit stress could be reached much faster, potentially producing the collapse of the structure.

- The fact that the upwards loading is the most critical case is emphasized in the second case study related to Jeju World Cup Stadium dome that was collapsed due to this loading condition.
- The difference between the panels of the dome in the case study 1 and 2 is that even though the uplift wind loading is much greater in the case of Jeju dome, the size of the panels in the Seoul dome is 5 times longer and 2 times wider. That is why displacements in the case of Seoul Southwestern Stadium dome are greater although stresses are smaller due to stricter loading conditions.
- This fact gives a thought about that the influence of the scale exists in this kind of panels, because it is observable that even the panels of Jeju dome are much smaller than the ones in the Seoul Southwestern dome, the values of the maximum stress are much higher. In the Seoul dome, the values of all cases and panels did not reach maximum allowable stress while in Jeju dome, almost all values are higher.
- Besides, it is also learnt that the normal fabric used for stadium domes is Sheerfill-II (used also in the Seoul Southwestern dome), but when the wind loading condition is extreme, a stronger fabric is needed as is the case of Jeju dome.

For all that reasons, a further parametric study was made to find design limitations on this kind of structures. From the parametric study the following conclusions are made:

- The following three parameters determine the geometry of regular barrel vault shaped membranes are: the arch curvature, the width of the panel, and the scale of the arch.
- The effect of the scale of the arch is negligible as the maximum stresses are almost equivalent when the arch curvature and width of the panel are kept constant. This means that considering only these last two parameters mentioned, any span can be covered.
- The arch curvature influences on the achievement of a balanced initial stress distribution when performing the form-finding analysis. If the curvature is increased, the uniformly distributed initial stress is more difficult to reach.
- The width of the panel has a smaller influence on the achievement of the balanced initial stress distribution during the form-finding analysis. However, panels with narrower widths reach a uniform stress distribution easier than the ones with wider spans between arches.
- The stress-deformation analysis should be performed under downwards loading (snow) and upwards loading (wind). And the maximum stresses under downwards loading are higher in the warp direction of the fabric while under upwards loading are higher in the fill direction.

- As the fabric strips ultimate tensile strength is lower in the fill direction than in the warp direction, it is the fill direction that gives the limitations for the design. Besides, as the upwards loading produce higher stresses in the fill direction than the downwards loading, the limitations are given by the upwards loading case in the fill direction.
- When looking at the results from the stress-deformation analysis for the arch curvature models, it is found that the lower curvatures have higher stresses. However, when the curvature of the arch is increased, negative stresses appear in the panels. This means that the membrane can wrinkle and thus possible ponding problems can also appear.
- By analyzing different widths for each arch curvature case, the limitations of width for each arch curvature are found. Besides, the models that result in wrinkle conditions are also removed from the design safety cases. These two conditions, added to the fact that the scale parameter can be neglected, lead to the development of the safe design aid chart illustrated in Fig. 8.2-15.
- For a more variety of design combinations, one grade of irregularity is added to the study. This includes the asymmetry about the transverse axis and the asymmetry about the longitudinal axis, aiming to find a similar safe design combination graph as made for the regular barrel vault shaped membranes.

- When adding asymmetry about the transverse axis, curved barrel vault shaped membrane panels are created. This type of panel is defined by the opening angle, the width of the panel in the center, and the arch curvature. Besides, any span can be covered by combining the other parameters.
- It was found that the behavior under upwards loading in the fill direction of a panel, is equivalent to the behavior of a regular panel with the same width as that in the center of the curved panel. This happens because in the fill direction under upwards loading, the maximum stress is always reached in the center of the panel. So curved panels have the same limitations as the regular panels with the same width as in the center of the curved panel regardless of the opening angle.
- However, the opening angle is limited by the behavior of the structure under downwards loading in the fill direction. The maximum stress in this condition increases linearly with the increment of the opening angle.
- Besides, it is found that this linear increment of the stress has the same rate regardless of the width chosen if the arch curvature is kept constant. This means that for the same arch curvature the increase of the stress under downwards loading in the fill direction is linear and it keeps the same rate, thus the same rate can be applied to any width.

- With this finding and the relationship between the maximum allowable stress and opening angle (Fig. 8.3-15), any opening angle can be calculated for the chosen arch curvature and width in the center.
- Both limitations, given by the downwards loading and upwards loading in the fill direction, are plotted in a safe design aid chart (Fig. 8.3-20). With this safe design aid chart for the curved panels all the limitations for the different parameter combinations of arch curvature, width in the center and opening angle can be read.
- In the case of adding asymmetry about the longitudinal axis, inclined panels are created. The parameters defining this type of panels are: the arch curvature, the inclination angle, and width of the panel. Besides, the formulas for calculating the scale of the second arch in relation with the first arch and the other parameter chosen is also driven.
- Most critical case for inclined panels is the downward loading in the fill direction (as it happens in the case studies that also used inclined panels).
- The incremental rate of the stress in the fill direction under upwards loading when the inclination angle is increased is not similar for the different panel widths when the curvature is kept constant as it happens with curved panels due to the scale factor of the second arch.

- However, the increasing rate is similar for different arch curvatures when the width is kept constant. This happens because the inclination angle is independent of the arch curvature but dependent upon the width of the panel, and maximum stresses are obtained in the central transverse section which applies for all panels regardless of the arch curvature.
- With all of this finding, a relationship between the maximum allowable stress and inclination angle is also determined for obtaining the limitations of the inclined panels (Fig. 8.4-15).
- Besides, the resulting values for the main widths and curvatures are plotted in a safe design aid chart represented in Fig. 8.4-19, where in addition, the combinations where wrinkle appears are excluded. Using this 3D chart or the formula explained earlier, the inclination angle limitations can be found for any arch curvature and width combination.
- Simple design examples are also described to show the application of this study. From the integration of the structure in the urban context to the adaptation to an organic landscape or even the covering of a domed building are some of the possible applications of the safe design aid charts created for regular, curved and inclined panels. However, the examples illustrated in this thesis are just simple and basic applications, and more complex designs can be made using the same procedure for each type of panel.

Summarizing, this thesis provides design guidance that can be considered in the first stage of the projects that use barrel vault shaped membranes, as well as to give a detailed explanation on the modeling and analysis of tensile structures.

References

- Ali-Nezhad, F.M. & Eskandari, H., 2012. Effect of Architectural Design of Greenhouse on Solar Radiation Interception and Crops Growth Conditions. *International Journal of Agriculture and Crop Sciences*, 4(3), pp.122–127.
- Ambroziak, A. & Kłosowski, P., 2014. Mechanical properties for preliminary design of structures made from PVC coated fabric. *Construction and Building Materials*, 50, pp.74–81.
- Argyris, J.H., Angelopoulos, T. & Bichat, B., 1974. A general method for the shape finding of lightweight tension structures. *Computer Methods in Applied Mechanics and Engineering*, 3(1), pp.135–149.
- Barnes, M.R., 1999. Form finding and analysis of tension structures by dynamic relaxation. *International Journal of Space Structures*, 14(2), pp.89–104.
- Berger, H., 2012. Creating Architecture with Tensile Membrane Structures. *IASS-APCS*.
- Berger, H., 1999. Form and function of tensile structures for permanent buildings. *Engineering Structures*, 21(8), pp.669–679.
- Berger, H., 1996. *Light structures, structures of light: The art and engineering of tensile architecture*, Birkhauser.
- Bletzinger, K.-U. & Ramm, E., 2001. Structural optimization and form finding of light weight structures. *Computers & Structures*, 79(22), pp.2053–2062.

- Bradshaw, R., Campbell, D., Gargari, M., Mirmiran, A., Tripeny, P., 2002. Special structures: past, present, and future. *Journal of Structural Engineering*, 128(6), pp.691–709.
- Bridgens, B. & Birchall, M., 2012. Form and function: The significance of material properties in the design of tensile fabric structures. *Engineering Structures*, 44, pp.1–12.
- Brzozowski, A., Freeman, G. & Lee, J.C., 2005. The Roof Structure of the Jeju Worldcup Stadium. In *Structures Congress 2005 Metropolis and Beyond*. ASCE, pp. 1–12.
- Crisfield, M.A., Remmers, J.J., Verhoosel, C.V., others, 2012. *Nonlinear finite element analysis of solids and structures*, John Wiley & Sons.
- Engel, H., 1981. *Structure Systems*, Van Nostrand Reinhold Company.
- Fang, R., 2009. *The design and construction of fabric structures*. Massachusetts Institute of Technology.
- Forster, B. & Mollaert, M., 2004. *European design guide for tensile surface structures*, Tensinet.
- Gosling, P., Bridgens, B., Albrecht, A., Alpermann, H., Angeleri, A., Barnes, M., Bartle, N., Canobbio, R., Dieringer, F., Gellin, S., others, 2013. Analysis and design of membrane structures: Results of a round robin exercise. *Engineering Structures*, 48, pp.313–328.
- Greco, L. & Cuomo, M., 2012. On the force density method for slack cable nets. *International Journal of Solids and Structures*, 49(13), pp.1526–1540.
- Haug, E., Milcent, G., Gelenne, P., Kermel, P., Gawenat, B., Michalski, A., 2012. Simulation of folding and stowing of structural membranes. *IASS-APCS*.

- Hills, S., Birks, R. & McKenzie, B., 2002. The Millennium Dome“ Watercycle” experiment: to evaluate water efficiency and customer perception at a recycling scheme for 6 million visitors. *Water Science & Technology*, 46(6), pp.233–240.
- Iványi, P., 2013. A new conceptual design tool for cable-membrane structures. *Advances in Engineering Software*, 57, pp.33–39.
- Kim, J.-S., Choi, J.-I. & Cho, D.-W., 2010. Design process of free-formed dome structure; Southwestern Dome Stadium. *Proceedings of the International Association for Shell and Spatial Structures*.
- Knebel, K., Sanchez-Alvarez, J. & Zimmermann, S., 2002. The structural making of the Eden domes. *Space Structures*, 5(1), pp.245–254.
- Lan, T.T., 2012. Advances of Spatial Structures in China - Recent developments and applications. *IASS-APCS*.
- Lienhard, J. & Knippers, J., 2012. Permanent and convertible membrane structures with intricate bending-active support systems. *IASS-APCS*.
- Maurin, B. & Motro, R., 1998. The surface stress density method as a form-finding tool for tensile membranes. *Engineering Structures*, 20(8), pp.712–719.
- McGuire, W., Gallagher, R.H. & Ziemian, R.D., 1979. *Matrix structural analysis*, Wiley New York.
- Mendez Echenagucia, T. & Sassone, M., 2012. Multi Objective Oriented design of Shell Structures. *IASS-APCS*.
- Miki, M. & Kawaguchi, K., 2010. Extended force density method for form-finding of tension structures. *Journal of the International Association for Shell and Spatial Structures*, 51(4), p.291.
- Olsson, J., 2012. *Form finding and size optimization-Implementation of beam elements and size optimization in real time form finding using dynamic relaxation*. Chalmers University of Technology.

- Otto, F. & Rasch, B., 1996. *Finding Form: Towards an Architecture of the Minimal*, Axel Menges.
- Rezaiee Pajand, M. & Moghaddasie, B., 2009. Some geometrical bases for incremental-iterative methods. *International Journal of Engineering*, 22.
- Sakai, K., Ishihara, O., Sasaguchi, K., Baba, H., Sato, T., 1999. A simulation of an underground heat storage system using midnight electric power at Park Dome Kumamoto. In *Proc of Building Simulation*. pp. 507–512.
- Sakamoto, H., Park, K. & Miyazaki, Y., 2007. Evaluation of membrane structure designs using boundary web cables for uniform tensioning. *Acta Astronautica*, 60(10), pp.846–857.
- Sanchez, J., Serna, M.A. & Morer, P., 2007. A multi-step force–density method and surface-fitting approach for the preliminary shape design of tensile structures. *Engineering Structures*, 29(8), pp.1966–1976.
- Schek, H.-J., 1974. The force density method for form finding and computation of general networks. *Computer Methods in Applied Mechanics and Engineering*, 3(1), pp.115–134.
- Symeonidou, I., 2012. From Cable Nets to Surface Nets: A case study. *IASS-APCS*.
- Tabarrok, B. & Qin, Z., 1992. Nonlinear analysis of tension structures. *Computers & Structures*, 45(5), pp.973–984.
- Veenendaal, D. & Block, P., 2012. An overview and comparison of structural form finding methods for general networks. *International Journal of Solids and Structures*, 49(26), pp.3741–3753.
- Wakefield, D., 1999. Engineering analysis of tension structures: theory and practice. *Engineering Structures*, 21(8), pp.680–690.

- Weaver, W., Johnston, P.R. & Douglas, A., 1984. Finite elements for structural analysis. *Journal of Applied Mechanics*, 51, p.705.
- Winslow, P., Pellegrino, S. & Sharma, S., 2010. Multi-objective optimization of free-form grid structures. *Structural and Multidisciplinary Optimization*, 40(1-6), pp.257–269.
- Ye, J., Feng, R., Zhou, S., Tian, J., 2012. The modified force-density method for form-finding of membrane structures. *International Journal of Steel Structures*, 12(3), pp.299–310.

Appendices

In this appendices an example of the input and output data for one of the models is presented. The following data files correspond to a regular barrel vault shaped membrane with 38 degrees arch curvature and 6 meters width. The initial data and the results for form-finding analysis and stress-deformation analysis for both cases, downwards loading and upwards loading, are shown. However, only a portion of the output data file is shown for space reasons.

From page 262 till 269, the initial input data for the form-finding analysis can be read. From page 270 to 281, the final results after obtaining a balanced initial stress distribution are presented. From page 282 to 293, the initial data for the stress-deformation analysis under downwards loading with the updated coordinates found in the form-finding analysis can be read. In this file, nodal downwards forces are included. From page 293 to 304, the results under downwards loading with the final maximum stress are shown. In the same way, from 305 to 315, the initial for the stress-deformation analysis under upwards loading is represented, and from 316 to 327, the results are shown.

This procedure is done for each of the models with different variables analyzed in this thesis.

==== BARREL VAULT _curvature38 width6_ Shape analysis ====

3 1 1
3 3 1
153 256
3 1

clea tfor
clea tdis
clea tsrs
clea tsrn
nonl

100 50 0.01e-10 0 0

node

1	0.000000	0.000000	0.000000	0
2	69.801903	0.000000	22.396667	0
3	143.653870	0.000000	42.832476	0
4	222.870827	0.000000	61.152548	0
5	297.819328	0.000000	75.153917	0
6	369.630241	0.000000	85.600668	0
7	446.246147	0.000000	93.599677	0
8	522.480583	0.000000	98.375160	0
9	598.198318	0.000000	99.999124	0
10	673.486900	0.000000	98.539877	0
11	750.972939	0.000000	93.829483	0
12	826.968765	0.000000	86.024290	0
13	901.795769	0.000000	75.217617	0
14	978.141594	0.000000	60.941446	0
15	1053.578758	0.000000	43.534598	0
16	1126.350021	0.000000	23.543227	0
17	1200.000000	0.000000	0.000000	0
18	0.000000	75.000000	0.000000	0
19	69.801903	75.000000	22.396667	0
20	143.653870	75.000000	42.832476	0
21	222.870827	75.000000	61.152548	0
22	297.819328	75.000000	75.153917	0
23	369.630241	75.000000	85.600668	0
24	446.246147	75.000000	93.599677	0
25	522.480583	75.000000	98.375160	0
26	598.198318	75.000000	99.999124	0
27	673.486900	75.000000	98.539877	0
28	750.972939	75.000000	93.829483	0
29	826.968765	75.000000	86.024290	0
30	901.795769	75.000000	75.217617	0
31	978.141594	75.000000	60.941446	0
32	1053.578758	75.000000	43.534598	0
33	1126.350021	75.000000	23.543227	0
34	1200.000000	75.000000	0.000000	0
35	0.000000	150.000000	0.000000	0
36	69.801903	150.000000	22.396667	0
37	143.653870	150.000000	42.832476	0
38	222.870827	150.000000	61.152548	0
39	297.819328	150.000000	75.153917	0
40	369.630241	150.000000	85.600668	0
41	446.246147	150.000000	93.599677	0
42	522.480583	150.000000	98.375160	0
43	598.198318	150.000000	99.999124	0
44	673.486900	150.000000	98.539877	0
45	750.972939	150.000000	93.829483	0
46	826.968765	150.000000	86.024290	0
47	901.795769	150.000000	75.217617	0
48	978.141594	150.000000	60.941446	0

49	1053.578758	150.000000	43.534598	0
50	1126.350021	150.000000	23.543227	0
51	1200.000000	150.000000	0.000000	0
52	0.000000	225.000000	0.000000	0
53	69.801903	225.000000	22.396667	0
54	143.653870	225.000000	42.832476	0
55	222.870827	225.000000	61.152548	0
56	297.819328	225.000000	75.153917	0
57	369.630241	225.000000	85.600668	0
58	446.246147	225.000000	93.599677	0
59	522.480583	225.000000	98.375160	0
60	598.198318	225.000000	99.999124	0
61	673.486900	225.000000	98.539877	0
62	750.972939	225.000000	93.829483	0
63	826.968765	225.000000	86.024290	0
64	901.795769	225.000000	75.217617	0
65	978.141594	225.000000	60.941446	0
66	1053.578758	225.000000	43.534598	0
67	1126.350021	225.000000	23.543227	0
68	1200.000000	225.000000	0.000000	0
69	0.000000	300.000000	0.000000	0
70	69.801903	300.000000	22.396667	0
71	143.653870	300.000000	42.832476	0
72	222.870827	300.000000	61.152548	0
73	297.819328	300.000000	75.153917	0
74	369.630241	300.000000	85.600668	0
75	446.246147	300.000000	93.599677	0
76	522.480583	300.000000	98.375160	0
77	598.198318	300.000000	99.999124	0
78	673.486900	300.000000	98.539877	0
79	750.972939	300.000000	93.829483	0
80	826.968765	300.000000	86.024290	0
81	901.795769	300.000000	75.217617	0
82	978.141594	300.000000	60.941446	0
83	1053.578758	300.000000	43.534598	0
84	1126.350021	300.000000	23.543227	0
85	1200.000000	300.000000	0.000000	0
86	0.000000	375.000000	0.000000	0
87	69.801903	375.000000	22.396667	0
88	143.653870	375.000000	42.832476	0
89	222.870827	375.000000	61.152548	0
90	297.819328	375.000000	75.153917	0
91	369.630241	375.000000	85.600668	0
92	446.246147	375.000000	93.599677	0
93	522.480583	375.000000	98.375160	0
94	598.198318	375.000000	99.999124	0
95	673.486900	375.000000	98.539877	0
96	750.972939	375.000000	93.829483	0
97	826.968765	375.000000	86.024290	0
98	901.795769	375.000000	75.217617	0
99	978.141594	375.000000	60.941446	0
100	1053.578758	375.000000	43.534598	0
101	1126.350021	375.000000	23.543227	0
102	1200.000000	375.000000	0.000000	0
103	0.000000	450.000000	0.000000	0
104	69.801903	450.000000	22.396667	0
105	143.653870	450.000000	42.832476	0
106	222.870827	450.000000	61.152548	0
107	297.819328	450.000000	75.153917	0
108	369.630241	450.000000	85.600668	0

109	446.246147	450.000000	93.599677	0
110	522.480583	450.000000	98.375160	0
111	598.198318	450.000000	99.999124	0
112	673.486900	450.000000	98.539877	0
113	750.972939	450.000000	93.829483	0
114	826.968765	450.000000	86.024290	0
115	901.795769	450.000000	75.217617	0
116	978.141594	450.000000	60.941446	0
117	1053.578758	450.000000	43.534598	0
118	1126.350021	450.000000	23.543227	0
119	1200.000000	450.000000	0.000000	0
120	0.000000	525.000000	0.000000	0
121	69.801903	525.000000	22.396667	0
122	143.653870	525.000000	42.832476	0
123	222.870827	525.000000	61.152548	0
124	297.819328	525.000000	75.153917	0
125	369.630241	525.000000	85.600668	0
126	446.246147	525.000000	93.599677	0
127	522.480583	525.000000	98.375160	0
128	598.198318	525.000000	99.999124	0
129	673.486900	525.000000	98.539877	0
130	750.972939	525.000000	93.829483	0
131	826.968765	525.000000	86.024290	0
132	901.795769	525.000000	75.217617	0
133	978.141594	525.000000	60.941446	0
134	1053.578758	525.000000	43.534598	0
135	1126.350021	525.000000	23.543227	0
136	1200.000000	525.000000	0.000000	0
137	0.000000	600.000000	0.000000	0
138	69.801903	600.000000	22.396667	0
139	143.653870	600.000000	42.832476	0
140	222.870827	600.000000	61.152548	0
141	297.819328	600.000000	75.153917	0
142	369.630241	600.000000	85.600668	0
143	446.246147	600.000000	93.599677	0
144	522.480583	600.000000	98.375160	0
145	598.198318	600.000000	99.999124	0
146	673.486900	600.000000	98.539877	0
147	750.972939	600.000000	93.829483	0
148	826.968765	600.000000	86.024290	0
149	901.795769	600.000000	75.217617	0
150	978.141594	600.000000	60.941446	0
151	1053.578758	600.000000	43.534598	0
152	1126.350021	600.000000	23.543227	0
153	1200.000000	600.000000	0.000000	0

0,/////////
elem mak3 3

1	18 1 2	1	0	0
2	2 19 18	1	0	0
3	19 2 3	1	0	0
4	3 20 19	1	0	0
5	20 3 4	1	0	0
6	4 21 20	1	0	0
7	21 4 5	1	0	0
8	5 22 21	1	0	0
9	22 5 6	1	0	0
10	6 23 22	1	0	0
11	23 6 7	1	0	0
12	7 24 23	1	0	0
13	24 7 8	1	0	0

14	8	25	24	1	0	0
15	25	8	9	1	0	0
16	9	26	25	1	0	0
17	26	9	10	1	0	0
18	10	27	26	1	0	0
19	27	10	11	1	0	0
20	11	28	27	1	0	0
21	28	11	12	1	0	0
22	12	29	28	1	0	0
23	29	12	13	1	0	0
24	13	30	29	1	0	0
25	30	13	14	1	0	0
26	14	31	30	1	0	0
27	31	14	15	1	0	0
28	15	32	31	1	0	0
29	32	15	16	1	0	0
30	16	33	32	1	0	0
31	33	16	17	1	0	0
32	17	34	33	1	0	0
33	35	18	19	1	0	0
34	19	36	35	1	0	0
35	36	19	20	1	0	0
36	20	37	36	1	0	0
37	37	20	21	1	0	0
38	21	38	37	1	0	0
39	38	21	22	1	0	0
40	22	39	38	1	0	0
41	39	22	23	1	0	0
42	23	40	39	1	0	0
43	40	23	24	1	0	0
44	24	41	40	1	0	0
45	41	24	25	1	0	0
46	25	42	41	1	0	0
47	42	25	26	1	0	0
48	26	43	42	1	0	0
49	43	26	27	1	0	0
50	27	44	43	1	0	0
51	44	27	28	1	0	0
52	28	45	44	1	0	0
53	45	28	29	1	0	0
54	29	46	45	1	0	0
55	46	29	30	1	0	0
56	30	47	46	1	0	0
57	47	30	31	1	0	0
58	31	48	47	1	0	0
59	48	31	32	1	0	0
60	32	49	48	1	0	0
61	49	32	33	1	0	0
62	33	50	49	1	0	0
63	50	33	34	1	0	0
64	34	51	50	1	0	0
65	52	35	36	1	0	0
66	36	53	52	1	0	0
67	53	36	37	1	0	0
68	37	54	53	1	0	0
69	54	37	38	1	0	0
70	38	55	54	1	0	0
71	55	38	39	1	0	0
72	39	56	55	1	0	0
73	56	39	40	1	0	0

74	40	57	56	1	0	0
75	57	40	41	1	0	0
76	41	58	57	1	0	0
77	58	41	42	1	0	0
78	42	59	58	1	0	0
79	59	42	43	1	0	0
80	43	60	59	1	0	0
81	60	43	44	1	0	0
82	44	61	60	1	0	0
83	61	44	45	1	0	0
84	45	62	61	1	0	0
85	62	45	46	1	0	0
86	46	63	62	1	0	0
87	63	46	47	1	0	0
88	47	64	63	1	0	0
89	64	47	48	1	0	0
90	48	65	64	1	0	0
91	65	48	49	1	0	0
92	49	66	65	1	0	0
93	66	49	50	1	0	0
94	50	67	66	1	0	0
95	67	50	51	1	0	0
96	51	68	67	1	0	0
97	69	52	53	1	0	0
98	53	70	69	1	0	0
99	70	53	54	1	0	0
100	54	71	70	1	0	0
101	71	54	55	1	0	0
102	55	72	71	1	0	0
103	72	55	56	1	0	0
104	56	73	72	1	0	0
105	73	56	57	1	0	0
106	57	74	73	1	0	0
107	74	57	58	1	0	0
108	58	75	74	1	0	0
109	75	58	59	1	0	0
110	59	76	75	1	0	0
111	76	59	60	1	0	0
112	60	77	76	1	0	0
113	77	60	61	1	0	0
114	61	78	77	1	0	0
115	78	61	62	1	0	0
116	62	79	78	1	0	0
117	79	62	63	1	0	0
118	63	80	79	1	0	0
119	80	63	64	1	0	0
120	64	81	80	1	0	0
121	81	64	65	1	0	0
122	65	82	81	1	0	0
123	82	65	66	1	0	0
124	66	83	82	1	0	0
125	83	66	67	1	0	0
126	67	84	83	1	0	0
127	84	67	68	1	0	0
128	68	85	84	1	0	0
129	86	69	70	1	0	0
130	70	87	86	1	0	0
131	87	70	71	1	0	0
132	71	88	87	1	0	0
133	88	71	72	1	0	0

134	72 89 88	1	0	0
135	89 72 73	1	0	0
136	73 90 89	1	0	0
137	90 73 74	1	0	0
138	74 91 90	1	0	0
139	91 74 75	1	0	0
140	75 92 91	1	0	0
141	92 75 76	1	0	0
142	76 93 92	1	0	0
143	93 76 77	1	0	0
144	77 94 93	1	0	0
145	94 77 78	1	0	0
146	78 95 94	1	0	0
147	95 78 79	1	0	0
148	79 96 95	1	0	0
149	96 79 80	1	0	0
150	80 97 96	1	0	0
151	97 80 81	1	0	0
152	81 98 97	1	0	0
153	98 81 82	1	0	0
154	82 99 98	1	0	0
155	99 82 83	1	0	0
156	83 100 99	1	0	0
157	100 83 84	1	0	0
158	84 101 100	1	0	0
159	101 84 85	1	0	0
160	85 102 101	1	0	0
161	103 86 87	1	0	0
162	87 104 103	1	0	0
163	104 87 88	1	0	0
164	88 105 104	1	0	0
165	105 88 89	1	0	0
166	89 106 105	1	0	0
167	106 89 90	1	0	0
168	90 107 106	1	0	0
169	107 90 91	1	0	0
170	91 108 107	1	0	0
171	108 91 92	1	0	0
172	92 109 108	1	0	0
173	109 92 93	1	0	0
174	93 110 109	1	0	0
175	110 93 94	1	0	0
176	94 111 110	1	0	0
177	111 94 95	1	0	0
178	95 112 111	1	0	0
179	112 95 96	1	0	0
180	96 113 112	1	0	0
181	113 96 97	1	0	0
182	97 114 113	1	0	0
183	114 97 98	1	0	0
184	98 115 114	1	0	0
185	115 98 99	1	0	0
186	99 116 115	1	0	0
187	116 99 100	1	0	0
188	100 117 116	1	0	0
189	117 100 101	1	0	0
190	101 118 117	1	0	0
191	118 101 102	1	0	0
192	102 119 118	1	0	0
193	120 103 104	1	0	0

194	104	121	120	1	0	0
195	121	104	105	1	0	0
196	105	122	121	1	0	0
197	122	105	106	1	0	0
198	106	123	122	1	0	0
199	123	106	107	1	0	0
200	107	124	123	1	0	0
201	124	107	108	1	0	0
202	108	125	124	1	0	0
203	125	108	109	1	0	0
204	109	126	125	1	0	0
205	126	109	110	1	0	0
206	110	127	126	1	0	0
207	127	110	111	1	0	0
208	111	128	127	1	0	0
209	128	111	112	1	0	0
210	112	129	128	1	0	0
211	129	112	113	1	0	0
212	113	130	129	1	0	0
213	130	113	114	1	0	0
214	114	131	130	1	0	0
215	131	114	115	1	0	0
216	115	132	131	1	0	0
217	132	115	116	1	0	0
218	116	133	132	1	0	0
219	133	116	117	1	0	0
220	117	134	133	1	0	0
221	134	117	118	1	0	0
222	118	135	134	1	0	0
223	135	118	119	1	0	0
224	119	136	135	1	0	0
225	137	120	121	1	0	0
226	121	138	137	1	0	0
227	138	121	122	1	0	0
228	122	139	138	1	0	0
229	139	122	123	1	0	0
230	123	140	139	1	0	0
231	140	123	124	1	0	0
232	124	141	140	1	0	0
233	141	124	125	1	0	0
234	125	142	141	1	0	0
235	142	125	126	1	0	0
236	126	143	142	1	0	0
237	143	126	127	1	0	0
238	127	144	143	1	0	0
239	144	127	128	1	0	0
240	128	145	144	1	0	0
241	145	128	129	1	0	0
242	129	146	145	1	0	0
243	146	129	130	1	0	0
244	130	147	146	1	0	0
245	147	130	131	1	0	0
246	131	148	147	1	0	0
247	148	131	132	1	0	0
248	132	149	148	1	0	0
249	149	132	133	1	0	0
250	133	150	149	1	0	0
251	150	133	134	1	0	0
252	134	151	150	1	0	0
253	151	134	135	1	0	0

```

254      135 152 151      1  0  0
255      152 135 136      1  0  0
256      136 153 152      1  0  0
0,,,,,,,,,
mate ortr
1  1.0    0.0   1230.0   950.0  0.804  0.620  96.26
0,,,,,,,,,
strs
1      5.0          5.0      0.0    1
256    5.0          5.0      0.0    0
0,,,,,,,,,
b.c.
1      1  1  1  1
18     1  1  1  0
136    1  1  1  1
153    1  1  1  0
34     1  1  1  0
35     1  1  1  0
51     1  1  1  0
52     1  1  1  0
68     1  1  1  0
69     1  1  1  0
85     1  1  1  0
86     1  1  1  0
102    1  1  1  0
103    1  1  1  0
119    1  1  1  0
120    1  1  1  0
0,,,,,,,,,
end

```

```

*****
***
***          =====
***                   NASS-2004
***          NONLINEAR ANALYSIS FOR SPATIAL STRUCTURES
***          =====
***
***                   developed by
***                   SEUNG-DEOG KIM, Semyung University
***
*****

```

TITLE : ===== BARREL VAULT _curvature38 width6_ Shape analysis =====

```

Kind of dimension          = 3 ( 2 for 2-D, 3 for 3-D )
Kind of problem (1)       = 1 ( 1 for STATIC, 2 for DYNAMIC )
Kind of problem (2)       = 1 ( 0 for LINEAR ANALYSIS
                               1 for EQUILIBLIUM-FINDING
                               2 for SHAPE-FINDING
                               3 for STRESS-DEFORMATION by FORCE
                               4 for STRESS-DEFORMATION by DISPL
                               5 for 1 + 3
                               6 for 1 + 4
                               7 for 2 + 3
                               8 for 2 + 4
                               )

```

```

Maximum DOF of each node   = 3
Maximum node of each element = 3
Outputing level            = 1

Total nodes                 = 153
Total elements              = 256
Kinds of Material           = 1

Total DOFs                  = 459

```

```

Integrating points for IN-PLANE & BENDING = 3
Integrating points for SHEAR              = 1

```

/// Memory Check : kaend= 41519 , k1= 300000 ///

/// Memory Check : klend= 3169 , k2= 20000 ///

/// Memory Check : kbend= 421362 , k3=8100000 ///

... total DOF x total DOF = 459 x 459 = 210681 ...

===== DATA FOR NONLINEAR ANALYSIS =====

Total Step = 100
Total Iteration = 50
Error = .10000E-11
Modification On/Off = 0 (Off for 0)
Determinant On/Off = 0 (On for 1)

Control Node = 0
Control DOF = 0
Displacement = .00000E+00

===== DATA FOR INITIAL IMPERFECTION =====

Imperfection = .00000E+00
Mode Number = 0

===== DATA FOR SEMI-RIGID FACTOR =====

Semi-Rigid = .10000E+01

49	.10517E+04	.14970E+03	.33602E+02	.40359E-11	.15262E-10	.45475E-12
50	.11251E+04	.14983E+03	.17522E+02	.26716E-11	.21885E-11	.34106E-12
51	.12000E+04	.15000E+03	.00000E+00	-.24074E-11	-.53433E-11	.57791E-12
52	.00000E+00	.22500E+03	.00000E+00	-.21885E-11	.76739E-11	-.57554E-12
53	.71297E+02	.22488E+03	.15489E+02	.17053E-12	-.28706E-11	.72475E-12
54	.14589E+03	.22479E+03	.30875E+02	.56843E-13	-.51443E-11	.14495E-11
55	.22533E+03	.22474E+03	.45573E+02	.96634E-12	-.17906E-11	.19362E-11
56	.30008E+03	.22470E+03	.57287E+02	.21600E-11	-.62528E-12	.16875E-11
57	.37150E+03	.22465E+03	.66274E+02	.44054E-11	.50591E-11	.11067E-11
58	.44755E+03	.22462E+03	.73286E+02	.71054E-11	.62244E-11	.11493E-11
59	.52316E+03	.22462E+03	.77523E+02	.87255E-11	.61107E-11	.56177E-12
60	.59823E+03	.22462E+03	.78972E+02	.10004E-10	.73612E-11	.45297E-13
61	.67286E+03	.22462E+03	.77670E+02	.11227E-10	.83560E-11	-.30376E-12
62	.74971E+03	.22463E+03	.73488E+02	.11568E-10	.97202E-11	-.26290E-12
63	.82513E+03	.22468E+03	.66642E+02	.11539E-10	.15262E-10	-.42277E-12
64	.89955E+03	.22471E+03	.57339E+02	.12591E-10	.19213E-10	-.19895E-12
65	.97572E+03	.22476E+03	.45392E+02	.12562E-10	.19384E-10	-.63238E-12
66	.10513E+04	.22483E+03	.31437E+02	.11170E-10	.16030E-10	-.94502E-12
67	.11249E+04	.22492E+03	.16313E+02	.66507E-11	.29274E-11	-.83844E-12
68	.12000E+04	.22500E+03	.00000E+00	-.25915E-11	-.65086E-11	.62573E-12
69	.00000E+00	.30000E+03	.00000E+00	-.17053E-12	.94929E-11	-.85265E-13
70	.71348E+02	.29998E+03	.15122E+02	.28422E-12	-.70486E-11	.97344E-12
71	.14598E+03	.29999E+03	.30180E+02	-.28137E-11	-.12022E-10	.98765E-12
72	.22545E+03	.30000E+03	.44618E+02	-.52580E-11	-.98335E-11	.58265E-12
73	.30017E+03	.30000E+03	.56153E+02	-.61391E-11	-.92655E-11	.47962E-12
74	.37160E+03	.30000E+03	.65028E+02	-.63096E-11	-.34106E-11	.23803E-12
75	.44761E+03	.30000E+03	.71960E+02	-.57128E-11	-.14779E-11	-.74607E-13
76	.52318E+03	.30000E+03	.76155E+02	-.55138E-11	-.13927E-11	.14122E-12
77	.59820E+03	.30000E+03	.77590E+02	-.52296E-11	.68212E-12	.28377E-12
78	.67283E+03	.30000E+03	.76300E+02	-.42064E-11	.23022E-11	.88107E-12
79	.74962E+03	.30000E+03	.72163E+02	-.26432E-11	.33822E-11	.12115E-11
80	.82503E+03	.30000E+03	.65393E+02	-.17053E-12	.94929E-11	.18119E-11
81	.89944E+03	.30000E+03	.56208E+02	.34959E-11	.14495E-10	.15312E-11
82	.97556E+03	.30000E+03	.44448E+02	.69633E-11	.15348E-10	.75673E-12
83	.10513E+04	.30001E+03	.30716E+02	.86970E-11	.14182E-10	.33396E-12
84	.11247E+04	.30002E+03	.15959E+02	.61107E-11	.33538E-11	-.68923E-12
85	.12000E+04	.30000E+03	.00000E+00	-.80569E-12	-.66791E-11	.14778E-12
86	.00000E+00	.37500E+03	.00000E+00	.16200E-11	.98908E-11	.37659E-12
87	.71281E+02	.37508E+03	.15484E+02	.17621E-11	-.94076E-11	.13500E-11
88	.14588E+03	.37516E+03	.30871E+02	-.23874E-11	-.17025E-10	.70344E-12
89	.22529E+03	.37524E+03	.45565E+02	-.46043E-11	-.16229E-10	.28422E-12
90	.30007E+03	.37529E+03	.57285E+02	-.68496E-11	-.16598E-10	-.36948E-12
91	.37148E+03	.37532E+03	.66270E+02	-.73612E-11	-.10601E-10	-.48672E-12
92	.44753E+03	.37537E+03	.73284E+02	-.73896E-11	-.80433E-11	-.56488E-12
93	.52314E+03	.37538E+03	.77522E+02	-.74465E-11	-.75033E-11	-.53113E-12
94	.59820E+03	.37538E+03	.78972E+02	-.69349E-11	-.49738E-11	-.13500E-12
95	.67284E+03	.37538E+03	.77671E+02	-.62244E-11	-.36664E-11	.48672E-12
96	.74968E+03	.37538E+03	.73491E+02	-.46896E-11	-.19327E-11	.13305E-11
97	.82512E+03	.37535E+03	.66644E+02	-.15348E-11	.40075E-11	.18616E-11
98	.89954E+03	.37530E+03	.57342E+02	.28706E-11	.84981E-11	.17941E-11
99	.97568E+03	.37527E+03	.45401E+02	.70770E-11	.10544E-10	.14886E-11
100	.10513E+04	.37521E+03	.31439E+02	.90097E-11	.10175E-10	-.62528E-12
101	.11248E+04	.37513E+03	.16336E+02	.76739E-11	.24727E-11	-.46185E-12
102	.12000E+04	.37500E+03	.00000E+00	.66697E-12	-.57412E-11	-.31226E-12
103	.00000E+00	.45000E+03	.00000E+00	.28137E-11	.83844E-11	.83134E-12
104	.71073E+02	.45016E+03	.16631E+02	.32117E-11	-.10857E-10	.15064E-11
105	.14554E+03	.45028E+03	.33014E+02	-.13074E-11	-.19270E-10	.19185E-12
106	.22490E+03	.45041E+03	.48491E+02	-.56559E-11	-.20577E-10	-.98765E-12
107	.29967E+03	.45049E+03	.60720E+02	-.85549E-11	-.20947E-10	-.17479E-11
108	.37116E+03	.45053E+03	.70040E+02	-.11113E-10	-.16200E-10	-.22098E-11

109	.44731E+03	.45059E+03	.77282E+02	-.13216E-10	-.14012E-10	-.20535E-11
110	.52302E+03	.45062E+03	.81645E+02	-.14666E-10	-.12705E-10	-.16200E-11
111	.59820E+03	.45063E+03	.83136E+02	-.15547E-10	-.10402E-10	-.66791E-12
112	.67293E+03	.45062E+03	.81798E+02	-.15604E-10	-.81855E-11	.30376E-12
113	.74989E+03	.45059E+03	.77495E+02	-.14211E-10	-.64801E-11	.16982E-11
114	.82541E+03	.45055E+03	.70431E+02	-.10601E-10	-.19043E-11	.26930E-11
115	.89988E+03	.45050E+03	.60788E+02	-.48317E-11	.21885E-11	.27622E-11
116	.97607E+03	.45041E+03	.48320E+02	.13074E-11	.42348E-11	.17870E-11
117	.10517E+04	.45032E+03	.33605E+02	.57412E-11	.50022E-11	.42633E-12
118	.11251E+04	.45019E+03	.17524E+02	.59686E-11	.82423E-12	-.16129E-11
119	.12000E+04	.45000E+03	.00000E+00	.16548E-11	-.38654E-11	-.37170E-12
120	.00000E+00	.52500E+03	.00000E+00	.40927E-11	.49738E-11	.12861E-11
121	.70638E+02	.52517E+03	.18762E+02	-.48601E-11	-.82991E-11	-.10800E-11
122	.14486E+03	.52527E+03	.36848E+02	-.19298E-10	-.16200E-10	-.52154E-11
123	.22415E+03	.52538E+03	.53582E+02	-.32003E-10	-.17621E-10	-.79865E-11
124	.29900E+03	.52546E+03	.66613E+02	-.40558E-10	-.18701E-10	-.84270E-11
125	.37058E+03	.52548E+03	.76438E+02	-.48630E-10	-.16399E-10	-.77662E-11
126	.44689E+03	.52553E+03	.84023E+02	-.55678E-10	-.14154E-10	-.66009E-11
127	.52282E+03	.52555E+03	.88574E+02	-.58776E-10	-.13443E-10	-.43059E-11
128	.59820E+03	.52558E+03	.90128E+02	-.58066E-10	-.11624E-10	-.14069E-11
129	.67314E+03	.52557E+03	.88735E+02	-.55280E-10	-.10433E-10	.12310E-11
130	.75030E+03	.52553E+03	.84245E+02	-.48885E-10	-.96350E-11	.36664E-11
131	.82597E+03	.52550E+03	.76848E+02	-.37602E-10	-.67075E-11	.49489E-11
132	.90058E+03	.52546E+03	.66680E+02	-.24443E-10	-.41780E-11	.54605E-11
133	.97680E+03	.52539E+03	.53402E+02	-.12164E-10	-.29559E-11	.35527E-11
134	.10524E+04	.52529E+03	.37486E+02	-.18190E-11	-.13074E-11	.19185E-11
135	.11255E+04	.52519E+03	.19771E+02	.18190E-11	-.20179E-11	.29843E-12
136	.12000E+04	.52500E+03	.00000E+00	.16769E-11	-.13642E-11	-.51159E-12
137	.00000E+00	.60000E+03	.00000E+00	-.93792E-12	.11371E-11	-.25580E-12
138	.69802E+02	.60000E+03	.22397E+02	.26148E-11	.21074E-11	.66791E-12
139	.14365E+03	.60000E+03	.42832E+02	.11539E-10	.24964E-11	.26361E-11
140	.22287E+03	.60000E+03	.61153E+02	.22396E-10	.15692E-11	.44622E-11
141	.29782E+03	.60000E+03	.75154E+02	.30923E-10	.17374E-11	.49774E-11
142	.36963E+03	.60000E+03	.85601E+02	.39051E-10	.11154E-11	.46434E-11
143	.44625E+03	.60000E+03	.93600E+02	.45901E-10	.92482E-12	.37819E-11
144	.52248E+03	.60000E+03	.98375E+02	.48715E-10	.74563E-12	.20548E-11
145	.59820E+03	.60000E+03	.99999E+02	.48402E-10	-.33407E-12	.20428E-13
146	.67349E+03	.60000E+03	.98540E+02	.46242E-10	-.12841E-11	-.18812E-11
147	.75097E+03	.60000E+03	.93829E+02	.40899E-10	-.23911E-11	-.34142E-11
148	.82697E+03	.60000E+03	.86024E+02	.32657E-10	-.39641E-11	-.41425E-11
149	.90180E+03	.60000E+03	.75218E+02	.23306E-10	-.49793E-11	-.41425E-11
150	.97814E+03	.60000E+03	.60941E+02	.14211E-10	-.47012E-11	-.31193E-11
151	.10536E+04	.60000E+03	.43535E+02	.62812E-11	-.35898E-11	-.18403E-11
152	.11264E+04	.60000E+03	.23543E+02	.19043E-11	-.13358E-11	-.69633E-12
153	.12000E+04	.60000E+03	.00000E+00	.00000E+00	.00000E+00	.00000E+00

sum: .21503E-10 .11067E-09 -.54688E-11

<<< SUM OF FORCES & DISPLACEMENTS >>>

NODE	For-X	For-Y	For-Z	Dis-X	Dis-Y	Dis-Z
1	-.17853E+03	-.18327E+03	-.57285E+02	.00000E+00	.00000E+00	.00000E+00
2	-.72635E+01	-.37418E+03	.25208E+02	.00000E+00	.00000E+00	.00000E+00
3	-.97691E+01	-.39297E+03	.38878E+02	.00000E+00	.00000E+00	.00000E+00
4	-.98721E+01	-.39113E+03	.47186E+02	.00000E+00	.00000E+00	.00000E+00
5	-.82433E+01	-.36884E+03	.49503E+02	.00000E+00	.00000E+00	.00000E+00
6	-.66006E+01	-.37044E+03	.52956E+02	.00000E+00	.00000E+00	.00000E+00

7	-.47385E+01	-.37963E+03	.56493E+02	.00000E+00	.00000E+00	.00000E+00
8	-.24208E+01	-.37627E+03	.57213E+02	.00000E+00	.00000E+00	.00000E+00
9	-.72151E-01	-.37358E+03	.57198E+02	.00000E+00	.00000E+00	.00000E+00
10	.23278E+01	-.37826E+03	.57560E+02	.00000E+00	.00000E+00	.00000E+00
11	.46350E+01	-.38111E+03	.56771E+02	.00000E+00	.00000E+00	.00000E+00
12	.66661E+01	-.37635E+03	.53908E+02	.00000E+00	.00000E+00	.00000E+00
13	.84808E+01	-.37985E+03	.51015E+02	.00000E+00	.00000E+00	.00000E+00
14	.97045E+01	-.38497E+03	.46329E+02	.00000E+00	.00000E+00	.00000E+00
15	.96318E+01	-.38035E+03	.37921E+02	.00000E+00	.00000E+00	.00000E+00
16	.79730E+01	-.38082E+03	.26362E+02	.00000E+00	.00000E+00	.00000E+00
17	.17875E+03	-.19329E+03	-.57117E+02	.00000E+00	.00000E+00	.00000E+00
18	-.36264E+03	.24741E+00	-.96293E+02	.00000E+00	.00000E+00	.00000E+00
19	-.26238E-16	.26482E-16	.00000E+00	.18281E-03	-.52184E-04	-.71579E-03
20	-.42826E-17	-.16263E-18	-.39573E-17	.17738E-03	-.58404E-04	-.79353E-03
21	-.17347E-16	-.55294E-17	-.16941E-16	.31325E-03	-.13074E-03	-.16791E-02
22	.10408E-16	.81315E-18	-.12590E-16	.31679E-03	-.17279E-03	-.20516E-02
23	-.12902E-16	.12333E-17	-.27810E-16	.34234E-03	-.25065E-03	-.27622E-02
24	-.21684E-17	-.48789E-18	.59360E-17	.25860E-03	-.26221E-03	-.29388E-02
25	-.21142E-17	.65052E-18	-.87820E-17	.14876E-03	-.26442E-03	-.30053E-02
26	-.18364E-17	-.15179E-17	-.37351E-16	.35228E-04	-.30573E-03	-.33695E-02
27	.81315E-18	-.86736E-18	.94326E-17	-.76852E-04	-.27393E-03	-.30549E-02
28	.26563E-17	.21684E-17	.15585E-16	-.19004E-03	-.27461E-03	-.30320E-02
29	-.86736E-18	.10842E-17	.16263E-16	-.27924E-03	-.27503E-03	-.29550E-02
30	-.61257E-17	.11059E-16	-.22145E-16	-.26700E-03	-.20994E-03	-.23361E-02
31	.22172E-16	-.56487E-16	.10435E-16	-.19258E-03	-.14889E-03	-.16292E-02
32	.10343E-15	.65052E-16	.30629E-17	-.16659E-04	-.92253E-04	-.70829E-03
33	.29230E-15	-.27409E-15	.26780E-16	.90093E-04	-.12559E-03	-.29107E-03
34	.36229E+03	-.11455E+00	-.96094E+02	.00000E+00	.00000E+00	.00000E+00
35	-.36519E+03	.91998E-01	-.85430E+02	.00000E+00	.00000E+00	.00000E+00
36	-.46838E-16	.27756E-16	.10544E-16	.16152E-03	-.54980E-04	-.74956E-03
37	.17130E-16	.16046E-16	-.11384E-17	.33397E-03	-.82203E-04	-.17609E-02
38	-.26563E-17	-.86736E-18	.61257E-17	.51579E-03	-.16204E-03	-.31609E-02
39	.52584E-17	-.21684E-18	-.27349E-16	.52958E-03	-.21892E-03	-.39343E-02
40	.12035E-16	-.32526E-18	.15531E-16	.50107E-03	-.27773E-03	-.47342E-02
41	.54210E-18	.37947E-18	-.35562E-16	.43772E-03	-.35506E-03	-.58890E-02
42	.32526E-18	.14637E-17	-.33448E-16	.25721E-03	-.35421E-03	-.60475E-02
43	.37947E-18	.26021E-17	-.39302E-16	.64291E-04	-.37217E-03	-.62307E-02
44	-.79960E-17	-.13010E-17	-.11764E-16	-.11584E-03	-.33378E-03	-.57032E-02
45	-.27647E-17	-.15179E-17	-.16209E-16	-.26698E-03	-.30086E-03	-.51722E-02
46	.48857E-17	-.28189E-17	.77927E-18	-.34451E-03	-.26419E-03	-.43707E-02
47	-.10219E-16	.91073E-17	-.25208E-16	-.41628E-03	-.24712E-03	-.39974E-02
48	.21413E-16	.20383E-16	-.18974E-18	-.25719E-03	-.15819E-03	-.24613E-02
49	.51608E-16	.54210E-18	-.29409E-17	-.11317E-03	-.12305E-03	-.13846E-02
50	.50958E-16	-.18431E-16	-.19678E-16	-.76392E-04	-.98251E-04	-.79815E-03
51	.36502E+03	-.37128E-01	-.85379E+02	.00000E+00	.00000E+00	.00000E+00
52	-.36644E+03	.41053E-01	-.79590E+02	.00000E+00	.00000E+00	.00000E+00
53	.28623E-16	.12794E-16	-.58615E-17	.27024E-03	-.44425E-04	-.13880E-02
54	.17456E-16	.10842E-16	-.43910E-17	.40605E-03	-.51234E-04	-.23830E-02
55	.65052E-18	.00000E+00	.81451E-17	.52143E-03	-.86249E-04	-.36063E-02
56	-.62884E-17	-.17347E-17	-.26563E-17	.53691E-03	-.11809E-03	-.45624E-02
57	-.63697E-17	-.10842E-17	.27539E-16	.58092E-03	-.17775E-03	-.61537E-02
58	-.67763E-18	.00000E+00	-.24666E-17	.42430E-03	-.19016E-03	-.66169E-02
59	-.51245E-18	-.62342E-18	.16643E-16	.26106E-03	-.21659E-03	-.76145E-02
60	-.67763E-18	.75894E-18	-.47759E-16	.34902E-04	-.22612E-03	-.77760E-02
61	.00000E+00	-.43368E-18	-.16724E-16	-.18112E-03	-.20387E-03	-.72667E-02
62	.52042E-17	-.65052E-18	-.45591E-16	-.39293E-03	-.20804E-03	-.71033E-02
63	.23039E-17	-.58547E-17	-.12414E-16	-.51701E-03	-.20310E-03	-.63313E-02
64	.53668E-17	-.49873E-17	-.42013E-17	-.51074E-03	-.16905E-03	-.49874E-02
65	.35101E-17	.00000E+00	-.34315E-16	-.48131E-03	-.13277E-03	-.39308E-02
66	-.19570E-16	-.23636E-16	-.15206E-16	-.28083E-03	-.81655E-04	-.22162E-02

67	.32851E-16	-.24720E-16	.15924E-17	-.98142E-04	-.44835E-04	-.82833E-03
68	.36635E+03	-.21668E-01	-.79579E+02	.00000E+00	.00000E+00	.00000E+00
69	-.36679E+03	.19909E-01	-.77734E+02	.00000E+00	.00000E+00	.00000E+00
70	.28731E-17	-.75894E-18	-.21711E-16	.26069E-03	-.65606E-05	-.14785E-02
71	-.27105E-19	-.65052E-18	-.15206E-16	.29587E-03	.16643E-04	-.20938E-02
72	-.30629E-17	-.13010E-17	-.12739E-16	.53832E-03	.12438E-04	-.41129E-02
73	-.93377E-17	.00000E+00	-.49060E-17	.52933E-03	.16194E-04	-.49818E-02
74	-.11953E-16	.00000E+00	-.61257E-17	.54800E-03	-.10354E-05	-.64524E-02
75	.39302E-18	.10842E-18	.49060E-16	.44969E-03	.63895E-05	-.76705E-02
76	-.74539E-18	-.54210E-19	.16263E-16	.24530E-03	.10831E-04	-.81663E-02
77	.40658E-18	.00000E+00	-.33448E-16	.95374E-05	.58144E-05	-.85272E-02
78	-.47976E-17	.00000E+00	.30791E-16	-.22894E-03	.43247E-05	-.85530E-02
79	-.15179E-17	.00000E+00	.23446E-16	-.38637E-03	.31823E-05	-.71746E-02
80	.00000E+00	.00000E+00	-.10463E-16	-.48840E-03	-.22442E-04	-.60506E-02
81	-.75894E-18	-.21684E-18	.19624E-16	-.54291E-03	-.30098E-04	-.51203E-02
82	-.16805E-17	-.65052E-18	.35304E-17	-.41692E-03	-.20343E-04	-.33698E-02
83	-.13010E-17	-.13010E-17	-.55565E-17	-.34715E-03	-.81449E-05	-.23528E-02
84	-.26021E-17	.37947E-18	-.31713E-17	-.15246E-03	.22954E-05	-.96512E-03
85	.36679E+03	-.19213E-01	-.77735E+02	.00000E+00	.00000E+00	.00000E+00
86	-.36636E+03	.15348E-01	-.79581E+02	.00000E+00	.00000E+00	.00000E+00
87	-.54210E-18	-.21521E-16	.35846E-17	.12684E-03	.41191E-04	-.92711E-03
88	.10761E-16	.32851E-16	-.28243E-16	.31499E-03	.92303E-04	-.23283E-02
89	.13227E-16	.59631E-17	.71693E-17	.34246E-03	.10598E-03	-.31259E-02
90	.74539E-18	.86736E-18	.34911E-16	.54515E-03	.15824E-03	-.52346E-02
91	.49196E-17	-.39031E-17	.25397E-16	.49835E-03	.17117E-03	-.60468E-02
92	-.14908E-18	-.11926E-17	.18215E-16	.38410E-03	.20683E-03	-.69058E-02
93	.18974E-18	.86736E-18	-.10192E-16	.20555E-03	.23741E-03	-.75833E-02
94	.13010E-17	-.62342E-18	.70473E-18	-.17517E-04	.23766E-03	-.78188E-02
95	.26563E-17	.43368E-18	-.27810E-16	-.23309E-03	.21312E-03	-.73623E-02
96	.84568E-17	.10842E-17	.34261E-16	-.44128E-03	.21515E-03	-.71457E-02
97	.42284E-17	.65052E-18	.16507E-16	-.49488E-03	.14554E-03	-.55961E-02
98	-.81315E-18	.32526E-17	.18702E-17	-.50300E-03	.99728E-04	-.43611E-02
99	-.60173E-17	-.49873E-17	.16534E-17	-.47528E-03	.81837E-04	-.33104E-02
100	-.18323E-16	.13010E-16	-.15206E-16	-.41827E-03	.58623E-04	-.24437E-02
101	.20383E-16	.00000E+00	.13824E-17	-.21475E-03	.36416E-04	-.11324E-02
102	.36644E+03	-.40525E-01	-.79590E+02	.00000E+00	.00000E+00	.00000E+00
103	-.36501E+03	.35508E-01	-.85399E+02	.00000E+00	.00000E+00	.00000E+00
104	.92157E-16	-.84351E-16	-.46838E-16	.19551E-03	.10120E-03	-.12757E-02
105	-.90314E-16	-.95518E-16	.10978E-17	.15203E-03	.13476E-03	-.15196E-02
106	-.60824E-16	.12143E-16	-.73184E-18	.28665E-03	.17016E-03	-.26004E-02
107	-.61257E-17	.15396E-16	.10029E-17	.33169E-03	.19500E-03	-.34290E-02
108	.56921E-18	.30358E-17	-.28243E-16	.38112E-03	.26365E-03	-.46804E-02
109	-.90802E-18	.58547E-17	.10300E-17	.31040E-03	.33478E-03	-.55884E-02
110	-.19787E-17	-.10842E-17	.10869E-16	.14725E-03	.36688E-03	-.58872E-02
111	.10842E-17	.79960E-18	-.46621E-17	-.36901E-04	.38193E-03	-.62723E-02
112	.39031E-17	.00000E+00	-.11086E-16	-.21511E-03	.33780E-03	-.56873E-02
113	-.26021E-17	-.10842E-17	.37947E-18	-.39507E-03	.33159E-03	-.55627E-02
114	-.27105E-17	.00000E+00	-.15856E-16	-.44825E-03	.24786E-03	-.43783E-02
115	.75894E-18	-.21684E-18	.94326E-17	-.48481E-03	.19510E-03	-.36125E-02
116	-.11926E-17	-.58547E-17	.24882E-16	-.54365E-03	.17181E-03	-.32780E-02
117	-.10517E-16	-.14311E-16	-.83213E-17	-.27420E-03	.79643E-04	-.14731E-02
118	.22768E-17	-.29273E-17	.57463E-17	-.17300E-03	.46404E-04	-.80338E-03
119	.36520E+03	-.87434E-01	-.85407E+02	.00000E+00	.00000E+00	.00000E+00
120	-.36227E+03	.10651E+00	-.96186E+02	.00000E+00	.00000E+00	.00000E+00
121	-.20253E-15	.23549E-15	-.79906E-16	-.74855E-04	.11717E-03	-.29889E-03
122	-.11991E-15	-.50958E-16	.00000E+00	.13164E-03	.12862E-03	-.11791E-02
123	.32418E-16	.23094E-16	-.29111E-16	.23307E-03	.16629E-03	-.17945E-02
124	-.44994E-17	.73726E-17	.13119E-16	.22626E-03	.17555E-03	-.20206E-02
125	.00000E+00	.82399E-17	.10164E-17	.20734E-03	.19937E-03	-.23707E-02
126	-.56921E-18	-.39031E-17	.00000E+00	.18171E-03	.28367E-03	-.31334E-02

127	-.88091E-18	.32526E-18	-.57354E-16	.11109E-03	.37982E-03	-.39324E-02
128	-.18431E-17	-.43368E-18	.19976E-16	-.24581E-04	.31841E-03	-.34547E-02
129	-.21684E-18	.10842E-18	.17564E-16	-.14197E-03	.29857E-03	-.32478E-02
130	.43368E-18	-.69118E-18	.13878E-16	-.24972E-03	.27621E-03	-.30426E-02
131	.00000E+00	.37947E-17	.12251E-16	-.29743E-03	.22251E-03	-.25018E-02
132	.86736E-17	.49331E-17	.16426E-16	-.33312E-03	.18628E-03	-.21786E-02
133	-.57463E-17	-.15070E-16	.35508E-17	-.29157E-03	.12197E-03	-.15608E-02
134	.42284E-17	-.55294E-17	-.30412E-16	-.29564E-03	.10323E-03	-.13692E-02
135	.26834E-17	.24191E-17	-.12251E-16	-.15942E-04	.19610E-04	-.12051E-03
136	.36267E+03	-.25895E+00	-.96207E+02	.00000E+00	.00000E+00	.00000E+00
137	-.17869E+03	.18338E+03	-.57273E+02	.00000E+00	.00000E+00	.00000E+00
138	-.76235E+01	.37381E+03	.25091E+02	.00000E+00	.00000E+00	.00000E+00
139	-.99031E+01	.39281E+03	.38831E+02	.00000E+00	.00000E+00	.00000E+00
140	-.99146E+01	.39105E+03	.47164E+02	.00000E+00	.00000E+00	.00000E+00
141	-.82644E+01	.36881E+03	.49494E+02	.00000E+00	.00000E+00	.00000E+00
142	-.65998E+01	.37041E+03	.52954E+02	.00000E+00	.00000E+00	.00000E+00
143	-.47271E+01	.37962E+03	.56493E+02	.00000E+00	.00000E+00	.00000E+00
144	-.24050E+01	.37628E+03	.57215E+02	.00000E+00	.00000E+00	.00000E+00
145	-.51814E-01	.37358E+03	.57197E+02	.00000E+00	.00000E+00	.00000E+00
146	.23321E+01	.37826E+03	.57560E+02	.00000E+00	.00000E+00	.00000E+00
147	.46507E+01	.38112E+03	.56771E+02	.00000E+00	.00000E+00	.00000E+00
148	.66621E+01	.37636E+03	.53910E+02	.00000E+00	.00000E+00	.00000E+00
149	.84676E+01	.37988E+03	.51022E+02	.00000E+00	.00000E+00	.00000E+00
150	.96572E+01	.38505E+03	.46353E+02	.00000E+00	.00000E+00	.00000E+00
151	.95070E+01	.38051E+03	.37965E+02	.00000E+00	.00000E+00	.00000E+00
152	.75985E+01	.38121E+03	.26484E+02	.00000E+00	.00000E+00	.00000E+00
153	.17859E+03	.19318E+03	-.57126E+02	.00000E+00	.00000E+00	.00000E+00
sum:	-.20833E-10	-.11192E-09	.54143E-11			
max:				.58092E-03	.38193E-03	-.85530E-02

(((SUM OF STRESSES & STRAINES)))

ELEM	Sig-x	Sig-y	Tau-xy	Eps-x	Eps-y	Gam-xy
1	.50000E+01	.50000E+01	.00000E+00	.00000E+00	.00000E+00	.00000E+00
2	.49994E+01	.49995E+01	.29317E-04	-.20517E-06	-.96242E-07	.30456E-06
3	.49995E+01	.49997E+01	.18967E-04	-.20517E-06	-.34118E-09	.19704E-06
4	.49998E+01	.49996E+01	.19882E-04	.10623E-06	-.31068E-06	.20655E-06
5	.50003E+01	.50002E+01	.76519E-05	.10623E-06	-.12447E-09	.79492E-07
6	.50005E+01	.49997E+01	.27489E-04	.59606E-06	-.61604E-06	.28557E-06
7	.50015E+01	.50009E+01	.42413E-06	.59606E-06	-.46384E-11	.44060E-08
8	.50010E+01	.49998E+01	.49174E-04	.89029E-06	-.79684E-06	.51085E-06
9	.50022E+01	.50014E+01	-.23290E-04	.89029E-06	.67690E-10	-.24195E-06
10	.50015E+01	.50000E+01	.32671E-04	.12341E-05	-.98764E-06	.33940E-06
11	.50030E+01	.50019E+01	-.68700E-04	.12341E-05	-.42296E-09	-.71370E-06
12	.50018E+01	.49999E+01	.28380E-04	.15575E-05	-.13153E-05	.29483E-06
13	.50038E+01	.50024E+01	-.94998E-04	.15575E-05	-.11914E-08	-.98689E-06
14	.50020E+01	.49998E+01	.31336E-04	.17409E-05	-.14955E-05	.32553E-06
15	.50043E+01	.50026E+01	-.10738E-03	.17409E-05	-.22342E-08	-.11156E-05
16	.50021E+01	.49998E+01	.33982E-04	.18633E-05	-.16053E-05	.35302E-06
17	.50046E+01	.50028E+01	-.12779E-03	.18633E-05	-.39281E-08	-.13275E-05
18	.50018E+01	.49996E+01	.36800E-04	.17009E-05	-.15738E-05	.38230E-06
19	.50042E+01	.50026E+01	-.13814E-03	.17009E-05	-.52926E-08	-.14351E-05
20	.50016E+01	.49996E+01	.20647E-04	.15493E-05	-.14792E-05	.21449E-06
21	.50038E+01	.50023E+01	-.15334E-03	.15493E-05	-.75121E-08	-.15930E-05
22	.50011E+01	.49995E+01	-.11678E-05	.12256E-05	-.12654E-05	-.12131E-07
23	.50030E+01	.50018E+01	-.18593E-03	.12256E-05	-.10376E-07	-.19315E-05

24	.50006E+01	.49995E+01	-.57545E-04	.82154E-06	-.94949E-06	-.59781E-06
25	.50020E+01	.50012E+01	-.21335E-03	.82154E-06	-.12158E-07	-.22164E-05
26	.49997E+01	.49992E+01	-.10061E-03	.25622E-06	-.62131E-06	-.10451E-05
27	.50006E+01	.50004E+01	-.22882E-03	.25622E-06	-.14594E-07	-.23771E-05
28	.49985E+01	.49989E+01	-.14067E-03	-.46021E-06	-.23045E-06	-.14614E-05
29	.49989E+01	.49993E+01	-.22074E-03	-.46021E-06	-.13605E-07	-.22931E-05
30	.49964E+01	.49979E+01	-.12965E-03	-.14929E-05	.70193E-07	-.13469E-05
31	.49963E+01	.49977E+01	-.22532E-03	-.14929E-05	-.91221E-08	-.23407E-05
32	.49968E+01	.49960E+01	-.15685E-03	.00000E+00	-.20983E-05	-.16294E-05
33	.49999E+01	.49998E+01	.68697E-04	.00000E+00	-.96880E-07	.71367E-06
34	.49997E+01	.49996E+01	.79613E-04	-.26081E-07	-.18626E-06	.82706E-06
35	.49995E+01	.49994E+01	.41899E-04	-.26081E-07	-.31102E-06	.43527E-06
36	.49999E+01	.49993E+01	.37259E-04	.36048E-06	-.64225E-06	.38707E-06
37	.49999E+01	.49994E+01	.90006E-04	.36048E-06	-.61752E-06	.93504E-06
38	.50006E+01	.49993E+01	.87465E-04	.94699E-06	-.11096E-05	.90864E-06
39	.50011E+01	.49999E+01	.90382E-04	.94699E-06	-.79735E-06	.93894E-06
40	.50011E+01	.49993E+01	.11365E-03	.13753E-05	-.14729E-05	.11807E-05
41	.50019E+01	.50002E+01	.86158E-04	.13753E-05	-.98838E-06	.89506E-06
42	.50018E+01	.49994E+01	.11091E-03	.18867E-05	-.18308E-05	.11522E-05
43	.50026E+01	.50004E+01	.43268E-04	.18867E-05	-.13147E-05	.44950E-06
44	.50022E+01	.49992E+01	.94618E-04	.22957E-05	-.22563E-05	.98294E-06
45	.50034E+01	.50007E+01	-.71043E-05	.22957E-05	-.14944E-05	-.73804E-07
46	.50024E+01	.49991E+01	.64943E-04	.25372E-05	-.24985E-05	.67466E-06
47	.50038E+01	.50008E+01	-.48095E-04	.25372E-05	-.16050E-05	-.49964E-06
48	.50025E+01	.49991E+01	.35410E-04	.26514E-05	-.26144E-05	.36786E-06
49	.50041E+01	.50011E+01	-.10743E-03	.26514E-05	-.15751E-05	-.11161E-05
50	.50022E+01	.49998E+01	.14722E-05	.24522E-05	-.25357E-05	.15294E-07
51	.50038E+01	.50009E+01	-.14247E-03	.24522E-05	-.14835E-05	-.14800E-05
52	.50019E+01	.49989E+01	-.37133E-04	.22091E-05	-.23423E-05	-.38575E-06
53	.50035E+01	.50010E+01	-.15827E-03	.22091E-05	-.12715E-05	-.16442E-05
54	.50013E+01	.49989E+01	-.45755E-04	.17543E-05	-.20024E-05	-.47533E-06
55	.50028E+01	.50009E+01	-.17577E-03	.17543E-05	-.95740E-06	-.18260E-05
56	.50007E+01	.49989E+01	-.68289E-04	.12567E-05	-.15870E-05	-.70942E-06
57	.50021E+01	.50007E+01	-.18134E-03	.12567E-05	-.63031E-06	-.18839E-05
58	.49998E+01	.49987E+01	-.69495E-04	.63312E-06	-.11812E-05	-.72195E-06
59	.50012E+01	.50005E+01	-.12864E-03	.63312E-06	-.23428E-06	-.13364E-05
60	.49989E+01	.49985E+01	-.16687E-04	.68010E-07	-.83469E-06	-.17335E-06
61	.50003E+01	.50002E+01	-.12346E-04	.68010E-07	.71729E-07	-.12826E-06
62	.49996E+01	.49986E+01	.60669E-04	.57826E-06	-.11896E-05	.63026E-06
63	.49982E+01	.49969E+01	-.10645E-03	.57826E-06	-.20999E-05	-.11059E-05
64	.49979E+01	.49974E+01	-.12295E-03	.00000E+00	-.13966E-05	-.12773E-05
65	.49997E+01	.49996E+01	.72476E-04	.00000E+00	-.18534E-06	.75292E-06
66	.50000E+01	.49996E+01	.67071E-04	.27462E-06	-.41984E-06	.69677E-06
67	.49997E+01	.49992E+01	.53879E-04	.27462E-06	-.64207E-06	.55972E-06
68	.50002E+01	.49993E+01	.42132E-04	.65295E-06	-.89411E-06	.43769E-06
69	.49999E+01	.49989E+01	.10803E-03	.65295E-06	-.11083E-05	.11223E-05
70	.50010E+01	.49993E+01	.80345E-04	.12380E-05	-.13526E-05	.83467E-06
71	.50008E+01	.49991E+01	.11832E-03	.12380E-05	-.14700E-05	.12292E-05
72	.50015E+01	.49993E+01	.98965E-04	.17199E-05	-.17571E-05	.10281E-05
73	.50014E+01	.49992E+01	.12379E-03	.17199E-05	-.18284E-05	.12860E-05
74	.50023E+01	.49994E+01	.96892E-04	.22750E-05	-.21559E-05	.10066E-05
75	.50022E+01	.49992E+01	.94327E-04	.22750E-05	-.22540E-05	.97992E-06
76	.50027E+01	.49992E+01	.86383E-04	.26990E-05	-.26014E-05	.89739E-06
77	.50028E+01	.49994E+01	.59134E-04	.26990E-05	-.24971E-05	.61431E-06
78	.50029E+01	.49990E+01	.70538E-04	.29614E-05	-.28906E-05	.73278E-06
79	.50033E+01	.49996E+01	.45263E-04	.29614E-05	-.26136E-05	.47021E-06
80	.50029E+01	.49989E+01	.75757E-04	.30674E-05	-.30539E-05	.78700E-06
81	.50037E+01	.49999E+01	-.90672E-05	.30674E-05	-.25358E-05	-.94195E-07
82	.50024E+01	.49986E+01	.55141E-04	.28585E-05	-.30130E-05	.57283E-06
83	.50034E+01	.49999E+01	-.32244E-04	.28585E-05	-.23430E-05	-.33497E-06

84	.50020E+01	.49985E+01	.41956E-04	.25977E-05	-.28633E-05	.43586E-06
85	.50033E+01	.50002E+01	-.61106E-04	.25977E-05	-.20038E-05	-.63480E-06
86	.50013E+01	.49984E+01	.35618E-04	.21270E-05	-.25532E-05	.37002E-06
87	.50028E+01	.50002E+01	-.10039E-03	.21270E-05	-.15885E-05	-.10429E-05
88	.50008E+01	.49984E+01	-.18434E-05	.16430E-05	-.21395E-05	-.19150E-07
89	.50022E+01	.50003E+01	-.10668E-03	.16430E-05	-.11833E-05	-.11082E-05
90	.50001E+01	.49984E+01	-.16698E-05	.11107E-05	-.17461E-05	-.17347E-07
91	.50015E+01	.50001E+01	-.67681E-04	.11107E-05	-.83697E-06	-.70311E-06
92	.49999E+01	.49985E+01	.17060E-04	.88092E-06	-.14852E-05	.17723E-06
93	.50003E+01	.49991E+01	-.27659E-04	.88092E-06	-.11922E-05	-.28733E-06
94	.49997E+01	.49986E+01	.17733E-05	.71841E-06	-.13356E-05	.18422E-07
95	.49996E+01	.49984E+01	-.87965E-04	.71841E-06	-.13968E-05	-.91383E-06
96	.49984E+01	.49980E+01	-.56158E-04	.00000E+00	-.10400E-05	-.58340E-06
97	.49994E+01	.49992E+01	.58612E-04	.00000E+00	-.41921E-06	.60890E-06
98	.50002E+01	.49994E+01	.34873E-04	.50998E-06	-.70681E-06	.36228E-06
99	.49999E+01	.49991E+01	.37680E-04	.50998E-06	-.89341E-06	.39144E-06
100	.50004E+01	.49991E+01	.28356E-04	.86525E-06	-.11457E-05	.29458E-06
101	.50001E+01	.49988E+01	.99280E-04	.86525E-06	-.13516E-05	.10314E-05
102	.50011E+01	.49993E+01	.68419E-04	.13968E-05	-.15158E-05	.71078E-06
103	.50008E+01	.49988E+01	.10384E-03	.13968E-05	-.17551E-05	.10787E-05
104	.50017E+01	.49993E+01	.69543E-04	.18667E-05	-.18718E-05	.72245E-06
105	.50013E+01	.49988E+01	.12382E-03	.18667E-05	-.21547E-05	.12863E-05
106	.50025E+01	.49994E+01	.78928E-04	.24095E-05	-.22624E-05	.81995E-06
107	.50020E+01	.49987E+01	.82984E-04	.24095E-05	-.25995E-05	.86208E-06
108	.50028E+01	.49992E+01	.53197E-04	.28527E-05	-.27329E-05	.55264E-06
109	.50026E+01	.49989E+01	.54251E-04	.28527E-05	-.28894E-05	.56359E-06
110	.50031E+01	.49990E+01	.41672E-04	.31488E-05	-.30598E-05	.43291E-06
111	.50031E+01	.49990E+01	.42210E-04	.31488E-05	-.30531E-05	.43850E-06
112	.50031E+01	.49988E+01	.48093E-04	.32586E-05	-.32339E-05	.49962E-06
113	.50034E+01	.49993E+01	-.11768E-05	.32586E-05	-.30127E-05	-.12225E-07
114	.50027E+01	.49986E+01	.33809E-04	.30710E-05	-.31885E-05	.35122E-06
115	.50032E+01	.49993E+01	-.19063E-04	.30710E-05	-.28635E-05	-.19804E-06
116	.50023E+01	.49986E+01	.18132E-04	.28181E-05	-.30089E-05	.18836E-06
117	.50030E+01	.49995E+01	-.53838E-05	.28181E-05	-.25536E-05	-.55930E-07
118	.50017E+01	.49985E+01	.51826E-04	.23356E-05	-.26697E-05	.53839E-06
119	.50025E+01	.49995E+01	-.64608E-05	.23356E-05	-.21396E-05	-.67118E-07
120	.50012E+01	.49986E+01	.47824E-04	.18722E-05	-.22416E-05	.49682E-06
121	.50019E+01	.49995E+01	-.10668E-04	.18722E-05	-.17462E-05	-.11082E-06
122	.50006E+01	.49986E+01	.43742E-04	.13985E-05	-.18536E-05	.45441E-06
123	.50012E+01	.49993E+01	.12968E-04	.13985E-05	-.14853E-05	.13472E-06
124	.50002E+01	.49987E+01	.49619E-04	.99513E-06	-.14643E-05	.51546E-06
125	.50004E+01	.49990E+01	.18325E-04	.99513E-06	-.13351E-05	.19037E-06
126	.49999E+01	.49989E+01	.29152E-04	.63807E-06	-.11045E-05	.30285E-06
127	.50000E+01	.49990E+01	-.20255E-04	.63807E-06	-.10393E-05	-.21042E-06
128	.49990E+01	.49987E+01	.28706E-05	.00000E+00	-.66208E-06	.29821E-07
129	.49989E+01	.49987E+01	.86590E-05	.00000E+00	-.70661E-06	.89954E-07
130	.50001E+01	.49991E+01	-.30585E-04	.67283E-06	-.99866E-06	-.31773E-06
131	.49999E+01	.49989E+01	.28667E-05	.67283E-06	-.11455E-05	.29781E-07
132	.50004E+01	.49990E+01	-.11144E-04	.97743E-06	-.12962E-05	-.11576E-06
133	.50001E+01	.49986E+01	.57151E-04	.97743E-06	-.15151E-05	.59371E-06
134	.50012E+01	.49994E+01	.12559E-04	.14136E-05	-.14625E-05	.13047E-06
135	.50006E+01	.49986E+01	.64033E-04	.14136E-05	-.18711E-05	.66521E-06
136	.50020E+01	.49996E+01	.47148E-05	.18355E-05	-.16676E-05	.48980E-07
137	.50011E+01	.49985E+01	.72591E-04	.18355E-05	-.22614E-05	.75411E-06
138	.50027E+01	.49997E+01	-.91353E-06	.23755E-05	-.20541E-05	-.94902E-08
139	.50017E+01	.49984E+01	.31831E-04	.23755E-05	-.27324E-05	.33068E-06
140	.50031E+01	.49995E+01	-.31876E-04	.28376E-05	-.25227E-05	-.33115E-06
141	.50023E+01	.49985E+01	.34606E-04	.28376E-05	-.30595E-05	.35951E-06
142	.50034E+01	.49994E+01	-.14015E-04	.31453E-05	-.28549E-05	-.14560E-06
143	.50028E+01	.49987E+01	.51057E-04	.31453E-05	-.32336E-05	.53041E-06

144	.50034E+01	.49992E+01	.22494E-04	.32468E-05	-.30312E-05	.23368E-06
145	.50031E+01	.49989E+01	.52502E-04	.32468E-05	-.31887E-05	.54542E-06
146	.50029E+01	.49990E+01	.52681E-04	.30559E-05	-.29940E-05	.54727E-06
147	.50029E+01	.49990E+01	.56719E-04	.30559E-05	-.30093E-05	.58922E-06
148	.50026E+01	.49989E+01	.64817E-04	.28172E-05	-.28543E-05	.67335E-06
149	.50028E+01	.49992E+01	.80195E-04	.28172E-05	-.26704E-05	.83310E-06
150	.50018E+01	.49987E+01	.11630E-03	.23288E-05	-.25544E-05	.12082E-05
151	.50023E+01	.49993E+01	.69036E-04	.23288E-05	-.22424E-05	.71718E-06
152	.50013E+01	.49988E+01	.10438E-03	.18761E-05	-.21510E-05	.10843E-05
153	.50018E+01	.49993E+01	.52075E-04	.18761E-05	-.18541E-05	.54098E-06
154	.50007E+01	.49988E+01	.91025E-04	.13661E-05	-.17576E-05	.94562E-06
155	.50011E+01	.49993E+01	.55335E-04	.13661E-05	-.14655E-05	.57485E-06
156	.50001E+01	.49988E+01	.86659E-04	.87616E-06	-.13193E-05	.90026E-06
157	.50005E+01	.49992E+01	.35425E-04	.87616E-06	-.11046E-05	.36802E-06
158	.49998E+01	.49990E+01	.54709E-04	.44198E-06	-.86080E-06	.56835E-06
159	.50001E+01	.49994E+01	.30201E-04	.44198E-06	-.66207E-06	.31374E-06
160	.49994E+01	.49992E+01	.45551E-04	.00000E+00	-.39704E-06	.47321E-06
161	.49985E+01	.49981E+01	-.54358E-04	.00000E+00	-.99889E-06	-.56470E-06
162	.49997E+01	.49985E+01	-.90692E-04	.72560E-06	-.13738E-05	-.94216E-06
163	.49998E+01	.49986E+01	-.32718E-04	.72560E-06	-.12965E-05	-.33989E-06
164	.50003E+01	.49990E+01	-.52043E-04	.88144E-06	-.12456E-05	-.54065E-06
165	.49999E+01	.49986E+01	.28002E-04	.88144E-06	-.14622E-05	.29090E-06
166	.50014E+01	.50000E+01	-.49124E-04	.11280E-05	-.92591E-06	-.51032E-06
167	.50002E+01	.49986E+01	.59447E-05	.11280E-05	-.16676E-05	.61757E-07
168	.50021E+01	.50002E+01	-.85555E-04	.15969E-05	-.11810E-05	-.88879E-06
169	.50008E+01	.49985E+01	.14768E-04	.15969E-05	-.20540E-05	.15341E-06
170	.50029E+01	.50003E+01	-.83758E-04	.21414E-05	-.15663E-05	-.87012E-06
171	.50014E+01	.49985E+01	-.21679E-05	.21414E-05	-.25224E-05	-.22521E-07
172	.50033E+01	.50001E+01	-.93302E-04	.26272E-05	-.20464E-05	-.96927E-06
173	.50021E+01	.49986E+01	.61127E-05	.26272E-05	-.28548E-05	.63502E-07
174	.50036E+01	.50000E+01	-.69524E-04	.29481E-05	-.23757E-05	-.72226E-06
175	.50026E+01	.49987E+01	.48044E-04	.29481E-05	-.30316E-05	.49911E-06
176	.50036E+01	.49998E+01	-.57299E-05	.30448E-05	-.25501E-05	-.59526E-07
177	.50029E+01	.49990E+01	.57715E-04	.30448E-05	-.29945E-05	.59957E-06
178	.50032E+01	.49996E+01	.31168E-04	.28698E-05	-.25239E-05	.32379E-06
179	.50027E+01	.49990E+01	.75257E-04	.28698E-05	-.28556E-05	.78181E-06
180	.50028E+01	.49995E+01	.53846E-04	.26628E-05	-.24215E-05	.55938E-06
181	.50026E+01	.49992E+01	.10670E-03	.26628E-05	-.25563E-05	.11085E-05
182	.50021E+01	.49992E+01	.11597E-03	.21726E-05	-.21538E-05	.12047E-05
183	.50021E+01	.49992E+01	.11185E-03	.21726E-05	-.21533E-05	.11619E-05
184	.50015E+01	.49992E+01	.12209E-03	.17219E-05	-.17946E-05	.12683E-05
185	.50015E+01	.49993E+01	.86474E-04	.17219E-05	-.17596E-05	.89833E-06
186	.50008E+01	.49991E+01	.10587E-03	.12075E-05	-.14541E-05	.10999E-05
187	.50010E+01	.49993E+01	.79610E-04	.12075E-05	-.13193E-05	.82703E-06
188	.50000E+01	.49990E+01	.10450E-03	.66209E-06	-.10416E-05	.10856E-05
189	.50003E+01	.49994E+01	.47924E-04	.66209E-06	-.86118E-06	.49786E-06
190	.49996E+01	.49992E+01	.66465E-04	.20463E-06	-.59187E-06	.69047E-06
191	.49999E+01	.49996E+01	.59294E-04	.20463E-06	-.39694E-06	.61598E-06
192	.49997E+01	.49996E+01	.58069E-04	.00000E+00	-.18948E-06	.60325E-06
193	.49979E+01	.49974E+01	-.13345E-03	.00000E+00	-.13740E-05	-.13864E-05
194	.49984E+01	.49971E+01	-.12969E-03	.60319E-06	-.20414E-05	-.13473E-05
195	.49996E+01	.49986E+01	.35747E-04	.60319E-06	-.12430E-05	.37136E-06
196	.50002E+01	.50000E+01	-.33249E-04	.15221E-06	-.10305E-06	-.34541E-06
197	.49990E+01	.49985E+01	-.32780E-04	.15221E-06	-.92471E-06	-.34054E-06
198	.50011E+01	.50004E+01	-.13922E-03	.68225E-06	-.35111E-06	-.14463E-05
199	.49999E+01	.49988E+01	-.58217E-04	.68225E-06	-.11794E-05	-.60479E-06
200	.50021E+01	.50007E+01	-.16421E-03	.12220E-05	-.60827E-06	-.17059E-05
201	.50006E+01	.49989E+01	-.58678E-04	.12220E-05	-.15650E-05	-.60958E-06
202	.50030E+01	.50010E+01	-.17230E-03	.17772E-05	-.92583E-06	-.17899E-05
203	.50013E+01	.49988E+01	-.50722E-04	.17772E-05	-.20442E-05	-.52693E-06

204	.50035E+01	.50009E+01	-.16492E-03	.22553E-05	-.13224E-05	-.17132E-05
205	.50019E+01	.49989E+01	-.24087E-04	.22553E-05	-.23743E-05	-.25022E-06
206	.50039E+01	.50010E+01	-.13023E-03	.25643E-05	-.15593E-05	-.13529E-05
207	.50024E+01	.49991E+01	.21890E-04	.25643E-05	-.25502E-05	.22741E-06
208	.50039E+01	.50008E+01	-.67346E-04	.26358E-05	-.16705E-05	-.69963E-06
209	.50026E+01	.49992E+01	.34442E-04	.26358E-05	-.25246E-05	.35780E-06
210	.50036E+01	.50007E+01	-.33792E-04	.24699E-05	-.16175E-05	-.35105E-06
211	.50024E+01	.49992E+01	.73464E-04	.24699E-05	-.24233E-05	.76318E-06
212	.50032E+01	.50005E+01	.70402E-05	.22814E-05	-.15458E-05	.73137E-07
213	.50023E+01	.49994E+01	.85007E-04	.22814E-05	-.21553E-05	.88309E-06
214	.50024E+01	.50003E+01	.50848E-04	.18070E-05	-.13170E-05	.52824E-06
215	.50017E+01	.49993E+01	.99450E-04	.18070E-05	-.17964E-05	.10331E-05
216	.50018E+01	.50001E+01	.69201E-04	.13957E-05	-.10504E-05	.71889E-06
217	.50012E+01	.49994E+01	.10053E-03	.13957E-05	-.14564E-05	.10443E-05
218	.50010E+01	.49998E+01	.86160E-04	.91591E-06	-.84320E-06	.89507E-06
219	.50007E+01	.49994E+01	.61416E-04	.91591E-06	-.10429E-05	.63803E-06
220	.50001E+01	.49995E+01	.65196E-04	.38269E-06	-.56409E-06	.67729E-06
221	.50000E+01	.49995E+01	.52113E-04	.38269E-06	-.59304E-06	.54138E-06
222	.49994E+01	.49993E+01	.67733E-04	-.73300E-07	-.29677E-06	.70364E-06
223	.49995E+01	.49995E+01	.30154E-04	-.73300E-07	-.18928E-06	.31326E-06
224	.49997E+01	.49996E+01	.24490E-04	.00000E+00	-.20113E-06	.25442E-06
225	.49969E+01	.49961E+01	-.15432E-03	.00000E+00	-.20397E-05	-.16031E-05
226	.49966E+01	.49979E+01	-.21001E-03	-.13795E-05	-.91377E-08	-.21817E-05
227	.49965E+01	.49977E+01	-.14237E-03	-.13795E-05	-.10434E-06	-.14790E-05
228	.49989E+01	.49993E+01	-.24130E-03	-.42634E-06	-.14347E-07	-.25068E-05
229	.49984E+01	.49987E+01	-.13151E-03	-.42634E-06	-.34580E-06	-.13661E-05
230	.50006E+01	.50004E+01	-.22717E-03	.26194E-06	-.14433E-07	-.23599E-05
231	.49997E+01	.49993E+01	-.82916E-04	.26194E-06	-.59980E-06	-.86138E-06
232	.50019E+01	.50012E+01	-.18983E-03	.78808E-06	-.10750E-07	-.19721E-05
233	.50005E+01	.49995E+01	-.43662E-04	.78808E-06	-.91835E-06	-.45359E-06
234	.50031E+01	.50019E+01	-.17328E-03	.12523E-05	-.91141E-08	-.18001E-05
235	.50011E+01	.49994E+01	-.24527E-04	.12523E-05	-.13157E-05	-.25480E-06
236	.50039E+01	.50024E+01	-.18394E-03	.15955E-05	-.91379E-08	-.19109E-05
237	.50015E+01	.49995E+01	-.41854E-06	.15955E-05	-.15550E-05	-.43480E-08
238	.50045E+01	.50028E+01	-.17174E-03	.18254E-05	-.65153E-08	-.17841E-05
239	.50019E+01	.49996E+01	.35574E-04	.18254E-05	-.16694E-05	.36956E-06
240	.50045E+01	.50028E+01	-.12550E-03	.18455E-05	-.36901E-08	-.13037E-05
241	.50021E+01	.49997E+01	.40166E-04	.18455E-05	-.16182E-05	.41726E-06
242	.50042E+01	.50026E+01	-.10061E-03	.17153E-05	-.22363E-08	-.10452E-05
243	.50019E+01	.49997E+01	.53715E-04	.17153E-05	-.15477E-05	.55802E-06
244	.50038E+01	.50024E+01	-.82467E-04	.15526E-05	-.99838E-09	-.85671E-06
245	.50018E+01	.49999E+01	.40129E-04	.15526E-05	-.13180E-05	.41688E-06
246	.50029E+01	.50018E+01	-.51489E-04	.11840E-05	-.41164E-09	-.53489E-06
247	.50013E+01	.49998E+01	.50386E-04	.11840E-05	-.10511E-05	.52344E-06
248	.50022E+01	.50014E+01	-.23544E-04	.90934E-06	.40791E-10	-.24459E-06
249	.50009E+01	.49998E+01	.48836E-04	.90934E-06	-.84282E-06	.50734E-06
250	.50013E+01	.50008E+01	.31229E-06	.54324E-06	-.34084E-11	.32442E-08
251	.50005E+01	.49998E+01	.45153E-04	.54324E-06	-.56431E-06	.46907E-06
252	.50004E+01	.50002E+01	.25171E-04	.16440E-06	-.66410E-09	.26149E-06
253	.50000E+01	.49997E+01	.16800E-04	.16440E-06	-.29536E-06	.17453E-06
254	.49996E+01	.49997E+01	.21314E-04	-.17787E-06	-.38669E-09	.22142E-06
255	.49993E+01	.49993E+01	.36628E-04	-.17787E-06	-.20194E-06	.38051E-06
256	.50000E+01	.50000E+01	.00000E+00	.00000E+00	.00000E+00	.00000E+00
max:	.50046E+01	.50028E+01	-.24130E-03	.32586E-05	-.32339E-05	-.25068E-05

==== BARREL VAULT _curvature38 width6_Shape analysis =====

==== BARREL VAULT _curvature38 width6_ Stress-deformation_DOWNWARDS ==

3 1 3
3 3 1
153 256
3 1

clea tfor
clea tdis
clea tsrs
clea tsrn
nonl

100 50 0.01e-10 0 0

node

1	.00000E+00	.00000E+00	.00000E+00	0
2	.69802E+02	.00000E+00	.22397E+02	0
3	.14365E+03	.00000E+00	.42832E+02	0
4	.22287E+03	.00000E+00	.61153E+02	0
5	.29782E+03	.00000E+00	.75154E+02	0
6	.36963E+03	.00000E+00	.85601E+02	0
7	.44625E+03	.00000E+00	.93600E+02	0
8	.52248E+03	.00000E+00	.98375E+02	0
9	.59820E+03	.00000E+00	.99999E+02	0
10	.67349E+03	.00000E+00	.98540E+02	0
11	.75097E+03	.00000E+00	.93829E+02	0
12	.82697E+03	.00000E+00	.86024E+02	0
13	.90180E+03	.00000E+00	.75218E+02	0
14	.97814E+03	.00000E+00	.60941E+02	0
15	.10536E+04	.00000E+00	.43535E+02	0
16	.11264E+04	.00000E+00	.23543E+02	0
17	.12000E+04	.00000E+00	.00000E+00	0
18	.00000E+00	.75000E+02	.00000E+00	0
19	.70670E+02	.74820E+02	.18772E+02	0
20	.14491E+03	.74701E+02	.36863E+02	0
21	.22421E+03	.74608E+02	.53596E+02	0
22	.29904E+03	.74542E+02	.66620E+02	0
23	.37063E+03	.74491E+02	.76447E+02	0
24	.44694E+03	.74462E+02	.84028E+02	0
25	.52284E+03	.74441E+02	.88576E+02	0
26	.59823E+03	.74437E+02	.90126E+02	0
27	.67317E+03	.74443E+02	.88732E+02	0
28	.75034E+03	.74465E+02	.84242E+02	0
29	.82605E+03	.74495E+02	.76839E+02	0
30	.90062E+03	.74550E+02	.66672E+02	0
31	.97687E+03	.74620E+02	.53386E+02	0
32	.10524E+04	.74715E+02	.37483E+02	0
33	.11255E+04	.74819E+02	.19769E+02	0
34	.12000E+04	.75000E+02	.00000E+00	0
35	.00000E+00	.15000E+03	.00000E+00	0
36	.71101E+02	.14981E+03	.16639E+02	0
37	.14558E+03	.14968E+03	.33026E+02	0
38	.22494E+03	.14960E+03	.48500E+02	0
39	.29972E+03	.14950E+03	.60729E+02	0
40	.37120E+03	.14945E+03	.70047E+02	0
41	.44735E+03	.14941E+03	.77286E+02	0
42	.52306E+03	.14938E+03	.81647E+02	0
43	.59823E+03	.14937E+03	.83136E+02	0
44	.67297E+03	.14937E+03	.81797E+02	0
45	.74993E+03	.14941E+03	.77492E+02	0
46	.82546E+03	.14947E+03	.70423E+02	0
47	.89995E+03	.14951E+03	.60776E+02	0
48	.97611E+03	.14959E+03	.48311E+02	0

49	.10517E+04	.14970E+03	.33602E+02	0
50	.11251E+04	.14983E+03	.17522E+02	0
51	.12000E+04	.15000E+03	.00000E+00	0
52	.00000E+00	.22500E+03	.00000E+00	0
53	.71297E+02	.22488E+03	.15489E+02	0
54	.14589E+03	.22479E+03	.30875E+02	0
55	.22533E+03	.22474E+03	.45573E+02	0
56	.30008E+03	.22470E+03	.57287E+02	0
57	.37150E+03	.22465E+03	.66274E+02	0
58	.44755E+03	.22462E+03	.73286E+02	0
59	.52316E+03	.22462E+03	.77523E+02	0
60	.59823E+03	.22462E+03	.78972E+02	0
61	.67286E+03	.22462E+03	.77670E+02	0
62	.74971E+03	.22463E+03	.73488E+02	0
63	.82513E+03	.22468E+03	.66642E+02	0
64	.89955E+03	.22471E+03	.57339E+02	0
65	.97572E+03	.22476E+03	.45392E+02	0
66	.10513E+04	.22483E+03	.31437E+02	0
67	.11249E+04	.22492E+03	.16313E+02	0
68	.12000E+04	.22500E+03	.00000E+00	0
69	.00000E+00	.30000E+03	.00000E+00	0
70	.71348E+02	.29998E+03	.15122E+02	0
71	.14598E+03	.29999E+03	.30180E+02	0
72	.22545E+03	.30000E+03	.44618E+02	0
73	.30017E+03	.30000E+03	.56153E+02	0
74	.37160E+03	.30000E+03	.65028E+02	0
75	.44761E+03	.30000E+03	.71960E+02	0
76	.52318E+03	.30000E+03	.76155E+02	0
77	.59820E+03	.30000E+03	.77590E+02	0
78	.67283E+03	.30000E+03	.76300E+02	0
79	.74962E+03	.30000E+03	.72163E+02	0
80	.82503E+03	.30000E+03	.65393E+02	0
81	.89944E+03	.30000E+03	.56208E+02	0
82	.97556E+03	.30000E+03	.44448E+02	0
83	.10513E+04	.30001E+03	.30716E+02	0
84	.11247E+04	.30002E+03	.15959E+02	0
85	.12000E+04	.30000E+03	.00000E+00	0
86	.00000E+00	.37500E+03	.00000E+00	0
87	.71281E+02	.37508E+03	.15484E+02	0
88	.14588E+03	.37516E+03	.30871E+02	0
89	.22529E+03	.37524E+03	.45565E+02	0
90	.30007E+03	.37529E+03	.57285E+02	0
91	.37148E+03	.37532E+03	.66270E+02	0
92	.44753E+03	.37537E+03	.73284E+02	0
93	.52314E+03	.37538E+03	.77522E+02	0
94	.59820E+03	.37538E+03	.78972E+02	0
95	.67284E+03	.37538E+03	.77671E+02	0
96	.74968E+03	.37538E+03	.73491E+02	0
97	.82512E+03	.37535E+03	.66644E+02	0
98	.89954E+03	.37530E+03	.57342E+02	0
99	.97568E+03	.37527E+03	.45401E+02	0
100	.10513E+04	.37521E+03	.31439E+02	0
101	.11248E+04	.37513E+03	.16336E+02	0
102	.12000E+04	.37500E+03	.00000E+00	0
103	.00000E+00	.45000E+03	.00000E+00	0
104	.71073E+02	.45016E+03	.16631E+02	0
105	.14554E+03	.45028E+03	.33014E+02	0
106	.22490E+03	.45041E+03	.48491E+02	0
107	.29967E+03	.45049E+03	.60720E+02	0
108	.37116E+03	.45053E+03	.70040E+02	0

109	.44731E+03	.45059E+03	.77282E+02	0
110	.52302E+03	.45062E+03	.81645E+02	0
111	.59820E+03	.45063E+03	.83136E+02	0
112	.67293E+03	.45062E+03	.81798E+02	0
113	.74989E+03	.45059E+03	.77495E+02	0
114	.82541E+03	.45055E+03	.70431E+02	0
115	.89988E+03	.45050E+03	.60788E+02	0
116	.97607E+03	.45041E+03	.48320E+02	0
117	.10517E+04	.45032E+03	.33605E+02	0
118	.11251E+04	.45019E+03	.17524E+02	0
119	.12000E+04	.45000E+03	.00000E+00	0
120	.00000E+00	.52500E+03	.00000E+00	0
121	.70638E+02	.52517E+03	.18762E+02	0
122	.14486E+03	.52527E+03	.36848E+02	0
123	.22415E+03	.52538E+03	.53582E+02	0
124	.29900E+03	.52546E+03	.66613E+02	0
125	.37058E+03	.52548E+03	.76438E+02	0
126	.44689E+03	.52553E+03	.84023E+02	0
127	.52282E+03	.52555E+03	.88574E+02	0
128	.59820E+03	.52558E+03	.90128E+02	0
129	.67314E+03	.52557E+03	.88735E+02	0
130	.75030E+03	.52553E+03	.84245E+02	0
131	.82597E+03	.52550E+03	.76848E+02	0
132	.90058E+03	.52546E+03	.66680E+02	0
133	.97680E+03	.52539E+03	.53402E+02	0
134	.10524E+04	.52529E+03	.37486E+02	0
135	.11255E+04	.52519E+03	.19771E+02	0
136	.12000E+04	.52500E+03	.00000E+00	0
137	.00000E+00	.60000E+03	.00000E+00	0
138	.69802E+02	.60000E+03	.22397E+02	0
139	.14365E+03	.60000E+03	.42832E+02	0
140	.22287E+03	.60000E+03	.61153E+02	0
141	.29782E+03	.60000E+03	.75154E+02	0
142	.36963E+03	.60000E+03	.85601E+02	0
143	.44625E+03	.60000E+03	.93600E+02	0
144	.52248E+03	.60000E+03	.98375E+02	0
145	.59820E+03	.60000E+03	.99999E+02	0
146	.67349E+03	.60000E+03	.98540E+02	0
147	.75097E+03	.60000E+03	.93829E+02	0
148	.82697E+03	.60000E+03	.86024E+02	0
149	.90180E+03	.60000E+03	.75218E+02	0
150	.97814E+03	.60000E+03	.60941E+02	0
151	.10536E+04	.60000E+03	.43535E+02	0
152	.11264E+04	.60000E+03	.23543E+02	0
153	.12000E+04	.60000E+03	.00000E+00	0

0,/////////
elem mak3 3

1	18	1	2	1	0	0
2	2	19	18	1	0	0
3	19	2	3	1	0	0
4	3	20	19	1	0	0
5	20	3	4	1	0	0
6	4	21	20	1	0	0
7	21	4	5	1	0	0
8	5	22	21	1	0	0
9	22	5	6	1	0	0
10	6	23	22	1	0	0
11	23	6	7	1	0	0
12	7	24	23	1	0	0
13	24	7	8	1	0	0

14	8	25	24	1	0	0
15	25	8	9	1	0	0
16	9	26	25	1	0	0
17	26	9	10	1	0	0
18	10	27	26	1	0	0
19	27	10	11	1	0	0
20	11	28	27	1	0	0
21	28	11	12	1	0	0
22	12	29	28	1	0	0
23	29	12	13	1	0	0
24	13	30	29	1	0	0
25	30	13	14	1	0	0
26	14	31	30	1	0	0
27	31	14	15	1	0	0
28	15	32	31	1	0	0
29	32	15	16	1	0	0
30	16	33	32	1	0	0
31	33	16	17	1	0	0
32	17	34	33	1	0	0
33	35	18	19	1	0	0
34	19	36	35	1	0	0
35	36	19	20	1	0	0
36	20	37	36	1	0	0
37	37	20	21	1	0	0
38	21	38	37	1	0	0
39	38	21	22	1	0	0
40	22	39	38	1	0	0
41	39	22	23	1	0	0
42	23	40	39	1	0	0
43	40	23	24	1	0	0
44	24	41	40	1	0	0
45	41	24	25	1	0	0
46	25	42	41	1	0	0
47	42	25	26	1	0	0
48	26	43	42	1	0	0
49	43	26	27	1	0	0
50	27	44	43	1	0	0
51	44	27	28	1	0	0
52	28	45	44	1	0	0
53	45	28	29	1	0	0
54	29	46	45	1	0	0
55	46	29	30	1	0	0
56	30	47	46	1	0	0
57	47	30	31	1	0	0
58	31	48	47	1	0	0
59	48	31	32	1	0	0
60	32	49	48	1	0	0
61	49	32	33	1	0	0
62	33	50	49	1	0	0
63	50	33	34	1	0	0
64	34	51	50	1	0	0
65	52	35	36	1	0	0
66	36	53	52	1	0	0
67	53	36	37	1	0	0
68	37	54	53	1	0	0
69	54	37	38	1	0	0
70	38	55	54	1	0	0
71	55	38	39	1	0	0
72	39	56	55	1	0	0
73	56	39	40	1	0	0

74	40	57	56	1	0	0
75	57	40	41	1	0	0
76	41	58	57	1	0	0
77	58	41	42	1	0	0
78	42	59	58	1	0	0
79	59	42	43	1	0	0
80	43	60	59	1	0	0
81	60	43	44	1	0	0
82	44	61	60	1	0	0
83	61	44	45	1	0	0
84	45	62	61	1	0	0
85	62	45	46	1	0	0
86	46	63	62	1	0	0
87	63	46	47	1	0	0
88	47	64	63	1	0	0
89	64	47	48	1	0	0
90	48	65	64	1	0	0
91	65	48	49	1	0	0
92	49	66	65	1	0	0
93	66	49	50	1	0	0
94	50	67	66	1	0	0
95	67	50	51	1	0	0
96	51	68	67	1	0	0
97	69	52	53	1	0	0
98	53	70	69	1	0	0
99	70	53	54	1	0	0
100	54	71	70	1	0	0
101	71	54	55	1	0	0
102	55	72	71	1	0	0
103	72	55	56	1	0	0
104	56	73	72	1	0	0
105	73	56	57	1	0	0
106	57	74	73	1	0	0
107	74	57	58	1	0	0
108	58	75	74	1	0	0
109	75	58	59	1	0	0
110	59	76	75	1	0	0
111	76	59	60	1	0	0
112	60	77	76	1	0	0
113	77	60	61	1	0	0
114	61	78	77	1	0	0
115	78	61	62	1	0	0
116	62	79	78	1	0	0
117	79	62	63	1	0	0
118	63	80	79	1	0	0
119	80	63	64	1	0	0
120	64	81	80	1	0	0
121	81	64	65	1	0	0
122	65	82	81	1	0	0
123	82	65	66	1	0	0
124	66	83	82	1	0	0
125	83	66	67	1	0	0
126	67	84	83	1	0	0
127	84	67	68	1	0	0
128	68	85	84	1	0	0
129	86	69	70	1	0	0
130	70	87	86	1	0	0
131	87	70	71	1	0	0
132	71	88	87	1	0	0
133	88	71	72	1	0	0

134	72 89 88	1	0	0
135	89 72 73	1	0	0
136	73 90 89	1	0	0
137	90 73 74	1	0	0
138	74 91 90	1	0	0
139	91 74 75	1	0	0
140	75 92 91	1	0	0
141	92 75 76	1	0	0
142	76 93 92	1	0	0
143	93 76 77	1	0	0
144	77 94 93	1	0	0
145	94 77 78	1	0	0
146	78 95 94	1	0	0
147	95 78 79	1	0	0
148	79 96 95	1	0	0
149	96 79 80	1	0	0
150	80 97 96	1	0	0
151	97 80 81	1	0	0
152	81 98 97	1	0	0
153	98 81 82	1	0	0
154	82 99 98	1	0	0
155	99 82 83	1	0	0
156	83 100 99	1	0	0
157	100 83 84	1	0	0
158	84 101 100	1	0	0
159	101 84 85	1	0	0
160	85 102 101	1	0	0
161	103 86 87	1	0	0
162	87 104 103	1	0	0
163	104 87 88	1	0	0
164	88 105 104	1	0	0
165	105 88 89	1	0	0
166	89 106 105	1	0	0
167	106 89 90	1	0	0
168	90 107 106	1	0	0
169	107 90 91	1	0	0
170	91 108 107	1	0	0
171	108 91 92	1	0	0
172	92 109 108	1	0	0
173	109 92 93	1	0	0
174	93 110 109	1	0	0
175	110 93 94	1	0	0
176	94 111 110	1	0	0
177	111 94 95	1	0	0
178	95 112 111	1	0	0
179	112 95 96	1	0	0
180	96 113 112	1	0	0
181	113 96 97	1	0	0
182	97 114 113	1	0	0
183	114 97 98	1	0	0
184	98 115 114	1	0	0
185	115 98 99	1	0	0
186	99 116 115	1	0	0
187	116 99 100	1	0	0
188	100 117 116	1	0	0
189	117 100 101	1	0	0
190	101 118 117	1	0	0
191	118 101 102	1	0	0
192	102 119 118	1	0	0
193	120 103 104	1	0	0

194	104	121	120	1	0	0
195	121	104	105	1	0	0
196	105	122	121	1	0	0
197	122	105	106	1	0	0
198	106	123	122	1	0	0
199	123	106	107	1	0	0
200	107	124	123	1	0	0
201	124	107	108	1	0	0
202	108	125	124	1	0	0
203	125	108	109	1	0	0
204	109	126	125	1	0	0
205	126	109	110	1	0	0
206	110	127	126	1	0	0
207	127	110	111	1	0	0
208	111	128	127	1	0	0
209	128	111	112	1	0	0
210	112	129	128	1	0	0
211	129	112	113	1	0	0
212	113	130	129	1	0	0
213	130	113	114	1	0	0
214	114	131	130	1	0	0
215	131	114	115	1	0	0
216	115	132	131	1	0	0
217	132	115	116	1	0	0
218	116	133	132	1	0	0
219	133	116	117	1	0	0
220	117	134	133	1	0	0
221	134	117	118	1	0	0
222	118	135	134	1	0	0
223	135	118	119	1	0	0
224	119	136	135	1	0	0
225	137	120	121	1	0	0
226	121	138	137	1	0	0
227	138	121	122	1	0	0
228	122	139	138	1	0	0
229	139	122	123	1	0	0
230	123	140	139	1	0	0
231	140	123	124	1	0	0
232	124	141	140	1	0	0
233	141	124	125	1	0	0
234	125	142	141	1	0	0
235	142	125	126	1	0	0
236	126	143	142	1	0	0
237	143	126	127	1	0	0
238	127	144	143	1	0	0
239	144	127	128	1	0	0
240	128	145	144	1	0	0
241	145	128	129	1	0	0
242	129	146	145	1	0	0
243	146	129	130	1	0	0
244	130	147	146	1	0	0
245	147	130	131	1	0	0
246	131	148	147	1	0	0
247	148	131	132	1	0	0
248	132	149	148	1	0	0
249	149	132	133	1	0	0
250	133	150	149	1	0	0
251	150	133	134	1	0	0
252	134	151	150	1	0	0
253	151	134	135	1	0	0

```

254      135 152 151      1  0  0
255      152 135 136      1  0  0
256      136 153 152      1  0  0
0/////////
mate ortr
1  1.0  0.0  1230.0  950.0  0.804  0.620  96.26
0/////////
strs
1      5.0      5.0      0.0      1
256    5.0      5.0      0.0      0
0/////////
b.c.
1      1  1  1  1
18     1  1  1  0
136    1  1  1  1
153    1  1  1  0
34     1  1  1  0
35     1  1  1  0
51     1  1  1  0
52     1  1  1  0
68     1  1  1  0
69     1  1  1  0
85     1  1  1  0
86     1  1  1  0
102    1  1  1  0
103    1  1  1  0
119    1  1  1  0
120    1  1  1  0
0/////////
l.c.
1      0.0  0.0  -12.828759  0
2      0.0  0.0  -39.003405  0
3      0.0  0.0  -40.976413  0
4      0.0  0.0  -41.746564  0
5      0.0  0.0  -39.347932  0
6      0.0  0.0  -38.852821  0
7      0.0  0.0  -40.305889  0
8      0.0  0.0  -39.970300  0
9      0.0  0.0  -39.674305  0
10     0.0  0.0  -39.925463  0
11     0.0  0.0  -40.526596  0
12     0.0  0.0  -39.950715  0
13     0.0  0.0  -40.020674  0
14     0.0  0.0  -40.700737  0
15     0.0  0.0  -40.262236  0
16     0.0  0.0  -39.862924  0
17     0.0  0.0  -26.996996  0
18     0.0  0.0  -38.406077  0
19     0.0  0.0  -78.492358  0
20     0.0  0.0  -82.700150  0
21     0.0  0.0  -82.526890  0
22     0.0  0.0  -77.954091  0
23     0.0  0.0  -78.375031  0
24     0.0  0.0  -80.379247  0
25     0.0  0.0  -79.711252  0
26     0.0  0.0  -79.143544  0
27     0.0  0.0  -80.132961  0
28     0.0  0.0  -80.713548  0
29     0.0  0.0  -79.636197  0
30     0.0  0.0  -80.298245  0

```

31	0.0	0.0	-81.248007	0
32	0.0	0.0	-80.060662	0
33	0.0	0.0	-79.978188	0
34	0.0	0.0	-40.446893	0
35	0.0	0.0	-38.357453	0
36	0.0	0.0	-78.438146	0
37	0.0	0.0	-82.628596	0
38	0.0	0.0	-82.444007	0
39	0.0	0.0	-77.873691	0
40	0.0	0.0	-78.294509	0
41	0.0	0.0	-80.286950	0
42	0.0	0.0	-79.622553	0
43	0.0	0.0	-79.057505	0
44	0.0	0.0	-80.055972	0
45	0.0	0.0	-80.625550	0
46	0.0	0.0	-79.551417	0
47	0.0	0.0	-80.217444	0
48	0.0	0.0	-81.163812	0
49	0.0	0.0	-80.002453	0
50	0.0	0.0	-79.939779	0
51	0.0	0.0	-40.389671	0
52	0.0	0.0	-38.328311	0
53	0.0	0.0	-78.389686	0
54	0.0	0.0	-82.587731	0
55	0.0	0.0	-82.409948	0
56	0.0	0.0	-77.820734	0
57	0.0	0.0	-78.242351	0
58	0.0	0.0	-80.241498	0
59	0.0	0.0	-79.582354	0
60	0.0	0.0	-79.013140	0
61	0.0	0.0	-80.007468	0
62	0.0	0.0	-80.552987	0
63	0.0	0.0	-79.489793	0
64	0.0	0.0	-80.164962	0
65	0.0	0.0	-81.093893	0
66	0.0	0.0	-80.002789	0
67	0.0	0.0	-79.862943	0
68	0.0	0.0	-40.386297	0
69	0.0	0.0	-38.311708	0
70	0.0	0.0	-78.374065	0
71	0.0	0.0	-82.590901	0
72	0.0	0.0	-82.379181	0
73	0.0	0.0	-77.810892	0
74	0.0	0.0	-78.226056	0
75	0.0	0.0	-80.224369	0
76	0.0	0.0	-79.556472	0
77	0.0	0.0	-78.997751	0
78	0.0	0.0	-79.986993	0
79	0.0	0.0	-80.539029	0
80	0.0	0.0	-79.486312	0
81	0.0	0.0	-80.139454	0
82	0.0	0.0	-81.112661	0
83	0.0	0.0	-79.955797	0
84	0.0	0.0	-79.835373	0
85	0.0	0.0	-40.427280	0
86	0.0	0.0	-38.310613	0
87	0.0	0.0	-78.383833	0
88	0.0	0.0	-82.583867	0
89	0.0	0.0	-82.392520	0
90	0.0	0.0	-77.832885	0

91	0.0	0.0	-78.229484	0
92	0.0	0.0	-80.242020	0
93	0.0	0.0	-79.571850	0
94	0.0	0.0	-79.020166	0
95	0.0	0.0	-79.997005	0
96	0.0	0.0	-80.564715	0
97	0.0	0.0	-79.497255	0
98	0.0	0.0	-80.154539	0
99	0.0	0.0	-81.127220	0
100	0.0	0.0	-79.939634	0
101	0.0	0.0	-79.905360	0
102	0.0	0.0	-40.407921	0
103	0.0	0.0	-38.327741	0
104	0.0	0.0	-78.426380	0
105	0.0	0.0	-82.626505	0
106	0.0	0.0	-82.447128	0
107	0.0	0.0	-77.885246	0
108	0.0	0.0	-78.291288	0
109	0.0	0.0	-80.292908	0
110	0.0	0.0	-79.629786	0
111	0.0	0.0	-79.065675	0
112	0.0	0.0	-80.047330	0
113	0.0	0.0	-80.608753	0
114	0.0	0.0	-79.535601	0
115	0.0	0.0	-80.211482	0
116	0.0	0.0	-81.171978	0
117	0.0	0.0	-80.034133	0
118	0.0	0.0	-79.901886	0
119	0.0	0.0	-40.417893	0
120	0.0	0.0	-38.361290	0
121	0.0	0.0	-78.493906	0
122	0.0	0.0	-82.698321	0
123	0.0	0.0	-82.532580	0
124	0.0	0.0	-77.962428	0
125	0.0	0.0	-78.371314	0
126	0.0	0.0	-80.393037	0
127	0.0	0.0	-79.721998	0
128	0.0	0.0	-79.141305	0
129	0.0	0.0	-80.131223	0
130	0.0	0.0	-80.691961	0
131	0.0	0.0	-79.630350	0
132	0.0	0.0	-80.297737	0
133	0.0	0.0	-81.269625	0
134	0.0	0.0	-80.086868	0
135	0.0	0.0	-79.950069	0
136	0.0	0.0	-40.484327	0
137	0.0	0.0	-25.605719	0
138	0.0	0.0	-39.575692	0
139	0.0	0.0	-41.814299	0
140	0.0	0.0	-40.879582	0
141	0.0	0.0	-38.713364	0
142	0.0	0.0	-39.645998	0
143	0.0	0.0	-40.206444	0
144	0.0	0.0	-39.860258	0
145	0.0	0.0	-39.587130	0
146	0.0	0.0	-40.330077	0
147	0.0	0.0	-40.302911	0
148	0.0	0.0	-39.809608	0
149	0.0	0.0	-40.375121	0
150	0.0	0.0	-40.657414	0

```
151      0.0    0.0   -39.897922    0
152      0.0    0.0   -40.191393    0
153      0.0    0.0   -13.522907    0
0,,,,,,,,,
end
```


===== DATA FOR NONLINEAR ANALYSIS =====

Total Step = 100
Total Iteration = 50
Error = .10000E-11
Modification On/Off = 0 (Off for 0)
Determinant On/Off = 0 (On for 1)

Control Node = 0
Control DOF = 0
Displacement = .00000E+00

===== DATA FOR INITIAL IMPERFECTION =====

Imperfection = .00000E+00
Mode Number = 0

===== DATA FOR SEMI-RIGID FACTOR =====

Semi-Rigid = .10000E+01

49	.10494E+04	.14897E+03	.19777E+02	-.16371E-10	.16030E-10	.32543E-11
50	.11234E+04	.14949E+03	.74513E+01	-.96065E-11	.13301E-10	.19540E-11
51	.12000E+04	.15000E+03	.00000E+00	-.63149E-12	-.10061E-10	.47384E-12
52	.00000E+00	.22500E+03	.00000E+00	-.19895E-12	.12562E-10	-.49383E-12
53	.72928E+02	.22463E+03	.37601E+01	-.90949E-12	-.62528E-11	-.17764E-12
54	.14830E+03	.22429E+03	.13760E+02	-.67075E-11	-.82991E-11	-.24869E-13
55	.22771E+03	.22410E+03	.26737E+02	-.11653E-10	-.79581E-11	-.45475E-12
56	.30208E+03	.22401E+03	.38241E+02	-.13699E-10	-.71623E-11	-.15987E-12
57	.37304E+03	.22393E+03	.47427E+02	-.14609E-10	-.43201E-11	-.92726E-12
58	.44858E+03	.22389E+03	.54707E+02	-.15859E-10	-.36380E-11	-.71054E-12
59	.52368E+03	.22389E+03	.59128E+02	-.14893E-10	.56843E-12	-.51159E-12
60	.59826E+03	.22388E+03	.60641E+02	-.15461E-10	.27285E-11	-.44764E-12
61	.67239E+03	.22389E+03	.59279E+02	-.14722E-10	.52296E-11	.71054E-13
62	.74873E+03	.22391E+03	.54912E+02	-.12562E-10	.75033E-11	.66791E-12
63	.82363E+03	.22398E+03	.47802E+02	-.10573E-10	.77307E-11	.49738E-12
64	.89756E+03	.22405E+03	.38293E+02	-.61391E-11	.11482E-10	.13074E-11
65	.97333E+03	.22419E+03	.26564E+02	-.47180E-11	.88676E-11	.44054E-12
66	.10489E+04	.22442E+03	.14259E+02	-.13074E-11	.88676E-11	.22737E-12
67	.11232E+04	.22475E+03	.42298E+01	.48317E-11	.38654E-11	.29132E-12
68	.12000E+04	.22500E+03	.00000E+00	-.49938E-12	-.10914E-10	.15241E-12
69	.00000E+00	.30000E+03	.00000E+00	.85265E-12	.12847E-10	-.12967E-12
70	.72956E+02	.29994E+03	.28084E+01	.00000E+00	-.57412E-11	.54001E-12
71	.14841E+03	.29994E+03	.11992E+02	-.40359E-11	-.71623E-11	.19895E-12
72	.22788E+03	.29996E+03	.24489E+02	-.44906E-11	-.73896E-11	.14211E-12
73	.30223E+03	.29998E+03	.35771E+02	-.51728E-11	-.70486E-11	-.22027E-12
74	.37318E+03	.29999E+03	.44859E+02	-.50591E-11	-.56843E-11	-.49738E-13
75	.44866E+03	.29999E+03	.52094E+02	-.34674E-11	-.30695E-11	-.37659E-12
76	.52370E+03	.30000E+03	.56498E+02	-.38085E-11	-.19327E-11	-.15277E-12
77	.59821E+03	.30000E+03	.58008E+02	-.22737E-11	-.56843E-12	-.88818E-13
78	.67233E+03	.30000E+03	.56651E+02	-.17053E-12	.11369E-11	.22382E-12
79	.74858E+03	.30001E+03	.52305E+02	.60212E-12	.25011E-11	.46185E-12
80	.82347E+03	.30001E+03	.45237E+02	.26148E-11	.59117E-11	.94857E-12
81	.89738E+03	.30002E+03	.35817E+02	.28990E-11	.61391E-11	.81712E-12
82	.97311E+03	.30004E+03	.24306E+02	.56275E-11	.76170E-11	.69633E-12
83	.10488E+04	.30006E+03	.12430E+02	.67075E-11	.59117E-11	.13500E-12
84	.11230E+04	.30006E+03	.32257E+01	.52864E-11	.37517E-11	-.26645E-12
85	.12000E+04	.30000E+03	.00000E+00	-.47962E-13	-.11170E-10	-.14977E-12
86	.00000E+00	.37500E+03	.00000E+00	.85265E-12	.11795E-10	.21494E-12
87	.72915E+02	.37524E+03	.37705E+01	.59686E-12	-.55138E-11	.10090E-11
88	.14829E+03	.37556E+03	.13784E+02	.15916E-11	-.10232E-10	.62528E-12
89	.22766E+03	.37581E+03	.26752E+02	.26148E-11	-.10914E-10	.56843E-13
90	.30206E+03	.37595E+03	.38248E+02	.38654E-11	-.10573E-10	-.22737E-12
91	.37299E+03	.37602E+03	.47418E+02	.55707E-11	-.70486E-11	-.25580E-12
92	.44853E+03	.37609E+03	.54701E+02	.64233E-11	-.65938E-11	-.19895E-12
93	.52363E+03	.37611E+03	.59125E+02	.79581E-11	-.53433E-11	-.41211E-12
94	.59819E+03	.37612E+03	.60641E+02	.82991E-11	-.44338E-11	-.38369E-12
95	.67234E+03	.37611E+03	.59281E+02	.87539E-11	-.56843E-12	-.31264E-12
96	.74866E+03	.37611E+03	.54920E+02	.10061E-10	.11369E-11	.00000E+00
97	.82359E+03	.37607E+03	.47808E+02	.84128E-11	.42064E-11	-.17053E-12
98	.89753E+03	.37600E+03	.38287E+02	.10061E-10	.77307E-11	.80291E-12
99	.97329E+03	.37591E+03	.26553E+02	.89813E-11	.77307E-11	.63949E-13
100	.10489E+04	.37572E+03	.14231E+02	.80718E-11	.90949E-11	.85265E-13
101	.11231E+04	.37539E+03	.42223E+01	.55138E-11	.57980E-11	-.10942E-11
102	.12000E+04	.37500E+03	.00000E+00	.26290E-12	-.10914E-10	-.43587E-12
103	.00000E+00	.45000E+03	.00000E+00	.88107E-12	.99192E-11	.54712E-12
104	.72718E+02	.45048E+03	.68334E+01	.10175E-10	-.14211E-10	.20464E-11
105	.14779E+03	.45100E+03	.19246E+02	.16712E-10	-.17849E-10	.19327E-11
106	.22702E+03	.45137E+03	.33552E+02	.25864E-10	-.20577E-10	.19611E-11
107	.30141E+03	.45157E+03	.45637E+02	.30241E-10	-.18076E-10	.10232E-11
108	.37247E+03	.45167E+03	.55079E+02	.35527E-10	-.16939E-10	.11084E-11

109	.44816E+03	.45176E+03	.62503E+02	.40473E-10	-.14893E-10	.85265E-13
110	.52343E+03	.45180E+03	.66991E+02	.41553E-10	-.92086E-11	-.42633E-13
111	.59817E+03	.45182E+03	.68528E+02	.40188E-10	-.39790E-11	-.45475E-12
112	.67248E+03	.45180E+03	.67153E+02	.37517E-10	.68212E-12	-.72475E-12
113	.74899E+03	.45176E+03	.62732E+02	.33481E-10	.55707E-11	-.86686E-12
114	.82406E+03	.45170E+03	.55491E+02	.30411E-10	.11596E-10	.88107E-12
115	.89810E+03	.45161E+03	.45698E+02	.22681E-10	.12619E-10	.17764E-12
116	.97391E+03	.45142E+03	.33349E+02	.17621E-10	.15916E-10	.71765E-12
117	.10494E+04	.45114E+03	.19731E+02	.11198E-10	.13074E-10	-.37659E-12
118	.11234E+04	.45063E+03	.73747E+01	.77307E-11	.75602E-11	-.18048E-11
119	.12000E+04	.45000E+03	.00000E+00	.42455E-11	-.83276E-11	-.10156E-11
120	.00000E+00	.52500E+03	.00000E+00	.10886E-10	.56843E-11	.28137E-11
121	.72008E+02	.52552E+03	.12591E+02	-.15575E-10	-.26148E-11	-.33111E-11
122	.14651E+03	.52598E+03	.28716E+02	-.53262E-10	-.62528E-11	-.15575E-10
123	.22560E+03	.52627E+03	.44958E+02	-.98339E-10	-.75033E-11	-.25153E-10
124	.30015E+03	.52644E+03	.57933E+02	-.12921E-09	-.10800E-10	-.25977E-10
125	.37143E+03	.52650E+03	.67802E+02	-.15660E-09	-.12847E-10	-.25665E-10
126	.44744E+03	.52657E+03	.75465E+02	-.18554E-09	-.11028E-10	-.20435E-10
127	.52308E+03	.52660E+03	.80067E+02	-.19662E-09	-.10459E-10	-.12875E-10
128	.59818E+03	.52663E+03	.81643E+02	-.19605E-09	-.98908E-11	-.34959E-11
129	.67284E+03	.52662E+03	.80235E+02	-.18707E-09	-.60254E-11	.65654E-11
130	.74970E+03	.52657E+03	.75700E+02	-.16888E-09	-.72760E-11	.13941E-10
131	.82507E+03	.52652E+03	.68237E+02	-.14120E-09	-.88676E-11	.16371E-10
132	.89937E+03	.52644E+03	.58011E+02	-.10999E-09	-.72760E-11	.18588E-10
133	.97529E+03	.52630E+03	.44783E+02	-.76227E-10	-.75033E-11	.16939E-10
134	.10507E+04	.52606E+03	.29312E+02	-.43258E-10	-.32969E-11	.11539E-10
135	.11241E+04	.52565E+03	.13299E+02	-.12108E-10	.43769E-11	.29274E-11
136	.12000E+04	.52500E+03	.00000E+00	.93792E-11	-.22737E-12	-.10871E-11
137	.00000E+00	.60000E+03	.00000E+00	.22737E-11	-.44196E-11	-.22737E-12
138	.69802E+02	.60000E+03	.22397E+02	.13245E-10	.29772E-11	.25864E-11
139	.14365E+03	.60000E+03	.42832E+02	.33538E-10	.11763E-10	.95213E-11
140	.22287E+03	.60000E+03	.61153E+02	.61391E-10	.15714E-10	.15831E-10
141	.29782E+03	.60000E+03	.75154E+02	.82309E-10	.15918E-10	.16840E-10
142	.36963E+03	.60000E+03	.85601E+02	.99476E-10	.14630E-10	.15859E-10
143	.44625E+03	.60000E+03	.93600E+02	.11835E-09	.11578E-10	.12811E-10
144	.52248E+03	.60000E+03	.98375E+02	.12653E-09	.57971E-11	.73328E-11
145	.59820E+03	.60000E+03	.99999E+02	.12676E-09	-.27711E-12	.79758E-12
146	.67349E+03	.60000E+03	.98540E+02	.12233E-09	-.69429E-11	-.57625E-11
147	.75097E+03	.60000E+03	.93829E+02	.11175E-09	-.10176E-10	-.10751E-10
148	.82697E+03	.60000E+03	.86024E+02	.94133E-10	-.13034E-10	-.13031E-10
149	.90180E+03	.60000E+03	.75218E+02	.74920E-10	-.14245E-10	-.14111E-10
150	.97814E+03	.60000E+03	.60941E+02	.53660E-10	-.12307E-10	-.12548E-10
151	.10536E+04	.60000E+03	.43535E+02	.32003E-10	-.11166E-10	-.90097E-11
152	.11264E+04	.60000E+03	.23543E+02	.10857E-10	-.56275E-11	-.31477E-11
153	.12000E+04	.60000E+03	.00000E+00	.00000E+00	.00000E+00	.00000E+00
sum:				-.13390E-10	.43866E-11	-.41110E-10

<<< SUM OF FORCES & DISPLACEMENTS >>>

NODE	For-X	For-Y	For-Z	Dis-X	Dis-Y	Dis-Z
1	-.17853E+03	-.18327E+03	-.57285E+02	.00000E+00	.00000E+00	.00000E+00
2	-.14073E+03	-.76556E+03	.78931E+02	.00000E+00	.00000E+00	.00000E+00
3	-.19684E+03	-.12573E+04	.21884E+03	.00000E+00	.00000E+00	.00000E+00
4	-.13405E+03	-.14448E+04	.32313E+03	.00000E+00	.00000E+00	.00000E+00
5	-.67706E+02	-.14242E+04	.35364E+03	.00000E+00	.00000E+00	.00000E+00
6	-.35440E+02	-.14570E+04	.37760E+03	.00000E+00	.00000E+00	.00000E+00

7	-.23262E+02	-.14992E+04	.39601E+03	.00000E+00	.00000E+00	.00000E+00
8	-.94213E+01	-.14889E+04	.39699E+03	.00000E+00	.00000E+00	.00000E+00
9	-.43341E-01	-.14787E+04	.39527E+03	.00000E+00	.00000E+00	.00000E+00
10	.86165E+01	-.14988E+04	.39965E+03	.00000E+00	.00000E+00	.00000E+00
11	.15422E+02	-.15066E+04	.39877E+03	.00000E+00	.00000E+00	.00000E+00
12	.25884E+02	-.14810E+04	.38574E+03	.00000E+00	.00000E+00	.00000E+00
13	.39129E+02	-.14734E+04	.37201E+03	.00000E+00	.00000E+00	.00000E+00
14	.57371E+02	-.14223E+04	.33663E+03	.00000E+00	.00000E+00	.00000E+00
15	.89522E+02	-.12266E+04	.24777E+03	.00000E+00	.00000E+00	.00000E+00
16	.14090E+03	-.84348E+03	.97858E+02	.00000E+00	.00000E+00	.00000E+00
17	.33426E+03	-.17520E+03	-.11264E+03	.00000E+00	.00000E+00	.00000E+00
18	-.49193E+03	.10647E+02	-.83566E+02	.00000E+00	.00000E+00	.00000E+00
19	.00000E+00	.00000E+00	-.78492E+02	.13943E+01	-.44046E+00	-.63457E+01
20	.00000E+00	.00000E+00	-.82700E+02	.16755E+01	-.76309E+00	-.81509E+01
21	.00000E+00	.00000E+00	-.82527E+02	.14996E+01	-.90919E+00	-.86116E+01
22	.00000E+00	.00000E+00	-.77954E+02	.12092E+01	-.98069E+00	-.86666E+01
23	.00000E+00	.00000E+00	-.78375E+02	.91258E+00	-.10205E+01	-.86112E+01
24	.00000E+00	.00000E+00	-.80379E+02	.60625E+00	-.10393E+01	-.85467E+01
25	.00000E+00	.00000E+00	-.79711E+02	.31433E+00	-.10497E+01	-.85011E+01
26	.00000E+00	.00000E+00	-.79144E+02	.32695E-01	-.10541E+01	-.84872E+01
27	.00000E+00	.00000E+00	-.80133E+02	-.24568E+00	-.10536E+01	-.85033E+01
28	.00000E+00	.00000E+00	-.80714E+02	-.54007E+00	-.10439E+01	-.85567E+01
29	.00000E+00	.00000E+00	-.79636E+02	-.84246E+00	-.10233E+01	-.86274E+01
30	.00000E+00	.00000E+00	-.80298E+02	-.11522E+01	-.98215E+00	-.86854E+01
31	.00000E+00	.00000E+00	-.81248E+02	-.14577E+01	-.89386E+00	-.86339E+01
32	.00000E+00	.00000E+00	-.80061E+02	-.16451E+01	-.71359E+00	-.81503E+01
33	.00000E+00	.00000E+00	-.79978E+02	-.14005E+01	-.37055E+00	-.62997E+01
34	.56087E+03	.16209E+02	-.10244E+03	.00000E+00	.00000E+00	.00000E+00
35	-.61123E+03	.75124E+01	-.58943E+02	.00000E+00	.00000E+00	.00000E+00
36	.00000E+00	.00000E+00	-.78438E+02	.16451E+01	-.41346E+00	-.98726E+01
37	.00000E+00	.00000E+00	-.82629E+02	.22563E+01	-.80849E+00	-.13816E+02
38	.00000E+00	.00000E+00	-.82444E+02	.21442E+01	-.10101E+01	-.14962E+02
39	.00000E+00	.00000E+00	-.77874E+02	.17773E+01	-.11032E+01	-.15085E+02
40	.00000E+00	.00000E+00	-.78295E+02	.13606E+01	-.11514E+01	-.14945E+02
41	.00000E+00	.00000E+00	-.80287E+02	.90994E+00	-.11713E+01	-.14769E+02
42	.00000E+00	.00000E+00	-.79623E+02	.47037E+00	-.11819E+01	-.14649E+02
43	.00000E+00	.00000E+00	-.79058E+02	.40414E-01	-.11861E+01	-.14608E+02
44	.00000E+00	.00000E+00	-.80056E+02	-.38775E+00	-.11847E+01	-.14648E+02
45	.00000E+00	.00000E+00	-.80626E+02	-.83794E+00	-.11710E+01	-.14775E+02
46	.00000E+00	.00000E+00	-.79551E+02	-.12923E+01	-.11428E+01	-.14951E+02
47	.00000E+00	.00000E+00	-.80217E+02	-.17398E+01	-.10851E+01	-.15090E+02
48	.00000E+00	.00000E+00	-.81164E+02	-.21347E+01	-.96192E+00	-.14954E+02
49	.00000E+00	.00000E+00	-.80002E+02	-.22628E+01	-.72547E+00	-.13825E+02
50	.00000E+00	.00000E+00	-.79940E+02	-.17017E+01	-.34329E+00	-.10071E+02
51	.62919E+03	.13764E+02	-.62142E+02	.00000E+00	.00000E+00	.00000E+00
52	-.67317E+03	.92022E+00	-.35716E+02	.00000E+00	.00000E+00	.00000E+00
53	.00000E+00	.00000E+00	-.78390E+02	.16305E+01	-.24790E+00	-.11729E+02
54	.00000E+00	.00000E+00	-.82588E+02	.24100E+01	-.50220E+00	-.17115E+02
55	.00000E+00	.00000E+00	-.82410E+02	.23807E+01	-.63607E+00	-.18836E+02
56	.00000E+00	.00000E+00	-.77821E+02	.20039E+01	-.69377E+00	-.19046E+02
57	.00000E+00	.00000E+00	-.78242E+02	.15421E+01	-.72230E+00	-.18847E+02
58	.00000E+00	.00000E+00	-.80241E+02	.10297E+01	-.73045E+00	-.18579E+02
59	.00000E+00	.00000E+00	-.79582E+02	.52471E+00	-.73424E+00	-.18395E+02
60	.00000E+00	.00000E+00	-.79013E+02	.28468E-01	-.73545E+00	-.18331E+02
61	.00000E+00	.00000E+00	-.80007E+02	-.46578E+00	-.73382E+00	-.18391E+02
62	.00000E+00	.00000E+00	-.80553E+02	-.98258E+00	-.72222E+00	-.18576E+02
63	.00000E+00	.00000E+00	-.79490E+02	-.14978E+01	-.70031E+00	-.18840E+02
64	.00000E+00	.00000E+00	-.80165E+02	-.19909E+01	-.65674E+00	-.19046E+02
65	.00000E+00	.00000E+00	-.81094E+02	-.23893E+01	-.56677E+00	-.18828E+02
66	.00000E+00	.00000E+00	-.80003E+02	-.24288E+01	-.40793E+00	-.17178E+02

67	.00000E+00	.00000E+00	-.79863E+02	-.17014E+01	-.17474E+00	-.12083E+02
68	.67775E+03	.10630E+02	-.37403E+02	.00000E+00	.00000E+00	.00000E+00
69	-.69519E+03	-.61783E+01	-.26911E+02	.00000E+00	.00000E+00	.00000E+00
70	.00000E+00	.00000E+00	-.78374E+02	.16075E+01	-.41235E-01	-.12314E+02
71	.00000E+00	.00000E+00	-.82591E+02	.24338E+01	-.51045E-01	-.18188E+02
72	.00000E+00	.00000E+00	-.82379E+02	.24347E+01	-.36498E-01	-.20129E+02
73	.00000E+00	.00000E+00	-.77811E+02	.20565E+01	-.21683E-01	-.20382E+02
74	.00000E+00	.00000E+00	-.78226E+02	.15801E+01	-.14818E-01	-.20169E+02
75	.00000E+00	.00000E+00	-.80224E+02	.10482E+01	-.57366E-02	-.19866E+02
76	.00000E+00	.00000E+00	-.79556E+02	.52390E+00	-.16396E-02	-.19657E+02
77	.00000E+00	.00000E+00	-.78998E+02	.91756E-02	-.16325E-04	-.19582E+02
78	.00000E+00	.00000E+00	-.79987E+02	-.50282E+00	.43217E-03	-.19649E+02
79	.00000E+00	.00000E+00	-.80539E+02	-.10355E+01	.61107E-02	-.19858E+02
80	.00000E+00	.00000E+00	-.79486E+02	-.15634E+01	.12802E-01	-.20156E+02
81	.00000E+00	.00000E+00	-.80139E+02	-.20621E+01	.22745E-01	-.20391E+02
82	.00000E+00	.00000E+00	-.81113E+02	-.24496E+01	.38971E-01	-.20142E+02
83	.00000E+00	.00000E+00	-.79956E+02	-.24519E+01	.50182E-01	-.18286E+02
84	.00000E+00	.00000E+00	-.79835E+02	-.16795E+01	.42539E-01	-.12733E+02
85	.69422E+03	.69131E+01	-.29251E+02	.00000E+00	.00000E+00	.00000E+00
86	-.67899E+03	-.10590E+02	-.35172E+02	.00000E+00	.00000E+00	.00000E+00
87	.00000E+00	.00000E+00	-.78384E+02	.16345E+01	.16293E+00	-.11713E+02
88	.00000E+00	.00000E+00	-.82584E+02	.24134E+01	.40090E+00	-.17087E+02
89	.00000E+00	.00000E+00	-.82393E+02	.23749E+01	.56851E+00	-.18813E+02
90	.00000E+00	.00000E+00	-.77833E+02	.19858E+01	.65698E+00	-.19037E+02
91	.00000E+00	.00000E+00	-.78229E+02	.15148E+01	.69755E+00	-.18852E+02
92	.00000E+00	.00000E+00	-.80242E+02	.99522E+00	.72205E+00	-.18583E+02
93	.00000E+00	.00000E+00	-.79572E+02	.48633E+00	.73253E+00	-.18397E+02
94	.00000E+00	.00000E+00	-.79020E+02	-.11095E-01	.73547E+00	-.18331E+02
95	.00000E+00	.00000E+00	-.79997E+02	-.50443E+00	.73337E+00	-.18390E+02
96	.00000E+00	.00000E+00	-.80565E+02	-.10173E+01	.73137E+00	-.18571E+02
97	.00000E+00	.00000E+00	-.79497E+02	-.15259E+01	.72107E+00	-.18036E+02
98	.00000E+00	.00000E+00	-.80155E+02	-.20092E+01	.69576E+00	-.19055E+02
99	.00000E+00	.00000E+00	-.81127E+02	-.23947E+01	.63915E+00	-.18848E+02
100	.00000E+00	.00000E+00	-.79940E+02	-.24257E+01	.50739E+00	-.17208E+02
101	.00000E+00	.00000E+00	-.79905E+02	-.16993E+01	.26214E+00	-.12114E+02
102	.67133E+03	-.30795E+00	-.37938E+02	.00000E+00	.00000E+00	.00000E+00
103	-.63041E+03	-.14474E+02	-.60124E+02	.00000E+00	.00000E+00	.00000E+00
104	.00000E+00	.00000E+00	-.78426E+02	.16448E+01	.32253E+00	-.97976E+01
105	.00000E+00	.00000E+00	-.82627E+02	.22538E+01	.71531E+00	-.13768E+02
106	.00000E+00	.00000E+00	-.82447E+02	.21207E+01	.96302E+00	-.14939E+02
107	.00000E+00	.00000E+00	-.77885E+02	.17352E+01	.10848E+01	-.15083E+02
108	.00000E+00	.00000E+00	-.78291E+02	.13078E+01	.11396E+01	-.14961E+02
109	.00000E+00	.00000E+00	-.80293E+02	.84912E+00	.11706E+01	-.14779E+02
110	.00000E+00	.00000E+00	-.79630E+02	.40594E+00	.11836E+01	-.14654E+02
111	.00000E+00	.00000E+00	-.79066E+02	-.25076E-01	.11862E+01	-.14608E+02
112	.00000E+00	.00000E+00	-.80047E+02	-.45248E+00	.11814E+01	-.14645E+02
113	.00000E+00	.00000E+00	-.80609E+02	-.89900E+00	.11725E+01	-.14763E+02
114	.00000E+00	.00000E+00	-.79536E+02	-.13461E+01	.11508E+01	-.14940E+02
115	.00000E+00	.00000E+00	-.80211E+02	-.17813E+01	.11055E+01	-.15090E+02
116	.00000E+00	.00000E+00	-.81172E+02	-.21570E+01	.10139E+01	-.14971E+02
117	.00000E+00	.00000E+00	-.80034E+02	-.22662E+01	.81621E+00	-.13874E+02
118	.00000E+00	.00000E+00	-.79902E+02	-.17024E+01	.43532E+00	-.10149E+02
119	.60967E+03	-.66767E+01	-.60816E+02	.00000E+00	.00000E+00	.00000E+00
120	-.56065E+03	-.16643E+02	-.10082E+03	.00000E+00	.00000E+00	.00000E+00
121	.00000E+00	.00000E+00	-.78494E+02	.13696E+01	.35207E+00	-.61708E+01
122	.00000E+00	.00000E+00	-.82698E+02	.16452E+01	.70571E+00	-.81316E+01
123	.00000E+00	.00000E+00	-.82533E+02	.14471E+01	.89475E+00	-.86236E+01
124	.00000E+00	.00000E+00	-.77962E+02	.11496E+01	.98148E+00	-.86795E+01
125	.00000E+00	.00000E+00	-.78371E+02	.85379E+00	.10211E+01	-.86356E+01
126	.00000E+00	.00000E+00	-.80393E+02	.54740E+00	.10439E+01	-.85583E+01

127	.00000E+00	.00000E+00	-.79722E+02	.25769E+00	.10529E+01	-.85069E+01
128	.00000E+00	.00000E+00	-.79141E+02	-.22768E-01	.10542E+01	-.84854E+01
129	.00000E+00	.00000E+00	-.80131E+02	-.30252E+00	.10495E+01	-.84997E+01
130	.00000E+00	.00000E+00	-.80692E+02	-.59893E+00	.10403E+01	-.85445E+01
131	.00000E+00	.00000E+00	-.79630E+02	-.90247E+00	.10202E+01	-.86115E+01
132	.00000E+00	.00000E+00	-.80298E+02	-.12124E+01	.98276E+00	-.86694E+01
133	.00000E+00	.00000E+00	-.81270E+02	-.15088E+01	.91281E+00	-.86190E+01
134	.00000E+00	.00000E+00	-.80087E+02	-.16765E+01	.76806E+00	-.81736E+01
135	.00000E+00	.00000E+00	-.79950E+02	-.14254E+01	.45886E+00	-.64723E+01
136	.49147E+03	-.13993E+02	-.84786E+02	.00000E+00	.00000E+00	.00000E+00
137	-.32585E+03	.16911E+03	-.11009E+03	.00000E+00	.00000E+00	.00000E+00
138	-.14605E+03	.79840E+03	.85482E+02	.00000E+00	.00000E+00	.00000E+00
139	-.90684E+02	.12566E+04	.25263E+03	.00000E+00	.00000E+00	.00000E+00
140	-.57277E+02	.14503E+04	.34357E+03	.00000E+00	.00000E+00	.00000E+00
141	-.39939E+02	.14307E+04	.36070E+03	.00000E+00	.00000E+00	.00000E+00
142	-.24068E+02	.14553E+04	.37898E+03	.00000E+00	.00000E+00	.00000E+00
143	-.16288E+02	.15018E+04	.39727E+03	.00000E+00	.00000E+00	.00000E+00
144	-.80550E+01	.14901E+04	.39728E+03	.00000E+00	.00000E+00	.00000E+00
145	-.74762E+00	.14795E+04	.39546E+03	.00000E+00	.00000E+00	.00000E+00
146	.10132E+02	.14959E+04	.39899E+03	.00000E+00	.00000E+00	.00000E+00
147	.21218E+02	.15066E+04	.39824E+03	.00000E+00	.00000E+00	.00000E+00
148	.37806E+02	.14793E+04	.38356E+03	.00000E+00	.00000E+00	.00000E+00
149	.71736E+02	.14680E+04	.36430E+03	.00000E+00	.00000E+00	.00000E+00
150	.12672E+03	.14193E+04	.31838E+03	.00000E+00	.00000E+00	.00000E+00
151	.19111E+03	.12258E+04	.21546E+03	.00000E+00	.00000E+00	.00000E+00
152	.15363E+03	.80893E+03	.85229E+02	.00000E+00	.00000E+00	.00000E+00
153	.17859E+03	.19318E+03	-.57126E+02	.00000E+00	.00000E+00	.00000E+00
sum:	.13330E-10	.47180E-11	.40842E-10			
max:				-.24519E+01	.11862E+01	-.20391E+02

(((SUM OF STRESSES & STRAINES)))

ELEM	Sig-x	Sig-y	Tau-xy	Eps-x	Eps-y	Gam-xy
1	.50000E+01	.50000E+01	.00000E+00	.00000E+00	.00000E+00	.00000E+00
2	.10641E+02	.86329E+01	-.23214E+00	.22156E-02	.13652E-03	-.24116E-02
3	.10405E+02	.83388E+01	.44557E+00	.22156E-02	-.18701E-04	.46288E-02
4	.14810E+02	.94382E+01	.33846E+00	.50788E-02	-.17403E-02	.35161E-02
5	.17444E+02	.12720E+02	.25869E+00	.50788E-02	-.78385E-05	.26874E-02
6	.16357E+02	.89004E+01	.44827E+00	.66881E-02	-.33182E-02	.46568E-02
7	.21399E+02	.15181E+02	.13519E+00	.66881E-02	-.23165E-05	.14044E-02
8	.16799E+02	.85948E+01	.45168E+00	.72470E-02	-.39288E-02	.46923E-02
9	.22773E+02	.16036E+02	.64613E-01	.72470E-02	-.41192E-06	.67123E-03
10	.16961E+02	.86316E+01	.41140E+00	.73543E-02	-.39957E-02	.42738E-02
11	.23037E+02	.16200E+02	-.16097E-01	.73543E-02	-.10543E-06	-.16723E-03
12	.17219E+02	.88643E+01	.34989E+00	.74121E-02	-.39193E-02	.36349E-02
13	.23176E+02	.16286E+02	-.87777E-01	.74121E-02	-.15173E-05	-.91187E-03
14	.17339E+02	.90364E+01	.27238E+00	.73974E-02	-.38166E-02	.28296E-02
15	.23135E+02	.16257E+02	-.16428E+00	.73974E-02	-.49043E-05	-.17066E-02
16	.17401E+02	.91439E+01	.18685E+00	.73773E-02	-.37438E-02	.19411E-02
17	.23077E+02	.16215E+02	-.24554E+00	.73773E-02	-.10888E-04	-.25508E-02
18	.17389E+02	.91610E+01	.10051E+00	.73571E-02	-.37185E-02	.10441E-02
19	.23014E+02	.16168E+02	-.33803E+00	.73571E-02	-.19272E-04	-.35116E-02
20	.17383E+02	.91094E+01	.19650E-01	.73853E-02	-.37683E-02	.20414E-03
21	.23066E+02	.16190E+02	-.42037E+00	.73853E-02	-.30402E-04	-.43670E-02
22	.17208E+02	.89018E+01	-.56010E-01	.73784E-02	-.38724E-02	-.58187E-03
23	.23033E+02	.16158E+02	-.49864E+00	.73784E-02	-.41650E-04	-.51802E-02

24	.16771E+02	.85269E+01	-.11895E+00	.72680E-02	-.39816E-02	-.12357E-02
25	.22746E+02	.15971E+02	-.58106E+00	.72680E-02	-.51813E-04	-.60364E-02
26	.15832E+02	.79148E+01	-.16273E+00	.69043E-02	-.40122E-02	-.16906E-02
27	.21834E+02	.15391E+02	-.65250E+00	.69043E-02	-.65213E-04	-.67785E-02
28	.13670E+02	.69078E+01	-.20087E+00	.58035E-02	-.36589E-02	-.20867E-02
29	.19122E+02	.13700E+02	-.72132E+00	.58035E-02	-.73071E-04	-.74934E-02
30	.93971E+01	.55242E+01	-.26314E+00	.32328E-02	-.23224E-02	-.27336E-02
31	.12837E+02	.98092E+01	-.74605E+00	.32328E-02	-.60287E-04	-.77504E-02
32	.51588E+01	.51979E+01	-.46286E+00	.00000E+00	.10446E-03	-.48085E-02
33	.51487E+01	.51852E+01	.57997E+00	.00000E+00	.97763E-04	.60250E-02
34	.12734E+02	.10315E+02	.25832E+00	.28185E-02	.54002E-03	.26836E-02
35	.91760E+01	.58835E+01	.98588E+00	.28185E-02	-.17997E-02	.10242E-01
36	.17143E+02	.10689E+02	.67808E+00	.61598E-02	-.19492E-02	.70443E-02
37	.15007E+02	.80281E+01	.86846E+00	.61598E-02	-.33539E-02	.90220E-02
38	.18494E+02	.95331E+01	.76545E+00	.80123E-02	-.40488E-02	.79519E-02
39	.18659E+02	.97383E+01	.65653E+00	.80123E-02	-.39405E-02	.68203E-02
40	.18628E+02	.86040E+01	.69239E+00	.87278E-02	-.51145E-02	.71929E-02
41	.20336E+02	.10731E+02	.45938E+00	.87278E-02	-.39917E-02	.47722E-02
42	.18550E+02	.81562E+01	.56905E+00	.89564E-02	-.55347E-02	.59116E-02
43	.21027E+02	.11242E+02	.26810E+00	.89564E-02	-.39058E-02	.27852E-02
44	.18501E+02	.79837E+01	.42430E+00	.90295E-02	-.56846E-02	.44079E-02
45	.21361E+02	.11546E+02	.11344E+00	.90295E-02	-.38039E-02	.11784E-02
46	.18461E+02	.79225E+01	.28774E+00	.90363E-02	-.57224E-02	.29892E-02
47	.21479E+02	.11682E+02	-.25169E-01	.90363E-02	-.37375E-02	-.26147E-03
48	.18452E+02	.79126E+01	.15460E+00	.90359E-02	-.57272E-02	.16061E-02
49	.21504E+02	.11714E+02	-.15460E+00	.90359E-02	-.37204E-02	-.16060E-02
50	.18480E+02	.79238E+01	.25723E-01	.90511E-02	-.57336E-02	.26722E-03
51	.21447E+02	.11620E+02	-.29161E+00	.90511E-02	-.37821E-02	-.30294E-02
52	.18553E+02	.79497E+01	-.11227E+00	.90934E-02	-.57539E-02	-.11664E-02
53	.21373E+02	.11463E+02	-.42822E+00	.90934E-02	-.38991E-02	-.44486E-02
54	.18547E+02	.79365E+01	-.25805E+00	.90976E-02	-.57643E-02	-.26808E-02
55	.21191E+02	.11229E+02	-.57849E+00	.90976E-02	-.40259E-02	-.60096E-02
56	.18311E+02	.78501E+01	-.41216E+00	.89619E-02	-.57008E-02	-.42817E-02
57	.20770E+02	.10913E+02	-.75327E+00	.89619E-02	-.40838E-02	-.78253E-02
58	.17369E+02	.75749E+01	-.58013E+00	.83755E-02	-.53746E-02	-.60267E-02
59	.19836E+02	.10649E+02	-.93809E+00	.83755E-02	-.37519E-02	-.97454E-02
60	.14702E+02	.68653E+01	-.72269E+00	.66702E-02	-.43781E-02	-.75077E-02
61	.17671E+02	.10565E+02	-.10603E+01	.66702E-02	-.24252E-02	-.11015E-01
62	.94445E+01	.57103E+01	-.75086E+00	.31499E-02	-.21575E-02	-.78003E-02
63	.12829E+02	.99263E+01	-.67672E+00	.31499E-02	.68183E-04	-.70301E-02
64	.58103E+01	.60094E+01	-.42963E+00	.00000E+00	.53289E-03	-.44632E-02
65	.57944E+01	.59897E+01	.54510E+00	.00000E+00	.52246E-03	.56627E-02
66	.13415E+02	.11066E+02	.22448E+00	.28828E-02	.88467E-03	.23320E-02
67	.90996E+01	.56898E+01	.82475E+00	.28828E-02	-.19536E-02	.85679E-02
68	.17758E+02	.11278E+02	.47677E+00	.62756E-02	-.17314E-02	.49530E-02
69	.14262E+02	.69224E+01	.75086E+00	.62756E-02	-.40307E-02	.78003E-02
70	.19120E+02	.99194E+01	.57025E+00	.82693E-02	-.40515E-02	.59240E-02
71	.17546E+02	.79584E+01	.60140E+00	.82693E-02	-.50867E-02	.62476E-02
72	.19300E+02	.87566E+01	.53862E+00	.91740E-02	-.53927E-02	.55955E-02
73	.19119E+02	.85318E+01	.44720E+00	.91740E-02	-.55114E-02	.46458E-02
74	.19258E+02	.80997E+01	.45198E+00	.95688E-02	-.60569E-02	.46955E-02
75	.19851E+02	.88383E+01	.28741E+00	.95688E-02	-.56670E-02	.29857E-02
76	.19177E+02	.77374E+01	.33447E+00	.97393E-02	-.63853E-02	.34746E-02
77	.20201E+02	.90129E+01	.15603E+00	.97393E-02	-.57120E-02	.16209E-02
78	.19110E+02	.75443E+01	.22329E+00	.98112E-02	-.65450E-02	.23197E-02
79	.20361E+02	.91020E+01	.37346E-01	.98112E-02	-.57227E-02	.38797E-03
80	.19079E+02	.74589E+01	.11372E+00	.98414E-02	-.66143E-02	.11814E-02
81	.20417E+02	.91259E+01	-.74332E-01	.98414E-02	-.57343E-02	-.77220E-03
82	.19082E+02	.74484E+01	.33819E-02	.98509E-02	-.66275E-02	.35133E-04
83	.20402E+02	.90923E+01	-.19673E+00	.98509E-02	-.57597E-02	-.20438E-02

84	.19095E+02	.74900E+01	-.11985E+00	.98341E-02	-.65921E-02	-.12450E-02
85	.20339E+02	.90406E+01	-.32191E+00	.98341E-02	-.57735E-02	-.33442E-02
86	.19022E+02	.75529E+01	-.25075E+00	.97336E-02	-.64781E-02	-.26049E-02
87	.20192E+02	.90104E+01	-.46453E+00	.97336E-02	-.57086E-02	-.48258E-02
88	.18655E+02	.75825E+01	-.39143E+00	.94159E-02	-.62070E-02	-.40664E-02
89	.19901E+02	.91356E+01	-.63016E+00	.94159E-02	-.53871E-02	-.65465E-02
90	.17452E+02	.74318E+01	-.53154E+00	.85369E-02	-.55799E-02	-.55219E-02
91	.19249E+02	.96704E+01	-.78441E+00	.85369E-02	-.43981E-02	-.81489E-02
92	.14498E+02	.68971E+01	-.61403E+00	.64836E-02	-.42113E-02	-.63789E-02
93	.17609E+02	.10773E+02	-.83477E+00	.64836E-02	-.21654E-02	-.86721E-02
94	.96281E+01	.61257E+01	-.53413E+00	.30279E-02	-.18402E-02	-.55488E-02
95	.13224E+02	.10606E+02	-.46863E+00	.30279E-02	.52478E-03	-.48684E-02
96	.63157E+01	.66390E+01	-.21885E+00	.00000E+00	.86526E-03	-.22735E-02
97	.63405E+01	.66699E+01	.32709E+00	.00000E+00	.88158E-03	.33979E-02
98	.13503E+02	.11278E+02	.31673E-01	.28159E-02	.10501E-02	.32904E-03
99	.92905E+01	.60301E+01	.41424E+00	.28159E-02	-.17202E-02	.43034E-02
100	.17819E+02	.11450E+02	.76603E-01	.62125E-02	-.15896E-02	.79579E-03
101	.14112E+02	.68317E+01	.32896E+00	.62125E-02	-.40279E-02	.34174E-02
102	.19243E+02	.10032E+02	.13860E+00	.82955E-02	-.40131E-02	.14399E-02
103	.17185E+02	.74688E+01	.25152E+00	.82955E-02	-.53663E-02	.26129E-02
104	.19500E+02	.88087E+01	.16164E+00	.93026E-02	-.54687E-02	.16792E-02
105	.18637E+02	.77337E+01	.19103E+00	.93026E-02	-.60362E-02	.19845E-02
106	.19532E+02	.81177E+01	.15847E+00	.97800E-02	-.62173E-02	.16463E-02
107	.19298E+02	.78256E+01	.12764E+00	.97800E-02	-.63715E-02	.13260E-02
108	.19511E+02	.77477E+01	.12514E+00	.10004E-01	-.65927E-02	.13000E-02
109	.19593E+02	.78501E+01	.80768E-01	.10004E-01	-.65387E-02	.83906E-03
110	.19471E+02	.75433E+01	.92056E-01	.10105E-01	-.67819E-02	.95632E-03
111	.19729E+02	.78643E+01	.36161E-01	.10105E-01	-.66124E-02	.37566E-03
112	.19435E+02	.74446E+01	.53877E-01	.10140E-01	-.68624E-02	.55970E-03
113	.19792E+02	.78895E+01	-.85668E-02	.10140E-01	-.66275E-02	-.88996E-04
114	.19394E+02	.74165E+01	.14939E-01	.10126E-01	-.60653E-02	.15519E-03
115	.19810E+02	.79345E+01	-.61441E-01	.10126E-01	-.65919E-02	-.63828E-03
116	.19328E+02	.74484E+01	-.38166E-01	.10051E-01	-.67882E-02	-.39649E-03
117	.19805E+02	.80425E+01	-.11883E+00	.10051E-01	-.64745E-02	-.12345E-02
118	.19131E+02	.75000E+01	-.88506E-01	.98566E-02	-.66049E-02	-.91945E-03
119	.19747E+02	.82677E+01	-.18824E+00	.98566E-02	-.61997E-02	-.19556E-02
120	.18594E+02	.75239E+01	-.14252E+00	.94051E-02	-.62293E-02	-.14806E-02
121	.19605E+02	.87830E+01	-.27685E+00	.94051E-02	-.55646E-02	-.28761E-02
122	.17236E+02	.73940E+01	-.19169E+00	.83858E-02	-.54784E-02	-.19913E-02
123	.19185E+02	.98221E+01	-.36356E+00	.83858E-02	-.41965E-02	-.37769E-02
124	.14331E+02	.69365E+01	-.17845E+00	.63222E-02	-.40607E-02	-.18538E-02
125	.17714E+02	.11151E+02	-.39203E+00	.63222E-02	-.18359E-02	-.40726E-02
126	.96843E+01	.62907E+01	-.84852E-01	.29660E-02	-.17033E-02	-.88149E-03
127	.13596E+02	.11163E+02	-.21611E+00	.29660E-02	.86895E-03	-.22451E-02
128	.64705E+01	.68319E+01	.53225E-01	.00000E+00	.96710E-03	.55293E-03
129	.65967E+01	.69891E+01	.54447E-01	.00000E+00	.10501E-02	.56562E-03
130	.13278E+02	.11045E+02	-.21221E+00	.27847E-02	.95263E-03	-.22045E-02
131	.94128E+01	.62303E+01	-.77609E-01	.27847E-02	-.15894E-02	-.80625E-03
132	.17694E+02	.11262E+02	-.39385E+00	.62335E-02	-.17059E-02	-.40915E-02
133	.14184E+02	.68900E+01	-.18688E+00	.62335E-02	-.40140E-02	-.19414E-02
134	.19232E+02	.98934E+01	-.36605E+00	.83772E-02	-.41520E-02	-.38027E-02
135	.17233E+02	.74026E+01	-.19065E+00	.83772E-02	-.54669E-02	-.19806E-02
136	.19588E+02	.87782E+01	-.27670E+00	.93942E-02	-.55584E-02	-.28745E-02
137	.18587E+02	.75314E+01	-.13996E+00	.93942E-02	-.62166E-02	-.14540E-02
138	.19739E+02	.82743E+01	-.18861E+00	.98460E-02	-.61876E-02	-.19594E-02
139	.19125E+02	.75098E+01	-.95104E-01	.98460E-02	-.65912E-02	-.98799E-03
140	.19802E+02	.80499E+01	-.12406E+00	.10044E-01	-.64653E-02	-.12888E-02
141	.19323E+02	.74524E+01	-.38731E-01	.10044E-01	-.67807E-02	-.40236E-03
142	.19812E+02	.79381E+01	-.62772E-01	.10125E-01	-.65893E-02	-.65211E-03
143	.19398E+02	.74219E+01	.10490E-01	.10125E-01	-.68618E-02	.10897E-03

144	.19792E+02	.78887E+01	-.11150E-01	.10141E-01	-.66284E-02	-.11583E-03
145	.19432E+02	.74393E+01	.54443E-01	.10141E-01	-.68656E-02	.56559E-03
146	.19734E+02	.78655E+01	.34770E-01	.10109E-01	-.66148E-02	.36121E-03
147	.19469E+02	.75348E+01	.87896E-01	.10109E-01	-.67894E-02	.91311E-03
148	.19601E+02	.78492E+01	.76063E-01	.10011E-01	-.65450E-02	.79018E-03
149	.19508E+02	.77331E+01	.12617E+00	.10011E-01	-.66063E-02	.13107E-02
150	.19307E+02	.78210E+01	.12803E+00	.97903E-02	-.63822E-02	.13300E-02
151	.19537E+02	.81087E+01	.15403E+00	.97903E-02	-.62303E-02	.16001E-02
152	.18648E+02	.77294E+01	.18450E+00	.93150E-02	-.60484E-02	.19167E-02
153	.19513E+02	.88064E+01	.16076E+00	.93150E-02	-.54798E-02	.16701E-02
154	.17191E+02	.74658E+01	.24848E+00	.83023E-02	-.53733E-02	.25813E-02
155	.19192E+02	.99585E+01	.14024E+00	.83023E-02	-.40574E-02	.14569E-02
156	.14259E+02	.68818E+01	.32966E+00	.62993E-02	-.40713E-02	.34247E-02
157	.17855E+02	.11362E+02	.74922E-01	.62993E-02	-.17060E-02	.77833E-03
158	.95505E+01	.60810E+01	.41111E+00	.29941E-02	-.18366E-02	.42708E-02
159	.13814E+02	.11392E+02	.29197E-01	.29941E-02	.96734E-03	.30332E-03
160	.62093E+01	.65064E+01	.32794E+00	.00000E+00	.79526E-03	.34069E-02
161	.64489E+01	.68050E+01	-.21498E+00	.00000E+00	.95288E-03	-.22333E-02
162	.12886E+02	.10481E+02	-.46291E+00	.28345E-02	.61448E-03	-.48090E-02
163	.93458E+01	.60705E+01	-.52893E+00	.28345E-02	-.17138E-02	-.54948E-02
164	.17570E+02	.10858E+02	-.83206E+00	.63966E-02	-.20503E-02	-.86438E-02
165	.14344E+02	.68390E+01	-.61805E+00	.63966E-02	-.41720E-02	-.64206E-02
166	.19307E+02	.97465E+01	-.78760E+00	.85342E-02	-.43558E-02	-.81820E-02
167	.17456E+02	.74402E+01	-.53062E+00	.85342E-02	-.55733E-02	-.55124E-02
168	.19889E+02	.91345E+01	-.62988E+00	.94063E-02	-.53800E-02	-.65435E-02
169	.18648E+02	.75892E+01	-.39253E+00	.94063E-02	-.61958E-02	-.40778E-02
170	.20186E+02	.90174E+01	-.46465E+00	.97245E-02	-.56977E-02	-.48271E-02
171	.19013E+02	.75556E+01	-.25935E+00	.97245E-02	-.64694E-02	-.26942E-02
172	.20337E+02	.90400E+01	-.33135E+00	.98321E-02	-.57723E-02	-.34422E-02
173	.19093E+02	.74914E+01	-.12529E+00	.98321E-02	-.65898E-02	-.13015E-02
174	.20405E+02	.90943E+01	-.20140E+00	.98527E-02	-.57601E-02	-.20922E-02
175	.19085E+02	.74497E+01	-.51445E-02	.98527E-02	-.66283E-02	-.53444E-04
176	.20417E+02	.91244E+01	-.82800E-01	.98425E-02	-.57360E-02	-.86017E-03
177	.19078E+02	.74566E+01	.10815E+00	.98425E-02	-.66164E-02	.11235E-02
178	.20368E+02	.91049E+01	.31544E-01	.98152E-02	-.57244E-02	.32769E-03
179	.19111E+02	.75388E+01	.21519E+00	.98152E-02	-.65512E-02	.22355E-02
180	.20207E+02	.90141E+01	.14700E+00	.97437E-02	-.57149E-02	.15271E-02
181	.19173E+02	.77258E+01	.33227E+00	.97437E-02	-.63949E-02	.34518E-02
182	.19868E+02	.88455E+01	.28404E+00	.95779E-02	-.56705E-02	.29507E-02
183	.19261E+02	.80896E+01	.44466E+00	.95779E-02	-.60696E-02	.46193E-02
184	.19130E+02	.85295E+01	.43556E+00	.91845E-02	-.55211E-02	.45248E-02
185	.19313E+02	.87574E+01	.53591E+00	.91845E-02	-.54008E-02	.55674E-02
186	.17549E+02	.79510E+01	.59783E+00	.82767E-02	-.50966E-02	.62106E-02
187	.19079E+02	.98561E+01	.57260E+00	.82767E-02	-.40909E-02	.59484E-02
188	.14407E+02	.69853E+01	.75699E+00	.63523E-02	-.40592E-02	.78640E-02
189	.17773E+02	.11179E+02	.48428E+00	.63523E-02	-.18453E-02	.50309E-02
190	.93739E+01	.57657E+01	.82584E+00	.30563E-02	-.20530E-02	.85793E-02
191	.13714E+02	.11173E+02	.22122E+00	.30563E-02	.80147E-03	.22982E-02
192	.56708E+01	.58357E+01	.54486E+00	.00000E+00	.44117E-03	.56603E-02
193	.59442E+01	.61763E+01	-.42536E+00	.00000E+00	.62097E-03	-.44189E-02
194	.12467E+02	.97768E+01	-.67097E+00	.29532E-02	.14736E-03	-.69704E-02
195	.91548E+01	.56508E+01	-.75547E+00	.29532E-02	-.20308E-02	-.78483E-02
196	.17599E+02	.10604E+02	-.10652E+01	.65855E-02	-.23363E-02	-.11066E-01
197	.14556E+02	.68141E+01	-.73057E+00	.65855E-02	-.43370E-02	-.75896E-02
198	.19867E+02	.10683E+02	-.94674E+00	.83783E-02	-.37361E-02	-.98352E-02
199	.17385E+02	.75905E+01	-.58120E+00	.83783E-02	-.53686E-02	-.60378E-02
200	.20760E+02	.10924E+02	-.75287E+00	.89470E-02	-.40661E-02	-.78212E-02
201	.18291E+02	.78485E+01	-.41786E+00	.89470E-02	-.56897E-02	-.43409E-02
202	.21197E+02	.11235E+02	-.57872E+00	.90990E-02	-.40243E-02	-.60121E-02
203	.18552E+02	.79407E+01	-.26857E+00	.90990E-02	-.57632E-02	-.27900E-02

204	.21359E+02	.11443E+02	-.43972E+00	.90951E-02	-.39113E-02	-.45681E-02
205	.18556E+02	.79514E+01	-.12043E+00	.90951E-02	-.57544E-02	-.12511E-02
206	.21457E+02	.11626E+02	-.29648E+00	.90552E-02	-.37826E-02	-.30800E-02
207	.18488E+02	.79280E+01	.16144E-01	.90552E-02	-.57347E-02	.16771E-03
208	.21499E+02	.11706E+02	-.16468E+00	.90369E-02	-.37253E-02	-.17108E-02
209	.18453E+02	.79120E+01	.14704E+00	.90369E-02	-.57284E-02	.15275E-02
210	.21493E+02	.11693E+02	-.32591E-01	.90408E-02	-.37353E-02	-.33858E-03
211	.18467E+02	.79238E+01	.27860E+00	.90408E-02	-.57252E-02	.28942E-02
212	.21359E+02	.11547E+02	.10183E+00	.90278E-02	-.38024E-02	.10579E-02
213	.18493E+02	.79763E+01	.41979E+00	.90278E-02	-.56871E-02	.43610E-02
214	.21064E+02	.11269E+02	.26264E+00	.89689E-02	-.39015E-02	.27285E-02
215	.18567E+02	.81582E+01	.56143E+00	.89689E-02	-.55438E-02	.58324E-02
216	.20336E+02	.10723E+02	.44687E+00	.87333E-02	-.40002E-02	.46423E-02
217	.18630E+02	.85972E+01	.69087E+00	.87333E-02	-.51226E-02	.71771E-02
218	.18642E+02	.97324E+01	.65137E+00	.80027E-02	-.39359E-02	.67668E-02
219	.18415E+02	.94494E+01	.76438E+00	.80027E-02	-.40853E-02	.79408E-02
220	.15170E+02	.81174E+01	.86886E+00	.62338E-02	-.33662E-02	.90262E-02
221	.17160E+02	.10597E+02	.68117E+00	.62338E-02	-.20574E-02	.70764E-02
222	.94748E+01	.59786E+01	.98133E+00	.29994E-02	-.18949E-02	.10195E-01
223	.13051E+02	.10434E+02	.24783E+00	.29994E-02	.45702E-03	.25746E-02
224	.50491E+01	.50612E+01	.57321E+00	.00000E+00	.32286E-04	.59548E-02
225	.52690E+01	.53351E+01	-.46377E+00	.00000E+00	.17689E-03	-.48179E-02
226	.12428E+02	.95540E+01	-.74079E+00	.30672E-02	-.61909E-04	-.76957E-02
227	.91269E+01	.54412E+01	-.27415E+00	.30672E-02	-.22331E-02	-.28480E-02
228	.19019E+02	.13636E+02	-.73569E+00	.57617E-02	-.73444E-04	-.76428E-02
229	.13599E+02	.68832E+01	-.20504E+00	.57617E-02	-.36382E-02	-.21301E-02
230	.21782E+02	.15358E+02	-.66906E+00	.68846E-02	-.67286E-04	-.69505E-02
231	.15812E+02	.79197E+01	-.17045E+00	.68846E-02	-.39938E-02	-.17707E-02
232	.22712E+02	.15950E+02	-.58083E+00	.72540E-02	-.51571E-04	-.60340E-02
233	.16737E+02	.85060E+01	-.12879E+00	.72540E-02	-.39813E-02	-.13379E-02
234	.23086E+02	.16193E+02	-.49775E+00	.73990E-02	-.39917E-04	-.51709E-02
235	.17243E+02	.89140E+01	-.64556E-01	.73990E-02	-.38825E-02	-.67064E-03
236	.23043E+02	.16174E+02	-.42953E+00	.73765E-02	-.31600E-04	-.44622E-02
237	.17362E+02	.90966E+01	.10757E-01	.73765E-02	-.37680E-02	.11175E-03
238	.23039E+02	.16183E+02	-.34288E+00	.73673E-02	-.19534E-04	-.35620E-02
239	.17410E+02	.91705E+01	.91896E-01	.73673E-02	-.37216E-02	.95466E-03
240	.23067E+02	.16209E+02	-.25544E+00	.73737E-02	-.11131E-04	-.26536E-02
241	.17395E+02	.91426E+01	.17805E+00	.73737E-02	-.37415E-02	.18497E-02
242	.23156E+02	.16269E+02	-.17150E+00	.74063E-02	-.54518E-05	-.17817E-02
243	.17363E+02	.90528E+01	.26582E+00	.74063E-02	-.38151E-02	.27615E-02
244	.23153E+02	.16271E+02	-.98649E-01	.74029E-02	-.17322E-05	-.10248E-02
245	.17203E+02	.88584E+01	.34403E+00	.74029E-02	-.39150E-02	.35739E-02
246	.23111E+02	.16246E+02	-.21583E-01	.73845E-02	-.19901E-06	-.22422E-03
247	.17019E+02	.86576E+01	.40900E+00	.73845E-02	-.40062E-02	.42489E-02
248	.22748E+02	.16021E+02	.49564E-01	.72367E-02	-.21397E-06	.51490E-03
249	.16781E+02	.85872E+01	.44795E+00	.72367E-02	-.39246E-02	.46535E-02
250	.21279E+02	.15107E+02	.12768E+00	.66391E-02	-.20961E-05	.13264E-02
251	.16218E+02	.88013E+01	.43849E+00	.66391E-02	-.33311E-02	.45553E-02
252	.17653E+02	.12847E+02	.25675E+00	.51654E-02	-.10376E-04	.26673E-02
253	.14881E+02	.93939E+01	.33607E+00	.51654E-02	-.18334E-02	.34913E-02
254	.10831E+02	.86038E+01	.43373E+00	.23886E-02	-.17966E-04	.45058E-02
255	.10966E+02	.87717E+01	-.23141E+00	.23886E-02	.70649E-04	-.24040E-02
256	.50000E+01	.50000E+01	.00000E+00	.00000E+00	.00000E+00	.00000E+00
max:	.23176E+02	.16286E+02	-.10652E+01	.10141E-01	-.68656E-02	-.11066E-01

==== BARREL VAULT _curvature38 width6_ Stress-deformation_DOWNWARDS =====

==== BARREL VAULT _curvature38 width6_ Stress-deformation UPWARDS ====

3 1 3
3 3 1
153 256
3 1
clea tfor
clea tdis
clea tsrs
clea tsrn
nonl
100 50 0.01e-10 0 0

node				
1	.00000E+00	.00000E+00	.00000E+00	0
2	.69802E+02	.00000E+00	.22397E+02	0
3	.14365E+03	.00000E+00	.42832E+02	0
4	.22287E+03	.00000E+00	.61153E+02	0
5	.29782E+03	.00000E+00	.75154E+02	0
6	.36963E+03	.00000E+00	.85601E+02	0
7	.44625E+03	.00000E+00	.93600E+02	0
8	.52248E+03	.00000E+00	.98375E+02	0
9	.59820E+03	.00000E+00	.99999E+02	0
10	.67349E+03	.00000E+00	.98540E+02	0
11	.75097E+03	.00000E+00	.93829E+02	0
12	.82697E+03	.00000E+00	.86024E+02	0
13	.90180E+03	.00000E+00	.75218E+02	0
14	.97814E+03	.00000E+00	.60941E+02	0
15	.10536E+04	.00000E+00	.43535E+02	0
16	.11264E+04	.00000E+00	.23543E+02	0
17	.12000E+04	.00000E+00	.00000E+00	0
18	.00000E+00	.75000E+02	.00000E+00	0
19	.70670E+02	.74820E+02	.18772E+02	0
20	.14491E+03	.74701E+02	.36863E+02	0
21	.22421E+03	.74608E+02	.53596E+02	0
22	.29904E+03	.74542E+02	.66620E+02	0
23	.37063E+03	.74491E+02	.76447E+02	0
24	.44694E+03	.74462E+02	.84028E+02	0
25	.52284E+03	.74441E+02	.88576E+02	0
26	.59823E+03	.74437E+02	.90126E+02	0
27	.67317E+03	.74443E+02	.88732E+02	0
28	.75034E+03	.74465E+02	.84242E+02	0
29	.82605E+03	.74495E+02	.76839E+02	0
30	.90062E+03	.74550E+02	.66672E+02	0
31	.97687E+03	.74620E+02	.53386E+02	0
32	.10524E+04	.74715E+02	.37483E+02	0
33	.11255E+04	.74819E+02	.19769E+02	0
34	.12000E+04	.75000E+02	.00000E+00	0
35	.00000E+00	.15000E+03	.00000E+00	0
36	.71101E+02	.14981E+03	.16639E+02	0
37	.14558E+03	.14968E+03	.33026E+02	0
38	.22494E+03	.14960E+03	.48500E+02	0
39	.29972E+03	.14950E+03	.60729E+02	0
40	.37120E+03	.14945E+03	.70047E+02	0
41	.44735E+03	.14941E+03	.77286E+02	0
42	.52306E+03	.14938E+03	.81647E+02	0
43	.59823E+03	.14937E+03	.83136E+02	0
44	.67297E+03	.14937E+03	.81797E+02	0
45	.74993E+03	.14941E+03	.77492E+02	0
46	.82546E+03	.14947E+03	.70423E+02	0
47	.89995E+03	.14951E+03	.60776E+02	0
48	.97611E+03	.14959E+03	.48311E+02	0

49	.10517E+04	.14970E+03	.33602E+02	0
50	.11251E+04	.14983E+03	.17522E+02	0
51	.12000E+04	.15000E+03	.00000E+00	0
52	.00000E+00	.22500E+03	.00000E+00	0
53	.71297E+02	.22488E+03	.15489E+02	0
54	.14589E+03	.22479E+03	.30875E+02	0
55	.22533E+03	.22474E+03	.45573E+02	0
56	.30008E+03	.22470E+03	.57287E+02	0
57	.37150E+03	.22465E+03	.66274E+02	0
58	.44755E+03	.22462E+03	.73286E+02	0
59	.52316E+03	.22462E+03	.77523E+02	0
60	.59823E+03	.22462E+03	.78972E+02	0
61	.67286E+03	.22462E+03	.77670E+02	0
62	.74971E+03	.22463E+03	.73488E+02	0
63	.82513E+03	.22468E+03	.66642E+02	0
64	.89955E+03	.22471E+03	.57339E+02	0
65	.97572E+03	.22476E+03	.45392E+02	0
66	.10513E+04	.22483E+03	.31437E+02	0
67	.11249E+04	.22492E+03	.16313E+02	0
68	.12000E+04	.22500E+03	.00000E+00	0
69	.00000E+00	.30000E+03	.00000E+00	0
70	.71348E+02	.29998E+03	.15122E+02	0
71	.14598E+03	.29999E+03	.30180E+02	0
72	.22545E+03	.30000E+03	.44618E+02	0
73	.30017E+03	.30000E+03	.56153E+02	0
74	.37160E+03	.30000E+03	.65028E+02	0
75	.44761E+03	.30000E+03	.71960E+02	0
76	.52318E+03	.30000E+03	.76155E+02	0
77	.59820E+03	.30000E+03	.77590E+02	0
78	.67283E+03	.30000E+03	.76300E+02	0
79	.74962E+03	.30000E+03	.72163E+02	0
80	.82503E+03	.30000E+03	.65393E+02	0
81	.89944E+03	.30000E+03	.56208E+02	0
82	.97556E+03	.30000E+03	.44448E+02	0
83	.10513E+04	.30001E+03	.30716E+02	0
84	.11247E+04	.30002E+03	.15959E+02	0
85	.12000E+04	.30000E+03	.00000E+00	0
86	.00000E+00	.37500E+03	.00000E+00	0
87	.71281E+02	.37508E+03	.15484E+02	0
88	.14588E+03	.37516E+03	.30871E+02	0
89	.22529E+03	.37524E+03	.45565E+02	0
90	.30007E+03	.37529E+03	.57285E+02	0
91	.37148E+03	.37532E+03	.66270E+02	0
92	.44753E+03	.37537E+03	.73284E+02	0
93	.52314E+03	.37538E+03	.77522E+02	0
94	.59820E+03	.37538E+03	.78972E+02	0
95	.67284E+03	.37538E+03	.77671E+02	0
96	.74968E+03	.37538E+03	.73491E+02	0
97	.82512E+03	.37535E+03	.66644E+02	0
98	.89954E+03	.37530E+03	.57342E+02	0
99	.97568E+03	.37527E+03	.45401E+02	0
100	.10513E+04	.37521E+03	.31439E+02	0
101	.11248E+04	.37513E+03	.16336E+02	0
102	.12000E+04	.37500E+03	.00000E+00	0
103	.00000E+00	.45000E+03	.00000E+00	0
104	.71073E+02	.45016E+03	.16631E+02	0
105	.14554E+03	.45028E+03	.33014E+02	0
106	.22490E+03	.45041E+03	.48491E+02	0
107	.29967E+03	.45049E+03	.60720E+02	0
108	.37116E+03	.45053E+03	.70040E+02	0

109	.44731E+03	.45059E+03	.77282E+02	0
110	.52302E+03	.45062E+03	.81645E+02	0
111	.59820E+03	.45063E+03	.83136E+02	0
112	.67293E+03	.45062E+03	.81798E+02	0
113	.74989E+03	.45059E+03	.77495E+02	0
114	.82541E+03	.45055E+03	.70431E+02	0
115	.89988E+03	.45050E+03	.60788E+02	0
116	.97607E+03	.45041E+03	.48320E+02	0
117	.10517E+04	.45032E+03	.33605E+02	0
118	.11251E+04	.45019E+03	.17524E+02	0
119	.12000E+04	.45000E+03	.00000E+00	0
120	.00000E+00	.52500E+03	.00000E+00	0
121	.70638E+02	.52517E+03	.18762E+02	0
122	.14486E+03	.52527E+03	.36848E+02	0
123	.22415E+03	.52538E+03	.53582E+02	0
124	.29900E+03	.52546E+03	.66613E+02	0
125	.37058E+03	.52548E+03	.76438E+02	0
126	.44689E+03	.52553E+03	.84023E+02	0
127	.52282E+03	.52555E+03	.88574E+02	0
128	.59820E+03	.52558E+03	.90128E+02	0
129	.67314E+03	.52557E+03	.88735E+02	0
130	.75030E+03	.52553E+03	.84245E+02	0
131	.82597E+03	.52550E+03	.76848E+02	0
132	.90058E+03	.52546E+03	.66680E+02	0
133	.97680E+03	.52539E+03	.53402E+02	0
134	.10524E+04	.52529E+03	.37486E+02	0
135	.11255E+04	.52519E+03	.19771E+02	0
136	.12000E+04	.52500E+03	.00000E+00	0
137	.00000E+00	.60000E+03	.00000E+00	0
138	.69802E+02	.60000E+03	.22397E+02	0
139	.14365E+03	.60000E+03	.42832E+02	0
140	.22287E+03	.60000E+03	.61153E+02	0
141	.29782E+03	.60000E+03	.75154E+02	0
142	.36963E+03	.60000E+03	.85601E+02	0
143	.44625E+03	.60000E+03	.93600E+02	0
144	.52248E+03	.60000E+03	.98375E+02	0
145	.59820E+03	.60000E+03	.99999E+02	0
146	.67349E+03	.60000E+03	.98540E+02	0
147	.75097E+03	.60000E+03	.93829E+02	0
148	.82697E+03	.60000E+03	.86024E+02	0
149	.90180E+03	.60000E+03	.75218E+02	0
150	.97814E+03	.60000E+03	.60941E+02	0
151	.10536E+04	.60000E+03	.43535E+02	0
152	.11264E+04	.60000E+03	.23543E+02	0
153	.12000E+04	.60000E+03	.00000E+00	0

0,,,,,,,,,
elem mak3 3

1	18	1	2	1	0	0
2	2	19	18	1	0	0
3	19	2	3	1	0	0
4	3	20	19	1	0	0
5	20	3	4	1	0	0
6	4	21	20	1	0	0
7	21	4	5	1	0	0
8	5	22	21	1	0	0
9	22	5	6	1	0	0
10	6	23	22	1	0	0
11	23	6	7	1	0	0
12	7	24	23	1	0	0
13	24	7	8	1	0	0

14	8	25	24	1	0	0
15	25	8	9	1	0	0
16	9	26	25	1	0	0
17	26	9	10	1	0	0
18	10	27	26	1	0	0
19	27	10	11	1	0	0
20	11	28	27	1	0	0
21	28	11	12	1	0	0
22	12	29	28	1	0	0
23	29	12	13	1	0	0
24	13	30	29	1	0	0
25	30	13	14	1	0	0
26	14	31	30	1	0	0
27	31	14	15	1	0	0
28	15	32	31	1	0	0
29	32	15	16	1	0	0
30	16	33	32	1	0	0
31	33	16	17	1	0	0
32	17	34	33	1	0	0
33	35	18	19	1	0	0
34	19	36	35	1	0	0
35	36	19	20	1	0	0
36	20	37	36	1	0	0
37	37	20	21	1	0	0
38	21	38	37	1	0	0
39	38	21	22	1	0	0
40	22	39	38	1	0	0
41	39	22	23	1	0	0
42	23	40	39	1	0	0
43	40	23	24	1	0	0
44	24	41	40	1	0	0
45	41	24	25	1	0	0
46	25	42	41	1	0	0
47	42	25	26	1	0	0
48	26	43	42	1	0	0
49	43	26	27	1	0	0
50	27	44	43	1	0	0
51	44	27	28	1	0	0
52	28	45	44	1	0	0
53	45	28	29	1	0	0
54	29	46	45	1	0	0
55	46	29	30	1	0	0
56	30	47	46	1	0	0
57	47	30	31	1	0	0
58	31	48	47	1	0	0
59	48	31	32	1	0	0
60	32	49	48	1	0	0
61	49	32	33	1	0	0
62	33	50	49	1	0	0
63	50	33	34	1	0	0
64	34	51	50	1	0	0
65	52	35	36	1	0	0
66	36	53	52	1	0	0
67	53	36	37	1	0	0
68	37	54	53	1	0	0
69	54	37	38	1	0	0
70	38	55	54	1	0	0
71	55	38	39	1	0	0
72	39	56	55	1	0	0
73	56	39	40	1	0	0

74	40	57	56	1	0	0
75	57	40	41	1	0	0
76	41	58	57	1	0	0
77	58	41	42	1	0	0
78	42	59	58	1	0	0
79	59	42	43	1	0	0
80	43	60	59	1	0	0
81	60	43	44	1	0	0
82	44	61	60	1	0	0
83	61	44	45	1	0	0
84	45	62	61	1	0	0
85	62	45	46	1	0	0
86	46	63	62	1	0	0
87	63	46	47	1	0	0
88	47	64	63	1	0	0
89	64	47	48	1	0	0
90	48	65	64	1	0	0
91	65	48	49	1	0	0
92	49	66	65	1	0	0
93	66	49	50	1	0	0
94	50	67	66	1	0	0
95	67	50	51	1	0	0
96	51	68	67	1	0	0
97	69	52	53	1	0	0
98	53	70	69	1	0	0
99	70	53	54	1	0	0
100	54	71	70	1	0	0
101	71	54	55	1	0	0
102	55	72	71	1	0	0
103	72	55	56	1	0	0
104	56	73	72	1	0	0
105	73	56	57	1	0	0
106	57	74	73	1	0	0
107	74	57	58	1	0	0
108	58	75	74	1	0	0
109	75	58	59	1	0	0
110	59	76	75	1	0	0
111	76	59	60	1	0	0
112	60	77	76	1	0	0
113	77	60	61	1	0	0
114	61	78	77	1	0	0
115	78	61	62	1	0	0
116	62	79	78	1	0	0
117	79	62	63	1	0	0
118	63	80	79	1	0	0
119	80	63	64	1	0	0
120	64	81	80	1	0	0
121	81	64	65	1	0	0
122	65	82	81	1	0	0
123	82	65	66	1	0	0
124	66	83	82	1	0	0
125	83	66	67	1	0	0
126	67	84	83	1	0	0
127	84	67	68	1	0	0
128	68	85	84	1	0	0
129	86	69	70	1	0	0
130	70	87	86	1	0	0
131	87	70	71	1	0	0
132	71	88	87	1	0	0
133	88	71	72	1	0	0

134	72 89 88	1	0	0
135	89 72 73	1	0	0
136	73 90 89	1	0	0
137	90 73 74	1	0	0
138	74 91 90	1	0	0
139	91 74 75	1	0	0
140	75 92 91	1	0	0
141	92 75 76	1	0	0
142	76 93 92	1	0	0
143	93 76 77	1	0	0
144	77 94 93	1	0	0
145	94 77 78	1	0	0
146	78 95 94	1	0	0
147	95 78 79	1	0	0
148	79 96 95	1	0	0
149	96 79 80	1	0	0
150	80 97 96	1	0	0
151	97 80 81	1	0	0
152	81 98 97	1	0	0
153	98 81 82	1	0	0
154	82 99 98	1	0	0
155	99 82 83	1	0	0
156	83 100 99	1	0	0
157	100 83 84	1	0	0
158	84 101 100	1	0	0
159	101 84 85	1	0	0
160	85 102 101	1	0	0
161	103 86 87	1	0	0
162	87 104 103	1	0	0
163	104 87 88	1	0	0
164	88 105 104	1	0	0
165	105 88 89	1	0	0
166	89 106 105	1	0	0
167	106 89 90	1	0	0
168	90 107 106	1	0	0
169	107 90 91	1	0	0
170	91 108 107	1	0	0
171	108 91 92	1	0	0
172	92 109 108	1	0	0
173	109 92 93	1	0	0
174	93 110 109	1	0	0
175	110 93 94	1	0	0
176	94 111 110	1	0	0
177	111 94 95	1	0	0
178	95 112 111	1	0	0
179	112 95 96	1	0	0
180	96 113 112	1	0	0
181	113 96 97	1	0	0
182	97 114 113	1	0	0
183	114 97 98	1	0	0
184	98 115 114	1	0	0
185	115 98 99	1	0	0
186	99 116 115	1	0	0
187	116 99 100	1	0	0
188	100 117 116	1	0	0
189	117 100 101	1	0	0
190	101 118 117	1	0	0
191	118 101 102	1	0	0
192	102 119 118	1	0	0
193	120 103 104	1	0	0

194	104	121	120	1	0	0
195	121	104	105	1	0	0
196	105	122	121	1	0	0
197	122	105	106	1	0	0
198	106	123	122	1	0	0
199	123	106	107	1	0	0
200	107	124	123	1	0	0
201	124	107	108	1	0	0
202	108	125	124	1	0	0
203	125	108	109	1	0	0
204	109	126	125	1	0	0
205	126	109	110	1	0	0
206	110	127	126	1	0	0
207	127	110	111	1	0	0
208	111	128	127	1	0	0
209	128	111	112	1	0	0
210	112	129	128	1	0	0
211	129	112	113	1	0	0
212	113	130	129	1	0	0
213	130	113	114	1	0	0
214	114	131	130	1	0	0
215	131	114	115	1	0	0
216	115	132	131	1	0	0
217	132	115	116	1	0	0
218	116	133	132	1	0	0
219	133	116	117	1	0	0
220	117	134	133	1	0	0
221	134	117	118	1	0	0
222	118	135	134	1	0	0
223	135	118	119	1	0	0
224	119	136	135	1	0	0
225	137	120	121	1	0	0
226	121	138	137	1	0	0
227	138	121	122	1	0	0
228	122	139	138	1	0	0
229	139	122	123	1	0	0
230	123	140	139	1	0	0
231	140	123	124	1	0	0
232	124	141	140	1	0	0
233	141	124	125	1	0	0
234	125	142	141	1	0	0
235	142	125	126	1	0	0
236	126	143	142	1	0	0
237	143	126	127	1	0	0
238	127	144	143	1	0	0
239	144	127	128	1	0	0
240	128	145	144	1	0	0
241	145	128	129	1	0	0
242	129	146	145	1	0	0
243	146	129	130	1	0	0
244	130	147	146	1	0	0
245	147	130	131	1	0	0
246	131	148	147	1	0	0
247	148	131	132	1	0	0
248	132	149	148	1	0	0
249	149	132	133	1	0	0
250	133	150	149	1	0	0
251	150	133	134	1	0	0
252	134	151	150	1	0	0
253	151	134	135	1	0	0

```

254      135 152 151      1  0  0
255      152 135 136      1  0  0
256      136 153 152      1  0  0
0,/////////
mate ortr
1  1.0  0.0  1230.0  950.0  0.804  0.620  96.26
0,/////////
strs
1      5.0      5.0      0.0  1
256    5.0      5.0      0.0  0
0,/////////
b.c.
1      1  1  1  1
18     1  1  1  0
136    1  1  1  1
153    1  1  1  0
34     1  1  1  0
35     1  1  1  0
51     1  1  1  0
52     1  1  1  0
68     1  1  1  0
69     1  1  1  0
85     1  1  1  0
86     1  1  1  0
102    1  1  1  0
103    1  1  1  0
119    1  1  1  0
120    1  1  1  0
0,/////////
l.c.
1      -4.199438  0.000000  13.087875  0
2      -11.531476  1.394774  40.120357  0
3      -10.620623  3.118296  42.472682  0
4      -9.152241  4.256999  43.565555  0
5      -6.983997  4.663047  41.306973  0
6      -5.265375  5.000281  40.983058  0
7      -3.789071  5.445042  42.664885  0
8      -2.037000  5.552287  42.407476  0
9      -0.319066  5.575578  42.132100  0
10     1.407548  5.600458  42.377414  0
11     3.165093  5.594045  42.934154  0
12     4.843508  5.332478  42.184612  0
13     6.567058  5.039440  42.062166  0
14     8.385146  4.635991  42.529590  0
15     9.950389  3.832433  41.783538  0
16     11.450293  2.638383  41.038232  0
17     8.110347  0.747388  27.735446  0
18     -11.228859  0.681182  39.557714  0
19     -20.737911  3.372059  81.396125  0
20     -19.514636  5.904914  86.194896  0
21     -16.633040  7.458451  86.488718  0
22     -12.773280  8.033318  82.117964  0
23     -9.735417  8.735295  82.917727  0
24     -6.773015  9.341697  85.311348  0
25     -3.395082  9.485433  84.776024  0
26     -0.065595  9.487778  84.231931  0
27     3.323910  9.545097  85.226815  0
28     6.699501  9.374471  85.674662  0
29     9.899576  8.840058  84.254192  0
30     13.232574  8.250076  84.576829  0

```

31	16.496731	7.277993	85.130266	0
32	19.071113	5.569380	83.410445	0
33	21.463353	3.083872	82.848171	0
34	10.698277	0.438273	41.983480	0
35	-9.757946	0.397075	39.911927	0
36	-18.681236	1.989066	81.899328	0
37	-17.975047	3.643843	86.590988	0
38	-15.593465	4.732011	86.793635	0
39	-12.126058	5.186481	82.363349	0
40	-9.322256	5.707244	83.145368	0
41	-6.522368	6.135770	85.524701	0
42	-3.282220	6.249530	84.987118	0
43	-0.067580	6.254544	84.443077	0
44	3.203716	6.283382	85.453214	0
45	6.441007	6.136965	85.895156	0
46	9.465057	5.737743	84.484383	0
47	12.536198	5.277986	84.838465	0
48	15.421865	4.537947	85.439128	0
49	17.494360	3.330158	83.826549	0
50	19.153508	1.745199	83.443156	0
51	9.632866	0.235146	42.185688	0
52	-8.930553	0.212568	40.080348	0
53	-17.502195	0.985564	82.134028	0
54	-17.037173	1.792228	86.801901	0
55	-14.942591	2.325905	86.974643	0
56	-11.709344	2.558552	82.493409	0
57	-9.052052	2.835999	83.268923	0
58	-6.360378	3.046829	85.655660	0
59	-3.211625	3.104206	85.121077	0
60	-0.073883	3.103718	84.571259	0
61	3.117255	3.114314	85.579958	0
62	6.259166	3.020259	85.998548	0
63	9.165196	2.802619	84.601913	0
64	12.065304	2.549404	84.979674	0
65	14.714289	2.143444	85.587447	0
66	16.527198	1.519543	84.084052	0
67	17.862078	0.744786	83.672583	0
68	9.113695	0.074620	42.300065	0
69	-8.578700	0.067390	40.141527	0
70	-17.128252	0.133685	82.204181	0
71	-16.742430	0.124787	86.883421	0
72	-14.738620	0.074184	87.008829	0
73	-11.581039	0.043211	82.541714	0
74	-8.966530	0.049505	83.309744	0
75	-6.312532	0.020760	85.695647	0
76	-3.193523	0.008236	85.151129	0
77	-0.082541	-0.000968	84.612166	0
78	3.078570	-0.002482	85.616569	0
79	6.187242	-0.026587	86.042471	0
80	9.051040	-0.038857	84.657834	0
81	11.884489	-0.050907	85.017257	0
82	14.462527	-0.083477	85.679746	0
83	16.177047	-0.112401	84.117440	0
84	17.432532	-0.133722	83.739815	0
85	9.051995	-0.074960	42.358213	0
86	-8.645674	-0.067103	40.125959	0
87	-17.537983	-0.704247	82.122165	0
88	-17.091559	-1.540217	86.791037	0
89	-15.008125	-2.181932	86.947564	0
90	-11.757537	-2.478324	82.501932	0

91	-9.077800	-2.741493	83.255317	0
92	-6.386958	-3.008463	85.655562	0
93	-3.232267	-3.088536	85.109594	0
94	-0.093363	-3.106782	84.578662	0
95	3.095095	-3.116966	85.569451	0
96	6.235373	-3.069707	86.011175	0
97	9.133957	-2.875741	84.610985	0
98	12.017111	-2.644199	84.972565	0
99	14.664147	-2.305938	85.628585	0
100	16.455450	-1.745210	84.025574	0
101	17.813383	-1.026770	83.727473	0
102	9.413814	-0.235596	42.255128	0
103	-9.142742	-0.212450	40.031860	0
104	-18.792509	-1.658513	81.865082	0
105	-18.104355	-3.390100	86.569856	0
106	-15.734321	-4.610448	86.777064	0
107	-12.217674	-5.125741	82.365782	0
108	-9.374472	-5.625260	83.141426	0
109	-6.571605	-6.107828	85.529291	0
110	-3.321707	-6.239537	84.994079	0
111	-0.103317	-6.257928	84.451562	0
112	3.163731	-6.281290	85.445556	0
113	6.392578	-6.176740	85.877906	0
114	9.402761	-5.795295	84.470495	0
115	12.444686	-5.353087	84.841161	0
116	15.306835	-4.682293	85.461906	0
117	17.367357	-3.556817	83.880398	0
118	18.986431	-2.072589	83.436247	0
119	10.277495	-0.438275	42.056440	0
120	-10.153626	-0.396728	39.817388	0
121	-21.069059	-2.946859	81.314194	0
122	-19.749971	-5.685353	86.149940	0
123	-16.839014	-7.392944	86.459649	0
124	-12.896975	-8.010051	82.109755	0
125	-9.805535	-8.674948	82.911622	0
126	-6.837237	-9.330629	85.322328	0
127	-3.446008	-9.483706	84.785760	0
128	-0.111011	-9.490533	84.229170	0
129	3.272021	-9.535461	85.228006	0
130	6.636808	-9.397678	85.653722	0
131	9.819452	-8.874645	84.253704	0
132	13.107575	-8.288096	84.592308	0
133	16.330067	-7.373953	85.178834	0
134	18.840867	-5.760173	83.482297	0
135	21.054836	-3.503735	82.921803	0
136	11.817255	-0.747020	41.702540	0
137	-7.707794	-0.681135	26.302834	0
138	-11.390217	-2.560010	40.740151	0
139	-10.360235	-3.961444	43.388831	0
140	-8.456288	-4.658159	42.708947	0
141	-6.385824	-4.868868	40.684128	0
142	-4.847430	-5.283158	41.859603	0
143	-3.224764	-5.544393	42.589337	0
144	-1.479395	-5.588784	42.306143	0
145	0.228259	-5.564735	42.039880	0
146	1.983050	-5.606448	42.792008	0
147	3.707169	-5.452707	42.667752	0
148	5.360252	-5.130131	41.995783	0
149	7.149577	-4.784265	42.387699	0
150	8.880870	-4.158198	42.434985	0

```
151    10.297216  -3.083448  41.363014    0
152    11.849196  -1.478506  41.349210    0
153     4.414312  0.000000  13.800000    0
0,,,,,,,,,
end
```

```

*****
***                                     ***
***          =====                   ***
***                   NASS-2004         ***
***          NONLINEAR ANALYSIS FOR SPATIAL STRUCTURES ***
***          =====                   ***
***                                     ***
***                   developed by       ***
***                   SEUNG-DEOG KIM, Semyung University ***
***                                     ***
*****

```

TITLE : ===== BARREL VAULT _curvature38 width6_ Stress-deformation UPWARDS =====

```

Kind of dimension      = 3 ( 2 for 2-D, 3 for 3-D )
Kind of problem (1)   = 1 ( 1 for STATIC, 2 for DYNAMIC )
Kind of problem (2)   = 3 ( 0 for LINEAR ANALYSIS
                          1 for EQUILIBLIUM-FINDING
                          2 for SHAPE-FINDING
                          3 for STRESS-DEFORMATION by FORCE
                          4 for STRESS-DEFORMATION by DISPL
                          5 for 1 + 3
                          6 for 1 + 4
                          7 for 2 + 3
                          8 for 2 + 4
                          )

```

```

Maximum DOF of each node = 3
Maximum node of each element = 3
Outputing level = 1

Total nodes = 153
Total elements = 256
Kinds of Material = 1

Total DOFs = 459

```

```

Integrating points for IN-PLANE & BENDING = 3
Integrating points for SHEAR = 1

```

/// Memory Check : kaend= 41519 , k1= 300000 ///

/// Memory Check : klend= 3169 , k2= 20000 ///

/// Memory Check : kbend= 421362 , k3=8100000 ///

... total DOF x total DOF = 459 x 459 = 210681 ...

===== DATA FOR NONLINEAR ANALYSIS =====

Total Step = 100
Total Iteration = 50
Error = .10000E-11
Modification On/Off = 0 (Off for 0)
Determinant On/Off = 0 (On for 1)

Control Node = 0
Control DOF = 0
Displacement = .00000E+00

===== DATA FOR INITIAL IMPERFECTION =====

Imperfection = .00000E+00
Mode Number = 0

===== DATA FOR SEMI-RIGID FACTOR =====

Semi-Rigid = .10000E+01

49	.10545E+04	.15007E+03	.48370E+02	-.29331E-10	-.22737E-12	.75033E-11
50	.11271E+04	.15008E+03	.26395E+02	-.11028E-10	-.14381E-10	.64233E-11
51	.12000E+04	.15000E+03	.00000E+00	.19821E-10	.10232E-10	-.73224E-11
52	.00000E+00	.22500E+03	.00000E+00	.37176E-10	-.24897E-10	.13699E-10
53	.69132E+02	.22507E+03	.25331E+02	-.30241E-10	.11028E-10	-.14438E-10
54	.14264E+03	.22504E+03	.48108E+02	-.12017E-09	-.10687E-10	-.38511E-10
55	.22180E+03	.22502E+03	.68256E+02	-.19656E-09	-.19213E-10	-.48175E-10
56	.29683E+03	.22501E+03	.83474E+02	-.24852E-09	-.20293E-10	-.47180E-10
57	.36881E+03	.22500E+03	.94736E+02	-.29922E-09	-.28365E-10	-.41993E-10
58	.44566E+03	.22498E+03	.10330E+03	-.35232E-09	-.21203E-10	-.33033E-10
59	.52217E+03	.22499E+03	.10840E+03	-.37676E-09	-.21316E-10	-.17931E-10
60	.59820E+03	.22499E+03	.11013E+03	-.38187E-09	-.16087E-10	-.12044E-11
61	.67378E+03	.22499E+03	.10859E+03	-.37994E-09	-.15973E-10	.15888E-10
62	.75155E+03	.22498E+03	.10357E+03	-.35561E-09	-.10175E-10	.31392E-10
63	.82777E+03	.22502E+03	.95221E+02	-.30786E-09	-.93792E-11	.42007E-10
64	.90278E+03	.22502E+03	.83581E+02	-.25580E-09	-.64233E-11	.46640E-10
65	.97922E+03	.22503E+03	.68064E+02	-.19361E-09	-.16485E-11	.46015E-10
66	.10546E+04	.22504E+03	.48935E+02	-.12210E-09	-.61959E-11	.38114E-10
67	.11271E+04	.22505E+03	.26611E+02	-.35698E-10	-.48431E-10	.13870E-10
68	.12000E+04	.22500E+03	.00000E+00	.32443E-10	.36039E-10	-.12062E-10
69	.00000E+00	.30000E+03	.00000E+00	.16030E-10	-.51728E-10	.57980E-11
70	.69122E+02	.30002E+03	.25392E+02	-.26944E-10	.49795E-10	-.12164E-10
71	.14262E+03	.30001E+03	.48270E+02	-.54115E-10	-.68212E-12	-.17423E-10
72	.22179E+03	.30000E+03	.68523E+02	-.70827E-10	-.12506E-10	-.17138E-10
73	.29678E+03	.30000E+03	.83811E+02	-.79240E-10	-.86402E-11	-.15689E-10
74	.36879E+03	.30001E+03	.95128E+02	-.93110E-10	-.14552E-10	-.11951E-10
75	.44564E+03	.30000E+03	.10373E+03	-.10743E-09	-.65938E-11	-.96492E-11
76	.52216E+03	.30000E+03	.10884E+03	-.10959E-09	-.56275E-11	-.44160E-11
77	.59818E+03	.30000E+03	.11058E+03	-.11210E-09	-.34106E-11	.37303E-12
78	.67380E+03	.30000E+03	.10902E+03	-.10573E-09	-.29559E-11	.54783E-11
79	.75156E+03	.30000E+03	.10398E+03	-.95497E-10	.38654E-11	.93081E-11
80	.82780E+03	.30000E+03	.95583E+02	-.79353E-10	.40359E-11	.10999E-10
81	.90283E+03	.30000E+03	.83880E+02	-.61505E-10	.47748E-11	.10772E-10
82	.97922E+03	.29999E+03	.68290E+02	-.41609E-10	.75033E-11	.10346E-10
83	.10547E+04	.29999E+03	.49030E+02	-.15120E-10	-.36380E-11	.13358E-11
84	.11270E+04	.29999E+03	.26696E+02	.17053E-11	-.56502E-10	-.28422E-11
85	.12000E+04	.30000E+03	.00000E+00	.11600E-11	.51955E-10	-.11635E-12
86	.00000E+00	.37500E+03	.00000E+00	-.26262E-10	-.46043E-10	-.94360E-11
87	.69129E+02	.37496E+03	.25355E+02	.25580E-10	.65484E-10	.97202E-11
88	.14265E+03	.37495E+03	.48150E+02	.11676E-09	.13756E-10	.34703E-10
89	.22179E+03	.37496E+03	.68295E+02	.19634E-09	.57980E-11	.46668E-10
90	.29684E+03	.37497E+03	.83514E+02	.24886E-09	.10346E-10	.46171E-10
91	.36881E+03	.37499E+03	.94765E+02	.30332E-09	.85265E-11	.41410E-10
92	.44566E+03	.37502E+03	.10332E+03	.35629E-09	.12733E-10	.31875E-10
93	.52217E+03	.37501E+03	.10841E+03	.38244E-09	.11710E-10	.17273E-10
94	.59819E+03	.37501E+03	.11013E+03	.39392E-09	.17508E-10	.24158E-12
95	.67378E+03	.37501E+03	.10858E+03	.39233E-09	.16712E-10	-.18161E-10
96	.75154E+03	.37502E+03	.10355E+03	.36675E-09	.18986E-10	-.33722E-10
97	.82778E+03	.37500E+03	.95190E+02	.32094E-09	.19554E-10	-.44452E-10
98	.90279E+03	.37498E+03	.83542E+02	.26853E-09	.16371E-10	-.51614E-10
99	.97921E+03	.37498E+03	.68026E+02	.20430E-09	.14666E-10	-.49312E-10
100	.10546E+04	.37496E+03	.48890E+02	.13006E-09	-.12506E-11	-.42434E-10
101	.11270E+04	.37494E+03	.26614E+02	.40927E-10	-.30354E-10	-.15973E-10
102	.12000E+04	.37500E+03	.00000E+00	-.36522E-10	.35129E-10	.12947E-10
103	.00000E+00	.45000E+03	.00000E+00	-.26148E-10	-.18531E-10	-.94929E-11
104	.69175E+02	.44992E+03	.25147E+02	.25807E-10	.32401E-10	.10573E-10
105	.14275E+03	.44992E+03	.47611E+02	.77989E-10	.10800E-10	.22453E-10
106	.22190E+03	.44996E+03	.67427E+02	.11244E-09	.75033E-11	.25750E-10
107	.29693E+03	.44998E+03	.82397E+02	.13290E-09	.13415E-10	.23377E-10
108	.36891E+03	.44999E+03	.93480E+02	.15814E-09	.10232E-10	.19639E-10

109	.44574E+03	.45002E+03	.10192E+03	.17712E-09	.13074E-10	.14129E-10
110	.52222E+03	.45003E+03	.10694E+03	.18520E-09	.12847E-10	.71765E-11
111	.59820E+03	.45004E+03	.10863E+03	.18429E-09	.14666E-10	-.18474E-11
112	.67373E+03	.45003E+03	.10709E+03	.17815E-09	.11937E-10	-.91660E-11
113	.75147E+03	.45001E+03	.10213E+03	.16450E-09	.14552E-10	-.16769E-10
114	.82767E+03	.45000E+03	.93882E+02	.13824E-09	.11482E-10	-.18900E-10
115	.90266E+03	.44999E+03	.82404E+02	.11312E-09	.87539E-11	-.22112E-10
116	.97911E+03	.44995E+03	.67122E+02	.80718E-10	.73896E-11	-.18986E-10
117	.10546E+04	.44993E+03	.48281E+02	.43997E-10	.12506E-11	-.15604E-10
118	.11271E+04	.44990E+03	.26330E+02	-.79581E-12	-.12506E-11	-.32401E-11
119	.12000E+04	.45000E+03	.00000E+00	-.22853E-10	.38085E-11	.90297E-11
120	.00000E+00	.52500E+03	.00000E+00	.90949E-12	-.30695E-11	.14211E-12
121	.69346E+02	.52492E+03	.24464E+02	-.27626E-10	-.53433E-11	-.90665E-11
122	.14300E+03	.52494E+03	.46172E+02	-.64915E-10	-.63665E-11	-.17451E-10
123	.22220E+03	.52498E+03	.65379E+02	-.10607E-09	.15916E-11	-.22752E-10
124	.29724E+03	.52502E+03	.79941E+02	-.13279E-09	.48885E-11	-.23391E-10
125	.36915E+03	.52501E+03	.90744E+02	-.16098E-09	.44338E-11	-.20258E-10
126	.44590E+03	.52504E+03	.98993E+02	-.18838E-09	.55707E-11	-.15493E-10
127	.52232E+03	.52504E+03	.10390E+03	-.20134E-09	.35243E-11	-.81286E-11
128	.59820E+03	.52507E+03	.10557E+03	-.20577E-09	.90949E-12	.99476E-12
129	.67365E+03	.52506E+03	.10406E+03	-.20430E-09	-.79581E-12	.99192E-11
130	.75131E+03	.52503E+03	.99200E+02	-.19270E-09	-.19327E-11	.17707E-10
131	.82742E+03	.52502E+03	.91141E+02	-.16905E-09	-.34106E-11	.22482E-10
132	.90237E+03	.52501E+03	.79942E+02	-.14359E-09	-.17053E-11	.26432E-10
133	.97878E+03	.52498E+03	.65082E+02	-.11073E-09	.56843E-12	.24272E-10
134	.10543E+04	.52494E+03	.46809E+02	-.73896E-10	.34106E-11	.21743E-10
135	.11269E+04	.52493E+03	.25603E+02	-.35698E-10	.63665E-11	.10630E-10
136	.12000E+04	.52500E+03	.00000E+00	.53433E-11	-.19895E-12	-.15348E-11
137	.00000E+00	.60000E+03	.00000E+00	.34106E-12	-.31974E-13	.11369E-12
138	.69802E+02	.60000E+03	.22397E+02	-.28990E-11	-.15916E-11	-.73896E-12
139	.14365E+03	.60000E+03	.42832E+02	-.35811E-11	.99476E-12	-.98055E-12
140	.22287E+03	.60000E+03	.61153E+02	-.34674E-11	.22169E-11	-.94502E-12
141	.29782E+03	.60000E+03	.75154E+02	-.30695E-11	.12399E-11	-.49027E-12
142	.36963E+03	.60000E+03	.85601E+02	-.27853E-11	.13465E-11	-.45475E-12
143	.44625E+03	.60000E+03	.93600E+02	-.11084E-11	.54712E-12	-.19540E-12
144	.52248E+03	.60000E+03	.98375E+02	-.90949E-12	.41567E-12	-.40856E-13
145	.59820E+03	.60000E+03	.99999E+02	.82423E-12	.82778E-12	-.14966E-12
146	.67349E+03	.60000E+03	.98540E+02	.14495E-11	-.34905E-12	-.11724E-12
147	.75097E+03	.60000E+03	.93829E+02	.21316E-11	-.10190E-11	-.19540E-12
148	.82697E+03	.60000E+03	.86024E+02	.40359E-11	.65725E-13	-.57554E-12
149	.90180E+03	.60000E+03	.75218E+02	.38654E-11	-.12736E-11	-.66791E-12
150	.97814E+03	.60000E+03	.60941E+02	.43201E-11	-.59863E-12	-.71054E-12
151	.10536E+04	.60000E+03	.43535E+02	.54570E-11	-.15739E-11	-.15348E-11
152	.11264E+04	.60000E+03	.23543E+02	.38085E-11	-.26148E-11	-.86686E-12
153	.12000E+04	.60000E+03	.00000E+00	.00000E+00	.00000E+00	.00000E+00
sum:				.14623E-10	-.16035E-10	-.23137E-10

<<< SUM OF FORCES & DISPLACEMENTS >>>

NODE	For-X	For-Y	For-Z	Dis-X	Dis-Y	Dis-Z
1	-.17853E+03	-.18327E+03	-.57285E+02	.00000E+00	.00000E+00	.00000E+00
2	-.16713E+03	-.11367E+04	-.72205E+02	.00000E+00	.00000E+00	.00000E+00
3	-.18957E+02	-.11477E+04	-.43644E+02	.00000E+00	.00000E+00	.00000E+00
4	.11953E+01	-.10775E+04	-.48954E+02	.00000E+00	.00000E+00	.00000E+00
5	-.71067E+01	-.97233E+03	-.53121E+02	.00000E+00	.00000E+00	.00000E+00
6	-.12381E+02	-.94256E+03	-.56414E+02	.00000E+00	.00000E+00	.00000E+00

7	-.36715E+01	-.95247E+03	-.58998E+02	.00000E+00	.00000E+00	.00000E+00
8	-.14170E+01	-.93392E+03	-.59459E+02	.00000E+00	.00000E+00	.00000E+00
9	.36338E+01	-.92444E+03	-.59481E+02	.00000E+00	.00000E+00	.00000E+00
10	.96169E+01	-.93554E+03	-.60242E+02	.00000E+00	.00000E+00	.00000E+00
11	.17787E+02	-.95611E+03	-.61225E+02	.00000E+00	.00000E+00	.00000E+00
12	.19743E+02	-.96107E+03	-.59788E+02	.00000E+00	.00000E+00	.00000E+00
13	.21308E+02	-.99518E+03	-.58304E+02	.00000E+00	.00000E+00	.00000E+00
14	.20449E+02	-.10572E+04	-.54851E+02	.00000E+00	.00000E+00	.00000E+00
15	.13219E+02	-.11070E+04	-.43951E+02	.00000E+00	.00000E+00	.00000E+00
16	.69407E+01	-.11641E+04	-.24528E+02	.00000E+00	.00000E+00	.00000E+00
17	.32933E+03	-.57759E+03	-.10645E+03	.00000E+00	.00000E+00	.00000E+00
18	-.11901E+04	-.32553E+03	-.41933E+03	.00000E+00	.00000E+00	.00000E+00
19	-.20738E+02	.33721E+01	.81396E+02	-.13372E+01	.25450E+00	.56169E+01
20	-.19515E+02	.59049E+01	.86195E+02	-.18971E+01	.34979E+00	.92251E+01
21	-.16633E+02	.74585E+01	.86489E+02	-.19841E+01	.40592E+00	.11703E+02
22	-.12773E+02	.80333E+01	.82118E+02	-.17931E+01	.44784E+00	.13255E+02
23	-.97354E+01	.87353E+01	.82918E+02	-.14678E+01	.48279E+00	.14255E+02
24	-.67730E+01	.93417E+01	.85311E+02	-.10284E+01	.49910E+00	.14934E+02
25	-.33951E+01	.94854E+01	.84776E+02	-.53854E+00	.50884E+00	.15311E+02
26	-.63595E-01	.94878E+01	.84232E+02	-.29208E-01	.51172E+00	.15440E+02
27	.33239E+01	.95451E+01	.85227E+02	.47646E+00	.50939E+00	.15342E+02
28	.66995E+01	.93745E+01	.85675E+02	.97523E+00	.49433E+00	.14987E+02
29	.98996E+01	.88401E+01	.84254E+02	.14146E+01	.47283E+00	.14343E+02
30	.13233E+02	.82501E+01	.84577E+02	.17566E+01	.44237E+00	.13336E+02
31	.16497E+02	.72780E+01	.85130E+02	.19468E+01	.39399E+00	.11770E+02
32	.19071E+02	.55694E+01	.83410E+02	.18646E+01	.33119E+00	.94240E+01
33	.21463E+02	.30839E+01	.82848E+02	.13309E+01	.26020E+00	.59237E+01
34	.11414E+04	-.16724E+03	-.40113E+03	.00000E+00	.00000E+00	.00000E+00
35	-.13875E+02	-.17944E+03	-.50368E+03	.00000E+00	.00000E+00	.00000E+00
36	-.18681E+02	.19891E+01	.81899E+02	-.19254E+01	.28911E+00	.84555E+01
37	-.17975E+02	.36438E+01	.86591E+02	-.28368E+01	.39351E+00	.14508E+02
38	-.15593E+02	.47320E+01	.86794E+02	-.30345E+01	.45530E+00	.18848E+02
39	-.12126E+02	.51865E+01	.82363E+02	-.27781E+01	.50781E+00	.21603E+02
40	-.93223E+01	.57072E+01	.83145E+02	-.22891E+01	.55374E+00	.23386E+02
41	-.65224E+01	.61358E+01	.85525E+02	-.16084E+01	.57437E+00	.24600E+02
42	-.32822E+01	.62495E+01	.84987E+02	-.84028E+00	.58708E+00	.25271E+02
43	-.67580E-01	.62545E+01	.84443E+02	-.37559E-01	.59148E+00	.25496E+02
44	.32037E+01	.62834E+01	.85453E+02	.76129E+00	.58879E+00	.25311E+02
45	.64410E+01	.61370E+01	.85895E+02	.15450E+01	.56867E+00	.24668E+02
46	.94651E+01	.57377E+01	.84484E+02	.22257E+01	.54156E+00	.23506E+02
47	.12536E+02	.52780E+01	.84838E+02	.27402E+01	.50444E+00	.21688E+02
48	.15422E+02	.45379E+01	.85439E+02	.29962E+01	.44498E+00	.18889E+02
49	.17494E+02	.33302E+01	.83827E+02	.28082E+01	.36954E+00	.14768E+02
50	.19154E+02	.17452E+01	.83443E+02	.19622E+01	.25164E+00	.88730E+01
51	.13688E+04	-.90857E+02	-.49540E+03	.00000E+00	.00000E+00	.00000E+00
52	-.14874E+04	-.10150E+03	-.54511E+03	.00000E+00	.00000E+00	.00000E+00
53	-.17502E+02	.98556E+00	.82134E+02	-.21652E+01	.19466E+00	.98423E+01
54	-.17037E+02	.17922E+01	.86802E+02	-.32521E+01	.25120E+00	.17233E+02
55	-.14943E+02	.23259E+01	.86975E+02	-.35266E+01	.28036E+00	.22683E+02
56	-.11709E+02	.25586E+01	.82493E+02	-.32544E+01	.31378E+00	.26187E+02
57	-.90521E+01	.28360E+01	.83269E+02	-.26925E+01	.34841E+00	.28462E+02
58	-.63604E+01	.30468E+01	.85656E+02	-.18948E+01	.36004E+00	.30018E+02
59	-.32116E+01	.31042E+01	.85121E+02	-.98649E+00	.36763E+00	.30877E+02
60	-.73883E-01	.31037E+01	.84571E+02	-.33495E-01	.37055E+00	.31161E+02
61	.31173E+01	.31143E+01	.85580E+02	.91506E+00	.36958E+00	.30916E+02
62	.62592E+01	.30203E+01	.85999E+02	.18421E+01	.35396E+00	.30080E+02
63	.91652E+01	.28026E+01	.84602E+02	.26398E+01	.33583E+00	.28579E+02
64	.12065E+02	.25494E+01	.84980E+02	.32312E+01	.31276E+00	.26242E+02
65	.14714E+02	.21434E+01	.85587E+02	.35047E+01	.27243E+00	.22672E+02
66	.16527E+02	.15195E+01	.84084E+02	.32514E+01	.21499E+00	.17498E+02

67	.17862E+02	.74479E+00	.83673E+02	.22290E+01	.13081E+00	.10298E+02
68	.14822E+04	-.26973E+02	-.54129E+03	.00000E+00	.00000E+00	.00000E+00
69	-.15175E+04	-.35358E+02	-.55747E+03	.00000E+00	.00000E+00	.00000E+00
70	-.17128E+02	.13368E+00	.82204E+02	-.22263E+01	.40168E-01	.10270E+02
71	-.16742E+02	.12479E+00	.86883E+02	-.33627E+01	.22763E-01	.18090E+02
72	-.14739E+02	.74184E-01	.87009E+02	-.36620E+01	.17110E-03	.23905E+02
73	-.11581E+02	.43211E-01	.82542E+02	-.33884E+01	-.15702E-02	.27658E+02
74	-.89665E+01	.49505E-01	.83310E+02	-.28061E+01	.87978E-02	.30100E+02
75	-.63125E+01	.20760E-01	.85696E+02	-.19737E+01	.27891E-02	.31770E+02
76	-.31935E+01	.82360E-02	.85151E+02	-.10228E+01	.36144E-03	.32689E+02
77	-.82541E-01	-.96800E-03	.84612E+02	-.24087E-01	.22174E-04	.32989E+02
78	.30786E+01	-.24820E-02	.85617E+02	.97081E+00	.21388E-02	.32719E+02
79	.61872E+01	-.26587E-01	.86042E+02	.19408E+01	-.37832E-02	.31813E+02
80	.90510E+01	-.38857E-01	.84658E+02	.27734E+01	-.43874E-02	.30190E+02
81	.11884E+02	-.50907E-01	.85017E+02	.33869E+01	-.17077E-02	.27672E+02
82	.14463E+02	-.83477E-01	.85680E+02	.36642E+01	-.77444E-02	.23842E+02
83	.16177E+02	-.11240E+00	.84117E+02	.33854E+01	-.19280E-01	.18314E+02
84	.17433E+02	-.13372E+00	.83740E+02	.23103E+01	-.33931E-01	.10737E+02
85	.15187E+04	.36025E+02	-.55546E+03	.00000E+00	.00000E+00	.00000E+00
86	-.14814E+04	.25635E+02	-.54335E+03	.00000E+00	.00000E+00	.00000E+00
87	-.17538E+02	-.70425E+00	.82122E+02	-.21521E+01	-.12221E+00	.98706E+01
88	-.17092E+02	-.15402E+01	.86791E+02	-.32304E+01	-.20980E+00	.17279E+02
89	-.15008E+02	-.21819E+01	.86948E+02	-.35034E+01	-.27981E+00	.22730E+02
90	-.11758E+02	-.24783E+01	.82502E+02	-.32337E+01	-.31544E+00	.26229E+02
91	-.90778E+01	-.27415E+01	.83255E+02	-.26723E+01	-.33062E+00	.28495E+02
92	-.63870E+01	-.30085E+01	.85656E+02	-.18739E+01	-.35437E+00	.30039E+02
93	-.32323E+01	-.30885E+01	.85110E+02	-.96516E+00	-.36692E+00	.30888E+02
94	-.93363E-01	-.31068E+01	.84579E+02	-.12108E+01	-.37056E+00	.31161E+02
95	.30951E+01	-.31170E+01	.85569E+02	.93669E+00	-.36556E+00	.30904E+02
96	.62354E+01	-.30697E+01	.86011E+02	.18635E+01	-.36164E+00	.30059E+02
97	.91340E+01	-.28757E+01	.84611E+02	.26610E+01	-.34507E+00	.28546E+02
98	.12017E+02	-.26442E+01	.84973E+02	.32530E+01	-.31735E+00	.26200E+02
99	.14664E+02	-.23059E+01	.85629E+02	.35281E+01	-.28735E+00	.22625E+02
100	.16455E+02	-.17452E+01	.84026E+02	.32727E+01	-.24964E+00	.17451E+02
101	.17813E+02	-.10268E+01	.83727E+02	.22440E+01	-.19128E+00	.10278E+02
102	.14888E+04	.10495E+03	-.54320E+03	.00000E+00	.00000E+00	.00000E+00
103	-.13685E+04	.87241E+02	-.49754E+03	.00000E+00	.00000E+00	.00000E+00
104	-.18793E+02	-.16585E+01	.81865E+02	-.18978E+01	-.24193E+00	.85155E+01
105	-.18104E+02	-.33901E+01	.86570E+02	-.27931E+01	-.36392E+00	.14597E+02
106	-.15734E+02	-.46104E+01	.86777E+02	-.29959E+01	-.45151E+00	.18936E+02
107	-.12218E+02	-.51257E+01	.82366E+02	-.27437E+01	-.50630E+00	.21677E+02
108	-.93745E+01	-.56253E+01	.83141E+02	-.22547E+01	-.53644E+00	.23440E+02
109	-.65716E+01	-.61078E+01	.85529E+02	-.15727E+01	-.56898E+00	.24637E+02
110	-.33217E+01	-.62395E+01	.84994E+02	-.80417E+00	-.58631E+00	.25290E+02
111	-.10332E+00	-.62579E+01	.84452E+02	-.12245E-02	-.59159E+00	.25496E+02
112	.31637E+01	-.62813E+01	.85446E+02	.79794E+00	-.58559E+00	.25293E+02
113	.63926E+01	-.61767E+01	.85878E+02	.15818E+01	-.57628E+00	.24634E+02
114	.94028E+01	-.57953E+01	.84470E+02	.22615E+01	-.55126E+00	.23451E+02
115	.12445E+02	-.53531E+01	.84841E+02	.27764E+01	-.51117E+00	.21616E+02
116	.15307E+02	-.46823E+01	.85462E+02	.30354E+01	-.46102E+00	.18802E+02
117	.17367E+02	-.35568E+01	.83880E+02	.28508E+01	-.39334E+00	.14676E+02
118	.18986E+02	-.20726E+01	.83436E+02	.19894E+01	-.28821E+00	.88059E+01
119	.13879E+04	.18654E+03	-.50154E+03	.00000E+00	.00000E+00	.00000E+00
120	-.11430E+04	.15917E+03	-.40353E+03	.00000E+00	.00000E+00	.00000E+00
121	-.21069E+02	-.29469E+01	.81314E+02	-.12920E+01	-.25273E+00	.57017E+01
122	-.19750E+02	-.56854E+01	.86150E+02	-.18573E+01	-.32752E+00	.93242E+01
123	-.16839E+02	-.73929E+01	.86460E+02	-.19475E+01	-.39820E+00	.11797E+02
124	-.12897E+02	-.80101E+01	.82110E+02	-.17607E+01	-.44323E+00	.13328E+02
125	-.98055E+01	-.86749E+01	.82912E+02	-.14346E+01	-.46944E+00	.14306E+02
126	-.68372E+01	-.93306E+01	.85322E+02	-.99353E+00	-.49481E+00	.14970E+02

127	-.34460E+01	-.94837E+01	.84786E+02	-.50427E+00	-.50772E+00	.15331E+02
128	-.11101E+00	-.94905E+01	.84229E+02	.44373E-02	-.51191E+00	.15438E+02
129	.32720E+01	-.95355E+01	.85228E+02	.51136E+00	-.50785E+00	.15321E+02
130	.66368E+01	-.93977E+01	.85654E+02	.10114E+01	-.50054E+00	.14955E+02
131	.98195E+01	-.88746E+01	.84254E+02	.14496E+01	-.48123E+00	.14293E+02
132	.13108E+02	-.82881E+01	.84592E+02	.17920E+01	-.45024E+00	.13262E+02
133	.16330E+02	-.73740E+01	.85179E+02	.19835E+01	-.40905E+00	.11680E+02
134	.18841E+02	-.57602E+01	.83482E+02	.19015E+01	-.34986E+00	.93227E+01
135	.21055E+02	-.35037E+01	.82922E+02	.13757E+01	-.25530E+00	.58318E+01
136	.11889E+04	.34149E+03	-.41702E+03	.00000E+00	.00000E+00	.00000E+00
137	-.32760E+03	.54886E+03	-.10616E+03	.00000E+00	.00000E+00	.00000E+00
138	-.58400E+01	.11503E+04	-.22980E+02	.00000E+00	.00000E+00	.00000E+00
139	-.16039E+02	.11492E+04	-.45701E+02	.00000E+00	.00000E+00	.00000E+00
140	-.21403E+02	.10673E+04	-.55531E+02	.00000E+00	.00000E+00	.00000E+00
141	-.17660E+02	.96523E+03	-.56033E+02	.00000E+00	.00000E+00	.00000E+00
142	-.20942E+02	.95121E+03	-.59198E+02	.00000E+00	.00000E+00	.00000E+00
143	-.16697E+02	.95020E+03	-.60694E+02	.00000E+00	.00000E+00	.00000E+00
144	-.10552E+02	.93273E+03	-.60091E+02	.00000E+00	.00000E+00	.00000E+00
145	-.28934E+01	.92297E+03	-.59416E+02	.00000E+00	.00000E+00	.00000E+00
146	-.13300E-01	.94015E+03	-.59873E+02	.00000E+00	.00000E+00	.00000E+00
147	.59364E+01	.95329E+03	-.59341E+02	.00000E+00	.00000E+00	.00000E+00
148	.93415E+01	.95989E+03	-.57259E+02	.00000E+00	.00000E+00	.00000E+00
149	.53901E+01	.10002E+04	-.54233E+02	.00000E+00	.00000E+00	.00000E+00
150	.37380E+01	.10600E+04	-.49079E+02	.00000E+00	.00000E+00	.00000E+00
151	.19787E+02	.11090E+04	-.43146E+02	.00000E+00	.00000E+00	.00000E+00
152	.16513E+03	.11569E+04	-.72866E+02	.00000E+00	.00000E+00	.00000E+00
153	.17859E+03	.19318E+03	-.57126E+02	.00000E+00	.00000E+00	.00000E+00
sum:	-.12705E-10	.21089E-10	.23093E-10			
max:				.36642E+01	-.59159E+00	.32989E+02

(((SUM OF STRESSES & STRAINES)))

ELEM	Sig-x	Sig-y	Tau-xy	Eps-x	Eps-y	Gam-xy
1	.50000E+01	.50000E+01	.00000E+00	.00000E+00	.00000E+00	.00000E+00
2	.19006E+02	.18575E+02	-.73188E+00	.25277E-02	.51342E-02	-.76032E-02
3	.11201E+02	.88515E+01	-.26857E+00	.25277E-02	.10008E-05	-.27901E-02
4	.18571E+02	.18344E+02	-.75768E+00	.23243E-02	.51758E-02	-.78712E-02
5	.10701E+02	.85401E+01	-.29532E+00	.23243E-02	.14783E-06	-.30679E-02
6	.17893E+02	.18419E+02	-.83516E+00	.17245E-02	.56978E-02	-.86761E-02
7	.92279E+01	.76245E+01	-.25441E+00	.17245E-02	-.95295E-06	-.26429E-02
8	.17684E+02	.18727E+02	-.81991E+00	.13539E-02	.61581E-02	-.85177E-02
9	.83189E+01	.70600E+01	-.17146E+00	.13539E-02	-.10177E-05	-.17812E-02
10	.17703E+02	.18976E+02	-.75117E+00	.12063E-02	.64082E-02	-.78035E-02
11	.79582E+01	.68369E+01	-.25960E-01	.12063E-02	-.12294E-06	-.26968E-03
12	.17491E+02	.19020E+02	-.65581E+00	.10056E-02	.65928E-02	-.68129E-02
13	.74674E+01	.65330E+01	.11872E+00	.10056E-02	.81255E-06	.12334E-02
14	.17451E+02	.19115E+02	-.52770E+00	.91117E-03	.67189E-02	-.54821E-02
15	.72374E+01	.63911E+01	.26893E+00	.91117E-03	.17922E-05	.27938E-02
16	.17457E+02	.19166E+02	-.38320E+00	.88262E-03	.67687E-02	-.39809E-02
17	.71700E+01	.63508E+01	.42028E+00	.88262E-03	.35021E-05	.43661E-02
18	.17535E+02	.19196E+02	-.23294E+00	.92641E-03	.67494E-02	-.24199E-02
19	.72784E+01	.64187E+01	.58306E+00	.92641E-03	.41446E-05	.60572E-02
20	.17536E+02	.19146E+02	-.84379E-01	.96019E-03	.66958E-02	-.87657E-03
21	.73664E+01	.64766E+01	.71804E+00	.96019E-03	.75345E-05	.74593E-02
22	.17683E+02	.19128E+02	.63140E-01	.10908E-02	.65815E-02	.65593E-03
23	.76895E+01	.66790E+01	.83209E+00	.10908E-02	.93489E-05	.86442E-02

24	.17947E+02	.19090E+02	.19416E+00	.13302E-02	.63690E-02	.20170E-02
25	.82727E+01	.70387E+01	.92823E+00	.13302E-02	.68030E-05	.96429E-02
26	.18245E+02	.18986E+02	.29666E+00	.16402E-02	.60647E-02	.30819E-02
27	.90410E+01	.75208E+01	.95905E+00	.16402E-02	.12053E-04	.99631E-02
28	.18674E+02	.18859E+02	.35903E+00	.20726E-02	.56500E-02	.37298E-02
29	.10102E+02	.81802E+01	.89463E+00	.20726E-02	.12500E-04	.92939E-02
30	.19089E+02	.18636E+02	.35200E+00	.25552E-02	.51441E-02	.36568E-02
31	.11271E+02	.88965E+01	.68914E+00	.25552E-02	.26217E-05	.71591E-02
32	.14257E+02	.16532E+02	.32417E+00	.00000E+00	.60880E-02	.33677E-02
33	.12812E+02	.14732E+02	-.33443E+00	.00000E+00	.51374E-02	-.34743E-02
34	.16929E+02	.19727E+02	-.58417E+00	.87016E-04	.77049E-02	-.60686E-02
35	.13087E+02	.14941E+02	-.29293E+00	.87016E-04	.51781E-02	-.30431E-02
36	.16572E+02	.20293E+02	-.55931E+00	-.57238E-03	.85337E-02	-.58104E-02
37	.12265E+02	.14927E+02	-.34223E+00	-.57238E-03	.57007E-02	-.35552E-02
38	.15836E+02	.20506E+02	-.64307E+00	-.13105E-02	.92397E-02	-.66806E-02
39	.11155E+02	.14675E+02	-.34811E+00	-.13105E-02	.61611E-02	-.36164E-02
40	.15535E+02	.20844E+02	-.65604E+00	-.17752E-02	.97916E-02	-.68153E-02
41	.10392E+02	.14437E+02	-.29105E+00	-.17752E-02	.64092E-02	-.30235E-02
42	.15425E+02	.21122E+02	-.60974E+00	-.20462E-02	.10156E-01	-.63343E-02
43	.10003E+02	.14367E+02	-.15797E+00	-.20462E-02	.65904E-02	-.16411E-02
44	.15260E+02	.21273E+02	-.51130E+00	-.22789E-02	.10423E-01	-.53117E-02
45	.96226E+01	.14250E+02	-.28185E-01	-.22789E-02	.67157E-02	-.29281E-03
46	.15233E+02	.21427E+02	-.39374E+00	-.24007E-02	.10602E-01	-.40904E-02
47	.94029E+01	.14163E+02	.11385E+00	-.24007E-02	.67676E-02	.11828E-02
48	.15277E+02	.21531E+02	-.25931E+00	-.24334E-02	.10683E-01	-.26939E-02
49	.92949E+01	.14079E+02	.25684E+00	-.24334E-02	.67494E-02	.26682E-02
50	.15370E+02	.21582E+02	-.12309E+00	-.23910E-02	.10677E-01	-.12787E-02
51	.93227E+01	.14049E+02	.41077E+00	-.23910E-02	.66992E-02	.42672E-02
52	.15472E+02	.21565E+02	.18027E-01	-.22973E-02	.10592E-01	.18728E-03
53	.93818E+01	.13979E+02	.53501E+00	-.22973E-02	.65869E-02	.55579E-02
54	.15710E+02	.21541E+02	.14387E+00	-.20879E-02	.10411E-01	.14946E-02
55	.95774E+01	.13901E+02	.63719E+00	-.20879E-02	.63779E-02	.66194E-02
56	.16091E+02	.21499E+02	.24382E+00	-.17509E-02	.10118E-01	.25329E-02
57	.99493E+01	.13848E+02	.71450E+00	-.17509E-02	.60790E-02	.74227E-02
58	.16618E+02	.21432E+02	.31253E+00	-.12786E-02	.97026E-02	.32467E-02
59	.10471E+02	.13775E+02	.71918E+00	-.12786E-02	.56603E-02	.74712E-02
60	.17303E+02	.21360E+02	.31491E+00	-.67425E-03	.91787E-02	.32714E-02
61	.11183E+02	.13735E+02	.61618E+00	-.67425E-03	.51535E-02	.64012E-02
62	.17170E+02	.20970E+02	.24264E+00	-.52810E-03	.88555E-02	.25207E-02
63	.12976E+02	.15745E+02	.58500E+00	-.52810E-03	.60970E-02	.60773E-02
64	.17690E+02	.20808E+02	.31380E+00	.00000E+00	.83454E-02	.32599E-02
65	.16715E+02	.19594E+02	-.38005E+00	.00000E+00	.77045E-02	-.39482E-02
66	.15461E+02	.20138E+02	-.37505E+00	-.13745E-02	.90969E-02	-.38962E-02
67	.14600E+02	.19065E+02	-.23800E+00	-.13745E-02	.85304E-02	-.24725E-02
68	.15108E+02	.21092E+02	-.32753E+00	-.22845E-02	.10332E-01	-.34025E-02
69	.13440E+02	.19014E+02	-.25858E+00	-.22845E-02	.92352E-02	-.26863E-02
70	.14446E+02	.21407E+02	-.38574E+00	-.30279E-02	.11096E-01	-.40073E-02
71	.12450E+02	.18921E+02	-.27817E+00	-.30279E-02	.97834E-02	-.28898E-02
72	.14101E+02	.21737E+02	-.41278E+00	-.35240E-02	.11669E-01	-.42881E-02
73	.11793E+02	.18862E+02	-.24883E+00	-.35240E-02	.10151E-01	-.25850E-02
74	.13933E+02	.22023E+02	-.39355E+00	-.38470E-02	.12079E-01	-.40884E-02
75	.11408E+02	.18877E+02	-.15100E+00	-.38470E-02	.10419E-01	-.15687E-02
76	.13799E+02	.22228E+02	-.31900E+00	-.40898E-02	.12383E-01	-.33140E-02
77	.11087E+02	.18849E+02	-.63198E-01	-.40898E-02	.10599E-01	-.65654E-03
78	.13781E+02	.22413E+02	-.24271E+00	-.42258E-02	.12590E-01	-.25214E-02
79	.10878E+02	.18798E+02	.34039E-01	-.42258E-02	.10682E-01	.35362E-03
80	.13829E+02	.22539E+02	-.15470E+00	-.42682E-02	.12691E-01	-.16071E-02
81	.10767E+02	.18724E+02	.13156E+00	-.42682E-02	.10676E-01	.13667E-02
82	.13932E+02	.22602E+02	-.64237E-01	-.42255E-02	.12689E-01	-.66733E-03
83	.10746E+02	.18633E+02	.24207E+00	-.42255E-02	.10594E-01	.25148E-02

84	.14088E+02	.22605E+02	.34401E-01	-.41004E-02	.12590E-01	.35737E-03
85	.10780E+02	.18483E+02	.32515E+00	-.41004E-02	.10415E-01	.33778E-02
86	.14358E+02	.22574E+02	.11289E+00	-.38615E-02	.12382E-01	.11727E-02
87	.10917E+02	.18287E+02	.39239E+00	-.38615E-02	.10119E-01	.40764E-02
88	.14761E+02	.22519E+02	.17172E+00	-.34976E-02	.12061E-01	.17839E-02
89	.11180E+02	.18058E+02	.44432E+00	-.34976E-02	.97056E-02	.46159E-02
90	.15326E+02	.22456E+02	.20711E+00	-.29971E-02	.11625E-01	.21516E-02
91	.11614E+02	.17832E+02	.43763E+00	-.29971E-02	.91838E-02	.45463E-02
92	.15890E+02	.22335E+02	.19712E+00	-.24598E-02	.11129E-01	.20477E-02
93	.12430E+02	.18025E+02	.40113E+00	-.24598E-02	.88539E-02	.41672E-02
94	.16749E+02	.22301E+02	.16768E+00	-.17390E-02	.10532E-01	.17419E-02
95	.13429E+02	.18165E+02	.43054E+00	-.17390E-02	.83482E-02	.44727E-02
96	.19312E+02	.22830E+02	.16310E+00	.00000E+00	.94125E-02	.16944E-02
97	.18831E+02	.22230E+02	-.25600E+00	.00000E+00	.90961E-02	-.26595E-02
98	.14556E+02	.20077E+02	-.10120E+00	-.20710E-02	.96246E-02	-.10513E-02
99	.15627E+02	.21411E+02	-.11319E+00	-.20710E-02	.10329E-01	-.11759E-02
100	.14087E+02	.21044E+02	-.77813E-01	-.30832E-02	.10949E-01	-.80836E-03
101	.14307E+02	.21319E+02	-.10916E+00	-.30832E-02	.11094E-01	-.11340E-02
102	.13438E+02	.21342E+02	-.10628E+00	-.38050E-02	.11686E-01	-.11041E-02
103	.13408E+02	.21304E+02	-.12871E+00	-.38050E-02	.11666E-01	-.13371E-02
104	.13065E+02	.21635E+02	-.13553E+00	-.43000E-02	.12239E-01	-.14080E-02
105	.12817E+02	.21327E+02	-.12341E+00	-.43000E-02	.12076E-01	-.12821E-02
106	.12868E+02	.21912E+02	-.14377E+00	-.46406E-02	.12659E-01	-.14936E-02
107	.12443E+02	.21383E+02	-.71949E-01	-.46406E-02	.12380E-01	-.74744E-03
108	.12746E+02	.22141E+02	-.10614E+00	-.48888E-02	.12980E-01	-.11026E-02
109	.12153E+02	.21401E+02	-.40047E-01	-.48888E-02	.12589E-01	-.41603E-03
110	.12729E+02	.22336E+02	-.84708E-01	-.50305E-02	.13196E-01	-.87999E-03
111	.11959E+02	.21377E+02	-.39327E-02	-.50305E-02	.12690E-01	-.40854E-04
112	.12779E+02	.22470E+02	-.57427E-01	-.50772E-02	.13305E-01	-.59658E-03
113	.11843E+02	.21304E+02	.32122E-01	-.50772E-02	.12689E-01	.33370E-03
114	.12890E+02	.22543E+02	-.32490E-01	-.50342E-02	.13309E-01	-.33753E-03
115	.11799E+02	.21183E+02	.78382E-01	-.50342E-02	.12591E-01	.81428E-03
116	.13067E+02	.22554E+02	.66803E-02	-.48975E-02	.13204E-01	.69399E-04
117	.11817E+02	.20997E+02	.10693E+00	-.48975E-02	.12383E-01	.11108E-02
118	.13344E+02	.22542E+02	.23974E-01	-.46532E-02	.12993E-01	.24906E-03
119	.11928E+02	.20760E+02	.12868E+00	-.46532E-02	.12061E-01	.13368E-02
120	.13743E+02	.22467E+02	.35076E-01	-.42908E-02	.12671E-01	.36439E-03
121	.12153E+02	.20486E+02	.15356E+00	-.42908E-02	.11625E-01	.15952E-02
122	.14280E+02	.22394E+02	.49071E-01	-.38067E-02	.12243E-01	.50978E-03
123	.12587E+02	.20285E+02	.16228E+00	-.38067E-02	.11130E-01	.16858E-02
124	.15029E+02	.22343E+02	.40104E-01	-.31644E-02	.11700E-01	.41663E-03
125	.13257E+02	.20134E+02	.16231E+00	-.31644E-02	.10534E-01	.16862E-02
126	.16270E+02	.22423E+02	.36571E-01	-.22088E-02	.10974E-01	.37992E-03
127	.13890E+02	.19459E+02	.19117E+00	-.22088E-02	.94092E-02	.19860E-02
128	.19665E+02	.23269E+02	-.42436E-01	.00000E+00	.96444E-02	-.44084E-03
129	.19635E+02	.23231E+02	-.52923E-01	.00000E+00	.96245E-02	-.54979E-03
130	.13951E+02	.19485E+02	.18302E+00	-.21763E-02	.93968E-02	.19013E-02
131	.16311E+02	.22425E+02	.34870E-01	-.21763E-02	.10949E-01	.36225E-03
132	.13272E+02	.20116E+02	.16922E+00	-.31403E-02	.10505E-01	.17580E-02
133	.15068E+02	.22354E+02	.56625E-01	-.31403E-02	.11686E-01	.58825E-03
134	.12575E+02	.20266E+02	.17657E+00	-.38047E-02	.11118E-01	.18343E-02
135	.14278E+02	.22388E+02	.45601E-01	-.38047E-02	.12238E-01	.47373E-03
136	.12162E+02	.20485E+02	.14904E+00	-.42828E-02	.11618E-01	.15483E-02
137	.13746E+02	.22457E+02	.27058E-01	-.42828E-02	.12659E-01	.28109E-03
138	.11940E+02	.20757E+02	.12067E+00	-.46414E-02	.12050E-01	.12536E-02
139	.13353E+02	.22517E+02	.33579E-01	-.46414E-02	.12979E-01	.34883E-03
140	.11825E+02	.20994E+02	.11531E+00	-.48895E-02	.12374E-01	.11979E-02
141	.13074E+02	.22550E+02	.43874E-02	-.48895E-02	.13196E-01	.45579E-04
142	.11799E+02	.21179E+02	.76359E-01	-.50314E-02	.12586E-01	.79326E-03
143	.12891E+02	.22539E+02	-.27157E-01	-.50314E-02	.13305E-01	-.28212E-03

144	.11842E+02	.21303E+02	.35845E-01	-.50779E-02	.12690E-01	.37238E-03
145	.12783E+02	.22476E+02	-.60327E-01	-.50779E-02	.13309E-01	-.62671E-03
146	.11949E+02	.21374E+02	-.47370E-02	-.50370E-02	.12694E-01	-.49211E-04
147	.12725E+02	.22342E+02	-.79221E-01	-.50370E-02	.13205E-01	-.82298E-03
148	.12144E+02	.21403E+02	-.33621E-01	-.48973E-02	.12597E-01	-.34928E-03
149	.12746E+02	.22153E+02	-.11178E+00	-.48973E-02	.12993E-01	-.11612E-02
150	.12425E+02	.21384E+02	-.77086E-01	-.46558E-02	.12393E-01	-.80081E-03
151	.12848E+02	.21911E+02	-.13382E+00	-.46558E-02	.12671E-01	-.13902E-02
152	.12823E+02	.21340E+02	-.11160E+00	-.43042E-02	.12087E-01	-.11594E-02
153	.13061E+02	.21637E+02	-.13106E+00	-.43042E-02	.12244E-01	-.13615E-02
154	.13420E+02	.22306E+02	-.12207E+00	-.37965E-02	.11661E-01	-.12681E-02
155	.13478E+02	.21378E+02	-.11598E+00	-.37965E-02	.11699E-01	-.12049E-02
156	.14248E+02	.21288E+02	-.11748E+00	-.31112E-02	.11100E-01	-.12205E-02
157	.14059E+02	.21052E+02	-.76808E-01	-.31112E-02	.10976E-01	-.79792E-03
158	.15586E+02	.21420E+02	-.11930E+00	-.21099E-02	.10365E-01	-.12394E-02
159	.14490E+02	.20055E+02	-.94292E-01	-.21099E-02	.96439E-02	-.97956E-03
160	.18869E+02	.22277E+02	-.23857E+00	.00000E+00	.91210E-02	-.24784E-02
161	.19288E+02	.22800E+02	.16058E+00	.00000E+00	.93967E-02	.16682E-02
162	.13482E+02	.18190E+02	.42850E+00	-.17123E-02	.83398E-02	.44515E-02
163	.16773E+02	.22290E+02	.16859E+00	-.17123E-02	.10504E-01	.17514E-02
164	.12457E+02	.18034E+02	.40025E+00	-.24439E-02	.88459E-02	.41580E-02
165	.15914E+02	.22340E+02	.20393E+00	-.24439E-02	.11119E-01	.21185E-02
166	.11624E+02	.17831E+02	.45406E+00	-.29886E-02	.91767E-02	.47170E-02
167	.15336E+02	.22455E+02	.20522E+00	-.29886E-02	.11618E-01	.21320E-02
168	.11192E+02	.18055E+02	.43996E+00	-.34855E-02	.96940E-02	.45705E-02
169	.14774E+02	.22517E+02	.16866E+00	-.34855E-02	.12049E-01	.17521E-02
170	.10918E+02	.18281E+02	.38318E+00	-.38561E-02	.10111E-01	.39807E-02
171	.14359E+02	.22567E+02	.12272E+00	-.38561E-02	.12374E-01	.12749E-02
172	.10792E+02	.18491E+02	.33604E+00	-.40954E-02	.10415E-01	.34910E-02
173	.14094E+02	.22604E+02	.36593E-01	-.40954E-02	.12586E-01	.38015E-03
174	.10740E+02	.18627E+02	.24201E+00	-.42265E-02	.10592E-01	.25141E-02
175	.13930E+02	.22600E+02	-.56151E-01	-.42265E-02	.12690E-01	-.58333E-03
176	.10766E+02	.18725E+02	.14024E+00	-.42695E-02	.10679E-01	.14569E-02
177	.13831E+02	.22543E+02	-.15214E+00	-.42695E-02	.12694E-01	-.15806E-02
178	.10863E+02	.18793E+02	.36485E-01	-.42349E-02	.10686E-01	.37903E-03
179	.13771E+02	.22415E+02	-.23549E+00	-.42349E-02	.12598E-01	-.24464E-02
180	.11082E+02	.18854E+02	-.53534E-01	-.40964E-02	.10607E-01	-.55614E-03
181	.13801E+02	.22240E+02	-.32212E+00	-.40964E-02	.12395E-01	-.33464E-02
182	.11378E+02	.18868E+02	-.15376E+00	-.38658E-02	.10430E-01	-.15973E-02
183	.13903E+02	.22015E+02	-.38509E+00	-.38658E-02	.12090E-01	-.40005E-02
184	.11811E+02	.18882E+02	-.23302E+00	-.35225E-02	.10161E-01	-.24208E-02
185	.14098E+02	.21731E+02	-.40816E+00	-.35225E-02	.11664E-01	-.42402E-02
186	.12481E+02	.18928E+02	-.27096E+00	-.30076E-02	.97709E-02	-.28149E-02
187	.14503E+02	.21447E+02	-.39183E+00	-.30076E-02	.11101E-01	-.40706E-02
188	.13366E+02	.18964E+02	-.27453E+00	-.23116E-02	.92302E-02	-.28520E-02
189	.15090E+02	.21112E+02	-.33507E+00	-.23116E-02	.10364E-01	-.34809E-02
190	.14542E+02	.19060E+02	-.24775E+00	-.14180E-02	.85624E-02	-.25738E-02
191	.15385E+02	.20110E+02	-.36719E+00	-.14180E-02	.91170E-02	-.38145E-02
192	.16745E+02	.19632E+02	-.35971E+00	.00000E+00	.77242E-02	-.37369E-02
193	.17679E+02	.20795E+02	.31795E+00	.00000E+00	.83383E-02	.33030E-02
194	.13012E+02	.15778E+02	.57883E+00	-.52010E-03	.61080E-02	.60132E-02
195	.17170E+02	.20958E+02	.24221E+00	-.52010E-03	.88427E-02	.25163E-02
196	.11216E+02	.13772E+02	.61705E+00	-.67125E-03	.51704E-02	.64103E-02
197	.17300E+02	.21351E+02	.31888E+00	-.67125E-03	.91718E-02	.33126E-02
198	.10516E+02	.13799E+02	.73618E+00	-.12586E-02	.56573E-02	.76478E-02
199	.16650E+02	.21441E+02	.31226E+00	-.12586E-02	.96916E-02	.32439E-02
200	.99684E+01	.13846E+02	.70937E+00	-.17341E-02	.60643E-02	.73693E-02
201	.16120E+02	.21509E+02	.24644E+00	-.17341E-02	.10110E-01	.25601E-02
202	.95602E+01	.13893E+02	.62782E+00	-.20966E-02	.63806E-02	.65221E-02
203	.15689E+02	.21528E+02	.15351E+00	-.20966E-02	.10411E-01	.15948E-02

204	.94073E+01	.14004E+02	.54611E+00	-.22930E-02	.65968E-02	.56732E-02
205	.15480E+02	.21568E+02	.23671E-01	-.22930E-02	.10590E-01	.24591E-03
206	.93059E+01	.14035E+02	.41101E+00	-.23960E-02	.66962E-02	.42698E-02
207	.15360E+02	.21578E+02	-.11425E+00	-.23960E-02	.10678E-01	-.11868E-02
208	.93009E+01	.14089E+02	.26720E+00	-.24351E-02	.67561E-02	.27758E-02
209	.15279E+02	.21537E+02	-.25412E+00	-.24351E-02	.10688E-01	-.26399E-02
210	.93746E+01	.14148E+02	.11830E+00	-.24137E-02	.67700E-02	.12289E-02
211	.15214E+02	.21422E+02	-.38704E+00	-.24137E-02	.10610E-01	-.40208E-02
212	.96275E+01	.14259E+02	-.16135E-01	-.22805E-02	.67215E-02	-.16762E-03
213	.15271E+02	.21289E+02	-.51149E+00	-.22805E-02	.10433E-01	-.53136E-02
214	.99455E+01	.14337E+02	-.15834E+00	-.20726E-02	.65952E-02	-.16449E-02
215	.15375E+02	.21100E+02	-.60547E+00	-.20726E-02	.10166E-01	-.62899E-02
216	.10431E+02	.14470E+02	-.27524E+00	-.17649E-02	.64184E-02	-.28593E-02
217	.15538E+02	.20832E+02	-.65550E+00	-.17649E-02	.97769E-02	-.68097E-02
218	.11209E+02	.14676E+02	-.34069E+00	-.12669E-02	.61267E-02	-.35392E-02
219	.15940E+02	.20570E+02	-.64208E+00	-.12669E-02	.92383E-02	-.66702E-02
220	.12163E+02	.14848E+02	-.35364E+00	-.60375E-03	.56845E-02	-.36738E-02
221	.16546E+02	.20309E+02	-.56333E+00	-.60375E-03	.85671E-02	-.58521E-02
222	.12998E+02	.14922E+02	-.29923E+00	.26996E-04	.52162E-02	-.31086E-02
223	.16818E+02	.19681E+02	-.57498E+00	.26996E-04	.77287E-02	-.59732E-02
224	.12832E+02	.14757E+02	-.31828E+00	.00000E+00	.51508E-02	-.33064E-02
225	.14281E+02	.16562E+02	.33207E+00	.00000E+00	.61039E-02	.34497E-02
226	.11209E+02	.88610E+01	.65681E+00	.25282E-02	.56338E-05	.68233E-02
227	.19050E+02	.18628E+02	.34444E+00	.25282E-02	.51619E-02	.35782E-02
228	.10102E+02	.81782E+01	.89333E+00	.20736E-02	.10586E-04	.92804E-02
229	.18668E+02	.18850E+02	.35241E+00	.20736E-02	.56444E-02	.36610E-02
230	.91354E+01	.75786E+01	.97454E+00	.16792E-02	.11200E-04	.10124E-01
231	.18317E+02	.19016E+02	.29614E+00	.16792E-02	.60492E-02	.30764E-02
232	.83124E+01	.70635E+01	.91784E+00	.13463E-02	.68986E-05	.95350E-02
233	.17992E+02	.19121E+02	.20029E+00	.13463E-02	.63725E-02	.20808E-02
234	.76214E+01	.66346E+01	.81913E+00	.10644E-02	.71237E-05	.85096E-02
235	.17631E+02	.19105E+02	.68087E-01	.10644E-02	.65902E-02	.70732E-03
236	.74070E+01	.65021E+01	.72481E+00	.97656E-03	.78520E-05	.75297E-02
237	.17571E+02	.19164E+02	-.76985E-01	.97656E-03	.66921E-02	-.79976E-03
238	.72415E+01	.63956E+01	.58252E+00	.91149E-03	.39455E-05	.60515E-02
239	.17506E+02	.19182E+02	-.22638E+00	.91149E-03	.67542E-02	-.23517E-02
240	.71803E+01	.63565E+01	.42947E+00	.88726E-03	.27819E-05	.44616E-02
241	.17474E+02	.19179E+02	-.37642E+00	.88726E-03	.67721E-02	-.39104E-02
242	.71883E+01	.63609E+01	.27452E+00	.89096E-03	.21172E-05	.28519E-02
243	.17412E+02	.19097E+02	-.52479E+00	.89096E-03	.67256E-02	-.54518E-02
244	.74918E+01	.65481E+01	.13045E+00	.10156E-02	.73142E-06	.13551E-02
245	.17524E+02	.19046E+02	-.65281E+00	.10156E-02	.65984E-02	-.67817E-02
246	.78524E+01	.67711E+01	-.23138E-01	.11631E-02	-.15356E-06	-.24037E-03
247	.17610E+02	.18926E+02	-.75548E+00	.11631E-02	.64167E-02	-.78483E-02
248	.83873E+01	.71025E+01	-.15606E+00	.13818E-02	-.98498E-06	-.16212E-02
249	.17701E+02	.18705E+02	-.82374E+00	.13818E-02	.61240E-02	-.85574E-02
250	.93802E+01	.77191E+01	-.25298E+00	.17866E-02	-.99376E-06	-.26281E-02
251	.18023E+02	.18486E+02	-.82950E+00	.17866E-02	.56829E-02	-.86173E-02
252	.10573E+02	.84639E+01	-.31139E+00	.22706E-02	.30363E-05	-.32349E-02
253	.18503E+02	.18342E+02	-.76557E+00	.22706E-02	.52176E-02	-.79532E-02
254	.11038E+02	.87506E+01	-.27945E+00	.24615E-02	.90969E-06	-.29031E-02
255	.18865E+02	.18500E+02	-.74042E+00	.24615E-02	.51477E-02	-.76918E-02
256	.50000E+01	.50000E+01	.00000E+00	.00000E+00	.00000E+00	.00000E+00
max:	.19665E+02	.23269E+02	.97454E+00	-.50779E-02	.13309E-01	.10124E-01

==== BARREL VAULT _curvature38 width6_ Stress-deformation UPWARDS =====